STRUCTURE-BORNE SOUND TRANSMISSION WITHIN ELECTRIC POWER STEERING SYSTEMS

Dennis ZABEL

Ph.D. Thesis 2018

STRUCTURE-BORNE SOUND TRANSMISSION WITHIN ELECTRIC POWER STEERING SYSTEMS

Dennis ZABEL

Acoustics Research Centre

School of Computing, Science and Engineering

University of Salford, Salford, UK

Submitted in Partial Fulfilment of the Requirements of the Degree

of Doctor of Philosophy, August 2018

Contents

LIST OF FIGURES ..... **VI**

ACKNOWLEDGEMENTS ..... **XIV**

DECLARATION ..... **XV**

NOMENCLATURE ..... **XVI**

ABSTRACT ..... **XXII**

1 INTRODUCTION **1**

1.1 BACKGROUND 2

1.2 THE GENERAL APPROACH OF TRANSFER PATH ANALYSIS 5

1.3 EMBEDDED INTERNAL SOURCES 7

1.4 INTERNAL-SOURCE-PATH-RECEIVER-MODEL 8

1.5 THESIS OBJECTIVES 10

2 LITERATURE AND THEORY **13**

2.1 INTRODUCTION 14

2.2 MICRO-ELECTRO-MECHANICAL-SYSTEMS ACCELEROMETERS IN STRUCTURAL DYNAMICS 14

2.2.1 Performance evaluation *15*

2.2.2 Calibration methods and signal processing *16*

2.3 CHARACTERISATION OF STRUCTURE-BORNE SOUND SOURCES 18

2.3.1 Frequency response functions *18*

2.3.2 Contact force 19

2.3.3 Direct measurement of blocked force and free velocity 21

2.3.4 In-situ blocked force 23

2.3.5 On-board force validation 25

2.4 CONTRIBUTION OF STRUCTURE-BORNE SOUND SOURCES 27

2.4.1 Classical transfer path analysis 27

2.4.2 In-situ transfer path analysis 27

2.4.3 Transmissibility based transfer path analysis 28

2.4.4 Virtual acoustic prototyping 29

2.5 SUMMARY AND CONCLUDING REMARKS 29

3 SUBSTRUCTURING OF ELECTRIC POWER STEERING SYSTEMS 31

3.1 INTRODUCTION 32

3.2 ELECTRIC POWER STEERING SYSTEMS 34

3.2.1 Introduction 34

3.2.2 Functional principle 36

3.2.3 Boundary conditions 39

3.3 INTERNAL SOUND SOURCES AND RECEIVER 41

3.3.1 Introduction 41

3.3.2 Primary internal sources 42

3.3.3 Secondary internal sources 44

3.3.4 Internal receiver 45

3.4 TRANSMISSION PATHS AND INTERFACES 47

3.4.1 Introduction 47

3.4.2 External interfaces ... *48*

3.4.3 Internal interfaces ... *50*

3.4.4 Transmission paths ... *51*

3.5 SUMMARY AND CONCLUDING REMARKS ... 54

4 INDEPENDENT CHARACTERISATION OF INTERNAL STRUCTURE-BORNE SOUND SOURCES ... 58

4.1 INTRODUCTION ... 59

4.2 APPLICATION OF EMBEDDED ACCELEROMETERS FOR THE DETERMINATION OF IN-SITU BLOCKED FORCES ... 61

4.2.1 Introduction ... *61*

4.2.2 Methodology ... *64*

4.2.3 Limits of the methodology ... *68*

4.3 INTERNAL SOURCES WITH CONTINUOUS INTERFACES ... 70

4.3.1 Introduction ... *70*

4.3.2 Discretisation of continuous interfaces ... *71*

4.3.3 Discussion ... *73*

4.4 INTERNAL SOURCES WITH REVOLVING INTERFACES ... 75

4.4.1 Introduction ... *75*

4.4.2 Definition of revolving interfaces ... *77*

4.4.3 Methodology ... *79*

4.4.4 Limits of the methodology ... *83*

4.5 CASE STUDIES: IN-SITU BLOCKED FORCES OF INTERNAL SOURCES ... 84

4.5.1 Introduction ... *84*

4.5.2 Case study I: Electric motor ... 86

4.5.3 Case study II: Ball nut assembly ... 105

4.5.4 Case study III: Toothed belt ... 116

4.6 SUMMARY AND CONCLUDING REMARKS ... 130

5 CONTRIBUTION OF MULTIPLE INTERNAL STRUCTURE-BORNE SOUND SOURCES ... 132

5.1 INTRODUCTION ... 133

5.2 ADVANCED INTERNAL-SOURCE-PATH-RECEIVER-MODEL ... 134

5.2.1 Introduction ... 134

5.2.2 Model as basis for blocked force transmissibility ... 135

5.2.3 Blocked force transmissibility ... 137

5.3 BLOCKED FORCE TRANSMISSIBILITY TRANSFER PATH ANALYSIS ... 140

5.3.1 Introduction ... 140

5.3.2 Methodology to determine blocked force transmissibility ... 140

5.3.3 Validation method for blocked force transmissibility transfer path analysis ... 143

5.3.4 Drawback of blocked force transmissibility ... 145

5.4 CASE STUDIES: BLOCKED FORCE TRANSMISSIBILITY TRANSFER PATH ANALYSIS ... 146

5.4.1 Introduction ... 146

5.4.2 Case study I: Freely suspended steel beam ... 147

5.4.3 Case study II: Artificial excitation of electric power steering systems ... 152

5.4.4 Case study III: Realistic excitation of electric power steering systems ... 161

5.4.5 Coherence criterion ... 170

5.4.6 Concluding remarks ... 172

5.5 VIRTUAL COMPONENT ASSEMBLY ... 174

5.5.1 Motivation ... 174

5.5.2 Methodology ... 175

5.5.3 Benefits and risks for early development stages ... 177

5.6 KINEMATIC INFLUENCES ... 178

5.6.1 Introduction ... 178

5.6.2 Case study: Electric power steering system ... 179

5.6.3 Improvement of in-situ blocked forces ... 181

5.7 SUMMARY AND CONCLUDING REMARKS ... 182

6 CONCLUDING REMARKS AND FUTURE WORK ... 185

6.1 CONCLUDING REMARKS ... 186

6.2 FUTURE WORK ... 194

REFERENCES ... 197

List of Figures

Figure 1.1: Transfer path problem of sound generated by a vibrational source (A) and subsequently induced at interface (c) to receiver (B) 5

Figure 1.2: Internal-source-path-receiver-model (ISPRM) 9

Figure 2.1: Test setup for the calibration of MEMS accelerometers 17

Figure 2.2: Linear, time invariant system with excitation $\mathbf{f}_c$ at interface (c) and response $\mathbf{y}_b$ at interface (b) 19

Figure 2.3: Schematic depiction of the inverse identification of forces $\mathbf{f}_c$ at the contact interface (c) between source (A) and receiver (B) 20

Figure 2.4: Source with free boundary conditions at the interface where the source is coupled to a receiver when operated in the actual assembly 21

Figure 2.5: Source coupled to a receiver with blocked conditions at the interface where the source is coupled to a receiver when operated in the actual assembly 22

Figure 2.6: Schematic depiction of the methodology to determine in-situ blocked forces $\mathbf{f}_{bl,c}$ at interface (c) between source (A) and receiver (B) 24

Figure 2.7: On-board approach for the validation of experimentally determined in-situ blocked forces $\mathbf{f}_{bl}$ at the interface between source and receiver 26

Figure 3.1: Schematic of the functional principle of an electric power steering system 37

List of Figures

Figure 3.2: Schematic model of the transmission paths of the vibrational energy flux within an EPSapa system 38

Figure 3.3: EPSapa system with highlighted main components 43

Figure 3.4: Cross sectional view of an EPSapa system with highlighted external interfaces at one of the mounting feet with a vehicle 49

Figure 3.5: Cross sectional view of an EPSapa system with highlighted internal interfaces ... 51

Figure 3.6: Cross sectional view of an EPSapa system with the two identified internal transmission paths highlighted as blue and yellow line 52

Figure 4.1: Grooves machined into the housing of an electric motor to embed MEMS accelerometers in the vicinity of the actual contact interface (green) 67

Figure 4.2: Mass-spring system of a MEMS accelerometer embedded in a cavity of a rigid structure 67

Figure 4.3: Point connections (1…n) equally distributed over a symmetric and continuous interface 72

Figure 4.4: Point connections (1 and 2) at a revolving interface 76

Figure 4.5: Influence of a defective tooth at the interface on experimentally determined FRFs 78

Figure 4.6: Methodology for the independent characterisation of a structure-borne sound source with in-situ blocked forces at a revolving interface (c) 80

Figure 4.7: Methodology for the characterisation of a rotating toothed belt with in-situ blocked forces and transmissibility 82

List of Figures

Figure 4.8: Test setup used for the experimental determination of in-situ blocked forces of an electric motor (red coloured) 86

Figure 4.9: Schematic depiction of the interface between an electric motor and a receiver plate prepared with six MEMS accelerometers (2 accelerometers at each bolt) 88

Figure 4.10: Setup for the calibration of a MEMS accelerometer 89

Figure 4.11: Comparison of FRFs of a cantilever beam mounted on a shaker measured with a MEMS accelerometer (red curve) and a reference accelerometer (black curve); upper diagram: magnitude; lower diagram: phase 90

Figure 4.12: Filter for MEMS accelerometer (bottom) and result of calibrated x-axis (top) ... 91

Figure 4.13: Spectra of measured acceleration with a MEMS accelerometer when only x-direction is excited 92

Figure 4.14: Filter for MEMS accelerometer (bottom) and result of calibrated y-axis (top) ... 93

Figure 4.15: Measurement points for determination of in-situ blocked forces of an electric motor: 24 remote points (RP), validation point (RP20) and 3 coupling points (CP1 – CP3) .. 94

Figure 4.16: Signal-to-noise-ratio (SNR); top: SNR at all 24 remote points (RP); bottom: Signal and noise at RP10; Grid: 10 dB 95

Figure 4.17: Spectrum of the excitation at the remote points 96

Figure 4.18: Mobility between validation point and degrees of freedom at internal interface at bolts 97

Figure 4.19: Coherence functions between validation point and degrees of freedom at internal interface 98

List of Figures

Figure 4.20: Condition number of mobility matrix 99

Figure 4.21: Spectra of in-situ blocked forces of an electric motor (EM); axial direction; grid ordinate: 20 dB 100

Figure 4.22: Spectra of in-situ blocked forces of an electric motor (EM); radial direction; grid ordinate: 20 dB 100

Figure 4.23: Spectra of in-situ blocked forces of an electric motor (EM); tangential direction; grid ordinate: 20 dB 101

Figure 4.24: Spectrogram of in-situ blocked forces of an electric motor (EM) determined at one bolt which is used for the fixation; grid ordinate: 10dB 103

Figure 4.25: On-board validation of the in-situ blocked forces of an electric motor (EM); grid ordinate: 10 dB 104

Figure 4.26: Deviation of predicted and measured orders of an electric motor (EM) 105

Figure 4.27: Test setup for the determination of in-situ blocked forces of a ball nut assembly (BNA) 106

Figure 4.28: Interface between a ball nut assembly (BNA) and a bearing shell of the test rig; accelerometers embedded in outer ring of the ball bearing of a BNA in an array at 60° intervals at the coupling points (CP) 1-6 107

Figure 4.29: Measurement points: 25 remote points (RP) on bearing shell 108

Figure 4.30: Signal-to-noise-ratio (SNR); top: SNR at all 25 remote points (RP); bottom: SNR at RP 20, Grid 10 dB 109

Figure 4.31: Mobility between validation point and degrees of freedom at internal interface 110

Figure 4.32: Coherence functions between validation point and degrees of freedom at internal interface 111

Figure 4.33: Condition number of mobility matrix 112

Figure 4.34: Spectra of in-situ blocked forces of a ball nut assembly (BNA) at coupling points (CP); axial direction; grid ordinate: 10 dB 113

Figure 4.35: Spectra of in-situ blocked forces of a ball nut assembly (BNA) at coupling points (CP); radial direction; grid ordinate: 10 dB 113

Figure 4.36: Spectra of in-situ blocked forces of a ball nut assembly (BNA) at coupling points (CP); tangential direction; grid ordinate: 10 dB 114

Figure 4.37: On-board validation of the in-situ blocked forces of a ball nut assembly (BNA); grid ordinate: 10 dB 115

Figure 4.38: Test rig for the determination of in-situ blocked forces of a toothed belt 117

Figure 4.39: Schematic depiction of revolving interface of a toothed belt which meshes with a toothed disc (right interface) and the pinion of an electric motor (left interface) 118

Figure 4.40: Measurement points: 13 remote points (RP) and validation point (RP07) on right plate 119

Figure 4.41: Signal-to-noise-ratio (SNR); top: SNR at all 13 remote points (RP); bottom: SNR at RP07 on the right fixation in y-direction; Grid: 10 dB 120

Figure 4.42: Mobility functions between validation point and degrees of freedom at internal interface on toothed belt 121

Figure 4.43: Coherence functions between validation point and degrees of freedom at internal interface 122

Figure 4.44: Condition number of mobility matrix 123

Figure 4.45: On-board validation of the in-situ blocked forces of a toothed belt (TB) determined at the incoming meshing teeth (case 1); grid ordinate: 5 dB 125

Figure 4.46: On-board validation of the in-situ blocked forces of a TB determined at the centre of the driving discs (case 2), grid ordinate: 5 dB 126

Figure 4.47: Spectrogram of in-situ blocked forces of a toothed belt (TB) at the incoming meshing teeth according to coordinate direction; x-direction; grid ordinate: 5 dB 127

Figure 4.48: Spectrogram of in-situ blocked forces of a toothed belt (TB) at the incoming meshing teeth according to coordinate direction; y-direction; grid ordinate: 5 dB 127

Figure 4.49: Spectrogram of in-situ blocked forces of a toothed belt (TB) at the incoming meshing teeth according to coordinate direction; z-direction; grid ordinate: 5 dB 128

Figure 4.50: Spectra of the in-situ blocked forces of a toothed belt at the incoming teeth according to interface position; forces at pinion side; grid ordinate: 10 dB 129

Figure 4.51: Spectra of the in-situ blocked forces of a toothed belt at the incoming teeth according to interface position; lower diagram: forces at toothed disc side; grid ordinate: 10 dB 129

Figure 5.1: Advanced internal-source-path-receiver model 136

List of Figures

Figure 5.2: Methodology to determine blocked force transmissibility functions 141

Figure 5.3: Approach to validate the determined internal in-situ blocked forces $\mathbf{f}_{bl,i}$ of an overall source (A) 144

Figure 5.4: Test setup for the determination of the in-situ blocked forces at the external and internal interface and the corresponding BFT functions between interface (i) and (c) 147

Figure 5.5: In-situ blocked forces (left) and moments (right) at interface (i) and (c) 149

Figure 5.6: Comparison of transmissibility between external interface (c) and internal interface (i); upper diagram: blocked force transmissibility functions; lower diagram: blocked moment transmissibility functions 150

Figure 5.7: Predicted strength of source (A) at external interface (c) based on transmissibility and source strength of internal source (IA) at internal interface (i); upper diagram: in-situ blocked force; lower diagram: in-situ blocked moment 151

Figure 5.8: Principle of a bfTPA within an EPSapa system based on the external and internal in-situ blocked forces and the corresponding blocked force transmissibility functions 153

Figure 5.9: Adaptive test rig used for the determination of in-situ blocked forces of an EPSapa system 155

Figure 5.10: Validation of the external and internal in-situ blocked forces of an artificially excited EPSapa system mounted on a test rig; grid ordinate: 10 dB 157

Figure 5.11: MEMS accelerometers placed at pinion of electric motor 158

Figure 5.12: Contribution of in-situ blocked forces of electric motor and pinion to structure-borne sound of an artificially excited EPSapa system, grid ordinate: 10 dB 160

Figure 5.13: bfTPA of an EPSapa system with realistic boundary conditions 162

Figure 5.14: MEMS accelerometers placed at toothed belt (TB)..... 165

Figure 5.15: Grooves for MEMS accelerometers embedded at ball nut assembly (BNA) 166

Figure 5.16: MEMS accelerometers embedded at electric motor (EM)..... 166

Table 5.1: Main orders of the internal sources of an EPSapa system..... 167

Figure 5.17: Validation predicted blocked forces of an EPSapa system; grid ordinate: 10 dB 168

Figure 5.18: Contribution of the internal sources (components) of an EPSapa system to the structure-borne sound generated by the whole EPSapa system; grid ordinate: 10 dB 169

Figure 5.19: Mean values of coherence functions for coherence criterion 172

Figure 5.20: Approach of virtual component assembly..... 176

Figure 5.21: Change of the position of a toothed rack within the housing of an electric power steering system 179

Figure 5.22: Frequency response assurance criterion (FRAC) comparing 600° (end lock) and 0° (middle position) steering angle; row 1-4 frequency response function (FRFs) between the external interface DoFs of an EPSapa system and the defined test position on the test rig; row 5-7 FRFs between the internal interface DoFs of the ball nut assembly (BNA) and the defined test position on the test rig..... 181

Acknowledgements

Everybody who had the privilege to do a Ph.D. knows the struggle during writing the thesis. I am very glad that I had a solid background of family, friends and colleagues who always supported me during this period. If it would be possible I would like to mention all of them by name but that would exceed the limit of this acknowledgements.

First of all I have to thank Andy Moorhouse and Michael Sturm who were encouraging and inspiring supervisors during the whole time. I always felt welcome with any concern at any time. The time that I was able to spend in Salford was very valuable on a personal and professional level. Furthermore I would also like to thank Thomas Alber, Gerd Speidel and Andreas Lay for their advice and organisational support. Also I have to thank all my colleagues at Robert Bosch Automotive Steering GmbH and at the Acoustics Research Centre at the University of Salford for being critical, inspiring and challenging dialogue partners. The research project was funded by the industrial partner Robert Bosch Automotive Steering GmbH, this support is also gratefully acknowledged.

My parents who strongly supported me during the whole time of the project need to be mentioned in particular. Your never ending encouragement was a huge factor of success. Most of all my girlfriend Lena was a very important support during the whole Ph.D. She was always understanding and considerate. It would have been much harder without your support because you never stopped believing in me. I will always deeply appreciate that.

Declaration

Publications that are used within this thesis:

D. Zabel, M. Sturm, T. Alber, and A. Moorhouse, “Embedded MEMS accelerometers for the in-situ measurement of blocked forces in coupled structures,” in *DAGA 2017*, 2017, no. 1, pp. 7–10.

D. Zabel, T. Alber, M. Sturm, and A. Moorhouse, “Internal transfer path analysis based on in-situ blocked forces and transmissibility functions,” in *Proceedings of 24 International Congress on Sound and Vibration (ICSV 24)*, 2017.

Nomenclature

List of operators and conventions

a_0	Reference value acceleration ($10^{-6}\, m/s^2$)
(b)	Artificial excitation at interface b
f_0	Reference value force ($10^{-6}\, N$)
$\bar{f}_{bl}$	Predicted blocked force
j	Complex variable ($\sqrt{-1}$)
v_0	Reference value velocity ($5 \cdot 10^{-8}\, m/s$)
$v_c^{(b)}$	Artificial excitation at b and response at c
x	Scalar
$\mathbf{x}$	Vector
$\sum \mathbf{x}$	Sum of vectors
$\mathbf{X}$	Matrix
$[\mathbf{X}]^T$	Transpose of matrix
$[\mathbf{X}]^+$	Moore-Penrose pseudoinverse of rectangular matrix
$[\mathbf{X}]^{-1}$	Inverse of square matrix
$\tilde{y}$	Predicted kinematic quantity
$\hat{Y}$	Defective frequency response function

List of symbols

a	Acceleration
D	Damping
f	Force
H	Frequency response function (general)
i	Gear ratio
I	Interface area
K	Stiffness
M	Torque
m	Mass
n	Rotational speed
N	Number of discretisation points
O	Order
p	Pressure
T	Transmissibility
v	Velocity
$\mathbf{V}$	Velocity matrix
x	Position
y	Kinematic quantity
Y	Mobility

α	Angular velocity

$\mathbf{\Lambda}$	Angular velocity matrix
ξ	Influence
σ	Tension
τ	Moment
Ψ	Rotational quantities
ω	Frequency
Ω	Filter for calibration

List of indices

α	Angular velocity based
A	Source
a	Surface of source
AC	Assembly conditions
b	Surface of receiver
B	Receiver
bl	Blocked boundary conditions
BNA	Ball nut assembly
c	Contact zone at external interface
C	Coupled system
calc	Calculated
cont	Continuous
EM	Electric motor

EPS	Electric power steering system
fs	Free boundary condition of source
H	Housing
i	Contact zone at internal interface
k, m, n, o	Counting integer
left	Left end lock
mean	Mean values
meas	Measured
op	Operational
pre	Predicted
right	Right end lock
T	Transmissibility related
TB	Toothed belt
tot	Total amount
TR	Toothed rack
v	Velocity based
val	Validation
Y	Mobility based

List of abbreviations

aISPRM	Advanced internal-source-path-receiver-model
BB	Ball bearing

BFT	Blocked force transmissibility
bfTPA	Blocked force transmissibility transfer path analysis
BNA	Ball nut assembly
CP	Coupling point at interface
DoF	Degree of freedom
ECU	Electronic control unit
EM	Electric motor
EPS	Electric power steering
EPSapa	Electric power steering system with axle parallel servo motor
EPSc	Electric power steering system with column mounted servo
EPSdp	Electric power steering system with a second worm gear
FL	Front left
FR	Front right
FRAC	Frequency response assurance criterion
FRF	Frequency response function
H	Housing
IA	Internal source
IB	Internal receiver
ICE	Internal combustion engine
IEPE	Integrated electronic piezoelectric
IH	Impact hammer
ISPRM	Internal-source-path-receiver-model
iTPA	In-situ transfer path analysis

LTI	Linear and time invariant
MDof	Multiple degree of freedom
MEMS	Micro electro mechanical system
NVH	Noise, vibration and harshness
OBV	On-board validation
P	Pinion of electric motor
RBAS	Robert Bosch Automotive Steering GmbH
RL	Rear left
rpm	Revolution per minute
RR	Rear right
SC	Steering column
SNR	Signal-to-noise-ratio
SP	Steering pinion
SPL	Sound pressure level
SPRM	Source-Path-receiver-model
TB	Toothed belt
TD	Toothed disc
TPA	Transfer path analysis
TR	Toothed rack
Trod	Tie rod
VAP	Virtual acoustic prototyping
VCA	Virtual component assembly
VRR	Virtual road release

Abstract

Transfer path analysis (TPA) is an established and valuable tool in the automotive industry, to determine the contributions of structure-borne sound sources to receiver responses at target positions. The classical TPA approach is based on contact forces at the interface between source and receiver to characterise the dynamic loads induced by the source and frequency response functions (FRFs) to quantify the transfer paths of the sound from the interface locations to the target positions. With knowledge of the determined contributions it is then possible to decide whether source loads or FRFs must be improved to optimise the target quantities.

Recently a timesaving improvement to classical TPA has been proposed, where the loads are characterised using the in-situ blocked force method, so that dismantling of source and receiver is not necessary. This method is therefore called in-situ TPA. However, if the contributions of internal structure-borne sound sources to the overall vibro-acoustic behaviour of a product are desired it is of benefit if the target quantities are blocked forces. Thus it would be possible to virtually couple the product with the properties of an overall receiver. Therefore this thesis presents a TPA approach called “blocked force transmissibility transfer path analysis” (bfTPA). In this context, the proposed internal-source-path-receiver-model (ISPRM) poses the theoretical basis of bfTPA. The aim of the presented novel TPA is to determine the contribution of internal structure-borne sound sources to an overall target quantity of a product. The presented approach uses the vector of in-situ blocked forces measured externally at the contact interface of the overall product and a corresponding set of “blocked force transmissibility” (BFT) functions relating the external coupling degrees of freedom (DOFs) to the internal source DOFs in order

to propagate the external in-situ blocked forces back to multiple internal in-situ blocked forces. To prove the methodology of the presented approach three case studies, which increase in complexity, were carried out experimentally. The case studies concern a beam and an electric power steering system with paraxial servo unit (EPSapa), respectively.

EPSapa systems consist of multiple embedded vibrational components which are defined as “internal sources”. The electric motor, the ball nut assembly and the toothed belt are identified as the main internal sources of an EPSapa system. Hence they are characterised by means of experimentally determined blocked forces. For the determination, micro electro mechanical systems (MEMS) accelerometers are embedded at the so called “internal interfaces”. This poses a novel application of the in-situ method in combination with the dealing of continuous and revolving internal interfaces.

Concluding a further application of the bfTPA methodology is presented. It allows the external in-situ blocked forces of EPS systems or other products to be predicted based on internal in-situ blocked forces and the BFT functions within internal receivers such as housings, for instance. Hence, the proposed approach is called “virtual component assembly”. It offers the advantage to synthesize a virtual EPS system based on the in-situ blocked forces of its components which are determined on test benches.

Chapter 1

Introduction

1.1 **Background**

The noise, vibration and harshness (NVH) quality is amongst others a substantial sales argument for today's vehicles [1]. In order to be more precise, a pleasant sound in the vehicle interior is of importance for potential customers. At low driving speeds the sound in the interior of vehicles which are driven by internal combustion engines (ICE) is mainly dominated by the ICE. This leads to a beneficial masking effect of sound which is generated by vehicle components such as pumps, gears or electric power steering (EPS) systems, for instance [2]. However, the trend in today's automotive industry is for many reasons strongly towards vehicles with electric engines or at least hybrid drives [3]. Consequently in the near future the benefit of the masking effect by the ICE will likely not be present anymore since the sound emission of electric engines into the vehicle interior is usually lower compared to sound emitted by the ICE. As a consequence, the effort to develop vehicle components of high NVH quality will become even more significant for manufacturers of such components [4].

In order to guarantee an intended high NVH performance, experimental transfer path analysis (TPA) is a broadly used tool in the automotive industry to efficiently troubleshoot potential issues of vehicles and its components [5]. Out of the various TPA methods especially classical TPA is well established. The aim of TPA is to investigate the contribution of sound sources such as vehicle components to the sound characteristic at receiver locations, with a vehicle interior being an example. Therefore a kinematic target quantity on the receiver side such as sound pressure is propagated back to dynamic loads characterising the source strength at the interface between source and receiver. However, the drawback of classical TPA is the dependence on the receiver's structural behaviour since the dynamic loads which are generated by the source are characterised by contact forces [6]–[8]. As distinct from classical TPA in-situ TPA (iTPA) which

was recently proposed characterises the dynamic loads with in-situ blocked forces rather than contact forces [9],[10]. Hence the dynamic loads induced by the source into the receiver are characterised independently from the receiver. This fact yields significant advantages for the early development processes of vehicle components and any other product or machinery regarding the NVH performance [11], [12].

The limitation of both of the above mentioned TPA approaches is the fact that the source is treated as a black box without further interest of the embedded generation mechanisms of structure-borne sound within the source. However, it might be assumed that engineers want to gain insight into the source e.g. an EPS system for further improvement regarding a high NVH performance. Therefore the generation as well as the transmission of the structure-borne sound within the source need to be characterised and analysed. In the following of this thesis the embedded generation mechanisms of structure-borne sound within a source such as bearings or gears will be referred to as internal sources for simplicity reasons (compare section 1.3). Although both classical TPA as well as iTPA can be experimentally employed to fulfil the aforementioned task they only provide information about the contribution of the internal sources to a kinematic target quantity at the connection points between source and receiver. Unfortunately though, a kinematic target quantity cannot be used as input for further analysis on the receiver level if different receivers such as divergent vehicles should be considered. Hence it is obvious to define the target quantity of a TPA approach within a source as a dynamic force rather than a kinematic quantity. However, this implies that the transmission paths within the source need to be characterised by transmissibility functions [13]–[23] rather than frequency response functions (FRFs).

Robert Bosch Automotive Steering GmbH (RBAS) is a manufacturer of different vehicle components such as steering columns or EPS systems, for instance. For the sake of fulfilling the quality requirements of different vehicle manufacturers RBAS has a strong interest to provide EPS systems of high NVH performance. For that reason excessive research effort is carried out to ensure the intended quality. The research that is presented in this thesis is part of this effort. With the aim to improve the NVH comfort of EPS systems and other technical products a novel TPA method is developed. The developed method aims to analyse the contribution of the dynamic forces characterising the internal sources to the dynamic forces acting at the interface between a source such as an EPS system and a receiver such as a vehicle, for instance. The use of the methodology results in a significant benefit for engineering and development processes of vehicle components or any other product or machinery where NVH comfort plays a key role. With the help of the developed methodology the NVH performance of a product can be predicted based on the known characteristics of the internal sources and the transmission of sound within the product.

Before the aims and objectives of the thesis are introduced in section 1.5 at first the general approach of TPA will be outlined in section 1.2 since it forms the basis for the presented research. In section 1.4 the internal-source-path-receiver model (ISPRM) which is crucial for the development of the novel TPA approach is introduced. Before the introduction of ISPRM section 1.3 outlines an explanation of embedded structure-borne sound sources which are an important part of ISPRM since they build a black box model for the generation mechanisms of structure-borne sound within a source.

1.2 **The general approach of transfer path analysis**

As already briefly mentioned in section 1.1 the general aim of TPA is to determine the contribution of sound which is generated by a source such as an EPS system to a target quantity at a receiver location such as the interior of a vehicle. In order to fulfil the aim of TPA the transfer path problem (see Figure 1.1) which will be introduced in the following paragraph needs to be analysed. For this purpose different TPA approaches are available which are distinguished on the one hand on the characterisation of the generated sound and on the other hand on the description of the sound transfer to target locations on the receiver side.

If a vibrational source (A) such as an EPS system is coupled to a receiver (B) structure-borne sound is induced from the source to the receiver at interface (c) between source and receiver. Subsequently the induced sound is transmitted via transfer paths to target locations on receiver side (b). This physical relationship which is schematically illustrated by Figure 1.1 is generally known as transfer path problem of an assembly (C).

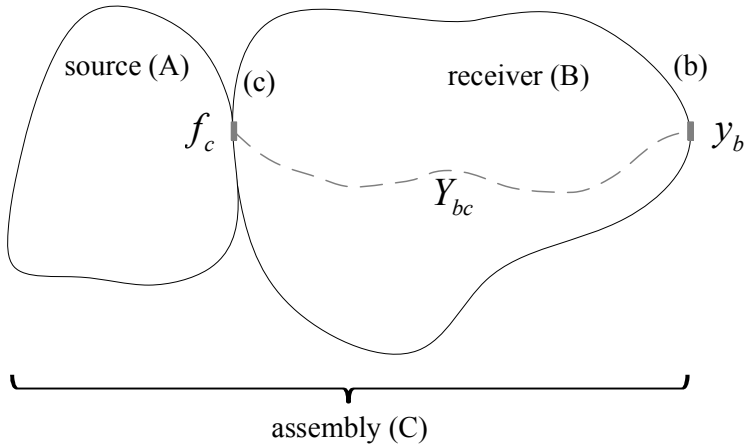

Figure 1.1: Transfer path problem of sound generated by a vibrational source (A) and subsequently induced at interface (c) to receiver (B)

At the extreme the sound which is generated by source (A) can cause an unpleasant sound characteristic at specific target locations (b) on receiver (B) e.g. the interior of a vehicle. For troubleshooting of this problem TPA methods are applied with the general aim to propagate a vector of kinematic target quantities $\mathbf{y}_b$ on receiver (B) back to a vector of dynamic loads $\mathbf{f}_c$ at degrees of freedom (DoFs) at interface (c) based on the following equation

$$\mathbf{y}_b = \mathbf{Y}_{bc}\mathbf{f}_c \tag{1.1}$$

For this purpose the transfer paths from DoFs at interface (c) to DoFs at target locations (b) on receiver (B) are characterised by FRFs which are contained in the FRF matrix $\mathbf{Y}_{bc}$ (see Figure 1.1). With knowledge of both the characteristics of the dynamic loads $\mathbf{f}_c$ and the transfer path behaviour $\mathbf{Y}_{bc}$ it is then possible to determine the contribution of the dynamic loads $\mathbf{f}_c$ to the measured target quantities $\mathbf{y}_b$ according to Eq. (1.1). Hence it is possible to modify either the source characterised by the dynamic loads $\mathbf{f}_c$ or the transfer paths $\mathbf{Y}_{bc}$ of the induced sound to improve the NVH performance of source (A) or receiver (B), respectively.

The presented thesis aims to develop a novel TPA methodology that can be applied for a source (A) such as an EPS system which consists of multiple internal sources such as electric motors and toothed belts. Furthermore the developed methodology which is introduced in chapter 5 focuses on the possibility to yield an independent description of the source as well as the internal sources. Therefore the transfer problem and the general methodology of TPA which are briefly outlined in this section play an important role within this thesis.

1.3 **Embedded internal sources**

In section 1.4 the internal-source-path-receiver-model (ISPRM) will be introduced which aims to gain insight into the black box that is used to characterise the strength of a source in terms of in-situ blocked forces. One important part of ISPRM is the description of the generation mechanisms of structure-borne sound within a source. Since these mechanisms are usually embedded within the source they are often not accessible with surface mounted measurement devices such as integrated electronic piezoelectric (IEPE) accelerometers. An example of such an internal sound generation mechanism is the tooth meshing of gears within any kind of housing. In the following of the thesis these sound generation mechanisms within a source will be referred to as internal sources (compare section 1.1).

For a potential improvement of a source[1] such as an EPS system it is necessary to understand and characterise the embedded internal sources. If this should be achieved through measurements no or only minor modifications of the source are favourable. In this manner a realistic vibrational behaviour of the internal sources and as a consequence also of the whole source is ensured. This precondition can be accomplished by using micro-electro-mechanical-systems (MEMS) accelerometers since they are available of small size of only a few millimetres. A detailed review of MEMS accelerometers is presented in section 2.2. Commercially available examples of such accelerometers can be found in [24] and [25], for instance.

The term “embedded” which in this thesis will often be omitted for simplicity should emphasize the fact that internal sources are usually surrounded by any sort of housing which is seen as part

[1] Within this thesis the term “product” will often be used equally to the term “structure-borne sound source” whereas the term “component” will be used synonymous to the term “internal source”.

of the source. Therefore the structure-borne sound emitted by the internal sources is transmitted via transfer paths within the housing to locations where the housing is connected to a receiver. These connections between the source and the receiver will be called “external interfaces”. However, in order to characterise the strength of the internal sources the interface between the internal source and the housing is of interest. If on the one hand the internal sources are treated as black boxes and on the other hand it is technically feasible to slightly modify the housing by adding grooves then it is consequently possible to have access to the relevant internal interfaces and therefore characterise the internal sources in-situ [26]–[29].

1.4 **Internal-source-path-receiver-model**

Before the aims and objectives of the thesis are presented in section 1.5 it is crucial to introduce at first a modelling approach which will be called “internal-source-path-receiver-model” (ISPRM). ISPRM is the proposal to extend the source-path-receiver-model (SPRM) firstly provided by Bolt and Ingard [30] in 1956 which aims to describe the sound transfer from a source via transmission paths to a receiver. The model is therefore the basis for many problem-solving approaches regarding NVH. However, a complex machinery or product usually does not consist of only one isolated embedded internal source. Therefore the hereafter presented extension of the well-known and established SPRM is a necessary step to deal with multiple internal sources and internal transmission paths. Hence ISPRM forms the basis for the novel TPA approach which will be presented in chapter 5 of this thesis.

In order to extend SPRM the black box which is used for a simplified characterisation of the source strength will be subdivided in n multiple internal sources and one internal receiver structure. The extension of SPRM and the subdivision of the source is schematically depicted

in Figure 1.2. Furthermore ISPRM takes into account that the source strength of a product is dependent on the partial contribution of the n internal source strengths in combination with their respective m internal transmission paths. Within this thesis the internal source strengths and the strength of the whole source are characterised with in-situ blocked forces. Since the transmission paths which are the relation between the internal source strength and the strength of the whole source are characterised with transmissibility functions the proposed novel TPA methodology will be called blocked force transmissibility transfer path analysis (bfTPA).

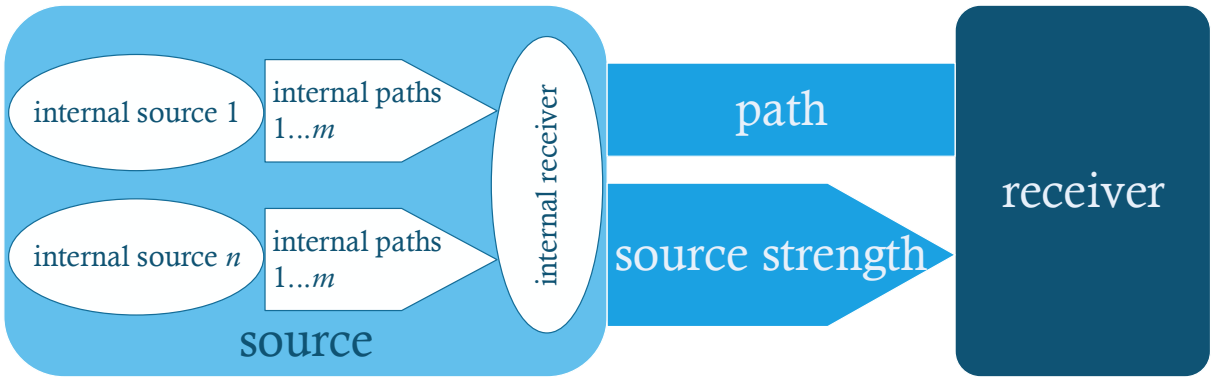

Figure 1.2: Internal-source-path-receiver-model (ISPRM)

In terms of an EPS system, the black box for the source would be the steering system itself while the internal sources would be all the components that are crucial for the functional principle and therefore generate vibration during the execution of a steering manoeuvre. These components respectively internal sources as well as the internal receiver and internal transmission paths will be introduced in chapter 3 for the case of one particular EPS system that is used within this thesis. A detailed discussion of the determined internal source strengths of an EPS in terms of in-situ blocked forces can be found in chapter 4. The TPA methodology to analyse

the partial contribution of multiple internal sources based on the here proposed ISPRM is introduced in chapter 5. Furthermore the aforementioned chapter contains a more in-depth discussion of ISPRM leading to the so called “advanced internal-source-path-receiver model”.

At this point it is briefly mentioned that ISPRM poses two possibilities. On the one hand it forms like already mentioned the basis for the proposed novel TPA method that will be introduced in chapter 5 and on the other hand the basis for the extension of the virtual acoustic prototyping (VAP) approach of an EPS system proposed by Bauer [31]. The methodology of the extended approach will be called virtual component assembly (VCA) and poses significant benefits for the development process regarding NVH quality.

1.5 **Thesis objectives**

The aim of the thesis concerns the proposal and the validation of a novel TPA methodology called bfTPA that can be carried out within a vibrational source such as an EPS system, for instance. In order to achieve the aim, two fundamental preliminary aims, which are outlined in the following, need to be fulfilled at first. Initially a general substructuring approach of a source such as an EPS system which consists of multiple internal sources and transmission paths needs to be developed and defined. This is a necessary step to identify meaningful interfaces for the characterisation of internal sources with in-situ blocked forces. The second preliminary aim involves the development of a relationship between in-situ blocked forces characterising the internal sources with the in-situ blocked forces of the whole source. This relationship poses the basis for bfTPA. In order to achieve the main aim of the thesis as well as the two preliminary aims several objectives need to be fulfilled. A list of all necessary objectives will be outlined in the following:

1. For the sake of fulfilling a worthwhile substructuring approach of an EPS system three questions have to be answered. The answering of the following three questions pose a fundamental objective of the presented thesis:
    - What are the prominent internal sources while a product is active and what are the internal receivers?
    - What are the main transmission paths for structure-borne sound within a product like an EPSapa system?
    - What are the interfaces between the defined internal sources and internal receivers within a product like an EPSapa system and how can they be described and discretised if the interfaces are continuous?
2. For the determination of the partial contribution of the internal sources to the overall source strength of an EPSapa system a bfTPA is conducted. The following three steps have to be achieved:
    - Conducting the bfTPA approach in a basic experiment using a steel beam to prove the general feasibility of the approach and therefore validate the methodology.
    - Characterisation of the prominent internal sources of an EPSapa system, namely the electric motor, the ball nut assembly and the toothed belt (compare section 3.3) in terms of in-situ blocked forces.
    - Experimental determination of the transmissibility functions within the internal receiver structure of an EPSapa system (compare subsection 3.3.4) between all DoFs at the relevant interfaces.

3. The kinematic of the whole EPSapa system changes during a steering manoeuvre because of its design (compare subsection 3.2.2). Therefore the changes in the transmissibility functions need to be investigated using the frequency assurance criterion (FRAC).
4. Verification of the feasibility of a measurement approach that offers the potential to determine highly accurate frequency response functions (FRFs) or transmissibility functions between multiple locations on the source and the receiver even for complex technical structures like EPS systems. For that reason a novel application using embedded MEMS accelerometers at locations not accessible with standard piezoelectric accelerometers is investigated and validated.

Chapter 2

Literature and theory

2.1 Introduction

This chapter reviews the most common and relevant literature to date which is related to the aims and objectives of the thesis. The purpose of this chapter is therefore to identify and outline gaps in the reviewed literature which this thesis tries to fill in. Therefore the chapter provides an overview of the research to date that has been carried out in the fields of

- MEMS accelerometers in structural dynamics in section 2.2,
- characterisation methods of structure-borne sound sources in section 2.3 and
- contribution of structure-borne sound sources in section 2.4.

Special attention will be focussed on the theory of blocked forces [11], [32], [33] especially the in-situ method by Moorhouse and Elliott [26], [27], [29], [34], the free velocity method [35], the in-situ transfer path analysis approach by Elliott and Moorhouse [9] and the blocked force transfer path analysis [36].

2.2 Micro-electro-mechanical-systems accelerometers in structural dynamics

Micro-electro-mechanical-systems (MEMS) accelerometers are based on a seismic mass system. This is further explained in [37], for instance. In the field of measurement devices MEMS accelerometers are used for condition monitoring and applications where a precise frequency detection is not necessarily important. An example is the use of MEMS accelerometers in modern communication technology such as mobile phones, for example. Because of their low price researchers also tried to investigate the use of MEMS devices for vibrational measurement tasks

in structural dynamics with the aim to determine the exact nature of the vibrations to be observed. This will be reviewed in the following of this section.

2.2.1 Performance evaluation

Accelerometers for the use in the field of structural dynamics are available in many different versions according to underlying measurement principle, frequency range, and sensitivity, for instance. In the following the use of MEMS accelerometers in structural dynamics will be reviewed.

Albarbar evaluated in [38] the performance of MEMS accelerometers by comparing them with standardized IEPE accelerometers commonly used in structural dynamics. The potential use for structural dynamics was shown but it was also proven that MEMS accelerometers need to be calibrated in a certain way. Additionally he showed that MEMS accelerometers can be successfully used for condition monitoring [39]. The potential of the integration of low-cost MEMS accelerometers in machinery was shown by Vollmer and Neumann [40].

A calibration methodology for the response signals provided by MEMS accelerometers was proposed by Badri et al. in [41]. Furthermore they proposed an adaptive filter to improve the performance of MEMS accelerometers for the use in structural dynamics and condition monitoring in [42].

Fisher investigated the use of MEMS accelerometers for inclination sensing in [43] and showed that MEMS accelerometers are susceptible for inclination and offset errors if used in the wrong way.

Recently research has been carried out by RBAS to investigate the use of MEMS accelerometers in the automotive industry. It was shown by Wienen [44] and Fauser [45] that MEMS accelerometers can be used for inverse force identification and the determination of in-situ blocked forces. In [44] Marschall investigated different possibilities for the embedding of MEMS accelerometers and calibration methods to improve the reliability of the investigated MEMS accelerometers. Schulz showed the potential of different MEMS accelerometers for the characterisation of steering systems [47].

The suitability of MEMS accelerometers for the measurement of vibration was shown by Béliveau et al. [8] and Albarbar et al. [9], [10]. Both showed that it is possible to measure vibrations in an exact manner if some boundary conditions are concerned.

2.2.2 Calibration methods and signal processing

Since MEMS accelerometers are usually not designed for complex vibrational measurement tasks it is necessary to at first calibrate the accelerometers in a distinct way. To fulfil this tasks in the literature it is proposed to apply digital filters on the measured time signals of acceleration to artificially force the signals provided by the MEMS accelerometer to be as precise as the ones measured with an IEPE accelerometer. These filters are usually applied after the measurement with MEMS accelerometers has been undertaken.

Albarbar proposed a test setup to compare MEMS accelerometers against a reference accelerometer. The test setup consists of a cantilever beam that is equipped with a MEMS accelerometer on top and an integrated electronics piezoelectric (IEPE) accelerometer on bottom which is used as reference (see Figure 2.1). Excitation $f_{excitation}$ is applied at one end of the beam

and the responses v_{ref} and v_{MEMS} at the other end are measured to determine a FRF (acceleration). The FRFs Y_{ref} and Y_{MEMS} are then compared against each other.

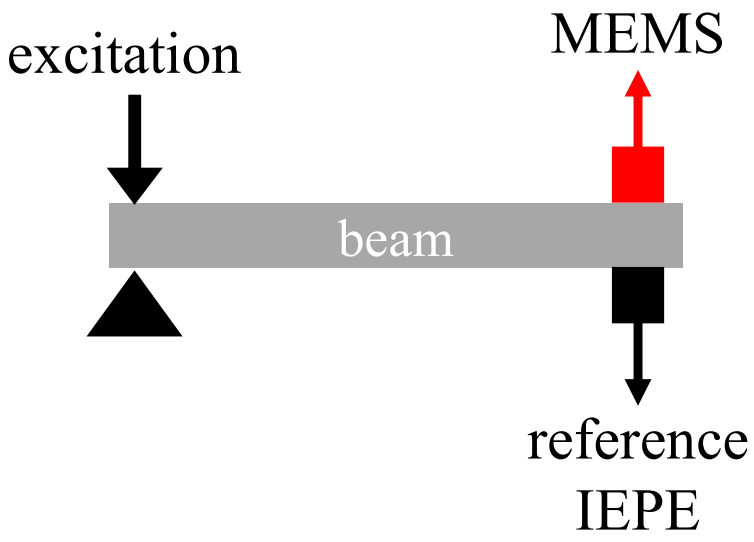

Figure 2.1: Test setup for the calibration of MEMS accelerometers

Badri proposed a calibration approach where the ratio between MEMS and reference accelerometer is used as calibration factor [11]. The calibration filter Ω is calculated as follows

$$\Omega(\omega) = \frac{Y_{ref}(\omega)}{Y_{MEMS}(\omega)} = \frac{\frac{v_{ref}(\omega)}{f_{exciation}(\omega)}}{\frac{v_{MEMS}(\omega)}{f_{excitation}(\omega)}} = \frac{v_{ref}(\omega)}{v_{MEMS}(\omega)} \tag{2.1}$$

If the measurement signal of the MEMS accelerometer is multiplied with the filter Ω it can be corrected.

2.3 Characterisation of structure-borne sound sources

A sensible optimisation progress of a product or machinery regarding NVH specifications should start with determining the characteristics of the source phenomena. Therefore a source can be characterised by determining its source strength. However, since a structure-borne sound source is usually coupled to a receiver an optimisation can also be achieved by reducing the sound transmission from the source to the receiver. Unfortunately it is not always possible to modify the transmission paths between a source and a receiver because it would affect the functional principle in a disadvantageous way. Therefore it would be of great benefit for engineers to be able to characterise the excitation of the receiver by the source in terms of a quantity that is independent from the receiver. Therefore, this section reviews receiver dependent and receiver independent source characterisation methods in the following.

2.3.1 Frequency response functions

A frequency response function (FRF) is used to describe the vibrational behaviour of linear, time invariant (LTI) systems. A FRF $\mathbf{H}_{bc}$ is expressed as the complex ratio of a kinematic response $\mathbf{y}_b$ to a kinetic excitation $\mathbf{f}_c$ according to the following equation

$$\mathbf{H}_{bc}(\omega) = \frac{\mathbf{y}_b(\omega)}{\mathbf{f}_c(\omega)} \tag{2.2}$$

The subscripts b and c denote the location of the response and the excitation, respectively. This is shown in Figure 2.2.

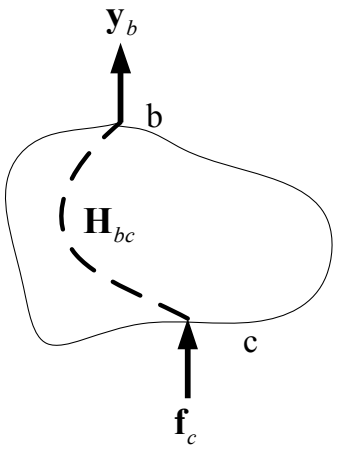

Figure 2.2: Linear, time invariant system with excitation $\mathbf{f}_c$ at interface (c) and response $\mathbf{y}_b$ at interface (b)

Therefore $\mathbf{H}_{bc}$ describes the structural behaviour of the system in the frequency domain according to an excitation at c. In the following of the report the radian frequency ω will be neglected for simplicity since all structure-borne sound phenomena has been analysed in the frequency domain within the scope of this thesis.

To improve the description of an LTI system the response to an excitation by a moment should be considered. Therefore moment excitation and moment mobilities was investigated by Elliot et al. [48], Jianxin and Mak [49] and Sanderson and Fredö [34]. Elliott et al. showed that the characterisation of a source can be significantly improved if moments at the interfaces between a source and a receiver are not omitted.

2.3.2 Contact force

The strength of a source can be described in terms of forces at the contact interface between a source and a receiver. These so called contact forces $\mathbf{f}_c$ are in contrast to the blocked forces not

an intrinsic quantity of the source (A) since they depend on the characteristics of the receiver (B) (Figure 2.3).

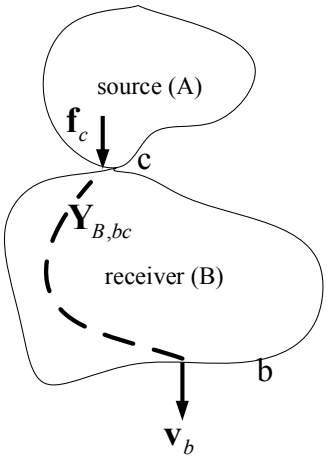

Figure 2.3: Schematic depiction of the inverse identification of forces $\mathbf{f}_c$ at the contact interface (c) between source (A) and receiver (B)

The contact forces $\mathbf{f}_c$ can be determined as follows

$$\mathbf{f}_c = \mathbf{Y}_{B,bc}^{+}\mathbf{v}_b \tag{2.3}$$

Therefore it is at first necessary to decouple source (A) and receiver (B) at interface (c) to determine the mobility $\mathbf{Y}_{B,bc}$. Afterwards the source (A) is coupled to receiver (B) to measure the velocities $\mathbf{v}_b$ on the receiver that are induced when source (A) is running. The reliability of the matrix inversion $\mathbf{Y}_{B,bc}^{+}$ of Eq. (2.3) can be improved by using regularisation techniques assuming the matrix can be inverted [51]–[57] and [58]. All results that are presented within the scope of the present thesis are achieved without applying any regularisation techniques. However it is possible to apply regularisation techniques as successfully shown in [53], [59], for instance.

2.3.3 Direct measurement of blocked force and free velocity

A meaningful and especially receiver independent characterisation of a source can be achieved in terms of two quantities. One is free velocity [35], [60] and the other quantity is blocked force [61]. Both approaches will be described in the following.

Free velocity

The free velocity vector $\mathbf{v}_{sf}$ is the velocity that can be determined if the boundary conditions of a source can be seen as free and therefore no vector of external forces $\mathbf{f}_s$ is present. In order to ensure that there are no external forces present the source needs to be freely suspended. This is symbolised by the blue dotted line in Figure 2.4.

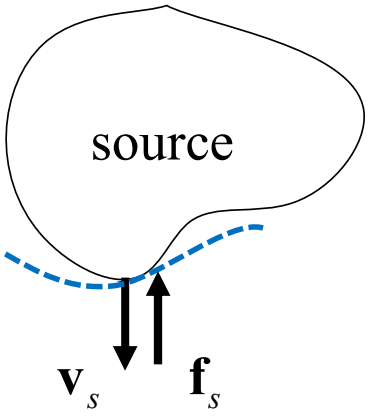

Figure 2.4: Source with free boundary conditions at the interface where the source is coupled to a receiver when operated in the actual assembly

In a freely suspended case the velocity $\mathbf{v}_s$ at the free boundary of the source is equal to the so called free velocity $\mathbf{v}_{sf}$

$$\mathbf{v}_{sf} = \mathbf{v}_s \Big|_{\mathbf{f}_s=0} \tag{2.4}$$

Since the source is freely suspended the free velocity is a quantity that characterises the source intrinsically and independent from a receiver.

Blocked force

Beside the free velocity the so called blocked force [62], [61], [63], [64] is a further quantity to characterise the strength of a source independently from an attached receiver structure. It can be measured using a receiver that ensures blocked conditions at the interface between source and receiver. Therefore the receiver should in theory be infinitively stiff and has an infinite mass. The blocked conditions at the interface are symbolised by the red dotted line shown in Figure 2.5.

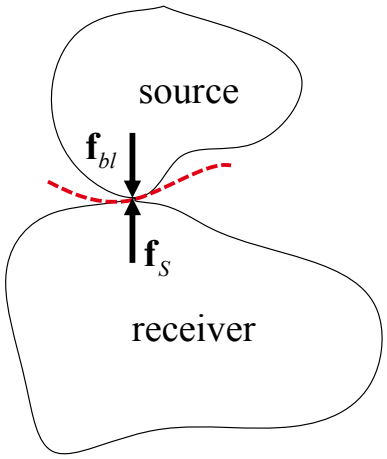

Figure 2.5: Source coupled to a receiver with blocked conditions at the interface where the source is coupled to a receiver when operated in the actual assembly

The blocked force $\mathbf{f}_{bl}$ is the force that is necessary to constrain the source and therefore set the velocity of the source $\mathbf{v}_s$ at the interface to zero as follows

$$\mathbf{f}_{bl} = -\mathbf{f}_s \Big|_{\mathbf{v}_s=0} \tag{2.5}$$

The blocked force $\mathbf{f}_{bl}$ is related to the free velocity $\mathbf{v}_{sf}$ as follows

$$\mathbf{f}_{bl} = \frac{\mathbf{v}_{sf}}{\mathbf{Y}_s} \tag{2.6}$$

Since the mobility of the source $\mathbf{Y}_s$ and the free velocity $\mathbf{v}_{sf}$ are independent from the receiver the blocked force must be independent from the receiver as well and is therefore a useful quantity for an intrinsic characterisation of a structure-borne sound source.

2.3.4 In-situ blocked force

In theory the blocked forces which characterise a source can be measured directly by using a force transducer between the source and an infinite stiff receiver with an infinite mass. However, in many cases such as a steering system it is not possible to measure the blocked forces directly. Therefore Moorhouse and Elliott [27], [29] provided a possibility to determine the blocked forces in-situ without the necessity to use force transducers. Furthermore the in-situ method has no need to dismount the source and the receiver which is a timesaving benefit. The methodology of the in-situ approach which is depicted in Figure 2.6 will be elucidated in the following.

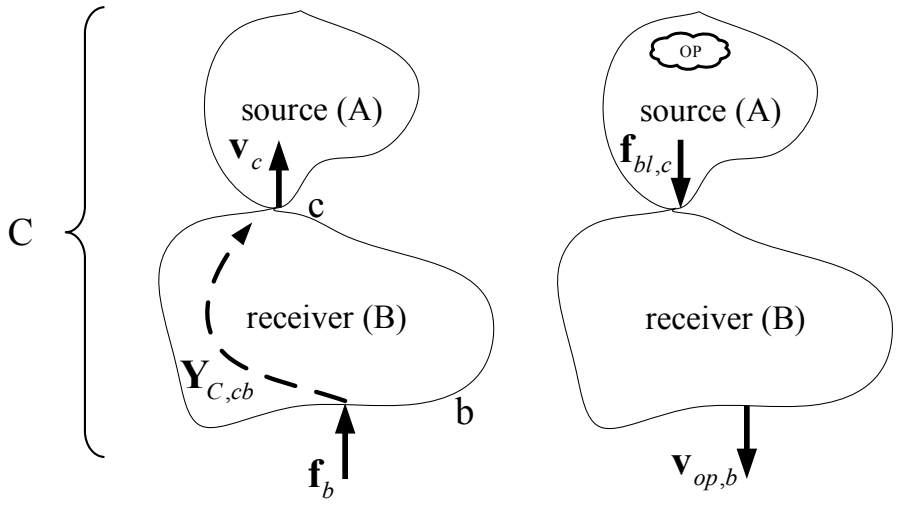

Figure 2.6: Schematic depiction of the methodology to determine in-situ blocked forces $\mathbf{f}_{bl,c}$ at interface (c) between source (A) and receiver (B)

To determine the in-situ blocked forces of a source a two-stage measurement has to be conducted. The first stage aims to determine the necessary passive characteristics of the coupled system in terms of an FRF. The FRF that is necessary to describe the passive system is the mobility $\mathbf{Y}_{C,cb}$. To obtain this quantity the coupled system is excited with a force $\mathbf{f}_b$ at random points (b) on the receiver structure. Simultaneously the velocity $\mathbf{v}_c$ at the interface (c) between the source and the receiver is measured. The complex ratio between the velocity and the force yields the necessary mobility which is represented by the following equation

$$\mathbf{Y}_{C,cb} = \frac{\mathbf{v}_c}{\mathbf{f}_b} \tag{2.7}$$

The second stage comprises the measurement of the operational properties of the coupled system in terms of velocities $\mathbf{v}_{op,b}$ at random positions on the receiver. With these two quantities the in-situ blocked forces $\mathbf{f}_{bl,c}$ at the interface (c) can be determined using the following equation

$$\mathbf{f}_{bl,c} = \left(\mathbf{Y}_{C,cb}^{T}\right)^{+} \mathbf{v}_{op,b} \tag{2.8}$$

The superscript $+$ indicates a Moore-Penrose pseudoinverse of the mobility matrix $\left(\mathbf{Y}_{C,cb}\right)^{T}$. Recent research in the fields of in-situ blocked forces of electric power steering systems was done by RBAS. In the following the research is briefly reviewed. Wang investigated the use of the in-situ blocked forces method for a steering system [65]. He showed that the in-situ blocked forces can be used to characterise a complex engineered system in a precise manner. A time domain approach for the use of in-situ blocked forces was provided by Sturm [66], [32] and Hudelmaier [67]. The use for in-situ blocked forces as part of the virtual acoustic prototype approach was shown by Sturm et al. [11].

Further research about in-situ blocked forces was conducted by Lennström et al. [33] for the source characterisation of a pump used in the automotive industry and by Picard for the case of a windscreen wiper of a vehicle [68]. Elliott and Moorhouse showed the potential of the in-situ method for the characterisation of a wind turbine [10], [69] and isolators [34]. De Klerk used the blocked forces for the characterisation of gear noise [70].

2.3.5 On-board force validation

After the determination of the in-situ blocked forces it is necessary to prove that the blocked forces are determined correctly to have confidence in the predicted forces. For that reason the determined in-situ blocked forces $\mathbf{f}_{bl}$ will be multiplied with a mobility matrix $\mathbf{Y}_{C,val}$, which contains the FRFs of the assembly C, to yield a predicted kinematic quantity such as velocity $\mathbf{v}_{C,val}$ on a position on the receiver as follows

$$\mathbf{v}_{C,val} = \mathbf{Y}_{C,val}\mathbf{f}_{bl} \tag{2.9}$$

If the source and receiver are not disassembled after the determining of the in-situ blocked forces the validation approach is the so called on-board validation (OBV) approach. The fact, that it is not necessary to remove the source, which would involve possible problems due to remounting, is the main advantage of the OBV approach. The approach is schematically shown in Figure 2.7.

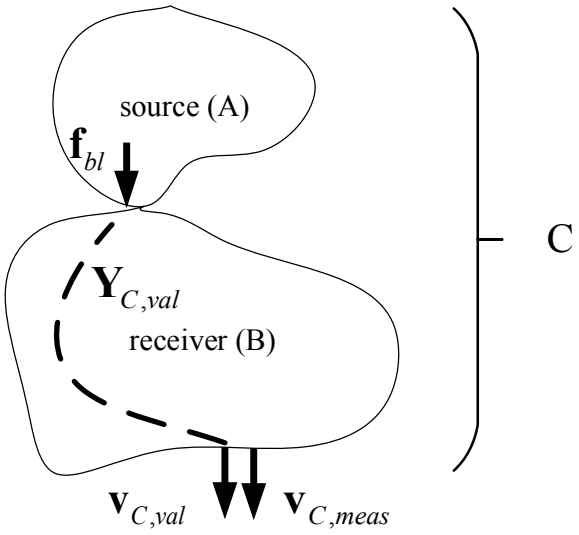

Figure 2.7: On-board approach for the validation of experimentally determined in-situ blocked forces $\mathbf{f}_{bl}$ at the interface between source and receiver

The predicted kinematic quantity according to the in-situ blocked forces can be compared towards a measured quantity $\mathbf{v}_{C,meas}$ on the same position on the receiver surface to ensure that the forces were determined in a precise manner.

2.4 Contribution of structure-borne sound sources

This section aims to review the engineering tool of transfer path analysis. This includes the classical TPA approach, the in-situ TPA (iTPA) approach and transmissibility based approaches. A recent review of TPA in general was provided by van der Seijs which can be found in [71] and [72]. Furthermore a review about experimental techniques to determine the contribution of commercial vehicles can be found in [5].

2.4.1 Classical transfer path analysis

The classical approach was first provided by Verheij [8], [73] in 1980. The approach is based on contact forces at the interface between a source and a receiver which can be determined directly with force transducers, via the mount stiffness method or via inverse methods [8]. The determined forces describe the strength of the source (A) while coupled to receiver (B) (see Figure 2.3). The necessary FRFs $\mathbf{H}_{bc}$ are determined while the source and the receiver are de-coupled. Based on the knowledge of the determined contact forces and the transmission in terms of FRF the contribution of the transfer paths to the response $\mathbf{y}_b$ on receiver (B) can be analysed for troubleshooting. Examples of classical TPA can be found in [74], [6] and [7] ,for instance.

2.4.2 In-situ transfer path analysis

An improvement of the family of classical TPA approaches was provided by Elliott and Moor-house [9]. The so called in-situ transfer path analysis (iTPA) has the advantage that source and receiver do not have to be dismounted to determine the forces since in-situ blocked forces are used as an input quantity rather than contact forces. This leads to a significant time saving while

conducting a TPA, compared to the classical approach. The idea of using in-situ blocked forces as the input quantity of a TPA will be used within this thesis for the methodology of a proposed novel bfTPA approach (section 5.3). Successful applications of iTPA can be found in [75], [11], [9] and [12], for instance.

2.4.3 Transmissibility based transfer path analysis

The general approach of transmissibility was introduced by Maia & Ribeiro in [15], [16] and [22]. They showed that rather than describing a structure in terms of FRFs transmissibilities, which is a relation between velocities, can be used. Further details will be outlined in subsection 5.3.2.

A recent application of the concept of transmissibility in TPA can be found in [17] by Gajdatsy et al. In general the transmissibility based TPA avoids determining forces at the interface between a source and a receiver and uses transmissibilities instead to describe the transmission of structure-borne sound.

Lage et al. investigated the relation between force and displacement transmissibility and showed that it is possible for an MDoF system to derive force transmissibility from displacement transmissibility and vice versa [19]. This relation is of use for the novel TPA approach that will be proposed in section 5.3.

2.4.4 Virtual acoustic prototyping

Moorhouse has shown that it is possible to generate a so called virtual acoustic prototype (VAP) which enables one to virtually listen to the generated sound of a source that not yet built [76]. This means that if a source could be characterised by blocked forces it is possible to predict the sound of the source when coupled to different receivers.

For EPS systems, in particular the EPSapa system (compare section 3.2), Bauer first showed that a VAP can be successfully build [31]. Subsequent studies by Sturm and Alber expanded the concept of VAP and carried out experimental case studies yielding very accurate VAPs [11], [12], [77]. Additionally Hesselmaier provided a VAP approach for EPS systems [78].

The trend in today's automotive industry is towards a so called virtual road release (VRR). This means that theoretically all the characteristics of a vehicle including the NVH performance can be simulated. As a consequence, potential problems can be detected at early development stages and therefore failure costs can be minimized.

2.5 Summary and concluding remarks

In the following of this section the literature and theoretical background, which is crucial for the understanding of this thesis, will be briefly summarised.

It was reviewed that in-situ blocked forces are to be preferred for the characterisation of a structure-borne sound source. In the following the reasons for the choice of in-situ blocked forces are explained. First, the characterisation method of in-situ blocked forces provides realistic boundary conditions compared to the approaches of direct measurement of free velocity and

blocked force. Secondly, in contrast to contact forces the characterisation is independent of an attached receiver structure. This yields a significant advantage towards VAP approaches. Furthermore in-situ blocked forces yield a useful input quantity for a transfer path analysis within a complex engineered product. A novelty of this thesis will be the characterisation of internal sources by determining their in-situ blocked forces. This will be shown in chapter 4.

Furthermore, the use of low-cost MEMS accelerometers was investigated by several researchers and by RBAS. The main research is focused on the general performance evaluation. The research in this thesis is focussed on the usage of MEMS for inverse force identification and especially for the in-situ blocked force method. This poses a novel application of the in-situ method.

The general approach of transmissibility and methodology of transmissibility based TPA is reviewed. The novelty of this work is using the already developed equations for a TPA approach. The equations will be applied to a beam to prove the general feasibility of the methodology and to an EPSapa system to prove the applicability to a complex product with multiple internal sources. The difference is based on the determination of transmissibility within the housing of an EPSapa system to relate internal and external in-situ blocked forces.

Chapter 3

Substructuring of electric power steering systems

3.1 **Introduction**

As already outlined in section 1.4 and 1.5 of the present thesis the substructuring of an overall vibrational structure-borne sound source, such as an electric power steering (EPS) system is initially crucial for a meaningful TPA approach within the overall source. Therefore, according to the already briefly introduced internal source-path-receiver model, the prominent internal sources, internal receivers and internal transmission paths within the overall source need to be defined. Moreover, the interfaces between the internal sources and the internal receivers, as well as the external interfaces between the overall source and an overall receiver, such as a vehicle need to be defined regarding their physical boundary conditions.

Within this thesis the first mentioned interfaces will be specified as “internal” interfaces since they are in most cases embedded within the overall source. Thus they cannot easily be accessed with measurement devices. An exception will be presented and discussed in this chapter. The second mentioned interfaces will be classified as “external” since they form the outer connection between the overall source, such as an EPS system, and the overall receiver such as a vehicle. In general, continuous interfaces and point connections between source and receiver are distinguished in the remainder of this thesis. This applies both for the internal and the external interfaces at which in-situ blocked forces are experimentally determined to conduct a bfTPA approach. Therefore a precise definition of all the necessary translational and rotational DoFs at the internal and external interfaces is an important step to successfully conduct a bfTPA approach.

For validation of the proposed novel bfTPA methodology (compare section 5.3), three experimental case studies are conducted within the scope of the present thesis. The aim of the first

case study is to generally validate the proposed methodology of bfTPA by using a freely suspended steel beam as an overall source. In subsection 5.4.2 the results of the case study are presented and discussed in detail. The two further case studies, which are presented in section 5.4, address the structure-borne sound transmission within an EPS system. More precisely, the chosen steering system is an EPSapa system where the electric motor (EM) is mounted in parallel with the front axle of a vehicle. In order to conduct a bfTPA within an EPSapa system, the whole system first needs to be sub-structured into its components and corresponding interfaces. Therefore a deep understanding of its functional principle is a necessary prerequisite. Only if the functional principle of the EPSapa system is fully understood, can all the necessary internal sources and internal receivers, the internal and the external interfaces and the transmission paths of structure-borne sound within an EPSapa system be identified and characterised.

Therefore, in section 3.2, the functional principle and some elementary boundary conditions of an EPSapa system are outlined and introduced. Section 3.3 continues the substructuring of the particular steering system with the definition of its primary and secondary internal sources as well as the internal receiver. Subsequently the transmission paths of structure-borne sound within an EPSapa system between the identified DoFs at the internal and external interfaces are introduced in section 3.4. In addition to the proposed substructuring approach of an EPSapa system this chapter elucidates in section 3.5 the possibility of employing the presented substructuring approach to any other product or machinery. The prerequisite is that the machinery consists of multiple internal sources, connected to an internal receiver according to the presented ISPRM.

At this point it has to be remarked that the proposed substructuring of an EPSapa system differs from general dynamic substructuring such as described in [79], [80] and [81]. This means that

solely the interfaces which separate the sources and receivers are defined including all necessary DoFs. However the term substructuring is used within the present thesis to elucidate the importance of defining internal sources, internal receivers, internal and external interfaces, transmission paths and the associated DoFs to be able to conduct a bfTPA approach.

3.2 Electric power steering systems

3.2.1 Introduction

Electric power steering systems, which widely replaced hydraulic steering systems (HDS) are used in a large number of today's passenger cars since they provide power only on demand. Therefore such steering systems are more energy efficient than HDS. This fact results in a lower fuel consumption in comparison with vehicles that use HDS rather than EPS systems [82], [83]. In addition to the energy benefits, assembly space can be saved in the engine bay since no hydraulic components such as pumps are needed.

As already mentioned in chapter 1 of the thesis, the NVH comfort in the vehicle interior plays an important role for the commercial success of the vehicle. As a consequence the structure-borne sound of EPS systems, transferred to the vehicle chassis, is considered since it is radiated from the surface of the vehicle chassis into the vehicle interior. This applies for other structure-borne sound sources which are attached to the vehicle chassis. Therefore, in automotive industry TPA methods, as outlined in section 2.4, are widely used to troubleshoot structure-borne sound issues which influence the NVH comfort in the vehicle interior in a negative way.

One of the many potential root causes of NVH issues in the vehicle interior can therefore be traced back to EPS systems. For that reason, in chapter 5 of the thesis the methodology of a

novel transmissibility based TPA approach is presented. The approach is developed to investigate the internal structure-borne sound generation mechanisms within an EPS system independently from the internal receiver which can be a housing, for instance. Therefore an EPSapa system, which is a particular type of EPS system, is chosen as the basis of two case studies. The case studies are carried out with the aim to validate the presented novel TPA methodology.

For this reason, in the following of this section at first the functional principle of an EPSapa system is fundamentally outlined. In general, besides the EPSapa system, two further categories of electric power steering systems are distinguished according to [82] and [83]. The abbreviations of these system are EPSdp [84] and EPSc [85]. The lower case letters “dp” stand for “dual pinion”. This type of EPS system has a second worm gear, used in combination with the electric motor, to provide a force which assists the driver to steer the vehicle. The EPSc system where the “c” stands for “column” generates the assisting force using an electric motor that is mounted at the steering column. Both EPS systems are used to steer compact or mid-size commercial vehicles while upper class and off-road vehicles are usually equipped with an EPSapa system.

Although only the EPSapa system is investigated in this thesis, the proposed novel TPA methodology can also be applied to EPSc and EPSdp systems. For this purpose the general rules which are summarised in section 3.5 are provided. After elucidating the functional principle of an EPSapa system in section 3.2.2 the boundary conditions of an EPSapa system are introduced and briefly discussed in section 3.2.3.

3.2.2 Functional principle

Since only steering systems of the type EPSapa are used within the scope of this thesis in the following of this subsection only the functional principle of an EPSapa system is outlined. A detailed description of the underlying functional principles of EPSc and EPSdp systems can be found in [82] and [83], for instance. Therefore the two aforementioned types of EPS systems are not further described. However, the three types of electric power steering systems are based on the so called “rack and pinion” principle. That simple principle allows to construct steering systems light in weight and precise in combination with a high haptic feedback from the road. Especially the haptic feedback is an important security factor for the drivers of vehicles while performing a steering manoeuvre.

When the driver of a vehicle turns the steering wheel with the intention to change the direction of driving the so called steering pinion (SP) which is part of a gear is set into rotation. On the drive side the SP is connected via the steering column (SC) with the steering wheel of the vehicle. On the output side the SP meshes with the so called toothed rack (TR) which is a straight bar with teeth on its surface. By means of that simple principle the steering system transforms the rotation of the steering wheel into a lateral movement of the TR from the left to the right side of the vehicle and vice versa. As the TR is connected to the tie rods of the vehicle, which are furthermore assembled to the wheels of the vehicle, the driver can change the direction of driving by simply turning the steering wheel. Hence, EPSapa systems make the driving experience more comfortable and also more secure by assisting the driver. The underlying sequence which is performed based on the functional principle of an EPSapa system is depicted by the following flow chart in Figure 3.1.

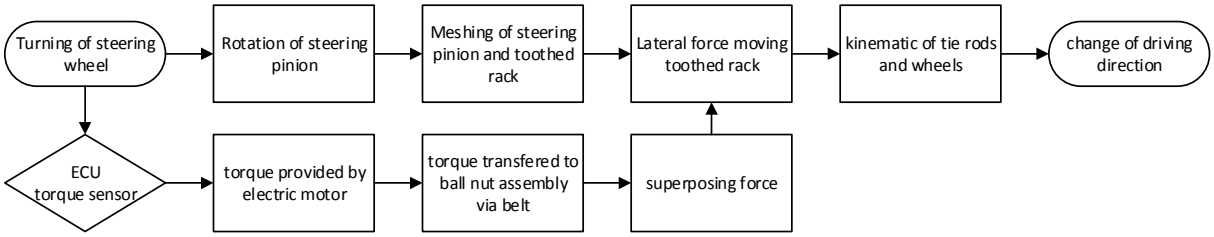

Figure 3.1: Schematic of the functional principle of an electric power steering system

In order to assist the driver with his endeavour to induce a steering manoeuvre the EM provides a servo torque according to the driving situation. Such a situation can be the parking processes at low vehicle speed or a lane change at high vehicle speeds, for instance. Therefore according to the specific situation, at first it has to be recognised by the electronic control unit (ECU) if the driver needs high power assistance or if there is only low power assistance necessary [82], [83]. In order to make that decision the actual driving situation which is characterised by the angular velocity of the steering wheel in combination with the driving speed of the vehicle is the decision criteria. Based on the aforementioned criteria the EM provides the servo torque that is needed to support the driver with his endeavour to steer the vehicle. Thereby the torque is calculated by the ECU.

The generated servo output torque of the EM is transferred via the so called toothed belt (TB) to the toothed disc of the so called ball nut assembly (BNA). Through the principle of the BNA the torque is then transferred into a translational force. This force is superposed to the steering force of the TR f_{TR} [82], [32]. This relation is condensed in the following equation

$$f_{TR} = i_{ST} M_{SP} + i_{EM} M_{EM} \tag{3.1}$$

where i_{SP} and i_{EM} are the ratios of the meshing between the steering pinion (SP) and the TR and the pinion (P) of the EM and the TB, respectively. The torque M_{SP} that is provided by the driver by turning the steering wheel is superposed to the assisting torque M_{EM} of the EM.

Because of this general functional principle multiple transmission paths for the vibrational energy flux within an EPSapa system exist. Figure 3.2 shows the identified transmission paths of the vibrational energy flux which is depicted as a red line within an EPSapa system.

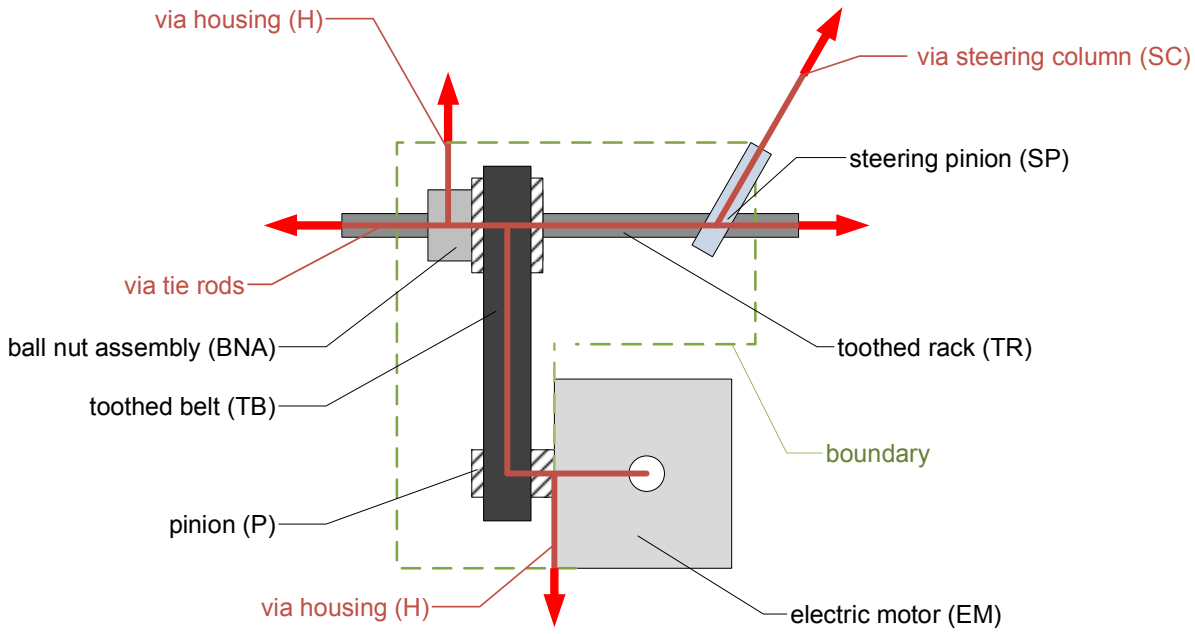

Figure 3.2: Schematic model of the transmission paths of the vibrational energy flux within an EPSapa system

Additionally in Figure 3.2 the coupling interfaces where the acoustic energy is transmitted from the EPSapa system to the vehicle are shown. These interfaces are the intersections between the boundary of the EPSapa system and the vehicle. They are depicted as red arrows in Figure 3.2. The following interfaces between an EPSapa system and a vehicle are generally defined:

- the steering column (SC),
- the tie rods and
- the housing (H) of the EPSapa system.

Previous research at RBAS has shown that only the connections between the housing (H) of the EPSapa system and the vehicle are dominant. Therefore only these interfaces are considered as important for the structure-borne sound transmission from the EPSapa system to the vehicle. A detailed discussion of all the interfaces and transmission paths, which are considered within the scope of the present thesis can be found in section 3.4 of this chapter.

3.2.3 Boundary conditions

For a meaningful conduction of a TPA approach (see section 2.3) it is at first necessary to define the boundary conditions of the source-path-receiver construct which should be analysed. This subsection intends to define in the following the aforementioned boundary conditions for the underlying case of an active EPSapa system coupled to a receiver such as a test rig or a vehicle, for instance. Two general categories of boundary conditions are distinguished in the following. At first the operational boundary conditions while the performing of a steering manoeuvre are defined. Second the mounting conditions of the steering system and its components with the test rig and the housing of the EPSapa system are defined, respectively.

Like already mentioned the sound in the vehicle interior while a parking manoeuvre at low vehicle speed is of interest for costumers in order to evaluate the NVH performance of the EPSapa system. The reason for this is that the internal combustion engine does not sufficiently mask the sound which is generated by the EPSapa system while the vehicle is been parked. This means that the structure-borne sound which is a result of the parking manoeuvre at low vehicle

speeds can be seen as a critical part of the “operational noise” of an EPSapa system. Therefore the definition of the operational boundary conditions for a bfTPA approach of an EPSapa system is based on the parking process of a vehicle.

At this point it is mentioned that in [32] Sturm described that also road induced noise while driving on uneven road surfaces such as rattle plays an important role for the NVH quality of an EPSapa system. However, within the present thesis only steering induced noise in the range between slow steering with an angular steering speed of 100°/sec and very fast steering with 600°/sec with an increment of 100°/sec is investigated. This is mainly because the bfTPA approach which is presented in the scope of this thesis is conducted in the frequency domain whereas the analysis of road induced noise requires a time domain approach [32], [66]. Constant steering speeds are easier to analyse in the frequency domain. Within the scope of the present thesis the defined range of angular speed while turning the steering wheel is one of the set boundary conditions for the conduction of the bfTPA approach which is presented in subsection 5.4.4. Furthermore the rotational speed of the components of an EPSapa system which are the most important operational boundary conditions in order to determine the in-situ blocked forces which characterise their structure-borne sound can be derived from the steering speed based on the internal ratios.

The second category of boundary conditions are the mounting conditions of the EPSapa system and its components and the definition of the external forces which act on the steering system. The mounting torque of the EPSapa system with the test rig should be the same as the mounting torque when the EPSapa system is assembled to a vehicle. The same applies to the mounting conditions of the components of an EPSapa system with the housing. This includes the mounting torque of the electric motor, the tension of the toothed belt and the fit between the ball

bearing of the ball nut assembly and the housing of the EPSapa system. An explicit discussion of the boundary conditions for each internal source can be found at the beginning of the subsections 4.5.2, 4.5.3 and 4.5.4 which contain case studies of the electric motor, the ball nut assembly and the toothed belt, respectively.

If a steering manoeuvre is performed the friction between the tires and the road surface needs to be overcome. This cause-effect relationship results in external forces which act at the tie rods against the steering forces. If a bfTPA approach of an EPSapa system is conducted on a test rig this fact needs to be considered in order to simulate the tie rod forces to conduct a meaningful analysis. Within this thesis the tie rod forces are treated as nearly equal to zero to reduce the complexity of the case study of a bfTPA of an EPSapa system which is presented in subsection 5.4.4. Therefore the torque that is provided by the electric motor of the EPSapa system is significantly lower than in case of a real parking manoeuvre of a car. Nevertheless this simplification offers the possibility to easily reproduce all the boundary conditions of an EPSapa system and its components on the corresponding test rigs.

3.3 Internal sound sources and receiver

3.3.1 Introduction

Based on the functional principle of an EPSapa system which is described in the previous section the main components regarding the NVH behaviour of an EPSapa system can be identified. These components will be called “internal sources” within the scope of the present thesis. They

generate the structure-borne sound that is transferred within an EPSapa system[2] via the internal receiver to the external connection points between the EPSapa system and an overall receiver such as a vehicle or a test rig, for instance.

In this section at first the primary and subsequently the secondary internal sources are outlined in subsection 3.3.2 and 3.3.3, respectively. The second mentioned internal sources are listed for the sake of completeness but are not included in the conducted bfTPA approach of an EPSapa system (compare case studies presented in subsection 5.4.3 and 5.4.4). However the aforementioned assumption is only valid for the structure-borne sound that is generated during a steering manoeuvre such as parking of a vehicle at low vehicle speed. If the sound in the vehicle interior of a vehicle is a consequence of excitation by an uneven surface of the road the secondary internal sources are important and need to be included within the bfTPA approach. The section is closed with an introduction of the internal receiver of an EPSapa system in subsection 3.3.4.

3.3.2 Primary internal sources

The EPS system which is used in the scope of this thesis is an EPSapa system. This means that the electric motor that provides the torque for the power assistance is mounted towards the housing of the EPS system in a parallel arrangement to the toothed rack. For the power assistance of the steering manoeuvre a force is generated which is superposed to the lateral movement of the TR. This is achieved because the so called pinion of the EM drives a toothed belt

[2] or any other overall source that consist of multiple internal structure-borne sound generation mechanisms

which in turn drives the toothed disc of the ball nut assembly. The BNA, which has a mechanical link to the TR via a ball chain, in turn transforms the torque provided by the EM into the lateral force which assists the driver with his endeavour to steer the vehicle. These fundamentals of the functional principle of an EPSapa system are already explained in more detail in subsection 3.2.2. An example of such an EPSapa system including the main components is depicted in Figure 3.3. All the referred components of an EPSapa system that are highlighted in Figure 3.3 will be categorized as primary internal sources, secondary internal sources and internal receiver in the scope of the subsections 3.3.2, 3.3.3 and 3.3.4, respectively.

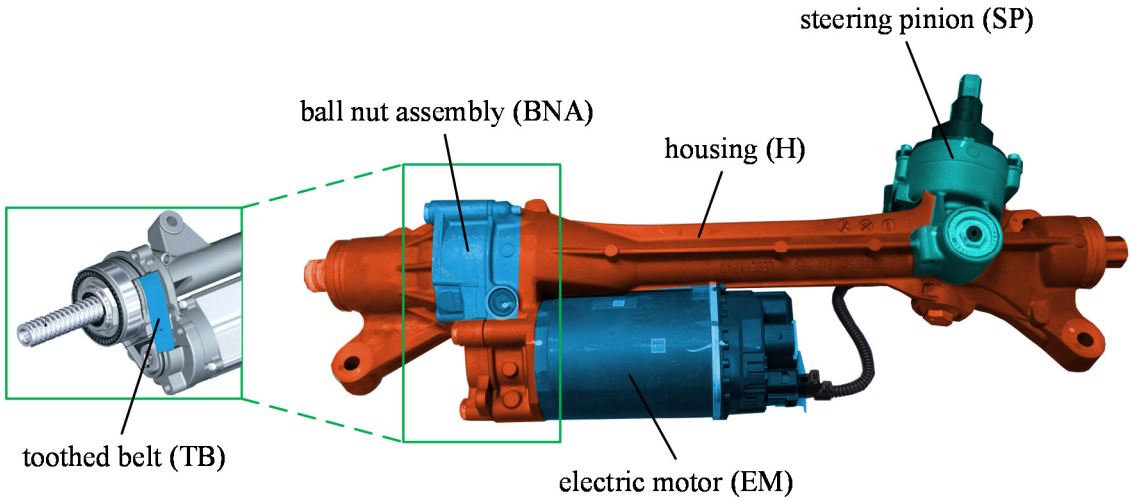

Figure 3.3: EPSapa system with highlighted main components

According to Pfeffer [86], research that has been carried out by RBAS and through closely analysing the functional principle of an EPSapa system three main prominent internal sources can be identified. The three identified internal sources of an EPSapa system generate structure-borne sound because of their functional principle during a steering manoeuvre such as parking of a vehicle, for instance. The challenge is to optimise their design regarding an optimised NVH behaviour of the whole EPSapa system which the internal sources are a crucial part of. Before

the three main internal sources of an EPSapa system are listed in the following it has to be remarked that transient effects, such as rattle noises, which result from excitation by the road surface will not be investigated within the scope of this thesis. But an assumption is made that the bfTPA methodology which is developed and presented in chapter 5 of this thesis can also be used in combination with the time domain approach by Sturm [32], [66] to determine the associated in-situ blocked forces and analyse their contribution.

The three dominant primary internal sources of an EPSapa system are identified as follows:

1. the electric motor,
2. the ball nut assembly and
3. the toothed belt

In section 4.5 all of the three identified primary internal sources of an EPSapa system are further investigated in the course of a case study. Hence further information about the characteristics of the three primary internal sources can be found in the subsections 4.5.2, 4.5.3 and 4.5.4. This subsection only intends to introduce the primary internal sources of an EPSapa system rather than discussing them in detail. The internal sources will be treated as a black box [87] within the further scope of this thesis. This means that no further substructuring of the three identified primary internal sources will be considered in the remainder of this thesis.

3.3.3 Secondary internal sources

Beside the three dominant internal sources which are listed in subsection 3.3.2 the steering pinion can be considered as a secondary and therefore not dominant internal source. The SP indeed transfers the torque provided by the driver who turns the steering wheel into a lateral movement

of the toothed rack and can therefore be seen as an important functional component. However, internal research at RBAS has shown that the SP is not to be seen as a dominant and therefore critical internal source during the operation of a steering manoeuvre. For that reason the SP is only mentioned for the sake of completeness. The SP as well as the primary internal sources are depicted in Figure 3.3 where they are highlighted in blue.

Although transient sound effects should not be considered within this thesis for the sake of completeness a further secondary source beside the SP is briefly introduced in the following. The yoke is a spring that is mounted between the housing of the EPSapa system and the toothed rack to preload the toothed rack. If the tolerances of the yoke are two wide a mechanical impact between the toothed rack and the yoke can result which can lead to rattle noises. However, during a parking manoeuvre the aforementioned secondary source is usually not to be seen as a key role for the NVH performance.

3.3.4 Internal receiver

Every complex product such as an EPSapa system consists besides the active vibrational components, which are defined as the internal sources, of passive parts as well. These parts, which are often important for the functional principle of the product because they embed the internal sources, can be considered as the internal receivers of the assembly (compare section 1.4). Since these passive parts of an assembly only embed the internal sources they do not generate structure-borne sound on their own. Although no structure-borne sound is generated, however the generated structure-borne sound of the internal sources is transmitted to the external interfaces of the assembly via the transmission paths within the internal receiver (compare Figure 1.2).

Hence it is important to define the internal receiver which is part of an overall structure-borne sound source in order to conduct a meaningful bfTPA approach within the overall source.

For the case of an EPSapa system the housing of the steering system is identified as the internal receiver. The reason for choosing the housing as the internal receiver is that the housing constitutes the interfaces between the overall receiver such as a vehicle, for instance, as well as between the internal sources. Both aforementioned “external” and “internal” interfaces will be further introduced in section 3.4. Thus on the one hand the housing embeds the internal sources introduced in section 3.3 and on the other hand it also forms the connection with the front axle carrier of a vehicle. Therefore the housing transmits the structure-borne sound which is induced by the EM, the BNA and the TB to the interface between the EPSapa system and the vehicle.

Figure 3.3 shows the housing of an EPSapa system, which embeds the EM, the BNA and the TB, depicted in orange. Just as the internal sources the internal receiver will be treated as black box. That way no further substructuring of the housing is needed. Therefore the only information that is needed about the housing, to conduct a bfTPA approach, are the in-situ blocked forces at the defined DoFs at the internal and external interfaces. Furthermore transmissibility functions called “blocked force transmissibility” (BFT) which will be introduced in section 5.2.3 are used to describe the transmission behaviour within the housing between the internal and external interfaces. Within the present thesis all the blocked force transmissibilities are calculated in the frequency domain. However in theory it is also possible to describe the transmissibility functions in the time domain. This yields the possibility to be able to investigate transient sound phenomena such as rattle noise, for instance.

3.4 Transmission paths and interfaces

3.4.1 Introduction

An important and major initial step, in conducting a bfTPA, is the definition of the interfaces as well as the transmission paths of structure-borne sound within an overall source. Since a bfTPA approach is based on transmissibility functions, it is important to include all necessary DoFs at the external and internal interfaces for a full description of the physical behaviour of the overall source. Otherwise important transmission paths within the overall source are omitted and the bfTPA would not be meaningful. A detailed discussion of this problem, which is typical for transmissibility based TPA, can be found in subsection 5.3.4 of this thesis. The identified transmission paths can be found in subsection 3.4.4.

It is proposed that the transmission paths are directly deduced from the DoFs at the external and internal interfaces which are defined according to the functional principle of the overall source such as an EPSapa system. Usually the overall source, to be analysed, is attached to an overall receiver such as a test rig or a vehicle. Therefore the connection between the overall source and the overall receiver are defined as the external interfaces. In general the internal interfaces are those between the defined internal sources and internal receiver structures. The difference between external and internal interfaces will be further explained in subsection 3.4.2 and subsection 3.4.3, respectively. In case of an EPSapa system the internal sources and the internal receiver are already defined in section 3.3. In the following, the interfaces between the aforementioned structures are introduced.

3.4.2 External interfaces

Steering systems are connected with a vehicle at multiple stiff connections where they are mounted against the front axle carrier. The stiff connections between a front axle carrier and a steering system are necessary to ensure feedback from the road which is important for the driver experience. This applies of course to EPSapa systems as well.

Unfortunately at these stiff connections structure-borne sound which is generated by the internal sources (compare section 3.3) of the EPSapa system is transferred from the housing of the EPSapa systems to the front axle carrier of the vehicle. Conveniently, these connections can be treated as point connections in most of the cases. Research that has been successfully conducted treating the connections of the EPS system with a vehicle or test rig as point connections can be found in [31], [32], [11], [12], for example.

In case of the EPSapa system that is used in the scope of this thesis four connections between the steering system and the vehicle exist. The connections can be seen as feet with holes where the EPSapa system is mounted against the front axle carrier of the vehicle using bolts. Therefore the four connections between the EPSapa system and the vehicle can be seen as highly stiff. One of the four connection points between the EPSapa system and the vehicle is exemplarily shown circled in red in Figure 3.4.

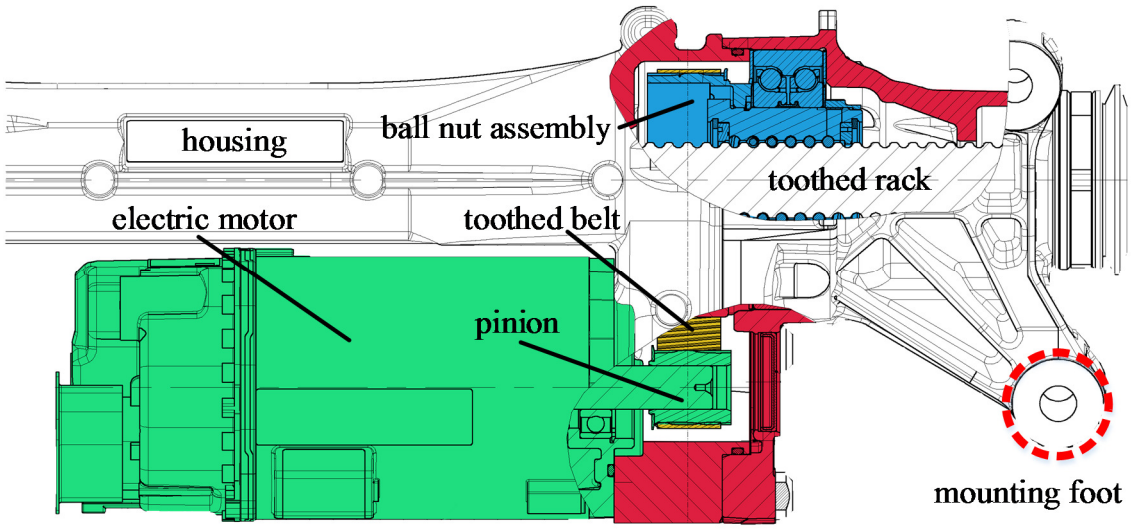

Figure 3.4: Cross sectional view of an EPSapa system with highlighted external interfaces at one of the mounting feet with a vehicle

The definition of the external interface is important since it is the target location for the bfTPA approach. Research that has been carried out by RBAS showed that it is for many cases sufficient to describe the external interface with three translational DoFs. The rotational DoFs are omitted and still a sufficient characterisation of the structure-borne sound at the external interface is achieved. For that reason within this thesis, rotational DoFs are omitted as well. Nevertheless in subsection 5.4.2 a bfTPA approach will be carried out using a steel beam where rotational DoFs are included. That way the validity of the proposed bfTPA methodology is proven.

In the case under consideration the external interface is characterised by determining three in-situ blocked forces at each connection point. In [88] van der Seijs showed that the interface between an EPSapa system and the vehicle behaves more or less as one stiff point and can therefore be treated as one point. This approach which is called virtual point transformation is not applied within this thesis. In total the EPSapa system is characterised with 12 vectors of in-situ blocked force at the connection points between the steering system and the vehicle.

3.4.3 Internal interfaces

Between every internal source which is outlined in section 3.3 and the internal receiver exists an internal interface. The physical characteristics of these interface are crucial for the transmission of the structure-borne sound between an internal source and an internal receiver. The precise characterisation of these interfaces is therefore important for the determination of the in-situ blocked forces. Thus it is also crucial for the conducting of the bfTPA approach. Therefore special attention needs to be focussed on defining the correct internal interfaces. This especially concerns the question if an interface is a continuous contact zone or if it can be treated as one or multiple point connections. If an interface can be treated as a point connection usually no further discretisation of the interface is needed. But in most cases, like an EPSapa system for example, the interfaces are continuous. This requires a spatial discretisation of the interface. A methodology to deal with these continuous interfaces will be outlined in section 4.3. The present section only aims to introduce and characterise the interfaces of an EPSapa system. This applies for the internal as well as the external interfaces of an EPSapa system.

Since three main internal sources of an EPSapa system were identified also three internal interfaces to be characterised exist. The locations of these three interfaces are schematically shown in Figure 3.5. The interface between the EM and the H, between the TB and the P and between the BNA and the H are highlighted with blue (1), purple (2) and yellow border (3) lines, respectively. In theory there would be a fourth internal interface between the SP and the housing of the EPSapa system. However, this interface will not be outlined in the following since the steering pinion is only considered as a secondary source in the scope of this thesis.

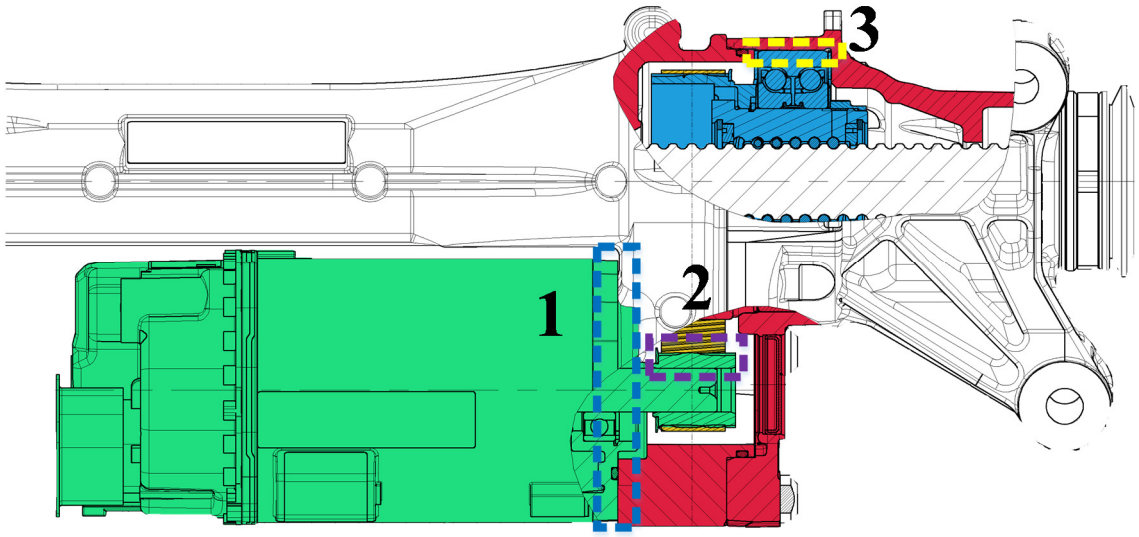

Figure 3.5: Cross sectional view of an EPSapa system with highlighted internal interfaces

The first interface to characterise with in-situ blocked forces is between the EM and the housing. Since it is a plain surface and can be seen as rotationally symmetric it is assumed to be the easiest to characterise. Additionally the stiffness of the interface can be assumed as being spatially constant. The second interface is between the BNA and the housing. Precisely the interface is chosen to be the surface of the outer ring of the ball bearing that embeds the BNA in the housing. The ball bearing therefore can be seen as part of the BNA. The last and probably most complicated interface, since it is revolving, is the interface between the TB and the pinion of the EM. The interfaces are all continuous admittedly, but differ in their shape and their dynamic behaviour.

3.4.4 Transmission paths

Besides the identification of the internal sources and internal receivers it is crucial, for conducting a bfTPA, to identify the main paths for the transmission of structure-borne sound within an

overall source. Naturally these paths follow if the necessary DoFs at the external and internal interfaces are defined since the transmission paths link the external and internal DoFs with each other. At this point it has to be mentioned that it is crucial to identify all relevant DoFs at the interface. Otherwise the structural behaviour and therefore also the correct transmission of structure-borne sound is not fully described. Nevertheless, in many cases some transmission paths within a product can be seen as dominant and some can be omitted because the path is blocked or fully damped.

This section therefore introduces the two main identified transmission paths for structure-borne sound within an EPSapa system. Figure 3.6 shows these two identified internal transmission paths within an EPSapa system as a blue and yellow line, respectively.

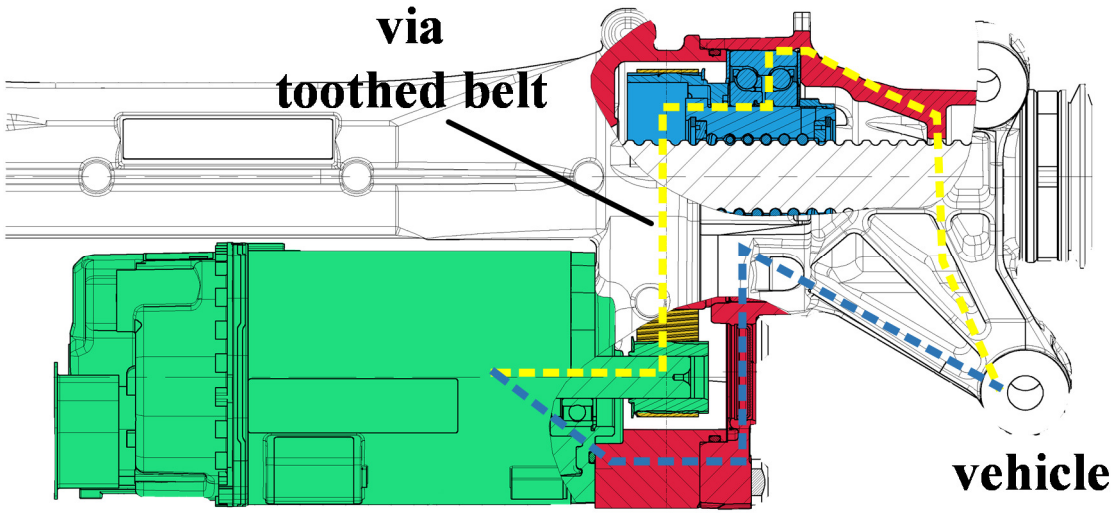

Figure 3.6: Cross sectional view of an EPSapa system with the two identified internal transmission paths highlighted as blue and yellow line

During a steering manoeuvre the EM provides a torque and in the following both identified transmission paths have their root cause each at the internal sound generation mechanisms

within the EM. Nevertheless according to the functional principle two main paths for the structure-borne sound that is generated within the EM can be identified. In the following no further distinction between all the DoFs which are contained within one transmission path will be made. All DoFs are seen to be combined within one transmission path for the sake of simplicity.

The first transmission path which is depicted in Figure 3.6 as a blue line runs via the plain interface between the EM (green) and the housing (red). The connection between the housing and the EM is therefore treated as three point connections. Within the housing the transmission path then proceeds to the external interfaces (compare subsection 3.4.2) between an EPSapa system and a vehicle. The second transmission path runs from the pinion of the EM, the toothed belt (TB) and then the ball nut assembly (BNA) to the housing of the EPSapa system. From there the structure-borne sound is then transmitted within the housing to the external connection points with the vehicle. The second path can be divided into two parts. The first path can be seen as the connection between the meshing of the pinion with the TB and the meshing of the TB with the toothed disc of BNA. The second part of the transmission path is the connection that follows after the meshing of TB and toothed disc until the connection between the EPSapa system and a vehicle.

The bearing of the BNA is introduced as a “transceiver structure”, since on one hand it generates structure-borne sound and on the other hand receives structure-borne sound from the BNA. A further transceiver structure within an EPSapa system is the toothed belt. The term “transceiver” is chosen in comparison with radio technology where a transceiver is a technical device that simultaneously transmits and receives radio waves. If the transceiver structures are engineered with high quality their contribution is usually expected as very low in comparison to the IAs. For that reason the transceiver structures can often be seen as part of the IAs. This can be an

advantage if the interface between the transceiver and the IB is easier to access than the interface between the transceiver and the IA.

Concluding, the internal transmission paths of the vibro-acoustic energy within an EPSapa system will be defined as follows

1. electric motor – housing
2. electric motor – toothed belt – ball nut assembly – housing
    a. electric motor – toothed belt – ball nut assembly
    b. ball nut assembly – housing

The experimental investigation of the aforementioned transmission paths of structure-borne sound within an EPSapa system can be found in section 5.4 of the present thesis.

3.5 **Summary and concluding remarks**

In the present chapter, at first electric power steering (EPS) systems in general and EPSapa systems in particular are introduced. Based on the functional principle, the EPSapa system is substructured into its main components regarding the NVH characteristics of the steering system. This is an important objective of the thesis since the detailed substructuring of the EPSapa system is the crucial basis for the success of the case studies that are presented in chapter 4 and chapter 5. The aforementioned case studies intend to prove the following two assumptions:

- It is possible to determine accurate and meaningful in-situ blocked force vectors at the internal interfaces of an EPSapa system that are identified in section 3.4.

- The determined in-situ blocked force vectors pose the input quantity of the proposed novel bfTPA approach since these forces characterise the strength of the internal sources which are defined in section 3.3.

In section 3.2 the functional principle and the boundary conditions of an EPS system are described. The EPSapa system is considered in detail, since it is part of the case studies that are carried out in the course of the present thesis. Based on that statement, all the relevant primary internal sources and the secondary internal sources of an EPSapa system are identified. When conducting a TPA, the definition of the interfaces plays a significant role in the preparation of the approach. The definition of the transmission paths within the internal receiver requires a profound knowledge of the physical behaviour at the internal and external interfaces. Hence, based on the defined internal and also the external interfaces the transmission paths within an EPSapa system are outlined in subsection 3.4.4. It was stated that the precise definition of the transmission paths is crucial for the success of bfTPA. This issue is later discussed in subsection 5.3.4. At this stage it is only mentioned that omitting relevant transmission paths within an overall source can reduce the meaning of the results of the bfTPA.

The methodology to substructure an EPSapa system, which is presented in this chapter, can also be applied to other products that consist of multiple internal sources and internal receivers. For this purpose the following steps can be followed to substructure an overall structure-borne sound source:

1. Identification of all parts of the product to be analysed that actively generate structure-borne sound according to the functional principle:
   These parts are defined as the internal sources and will be characterised by determining their source strength in terms of in-situ blocked forces. For simplicity, all

internal sources are treated as black boxes since the generation mechanism of structure-borne sound within the internal sources are often experimentally challenging. The limiting factor is the dimensions of the internal source. However, if it is possible to determine the internal generation mechanisms within an internal source a further substructuring is possible.

2. Identification of the component or components of a product that only transmit structure-borne sound instead of generating it on their own:
   These parts are defined as the internal receivers. An example of an internal receiver is the housing of an EPS system. Since every technical product needs some sort of housing, bearing or similar parts, it is always possible to identify at least one part of an assembly that is treated as an internal receiver.
3. Identification of the internal and external interfaces between the internal sources and the internal receivers, respectively:
   Not only the identification is of importance but also the description of the interfaces, particular if the interface is a point connection or a continuous area. If the interface is treated as a continuous area further assumptions about the discretisation need to be made. This will be discussed in subsection 4.3.2.
4. Definition of the transmission paths within the product:
   A transmission path begins at the interface between an internal source and an internal receiver and ends at the interface between the overall source and the overall receiver. One needs to avoid omitting relevant transmission paths. This is crucial since the paths are characterised with transmissibility functions rather than FRFs.

The four steps which are presented within this subsection can be followed in order to substructure an overall structure-borne sound source into its main internal sources, internal receivers and internal transmission paths within the internal receiver. Subsequently the methodology of bfTPA can be applied.

Chapter 4

Independent characterisation of internal structure-borne sound sources

4.1 **Introduction**

In chapter 5 of the present thesis a novel transmissibility based TPA methodology which is called “blocked force transmissibility transfer path analysis” (bfTPA) will be proposed. Within the scope of this thesis the validity of the proposed bfTPA methodology is proven by carrying out three experimental case studies. The results of the aforementioned experimental case studies are presented in subsection 5.4. As briefly mentioned in chapter 1 of this thesis, the conduction of the bfTPA initially requires the determination of external and internal in-situ blocked forces at the corresponding interfaces, respectively.

Within the context of this thesis the internal in-situ blocked forces characterise the vibrational strength of the defined embedded internal structure-borne sound sources within an overall structure-borne sound source (compare section 3.3). The experimentally determined vectors of internal in-situ blocked forces subsequently provide the input quantities (external source strengths) for the proposed bfTPA approach. Hence, the precise determination of the internal in-situ blocked forces is a crucial objective. This means, that in accordance with any other already existing TPA method[3], the proposed bfTPA method generally requires at first the precise definition of the conditions of the internal structure-borne sound sources.

Therefore, one important step within the definition of the internal sources[4] is the specification of the corresponding internal interfaces and DoFs between the internal sources and the internal

[3] This applies for transmissibility based and FRF based TPA methods.
[4] Within this thesis the term “internal source” is used rather than “internal structure-borne sound source” for reasons of simplicity.

receiver (compare section 3.4). The definition of the internal structure-borne sound sources embedded within the overall structure-borne sound source is conducted according to the developed internal-source-path-receiver-model (ISPRM). In section 1.4 of this thesis ISPRM was introduced and briefly outlined. Although the definition of the internal sources seems to be a fairly uncomplicated step in the course of a bfTPA, it is important to fulfil the step with care. Otherwise, wrong conclusions will be drawn for optimisation of the overall structure-borne sound source regarding NVH specifications.

In chapter 3 an EPSapa system was introduced and sub-structured into its three main internal sources, the internal receiver and the corresponding interfaces. In this chapter the three internal sources of an EPSapa system, which are the electric motor, the ball nut assembly and the toothed belt, are further investigated. Three different case studies are carried out, which comprise the experimental determination of the in-situ blocked forces of the three aforementioned prominent internal sources at the internal interfaces of an EPSapa system. Section 4.5 contains the results and the discussion of the determined aforementioned in-situ blocked forces.

A toothed belt of an EPSapa system can be seen as an internal source with a revolving interface rather than a system with a quasi-static interface. Therefore in section 4.4 a methodology to deal with an internal source is presented. Furthermore a second alternative way of determining the in-situ blocked forces of the toothed belt of an EPSapa system. In contrast to the internal interface between a toothed belt and the chosen internal receiver the interfaces between the electric motor and the ball nut assembly with an internal receiver, respectively, are continuous. For that reason in section 4.3 a methodology is proposed which aims to deal with the internal continuous interfaces within an overall structure-borne sound source such as an EPSapa system. It will be shown that a sufficient discretisation of the continuous internal interfaces of an electric

motor and a ball nut assembly with an internal receiver, respectively, is sufficient to yield meaningful results for the determined vectors of internal in-situ blocked forces.

In order to experimentally determine the in-situ blocked force vectors of the internal sources at first in section 4.2 a novel application of the in-situ method by Moorhouse and Elliott [27] is presented. The proposed novel application is based on the use of micro electro mechanical system (MEMS) accelerometers. It will be demonstrated that a specific type of small and low-cost MEMS accelerometers is useful for inverse force identification [89], [90] and therefore also for the in-situ blocked force method. In order to prove this assumption MEMS accelerometers are used for the determination of the vectors of in-situ blocked forces in the scope of the three case studies which are presented in section 4.5.

4.2 Application of embedded accelerometers for the determination of in-situ blocked forces

4.2.1 Introduction

In subsection 2.3.4 the underlying methodology for the determination of in-situ blocked forces, first presented by Moorhouse and Elliott in 2009, is outlined [27], [26]. Furthermore it was highlighted that for an accurate calculation of in-situ blocked forces, an accurate determination of FRFs is crucial (compare Eq. (2.8) and Eq. (2.7)). The aforementioned FRFs from multiple DoFs at the interface between a structure-borne sound source and a receiver to multiple arbitrary

locations[5] on the receiver side (compare Figure 2.6) can be determined either experimentally or analytically. However, in the following, only experimentally determined FRFs are considered. The reason is that the results that will be shown in subsection 4.5.2 and subsection 4.5.3 are also achieved experimentally.

The experimental determination of FRFs requires the measurement of acceleration at the interface DoFs between an overall structure-borne sound source and an overall receiver or between an internal source and an internal receiver[6], respectively (see Eq. (2.2)). For many products such as an EPSapa system, which is defined as an overall structure-borne sound source within this thesis, the determination of the necessary FRFs is in fact conveniently possible. The reason is, that the external interfaces can often be treated as point connections since the interface can be seen as stiff. Hence the choice of the DoFs at the interfaces is often obvious. Furthermore the external interfaces between the overall source and an overall receiver such as a vehicle or a test rig, for instance, are mostly accessible with surface mounted accelerometers. Hence, it is possible to determine the necessary FRFs (compare Figure 2.6) through measurement and subsequently calculate the vectors of external in-situ blocked forces. For the case of an EPSapa system this was already shown by research conducted at Robert Bosch Automotive Steering GmbH. Furthermore it was shown that the determined vectors of in-situ blocked forces yield a meaningful characterisation of the source strength of an EPSapa system if the external interfaces are each treated as point connections [11], [12]. A description of the external interfaces of an EPSapa system can be found in subsection 3.4.2 of the present thesis.

[5] The term location indicates a point and a corresponding DoF.
[6] Because of the inconvenience reciprocal measurement is often avoided.

Unfortunately, in case of an EPSapa system the internal interfaces are often either not conveniently accessible or totally inaccessible with standard surface mounted integrated electronic piezoelectric (IEPE) accelerometers. This is especially due to the fact that the size of most standard IEPE accelerometers is too large to even position them sufficiently close to the internal interface. Furthermore, the positioning of accelerometers changes the characteristics of the sensitive contact zone between an internal source and an internal receiver. Many products have inaccessible internal interfaces because of their complex and space-saving construction method. However, if the vectors of in-situ blocked forces of an internal source need to be determined, which is necessary for the conduction of a bfTPA approach, the problem of inaccessibility at the internal interfaces arises and needs to be solved.

However, if accelerometers are embedded at the sensitive contact interface between an internal source and an internal receiver the in-situ blocked force method can still be conducted as presented by Moorhouse and Elliott [27], [26]. Since MEMS accelerometers are to date available of low cost, small size and good measurement accuracy, e.g. [91], [25], [24], it is possible to place these types of accelerometers directly at the interface between an internal source and an internal receiver. Thus, yielding the possibility to determine the in-situ blocked forces of internal structure-borne sound sources such as the electric motor or the ball nut assembly of an EPSapa system, for example.

In the following the methodology for the determination of in-situ blocked forces through the application of MEMS accelerometers which are embedded at an internal interface will be introduced in subsection 4.2.2. Furthermore, the differences between the in-situ method and the

proposed application of the method using MEMS accelerometers will be elucidated. Subsequently potential improvement and the general limits of the proposed methodology are presented and discussed in subsection 4.2.3.

4.2.2 Methodology

The methodology to determine in-situ blocked forces at internal interfaces is basically comparable with the in-situ method proposed by Moorhouse and Elliott. Therefore, the aim of this subsection is to define the differences between both methodologies. Furthermore it will be stated how the proposed methodology expands the in-situ method in order to determine internal in-situ blocked forces.

The in-situ blocked force method, reviewed and discussed in section 2.3.4, gives the in-situ blocked forces calculated according to Eq. (2.7). Hence the in-situ method is based on an inverse force identification approach such as generally described in [92] and [93], for example. This means that for the calculation of the in-situ blocked forces the precise generation of a mobility matrix $\mathbf{Y}_{C,cb}$ (see Eq. (2.7)) is a key factor for the success of the methodology. Hence the proposed methodology for the determination of internal in-situ blocked forces is focussed on the mobility matrix $\mathbf{Y}_{C,cb}$ since the measurement of the operational velocities $\mathbf{v}_{op}$ does not differ from the in-situ method.

Like already mentioned, in order to generate the mobility matrix $\mathbf{Y}_{C,cb}$ simultaneous measurement of acceleration at the internal interfaces and excitation at the receiver side (b) is needed. Reciprocal measurement to determine the mobility matrix is often not possible, even for the determination of in-situ blocked forces at external interfaces. This issue is the same for the

determination of in-situ blocked forces at internal interfaces since the space around the internal interfaces is even reduced in comparison to the external interfaces of an EPSapa system. The measurement of acceleration at the internal interface and the derived velocity $\mathbf{v}_c$ is used to build the necessary mobility matrix $\mathbf{Y}_{C,cb}$ according to Eq. (2.7). In this point both methodologies share the same foundation since the coupled system is excited at the receiver side (b). However, the difference between both methods is the way how the acceleration at the interface (c) between an internal source and a receiver (see Figure 2.3) is determined.

Therefore the proposed use of embedded MEMS accelerometers for the determination of internal in-situ blocked forces can be seen as an adaption of the in-situ blocked force method. However, there are some differences between an approach with surface mounted accelerometers and the proposed use of embedded MEMS accelerometers.

In order to determine internal in-situ blocked forces it is proposed to slightly modify the sensitive internal interfaces in such a way that small MEMS accelerometers can be embedded at the internal interfaces. Where possible, existing small grooves or holes at the interface are used. However, often it is necessary to add small grooves to the interface. Hence, in contrast to the in-situ method the interface needs to be modified. This usually means that the internal source which is an embedded component of a product that is defined as an overall source needs to be disassembled. This can be seen as a potential downside of the proposed methodology and will therefore be further discussed in subsection 4.4.3.

If the proposed methodology is applied one has to pay attention that the boundary conditions between the internal source and the internal receiver stay the same in comparison to the unmodified state. The small size of MEMS accelerometers introduces only minor modifications to the very sensitive contact interface. Consequently, FRFs measured with MEMS accelerometers,

directly embedded in the flux of forces, are assumed to contain more meaningful information than FRFs measured with surface mounted accelerometers close to the contact zone. Nevertheless, the following questions should therefore be considered in detail:

1. Does the modification of the internal interface significantly change the contact zone between the internal source and the internal receiver in a way that a continuous interface is forced to be multiple point connections instead?
2. Does the modification prohibits the internal source from working in normal operational conditions?
3. Is it possible to mount the internal source towards the internal receiver in the same way as before the modifications to the internal interface are introduced?

Figure 4.1 shows an example of a modified internal interface between an internal source and an internal receiver. It shows the cylindrical contact surface of an electric motor (EM) with two additionally milled grooves[7] next to threaded holes used for mounting the EM to the housing. At this point it can be remarked that, alternatively, it would also be possible to modify the receiver structure which in this case is the housing of an EPSapa system.

[7] cross sectional area < 25 mm²: depth < 5 mm

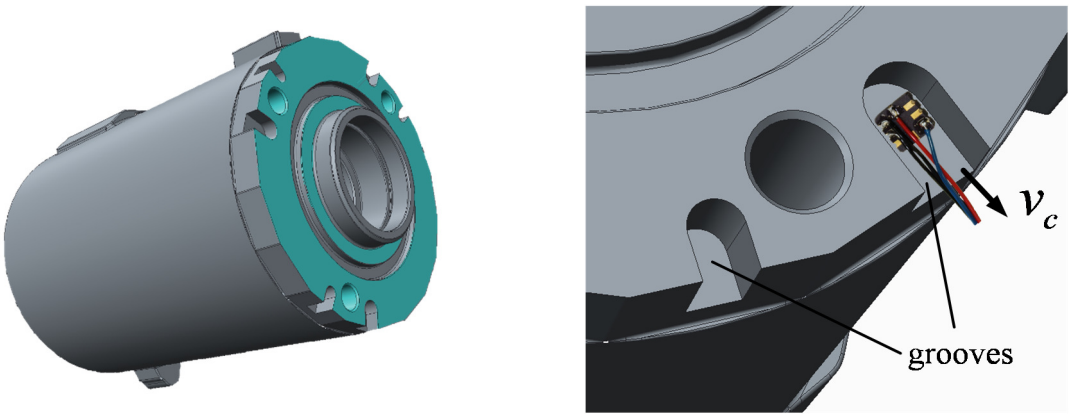

Figure 4.1: Grooves machined into the housing of an electric motor to embed MEMS accelerometers in the vicinity of the actual contact interface (green)

The embedded MEMS accelerometers record the velocity $\mathbf{v}_c$ at the internal interface which is necessary to determine the FRFs $\mathbf{Y}_{C,cb}$. In order to embed the MEMS accelerometers they have to be first placed carefully in the grooves. Additionally it is important to place them inside the grooves in such a way that the necessary DoFs for the determination of meaningful in-situ blocked forces can be measured. This means that no measurement direction of the MEMS accelerometer is blocked or significantly reduced. After the MEMS accelerometers are placed the cavities are filled with a resin or any other adhesive that provides the necessary stiffness $\mathbf{K}$ and a low damping factor $\mathbf{D}$ [94]. This means that the MEMS accelerometers will therefore become part of either the receiver structure or the internal source structure. That is schematically shown in Figure 4.2.

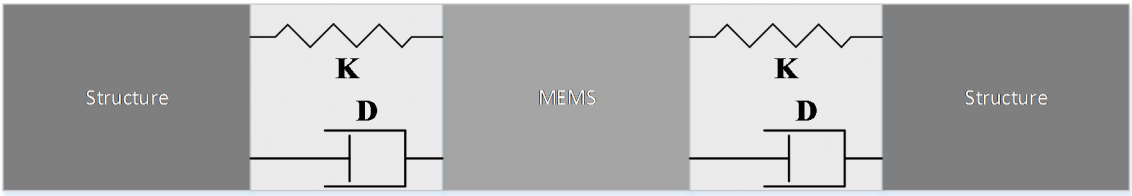

Figure 4.2: Mass-spring system of a MEMS accelerometer embedded in a cavity of a rigid structure

The results of the determined in-situ blocked forces will be outlined in subsection 4.5.2 and subsection 4.5.3.

4.2.3 Limits of the methodology

There are multiple boundary conditions which define the limits for the proposed methodology of embedded MEMS accelerometers at the interface between an internal source and an internal receiver in order to determine in-situ blocked forces. In the following of this subsection these limits will be elucidated and set in context with the already existing in-situ method.

If the in-situ blocked force method can be applied to characterise an overall source at its external interfaces often surface mounted IEPE accelerometers can be used which are conveniently placed at or very close to the interface. That way no further disassembling step of the overall source and the overall receiver is necessary. This poses a significant advantage of the in-situ method. However, if the in-situ blocked forces of an internal source need to be determined according to the methodology which was presented in subsection 4.2.2 the internal source and the internal receiver potentially need to be disassembled. This can be a complicated procedure which avoided in consideration of time-saving.

In addition it is also often required during the development process of the components of a product to determine the NVH properties during various prototype states. This presents the possibility to modify the component, which is seen as an internal source, before the components are assembled to an internal receiver such as a housing. Hence, the embedding of the MEMS accelerometers at the internal interface can be conveniently done during this stage. If this is considered at the beginning of the development cycle of a component the differences in time-saving between the in-situ method and the proposed method are minor.

Another potential limit of the method is if the available space at the internal interface is not sufficient. This is usually a consequence of a lightweight construction principle in the automotive industry towards saving of as much material as possible without reducing the stability of the product. However, since the interface forces are the same on the receiver side and the source side it is in theory possible to modify the receiver rather than the internal source [29], [79], [95].

MEMS accelerometers are often designed to measure vibration in a low frequency range. In general the frequency range of MEMS accelerometers is often rather narrow. However, during a steering manoeuvre a variety of vibration within a broad frequency range to an upper limit of 3 - 5 kHz is induced. Therefore it is desirable to be able to measure all phenomena within the frequency range to be analysed. In case of an EPSapa system the frequency range of the used MEMS accelerometers of 5 kHz is sufficiently high. However, this might not be true for other technical products which generate noise phenomena in a high frequency range of a couple kHz.

During the measurements that were conducted in the scope of this thesis it was observed that the signal-to-noise-ratio (SNR) of MEMS accelerometers is approximately 10 dB worse than the SNR of IEPE accelerometers. However, since the MEMS accelerometers are only used for the determination of FRFs this problem is manageable. In subsection 2.3.1 it was explained how FRFs are determined and that artificial excitation with an impact hammer or a shaker is used to construct the FRFs. Because of the principle of LTI systems theory the excitation can be adjusted so that the SNR is sufficiently high enough. This principle was used during the conduction of the case studies which are presented in section 4.5 and section 5.4.

4.3 Internal sources with continuous interfaces

4.3.1 Introduction

One can think of many cases where the external interface between the overall source and the overall receiver can be treated as a point connection at which the structure-borne sound is transferred from the overall source to the overall receiver. This assumption is especially true for a rigid coupling between the overall source such as an EPSapa system and the overall receiver such as a vehicle body or test rig, for instance. In automotive industry a rigid fixture is common for many couplings between vehicle components and the body of a vehicle because of stability reasons. In case of an EPSapa system the fixture between the steering system and the vehicle is rigid as well and is therefore treated as a single point connection.

However in contrast to the external interfaces of an EPSapa system the internal interfaces within an EPSapa system, which are introduced and defined in subsection 3.4.3, cannot be treated as single point connections. On the contrary the internal interfaces of an EPSapa system are continuous. Hence, in the following of this section the term continuous interface is further elucidated. This means that the transferred vibrational energy of the internal source is distributed over the whole connection surface between the internal source and the internal receiver. Therefore the question arises if the internal interfaces of an EPSapa system can be theoretically treated as multiple point connections for a convenient determination of meaningful internal in-situ blocked forces.

For that reason, in the following, dealing with continuous interfaces for the determination of internal in-situ blocked forces will be discussed. Thus, at first in subsection 4.3.2 a potential

concept to deal with continuous interfaces will be proposed. The concept is based on the discretisation of the interface while a second concept which is based on Fourier series is mentioned. Subsequently in subsection 4.3.3 the two concepts are briefly related to each other. At this point it is already remarked that only the first concept of discretisation was used within the scope of this thesis to determine the internal in-situ blocked forces. However, the concept of Fourier series is discussed for the sake of completeness and because it can be theoretically additionally applied to the concept of discretising a continuous interface.

4.3.2 Discretisation of continuous interfaces

One potential way to deal with the structure-borne sound transmitted through a continuous interface is to discretize the interface through multiple point connections. Therefore it is at first necessary to define the number of point connections needed to observe the physical behaviour of the internal interface sufficiently. This is summarized by the following equation, where I_{cont} is the continuous interface and I_k are the sub-interfaces which are used for the discretisation of the continuous interface as follows

$$I_{cont} = \sum_{k=1}^{n} I_k \tag{4.1}$$

This means that all the vibrational energy transmitted through the interface during the operation of a source can be observed from the chosen amount of the n point connections which each represent a sub-interface I_k. In other words, the interface is divided into multiple sub-areas which are represented by the defined n point connections and the corresponding DoFs.

One requirement for the success of the discretisation approach is the possibility to define the locations of the n points on the continuous interface equally distributed all over the interface. This way meaningful vectors of in-situ blocked forces $\mathbf{f}_{bl,k}$ in the n sub-interfaces can be determined. If the continuous interface is symmetric such as a cylindrical or a square interface it is furthermore possible to subdivide the interface equally distributed. This is depicted by Figure 4.3.

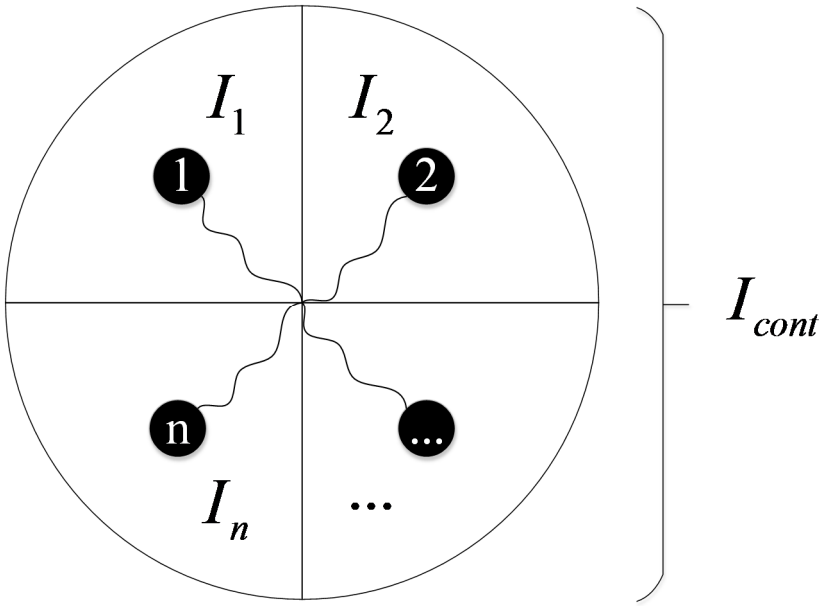

Figure 4.3: Point connections (1…n) equally distributed over a symmetric and continuous interface

Within the scope of this thesis all the defined internal interfaces of an EPSapa system are discretised through multiple point connections as depicted by Figure 4.3. This way the in-situ blocked force method can still be applied to determine the in-situ blocked forces at every discretisation point and the corresponding DoFs. Furthermore the methodology using embedded MEMS accelerometers which is proposed in section 4.2 can be applied in combination with the discretisation of a continuous interface. This means that the vector of in-situ blocked forces of

an internal source $\mathbf{f}_{bl,cont}$ is the sum of multiple in-situ blocked force vectors $\mathbf{f}_{bl,k}$ with n being the number of point connections used to discretise the continuous and internal interface.

$$\mathbf{f}_{bl,cont} = \sum_{k=1}^{n} \mathbf{f}_{bl,k} \tag{4.2}$$

Subsection 4.5.2 will show that the interface can be sufficiently discretised by three points and three corresponding translational DoFs per point for the case of an electric motor. The reason for that is the fact that the EM is mounted via three screws to the housing which hence logically yield the points for the discretisation. In contrast to the interface of the EM the interface between the BNA and the housing of an EPSapa system is curved and continuous. Therefore it cannot be discretised in an obvious way. A solution to that issue is presented in subsection 4.5.3.

4.3.3 Discussion

A Further way to deal with continuous interfaces is provided by Bonhoff [96]–[103]. He successfully showed that it is potentially possible to determine the mobility of a continuous interface based on spatial Fourier series. This methodology could also be applied for the source characterisation at a continuous interface if a sufficient amount of in-situ blocked forces was determined. The in-situ blocked force at the interface, e.g. between the BNA and the housing of an EPSapa system, can be considered as continuous and periodic, therefore yielding the spatial blocked interface force $\mathbf{f}_{bl,cont}$ as follows

$$\mathbf{f}_{bl,cont} = \frac{1}{N} \sum_{k=1}^{N} \mathbf{f}_{bl,k} e^{-\frac{j2\pi k}{N}} \tag{4.3}$$

In the previous equation N is the number of chosen discretisation points at the interface and $\mathbf{f}_{bl,k}$ the determined vectors of in-situ blocked forces at the N points. The discretisation points can be chosen to be equidistant (compare Figure 4.3).

However, for most cases it is assumed that the discretisation of a continuous interface can be conveniently achieved by treating the interface as multiple point connections. Hence all the vibrational energy is observed from the chosen amount of point connections. However, the question concerning the quantity of point connections which are necessary to characterise the interface arises. By conducting multiple case studies this question is answered for the internal interfaces of an EPSapa system in section 4.5. Nevertheless the following issues need to be kept in mind.

In theory only one point with three Cartesian coordinate directions is sufficient to yield an in-situ blocked force vector containing all necessary information about the source strength. This means that the dominant frequencies and the phase information can be analysed, for example. However, the magnitude of the vector yields only limited information since the information would be meaningless. This is a consequence that the vector of in-situ blocked forces was determined under the assumption that the energy flux is solely through that one point connection. Therefore Hannes Bonhoff proposed a different approach which was briefly shown above. Nevertheless it will be shown that the right choice of the location and the amount of the discretisation points yields meaningful results for the in-situ blocked forces of internal sources such as an EM or a BNA, for instance.

4.4 Internal sources with revolving interfaces

4.4.1 Introduction

The published literature which concern the characterisation of structure-borne sound sources by means of in-situ blocked forces usually defines static external interfaces between source and receiver. The research to date is listed as follows:

- EPS systems by Sturm [11], [12], [32], [66], Alber [77], [104], Bauer [31] and van der Seijs [36], [105], [106], [107]
- Beam by Moorhouse and Elliott [26], [108], [29], [69], [109], [110]
- Wind turbines by Moorhouse and Elliott [10]
- Pump by Lennström [111] and Elliott [28]

Hence, in most cases it is possible to define an interface between a structure-borne sound source and a receiver which can be seen as static or at least quasi static. The aforementioned assumption also applies for the continuous internal interfaces which are discussed in section 4.3. Because of the static or quasi static behaviour of the interface there is only relatively small movement between source and receiver. This often offers the possibility to conveniently place accelerometers at or close to the interface. Thus the necessary FRFs for obtaining of the in-situ blocked force method (compare subsection 2.3.4) can be experimentally determined. This holds for both point connections as well as for a continuous contact zone between an overall source and an overall receiver.

If the interface changes because the source which is a toothed belt, for instance, is revolving, a solution must be found to deal with the constant change of the interface. During a revolution of

the source the position at the revolving interface which is used for the determination of the necessary FRFs changes from position 1 to position 2, for instance. Hence the assumption is made that the FRFs $\mathbf{Y}_{c_1 b}$ and $\mathbf{Y}_{c_2 b}$ are different to some degree if the interface (c) is not homogenous. Such a revolving source with relative movement between position 1 and position 2 at the interface is schematically depicted by Figure 4.4.

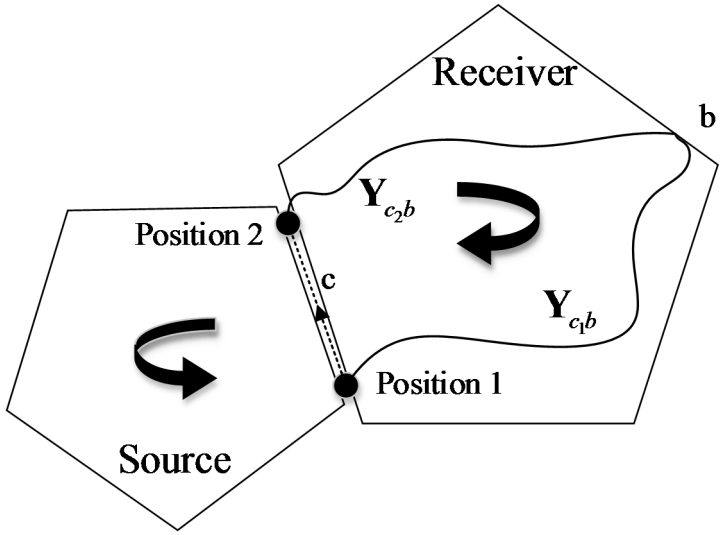

Figure 4.4: Point connections (1 and 2) at a revolving interface

In subsection 4.4.2 the term "revolving interface" will be defined in more detail and the basic equations will be introduced. Subsequently a potential methodology to determine in-situ blocked forces at revolving interfaces will be proposed and outlined in subsection 4.4.3. The chapter will close with a discussion of the limits of the proposed methodology in subsection 4.4.4. A case study of a source with revolving interfaces, in which the aforementioned methodology was applied, is in subsection 4.5.4.

4.4.2 Definition of revolving interfaces

If a structure-borne sound source is revolving, such as a toothed belt, it is assumed that the vector of in-situ blocked forces is dependent on the rotation. As a consequence, the interface behaviour between source and receiver changes constantly in relation to quantities such as rotational angle. These quantities, which influence the FRFs and as a consequence also the in-situ blocked forces are summarized in the following as Ψ. Hence, the vector of in-situ blocked forces $\mathbf{f}_{bl}$ which characterises the revolving source is expressed as a function of the aforementioned changing rotational quantities Ψ according to the following equation

$$\mathbf{f}_{bl}(\Psi) = \mathbf{Y}(\Psi)^{+}\,\mathbf{v}_{op}(\Psi) \tag{4.4}$$

Consequently, the question arises if the vector of in-situ blocked forces $\mathbf{f}_{bl}(\Psi)$ at a revolving interface can be characterised in the same manner as the vector of in-situ blocked forces at a static or quasi-static interface. In the following this question will be answered and it will be shown that the FRFs $\mathbf{Y}(\Psi)$ are not always dependent on the rotational quantities Ψ. It will be discussed that in case of the toothed belt of an EPSapa system the FRFs can be seen as constant or quasi constant if the toothed belt is produced without a defective tooth, for instance. This assumption is applied within the case study that is presented in subsection 4.5.4.

In contrast to a static or a quasi-static interface, a revolving interface is characterised through a constant change at the contact zone between a vibrational source and a passive receiver. In the literature to date the receiver is mostly seen as a passive part such as a housing, a building or a fixture, for instance. However, at a revolving interface the receiver can often not be seen as static or quasi static as a result of a significant movement at the interface.

The contact zone between source and receiver is dependent on quantities such as the angular position. This is also the case for the internal interface between the TD of a BNA and a TB of an EPSapa system which is described in subsection 3.2.2. Hence it is important for the bfTPA of an EPSapa system, that a solution to this issue is found. The interface between the TB and the TD changes because the TD and the TB are both revolving in order to transfer the torque of the electric motor into a lateral movement of the toothed rack. At this point it needs to be mentioned that also other revolving sources such as gears can be characterised in the same manner. However, the movement of the source means that the teeth of the disc and the teeth of the belt which together form the revolving interface are changing within one revolution. If for instance one of the teeth at the interface (c) is defective the FRFs $\hat{\mathbf{Y}}_{C,bc}$ between the interface (c) and the receiver side would change in contrast to a non-defective tooth characterised by $\mathbf{Y}_{C,bc}$. This is illustrated by Figure 4.5. Hence the determined in-situ blocked forces would also change according to Eq. (2.8). This limit of the methodology will be discussed in subsection 4.4.4.

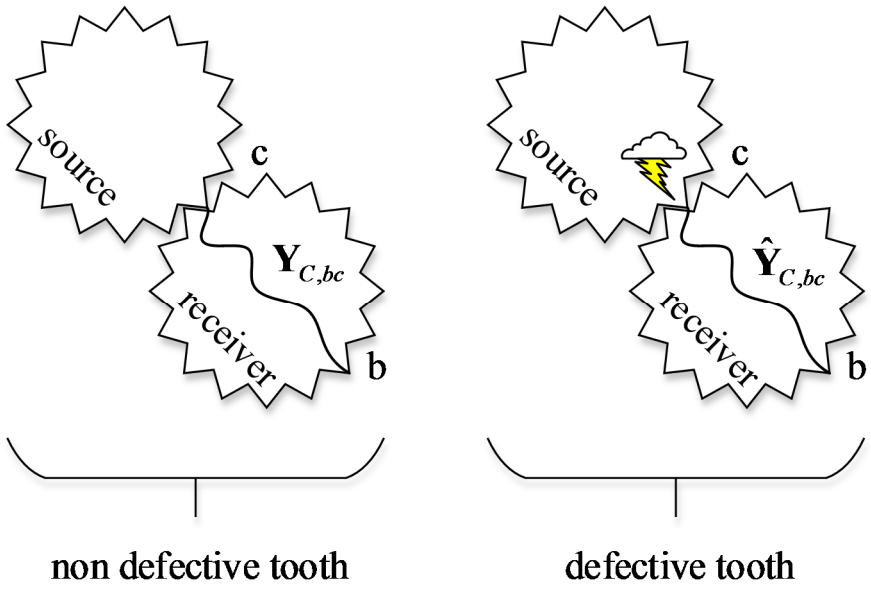

Figure 4.5: Influence of a defective tooth at the interface on experimentally determined FRFs

Nevertheless, since the gear ratio of the TD and the TB is constant an interface can be defined between the teeth of the TD and the TB. Although the internal interface changes during the cycle of a tooth mesh it is assumed that the equation of motion for the whole system does not change significantly. This means that the FRFs which are needed for the inverse calculation of the in-situ blocked forces are constant to a certain degree. The requirement for this assumption is a belt tension which is sufficiently high. However, in order to fulfil the functional task of the TB within an EPSapa system this requirement is fulfilled naturally.

4.4.3 Methodology

In the previous subsection the definition of a revolving internal interface is elucidated. However, in the following a methodology is introduced which aims to allow the determination of in-situ blocked forces at such interfaces. In order to determine the in-situ blocked forces according to Eq. (2.8) the placement of accelerometers at the interface (c) is however only necessary for the determination of the mobilities $\mathbf{Y}_{C,bc}$ when both the toothed belt and the toothed disk of the ball nut assembly are passive. Consequently the in-situ method can be applied if the accelerometers at the revolving interface are removed after the determination of the mobility matrix $\mathbf{Y}_{C,bc}$. That way it is possible to use MEMS accelerometers at the interface since their weight is assumed to have only a minor influence on the coupled system[8]. Additionally, the stiffness of the coupled system is not changed because of the MEMS accelerometers at the

[8] coupled system: source attached to receiver

interface. The approach to determine in-situ blocked forces at revolving interfaces is schematically shown in Figure 4.6.

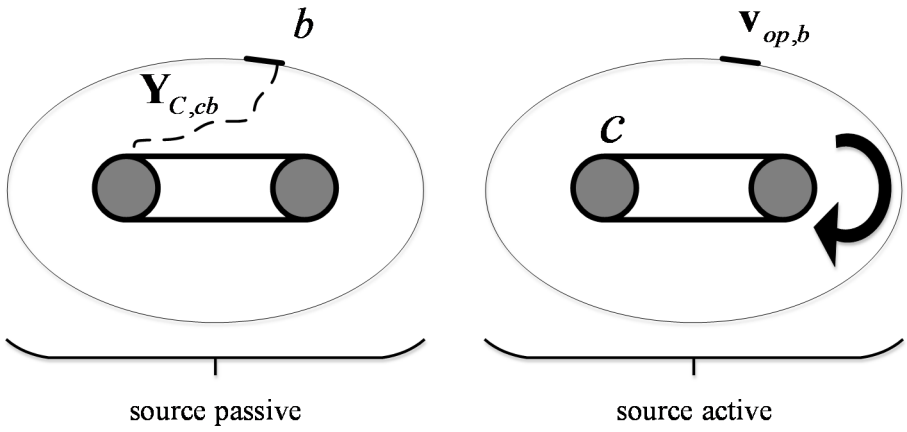

Figure 4.6: Methodology for the independent characterisation of a structure-borne sound source with in-situ blocked forces at a revolving interface (c)

The operational velocity $\mathbf{v}_{op,b}$ which is according to Eq. (2.8) necessary to calculate the in-situ blocked forces can be measured on the interface (b). This interface should be chosen as quasi static which in most cases is possible because the receiver can be defined in such a way. In case of an EPSapa system it is not necessary to solely define the revolving toothed disc as the receiver. In fact it is a big advantage if the housing of the EPSapa system is defined as receiver. Therefore the remote points are conveniently accessible with surface mounted IEPE accelerometers. This is schematically shown in Figure 4.6 on the right hand side. Based on the presented methodology one could design a specialized test rig which allows this two-stage approach because all revolving interfaces (c) are easily accessible. This yields the possibility of determining the in-situ blocked forces for a source with a revolving interface as described in subsection 2.3.4. In the following a further approach is presented which allows the determination of the blocked forces in-situ and without the need of a special test rig.

In subsection 5.4.3 and subsection 5.4.4 it will be shown that the vectors of in-situ blocked forces of the internal sources of an EPSapa system can be related with a blocked force transmissibility (BFT) matrix to the vector of in-situ blocked forces of the whole EPSapa system at its internal interfaces. Based on the functional principle of a steering system the in-situ blocked force vector $\mathbf{f}_{bl,EPS}$ of an EPSapa system can be expressed as follows

$$\mathbf{f}_{bl,EPS} = \mathbf{T}_{EM}\mathbf{f}_{bl,EM} + \mathbf{T}_{BB}\mathbf{f}_{bl,BB} \tag{4.5}$$

The right hand side of the equation contains the in-situ blocked force vectors of the electric motor (EM) $\mathbf{f}_{bl,EM}$ and the ball bearing (BB) of the ball nut assembly (BNA) $\mathbf{f}_{bl,BB}$ and the associated BFT matrices $\mathbf{T}_{EM}$ and $\mathbf{T}_{BB}$, respectively[9]. The relation between the internal and the external in-situ blocked force vectors and the corresponding transmissibility functions is shown in Figure 4.7 for the case of an EPSapa system. At this point it is remarked that this concept is applicable to every other revolving source which is connected through a bearing with a static receiver. Hence, the following methodology is not limited to the determination of in-situ blocked forces of a toothed belt within an EPSapa system.

[9] At this point it is only necessary to know that the BFT matrices yield the relation between blocked forces. However, in section 5.3 it will be explained in detail how these matrices are determined.

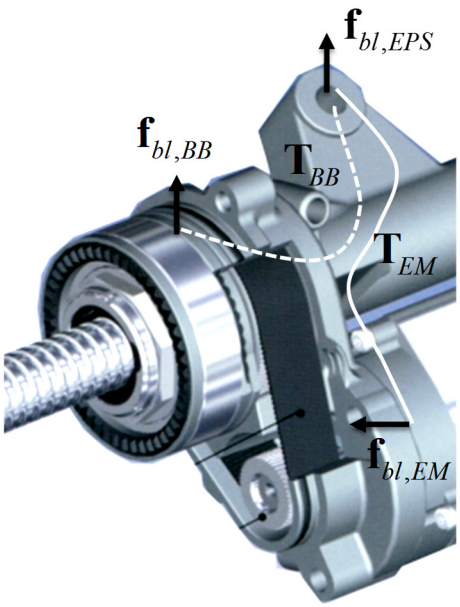

Figure 4.7: Methodology for the characterisation of a rotating toothed belt with in-situ blocked forces and transmissibility

The in-situ blocked force $\mathbf{f}_{bl.BB}$ that are determined at the ball bearing are the sum of the blocked forces of the BNA $\mathbf{f}_{bl,BNA}$ and the TB $\mathbf{f}_{bl,TB}$ as follows

$$\mathbf{f}_{bl,BB} = \mathbf{f}_{bl,BNA} + \mathbf{f}_{bl,TB} \tag{4.6}$$

Using Eq. (4.6) one can rewrite Eq. (4.5) as follows

$$\mathbf{f}_{bl,EPS} = \mathbf{T}_{EM}\mathbf{f}_{bl,EM} + \mathbf{T}_{BB}(\mathbf{f}_{bl,BNA} + \mathbf{f}_{bl,TB}) \tag{4.7}$$

Eq. (4.7) can now be solved for the unknown in situ blocked forces of TB $\mathbf{f}_{bl,TB}$ as follows

$$\mathbf{f}_{bl,TB} = \mathbf{T}_{BB}^{-1}(\mathbf{f}_{bl,EPS} - \mathbf{T}_{EM}\mathbf{f}_{bl,EM}) - \mathbf{f}_{bl,BNA} \tag{4.8}$$

The in-situ blocked forces of the EPSapa system $\mathbf{f}_{bl,EPS}$ can be determined for a particular operational state. This operational state is defined by a rotating speed of the EM and the BNA. Therefore the in-situ blocked forces of the EM $\mathbf{f}_{bl,EM}$ and the BNA $\mathbf{f}_{bl,BNA}$ can be independently

determined from each other for the same operational state. This is possible because of the receiver independent nature of blocked forces. The transmissibility matrices $\mathbf{T}_{BB}$ and $\mathbf{T}_{EM}$ can be determined while the EPSapa system is coupled with a receiver. Therefore it is possible to calculate the blocked forces of the toothed belt $\mathbf{f}_{bl,TB}$ according to Eq. (4.8).

4.4.4 Limits of the methodology

Although MEMS accelerometers which are of small size and low weight are used it is potentially possible that the MEMS accelerometers significantly change the weight of the source. In the case of a toothed belt, this influence is assumed to be negligible. Since the MEMS accelerometers which are placed at the interface for the sake of determining the necessary FRFs have to be removed during the operational measurements the equation of motion can be different during the FRF measurements and the operational state. That way the FRF matrix which needs to be pseudo inverted according to Eq. (4.4) does not correlate with the coupled system consisting of source and receiver during the operational state. One has to estimate the influence of this issue. Hence, a further investigation of a ratio between the weight of the source and the MEMS accelerometers is seen as useful.

Additionally the in-situ blocked force method is especially valid for LTI systems. Therefore the question arises if the in-situ blocked forces are also valid for a source with a resilient behaviour at the interface such as a toothed belt, for instance. However, in subsection 4.5.4 it will be shown that for a toothed belt on a test rig this effect is negligible. Nevertheless this might not be true for other resilient source. Hence further investigation should be focussed on resilient sources.

The third consideration is towards the revolving interface. In case of a toothed belt the interface is treated as only one meshing tooth on source and receiver side. However, one could think of

cases which do not allow such an assumption. Hence it would be necessary to prove that the FRFs do not significantly change as a consequence of the rotation of the source.

4.5 Case studies: In-situ blocked forces of internal sources

4.5.1 Introduction

The objectives of the presented thesis are listed and introduced in section 1.5. One of the stated objectives is the independent characterisation of the structure-borne sound generated by each of the prominent internal sources of an EPSapa system which are identified and explained in subsection 3.3.2. The achievement of this objective is crucial for fulfilling the main aim of the thesis, which is the implementation of a bfTPA to an EPSapa system. By conducting the bfTPA approach that will be proposed and outlined in detail in chapter 5 the question is answered which internal source contributes the most to the structure-borne sound of the chosen EPSapa system.

For the sake of the characterisation of an internal structure-borne sound source in section 2.3 it was already discussed and proposed that vectors of in-situ blocked forces are the preferred quantity. That way the characterisation of the three prominent internal sources of an EPSapa system is receiver independent. This means that the effect of the housing of the EPSapa system, which is defined as the internal receiver, can be neglected. Additionally, the determined vectors of in-situ blocked forces, which characterise the strength of the internal sources, serve as input quantity for the novel bfTPA method. However, in order to carry out the proposed bfTPA it is crucial to confirm that the vectors of in-situ blocked forces, characterising

the three main internal sources of an EPSapa system, can be experimentally determined accurately. This includes the different interface characteristics of each internal source.

For those reasons, three experimental case studies are carried out in order to prove that the necessary vectors of in-situ blocked forces can be experimentally determined using embedded MEMS accelerometers, as proposed in section 4.2. Furthermore the achieved results of the three case studies will prove that the discretisation of continuous interfaces according to the methodology proposed in section 4.3 yield meaningful results of in-situ blocked forces. Moreover the methodology, which is presented in section 4.4, is applied to deal with an internal source and its revolving interface.

The procedures of the three case studies are basically the same. First the test setup for the determination of the in-situ blocked forces and the test rig including the elementary boundary conditions are described. Secondly the characteristics of the internal interfaces are clarified. This involves especially the amount of discretisation points and the DoFs at the internal continuous interfaces. Then, the experimentally determined in-situ blocked forces at the internal interfaces are discussed. Since the in-situ blocked forces are determined through an inverse method, the determined forces are validated by means of on-board validation to prove the feasibility of the proposed approach using embedded MEMS accelerometers.

Subsection 4.5.2 and subsection 4.5.3 each outline the required test setup and the results of the determined in-situ blocked forces of an electric motor and a ball nut assembly, respectively. Both aforementioned case studies represent sources with continuous interfaces. The methodology to determine the in-situ blocked forces of a toothed belt, which is a source with a revolving

interface, is applied in subsection 4.5.4. The case study whose results are presented in this subsection prove the general feasibility of the methodology for revolving interfaces which is proposed in subsection 4.4.3 of this chapter.

4.5.2 Case study I: Electric motor

The electric motor was identified in section 3.3 as one of the three main internal structure-borne sound sources of an EPSapa system. Therefore, it is crucial for the success of a bfTPA, to determine the source strength of the EM [112] in a sufficiently accurate manner, taken as meaning that the deviation of the on-board validation does not exceed 3 to 5 dB. This is an important requirement since the in-situ blocked forces are the input quantity for a of the EPSapa system. In the following, the results of the case study are presented.

The used simple test setup, which consisted of two parts, is shown by Figure 4.8.

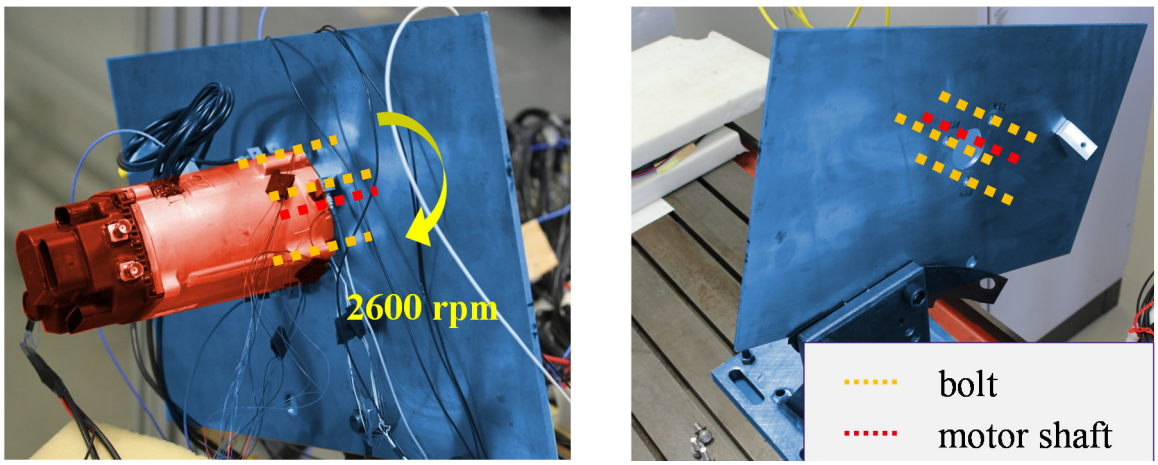

Figure 4.8: Test setup used for the experimental determination of in-situ blocked forces of an electric motor (red coloured)

The EM[10] under test (coloured red) was mounted against a thin steel plate (coloured blue). The steel plate functioned as a receiver and formed the second part of the test setup. It conveniently allows accelerometers to be placed at points remote from the interface, to apply the method proposed in section 4.2. The EM was attached to the plate with three bolts, which are symbolically represented by the three dotted orange lines. In this way a realistic mounting condition is generated as occurs in the EPSapa system. Furthermore, the number of bolts forms the basis for the discretisation of the interface between the EM and the plate. The thin steel plate had a drilled hole to carry through the pinion of the EM, symbolised in Figure 4.8 with the dotted red line. Hence the presented test setup generates the same boundary conditions as if the EM is mounted on the housing of an EPSapa. However, within an EPSapa system the EM is centred by a fit between the housing and the EM. In this case study the EM is not centred. The effect of the missing centring will be discussed in the course of the presentation of the achieved results.

However, the chosen test setup which is shown by Figure 4.8 allows the assumption that the interface between the EM and the receiver plate can be seen as continuous. Hence, no point connections between the EM and the plate which functions as receiver occur.

Close to each of the three bolts, two MEMS accelerometers were embedded, respectively. For the embedding of the accelerometers a two component adhesive was used which provided the necessary stiffness. The MEMS accelerometers are required for the determination of the in-situ blocked forces, which was described in subsection 4.2.2, and measure acceleration in two perpendicular directions. Figure 4.9 shows a cross sectional view of the interface with six embedded MEMS accelerometers in total.

[10] including the electronic control unit at the back of the EM

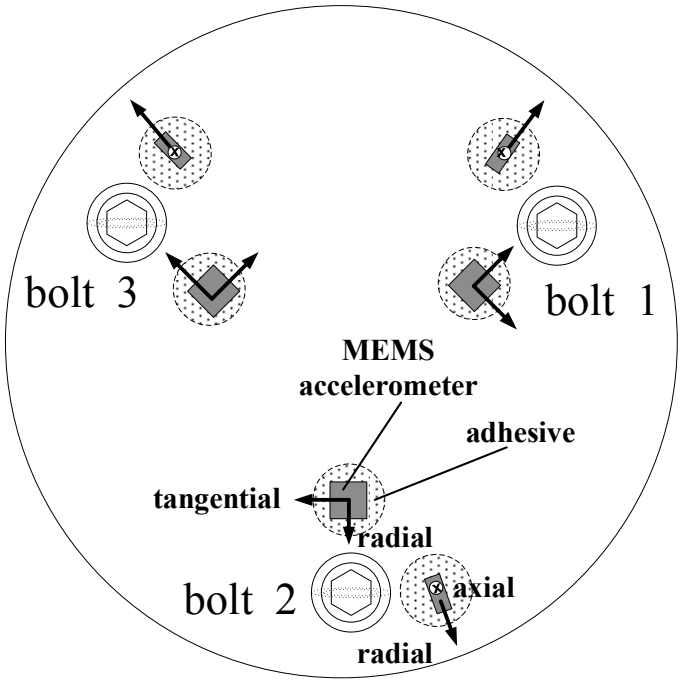

Figure 4.9: Schematic depiction of the interface between an electric motor and a receiver plate prepared with six MEMS accelerometers (2 accelerometers at each bolt)

The interface between the EM and any attached receiver such as the plate is a plain circular area which will be discretised with three points and three DoFs per point. The DoFs are chosen according to a cylindrical coordinate system. It is assumed that the vibration of an EM can be best described using radial, tangential and axial directions. Since the two embedded MEMS accelerometers at one point yield the acceleration in four directions but just three DoFs are needed to describe the source characteristics one radial direction is omitted. The locations of the accelerometers are chosen as close as possible to the three bolts since the assumption is made that the structure-borne sound will be transferred from the EM to the plate mainly via the three bolts. It is assumed to be ideal if the points would be the same as the middle of the bolts. Unfortunately this is not possible because the MEMS accelerometers cannot be placed in the bolts.

Before embedding the MEMS accelerometers they need to be calibrated. An approach for the calibration was reviewed in section 2.2.2 and will be used in the following. The MEMS accelerometers, which are used for the conduction of all following case studies, are calibrated in this way. For the calibration a bi-axial MEMS accelerometer is placed on top of a beam and the uni-axial IEPE accelerometer on the bottom at the same cross section. The perpendicular measurement directions are labelled “x” and “y” in the following. The setup for the calibration is shown in Figure 4.10.

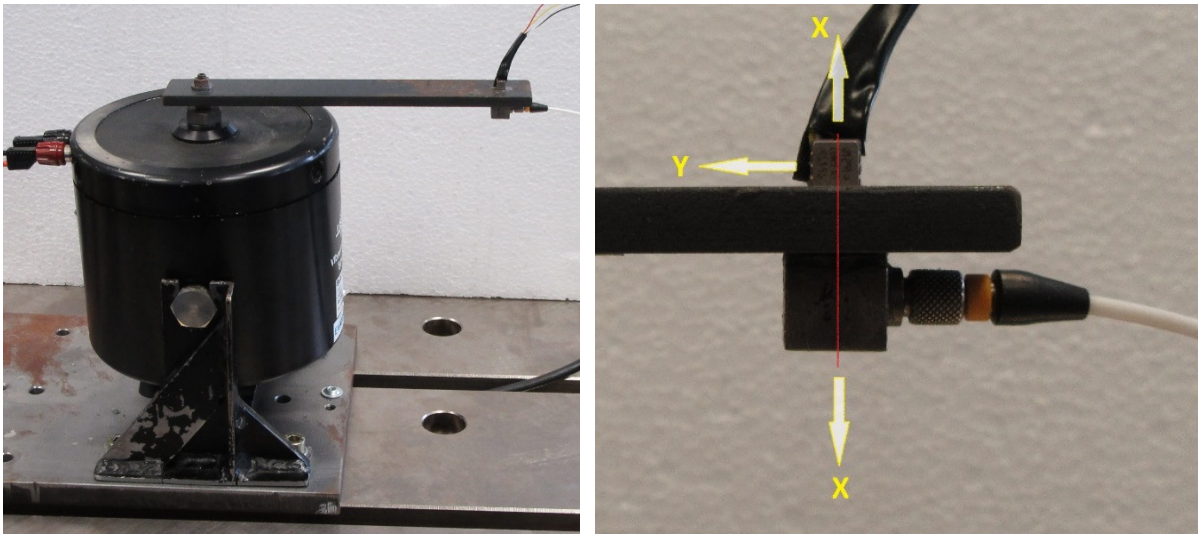

Figure 4.10: Setup for the calibration of a MEMS accelerometer

Figure 4.11 shows the comparison between FRFs of the beam, measured with a MEMS accelerometer and an integrated electronics piezoelectric (IEPE) accelerometer. It can be observed that in the frequency range below 1 kHz the agreement between the MEMS and the reference accelerometer is within 2 dB. However, above 1 kHz calibration of the MEMS accelerometer is needed since there is a drift in magnitude of the FRFs, which constantly increases with frequency.

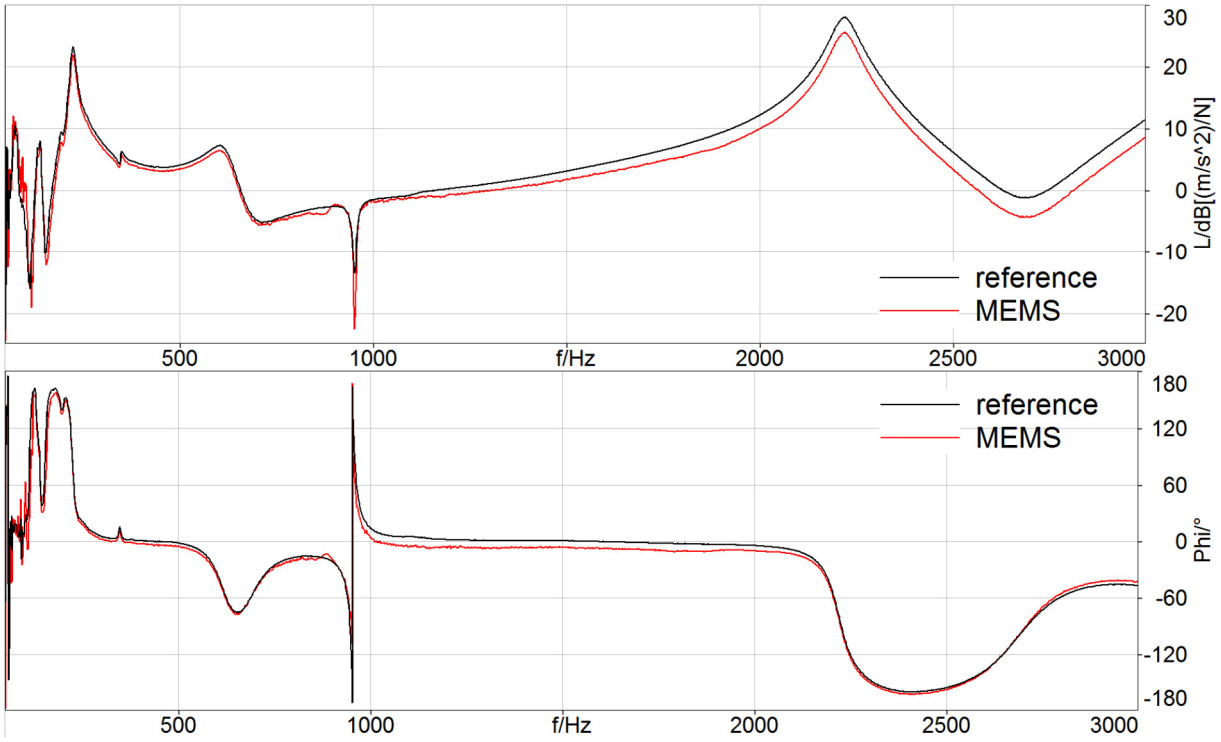

Figure 4.11: Comparison of FRFs of a cantilever beam mounted on a shaker measured with a MEMS accelerometer (red curve) and a reference accelerometer (black curve); upper diagram: magnitude; lower diagram: phase

The filter for the calibration of the MEMS accelerometer, which is determined according to Eq. (2.1), is shown on the bottom in Figure 4.12 for one of the two perpendicular axes of the MEMS accelerometer (x-direction). On top the calibrated measurement signal of the MEMS accelerometer is shown. No adjustments were made to the phase spectrum since, from Figure 4.11, this was considered unnecessary. In theory the phase can be calibrated as well if the calibration filter is multiplied with the complex time signal of the measured acceleration.

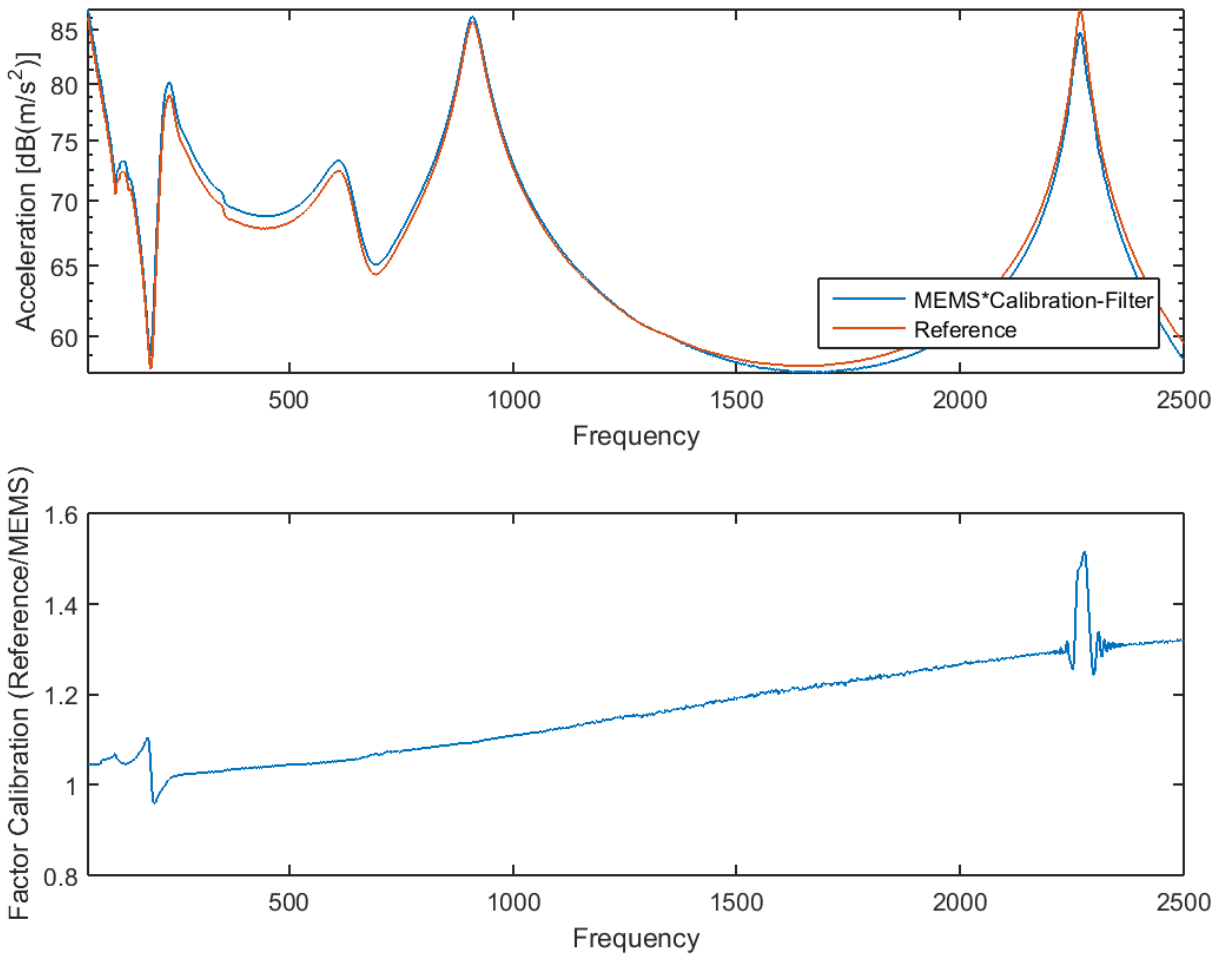

Figure 4.12: Filter for MEMS accelerometer (bottom) and result of calibrated x-axis (top)

It can be observed that by applying the filter the signal can be adjusted so as to agree with the IEPE accelerometers, especially above 1 kHz. This means that the deviation between the acceleration signals, measured with MEMS and IEPE accelerometer, is below 2 dB.

The lateral sensitivity of MEMS accelerometers, used in this case study, is shown in Figure 4.13. It shows the comparison between the spectra of the measured acceleration in the two perpendicular measurement directions of the MEMS accelerometer. In this case only the x-direction of the accelerometer was excited with the shaker.

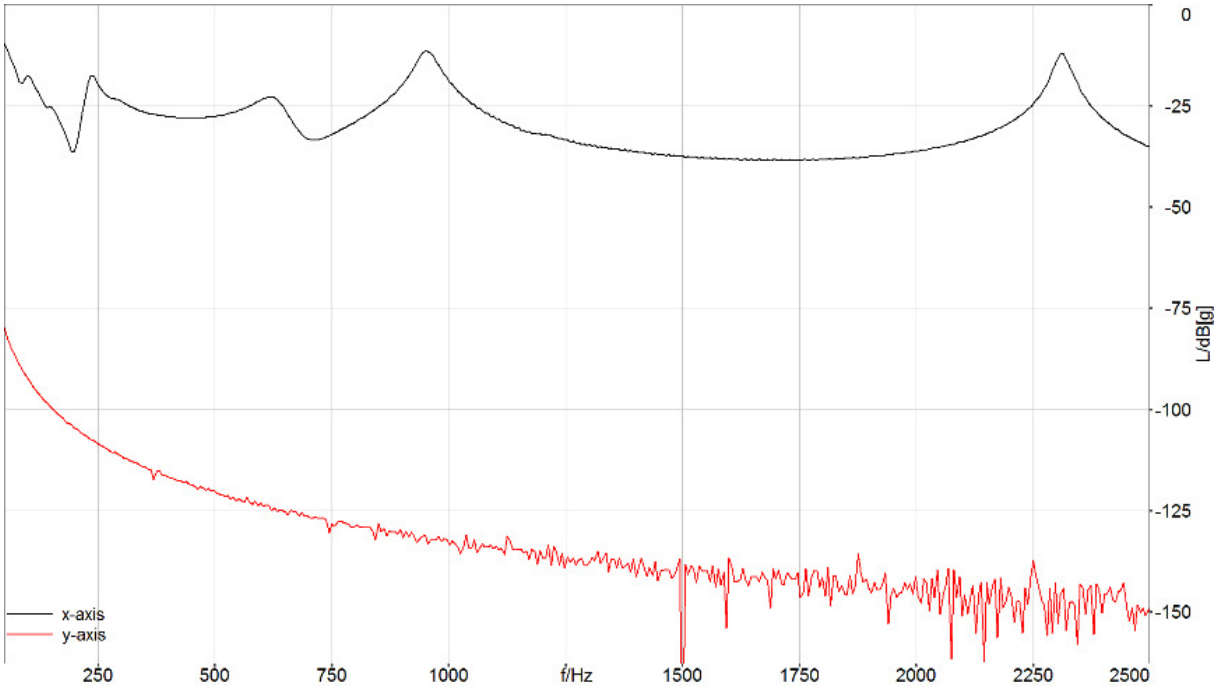

Figure 4.13: Spectra of measured acceleration with a MEMS accelerometer when only x-direction is excited

It can be observed that excitation in x-direction of the MEMS accelerometer yields a dominant measurement signal in this direction. There is no observable cross talk onto the y-axis spectrum which appears to consist purely of noise, at least 70 dB below the x-axis signal. For completeness in Figure 4.14 the calibration of the second measurement axis (y-direction) of the MEMS accelerometer is presented and shows similar characteristics to that from the x-direction.

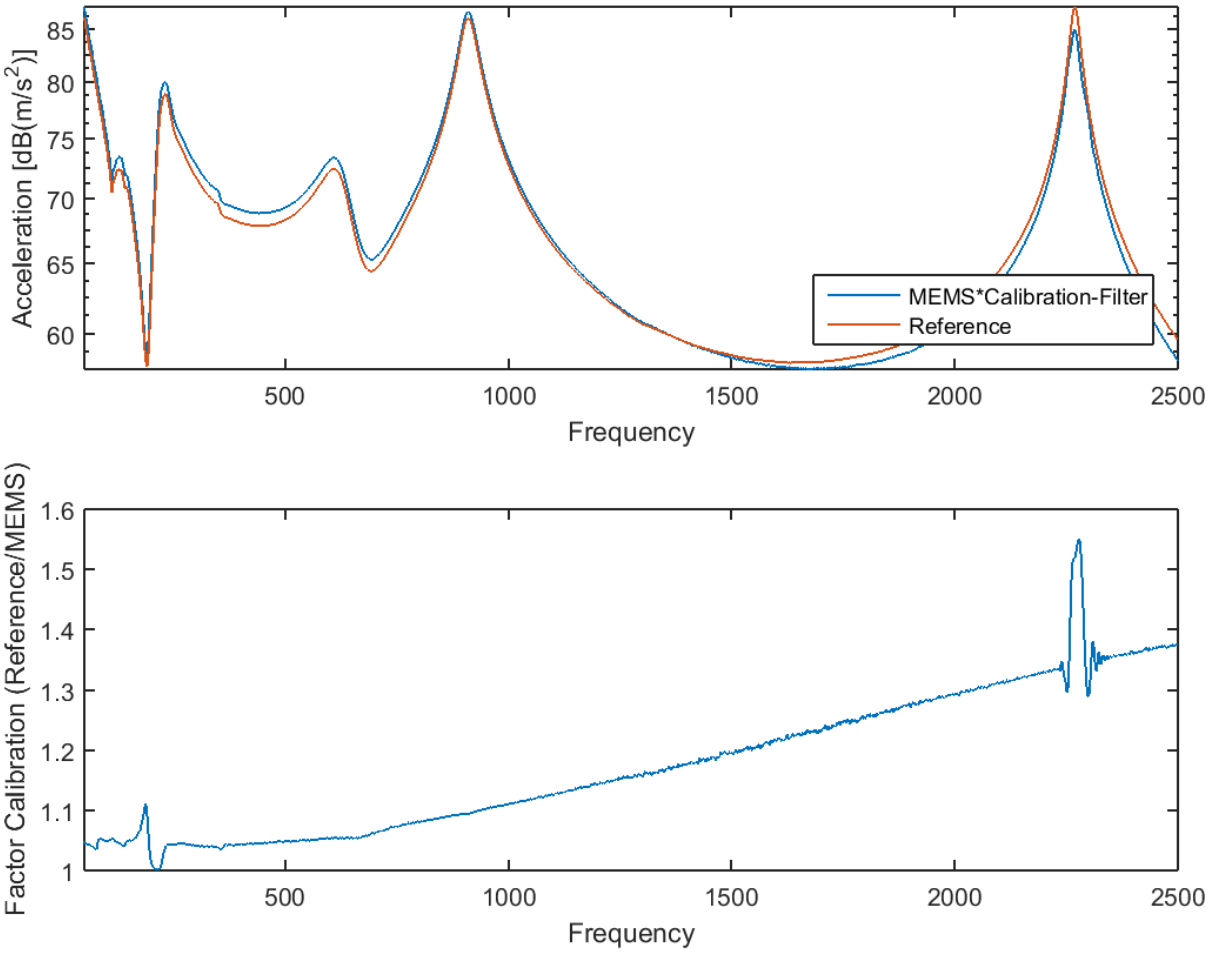

Figure 4.14: Filter for MEMS accelerometer (bottom) and result of calibrated y-axis (top)

The measurement points, namely remote points (RP) on the plate are shown in Figure 4.15. The point which is chosen out of the 24 remote points for the validation is labelled RP20.

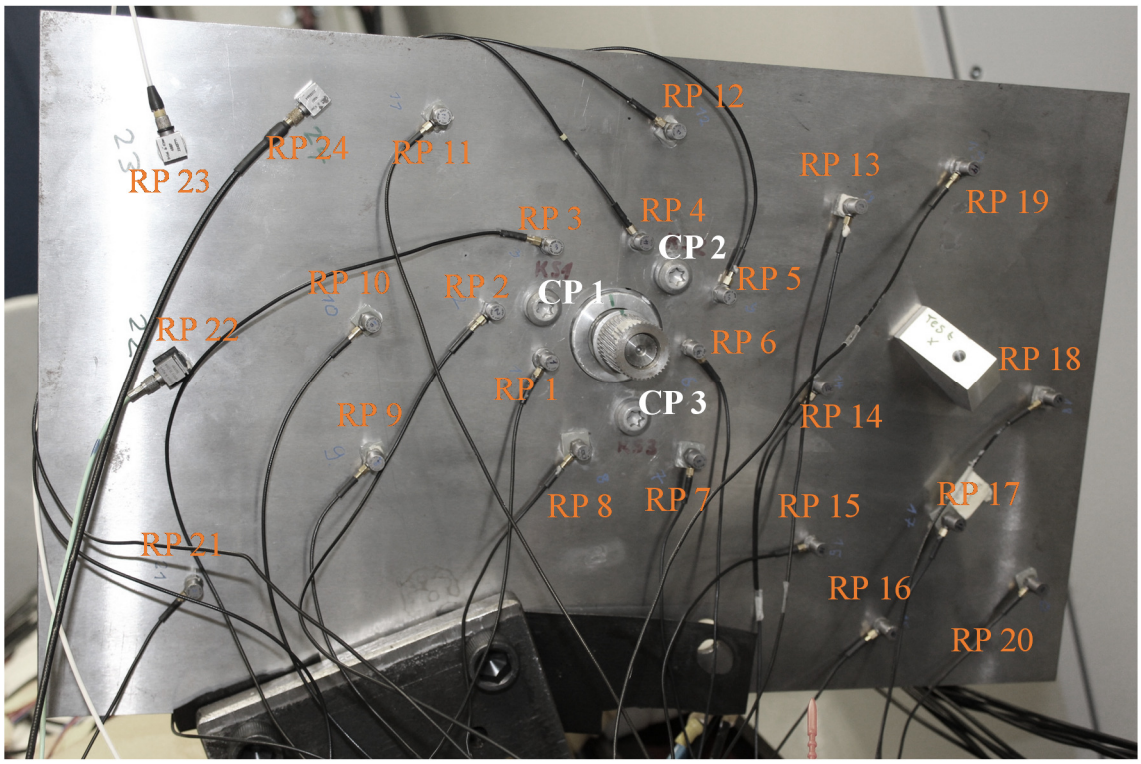

Figure 4.15: Measurement points for determination of in-situ blocked forces of an electric motor: 24 remote points (RP), validation point (RP20) and 3 coupling points (CP1 – CP3)

In the following preliminary measurement results for the determination of the in-situ blocked forces of an electric motor are shown. This includes the following analysis:

- the signal-to-noise-ratio (SNR),
- the force spectrum of the excitation at the remote points for the determination of the mobility functions,
- the coherence and mobility functions between the validation location and the DoFs at the internal interface and
- the condition number of the mobility matrix.

In subsection 4.5.3 and 4.5.4 the same preliminary analysis, except for the force spectrum, are shown for the case studies of a ball nut assembly and a toothed belt, respectively.

In order to be able to inversely calculate the in-situ blocked forces a sufficient SNR of the measured acceleration at the remote points on the receiver is required. A SNR of at least 10 dB is defined as sufficient. The colour diagram on top of Figure 4.16 shows the SNR at all of the 24 remote points. The worst SNR is at RP10. On the bottom the spectra of the acceleration signal and the noise at RP10 is shown. Frequencies with a SNR below 10 dB are marked red.

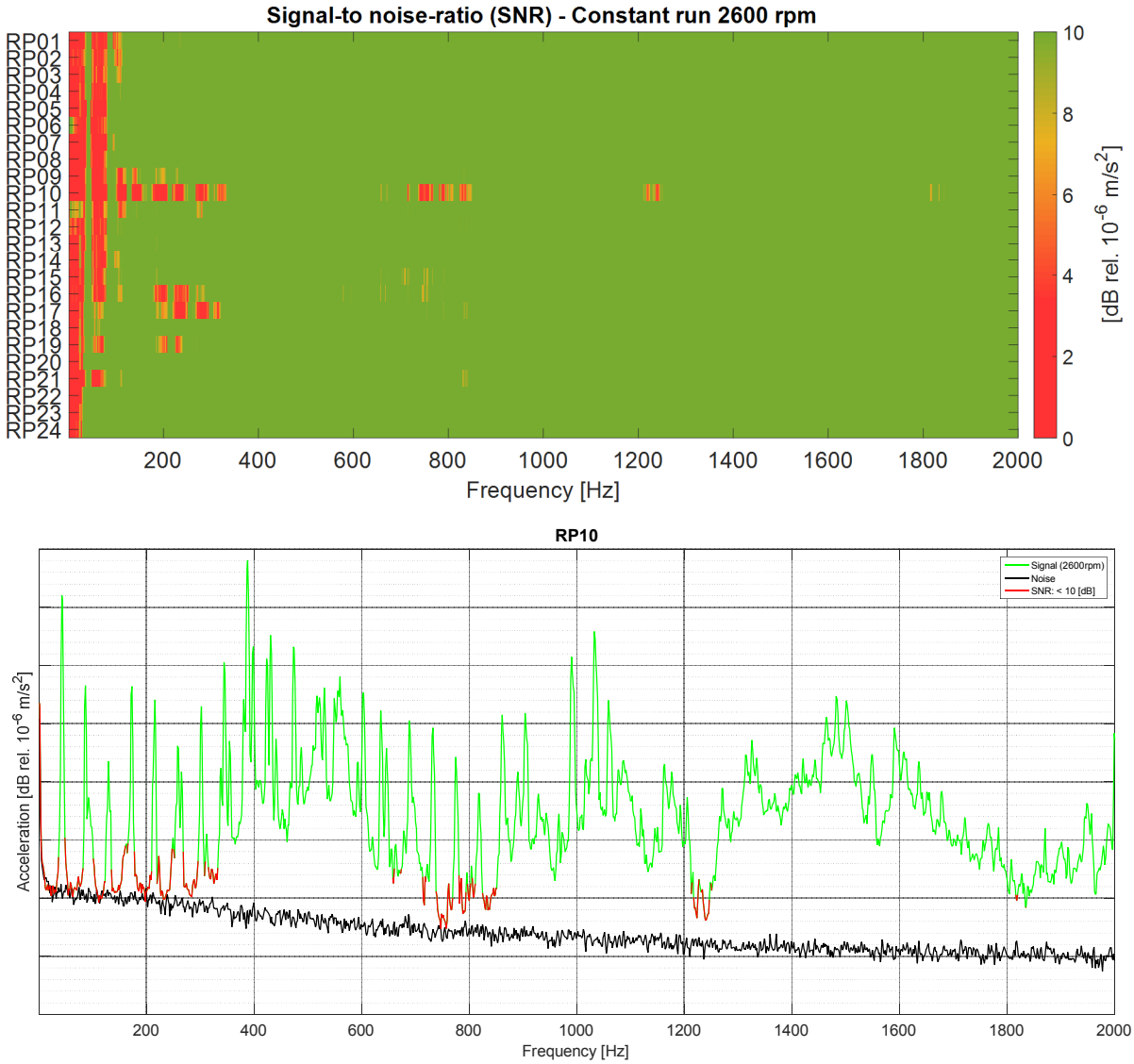

Figure 4.16: Signal-to-noise-ratio (SNR); top: SNR at all 24 remote points (RP); bottom: Signal and noise at RP10; Grid: 10 dB

It can be observed from the top diagram that the SNR at the 24 RPs is generally above 10 dB. The bottom diagrams shows that especially at the peaks, which refer to the orders of the electric motor, the SNR is always above 10 dB.

A drop of 10 dB in the spectrum of applied forces is taken as a guide to the highest frequency at which mobilities can be measured. As indicated in Figure 4.17 this upper bound is at 1800 Hz for this case. Above 1800 Hz the excitation force at the remote points is considered as too low for the determination of mobility functions.

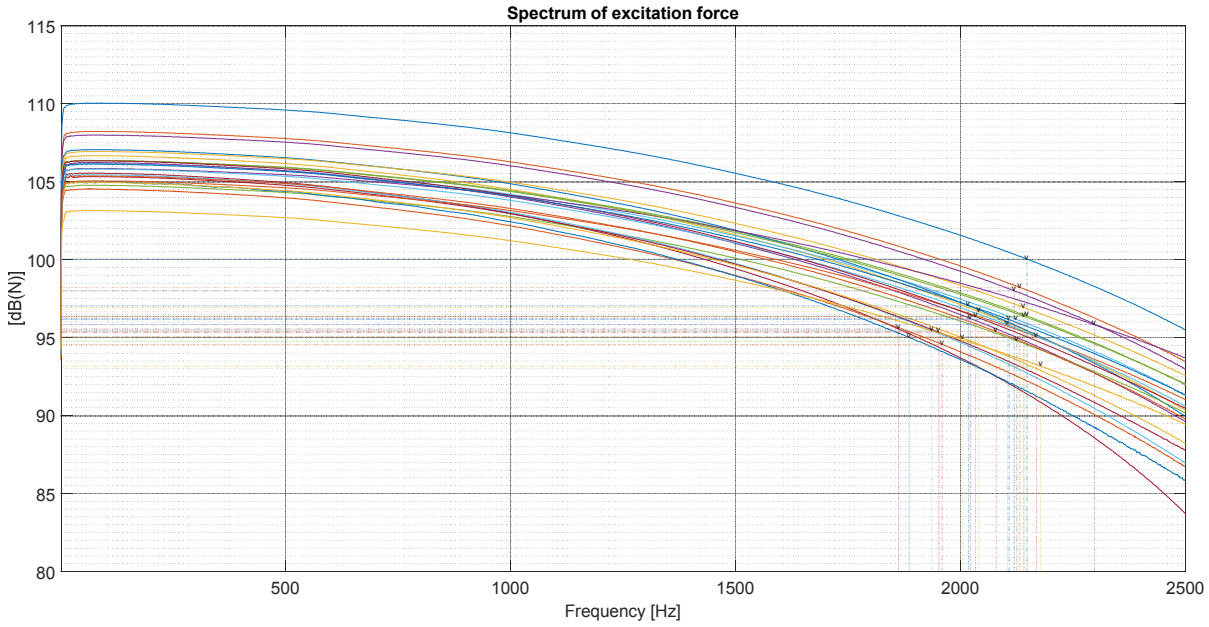

Figure 4.17: Spectrum of the excitation at the remote points

In Figure 4.18 the mobility functions between the validation point and the 9 DoFs at the internal interface between the EM and the plate are shown.

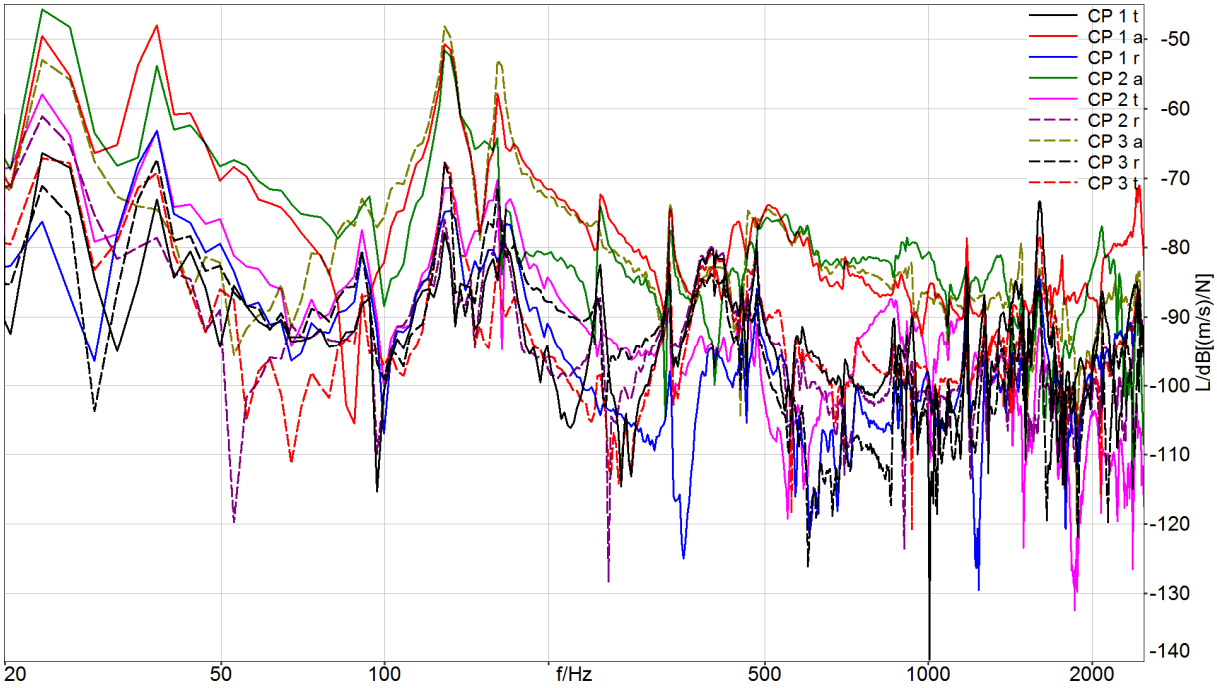

Figure 4.18: Mobility between validation point and degrees of freedom at internal interface at bolts

The assembly of the electric motor and the plate shows dominant resonances in the frequency range up to 2.5 kHz. Especially the mobility functions between the axial DoFs and the validation location are dominant in the shown frequency range.

The coherence is often chosen as a criterion to evaluate the quality of the FRFs. The coherence functions between the validation location on the plate and the 9 DoFs at the internal interface are shown in Figure 4.19.

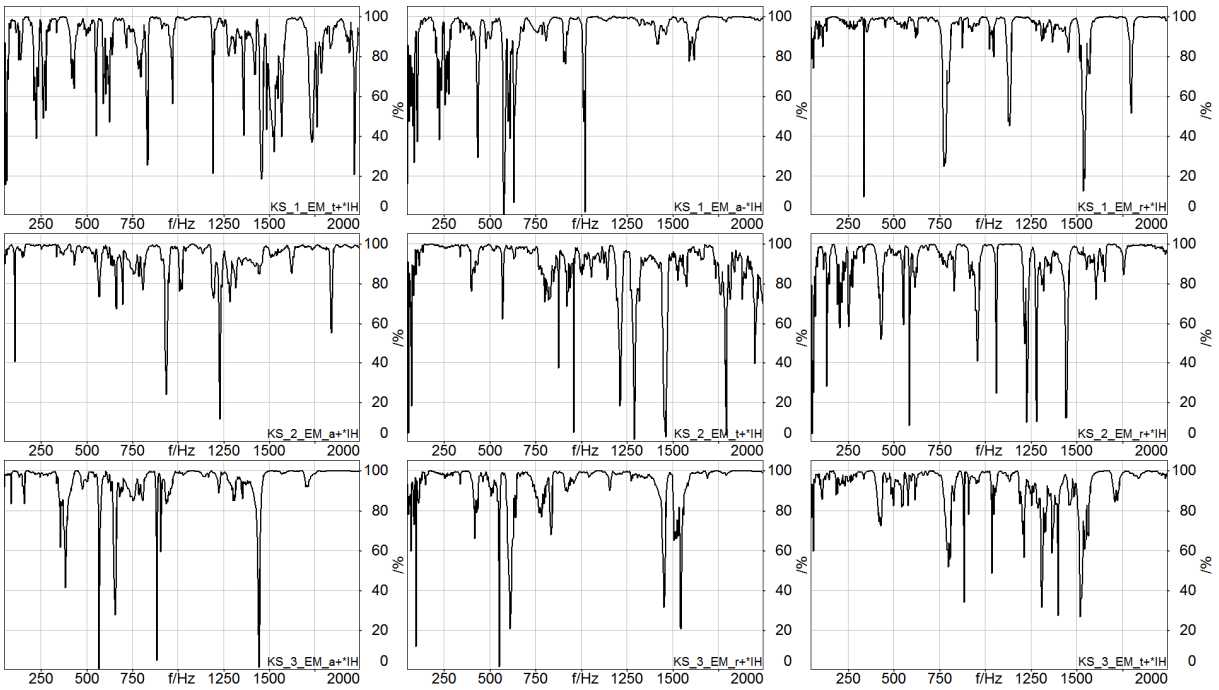

Figure 4.19: Coherence functions between validation point and degrees of freedom at internal interface

It can be observed that the coherence is generally above 95% in the frequency range above 100 Hz and below 200 Hz, except at the anti-resonances, which can be observed in Figure 4.18. This means that the test setup is a linear and time invariant system.

The condition number of a matrix is often taken as an indicator of the sensitivity of the system to inversion errors. In this case it is a criterion for the inversion of the mobility matrix, which is necessary for the calculation of in-situ blocked forces. Figure 4.20 shows the spectrum of the condition number of the matrix, which is used for the calculation of the in-situ blocked forces of an electric motor.

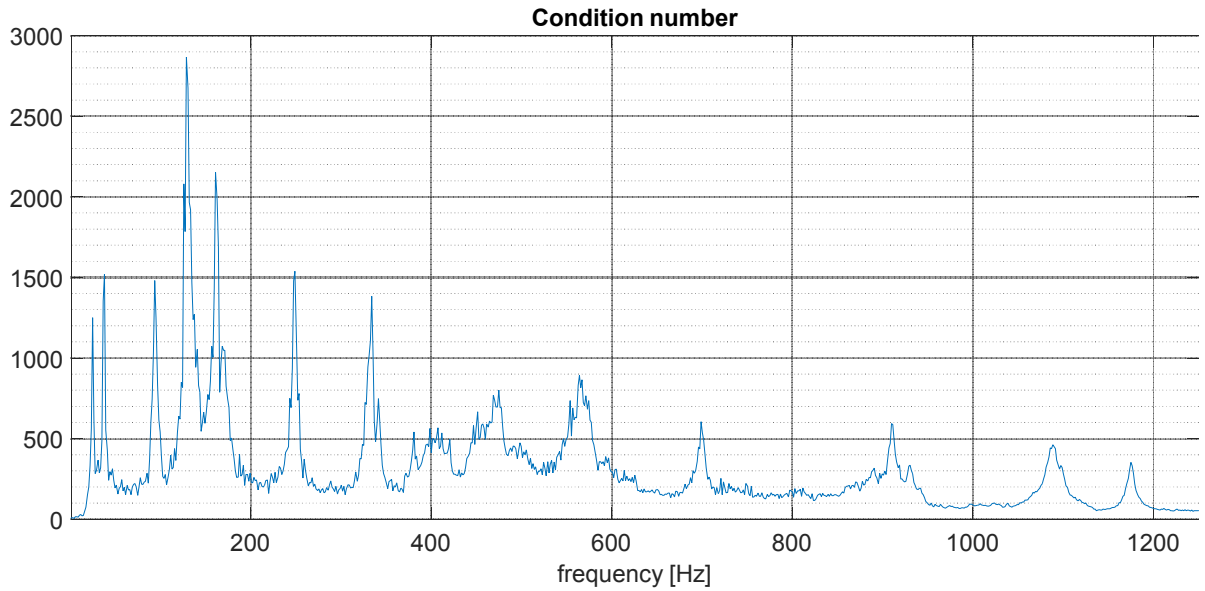

Figure 4.20: Condition number of mobility matrix

It can be observed that the condition number is significantly higher at frequencies which show a dominant resonance and anti-resonance behaviour of the assembly.

The spectra of the determined in-situ blocked forces of the EM are shown in Figure 4.21, Figure 4.22 and Figure 4.23 for a constant rotating speed of the EM with 2600 rpm. Such a so called "constant run" is chosen because most of the NVH requirements of an EPS system are specified for a constant steering speed which also means that the EM runs with a constant rotating speed. Every diagram shows the in-situ blocked forces in one direction at every of the three bolts in a frequency range from 10 Hz to 1250 Hz. Figure 4.21 shows the in-situ blocked forces in axial direction, Figure 4.22 in radial direction and Figure 4.23 in tangential direction (compare Figure 4.9). The blue curves show the forces at the first bolt, the red dotted curves at the second bolt and the yellow dashed curves at the third bolt (compare Figure 4.9).

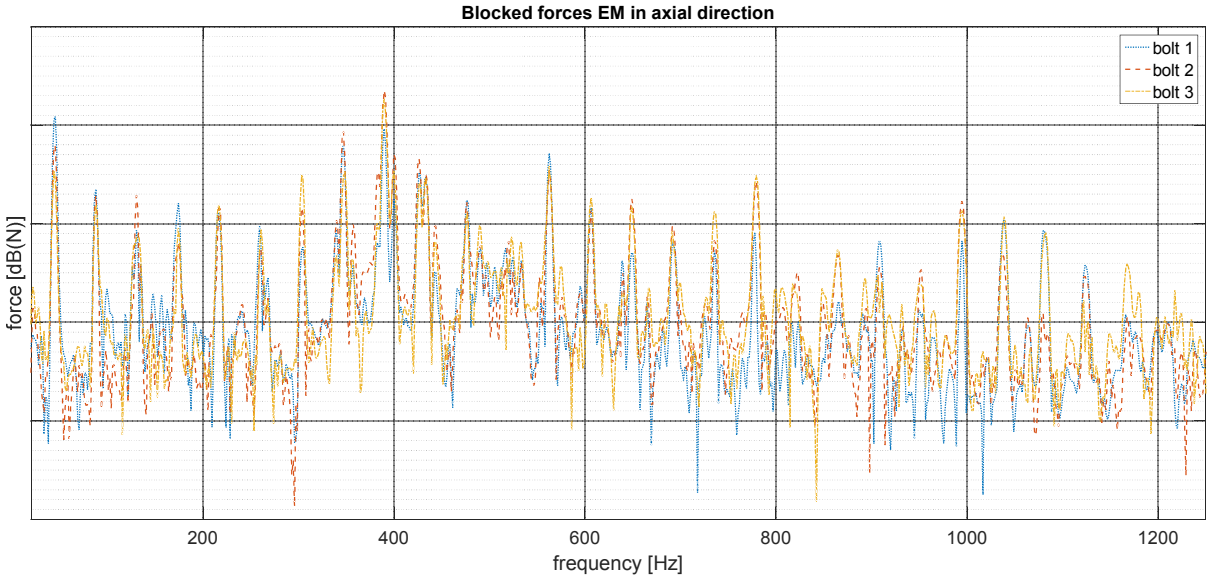

Figure 4.21: Spectra of in-situ blocked forces of an electric motor (EM); axial direction; grid ordinate: 20 dB

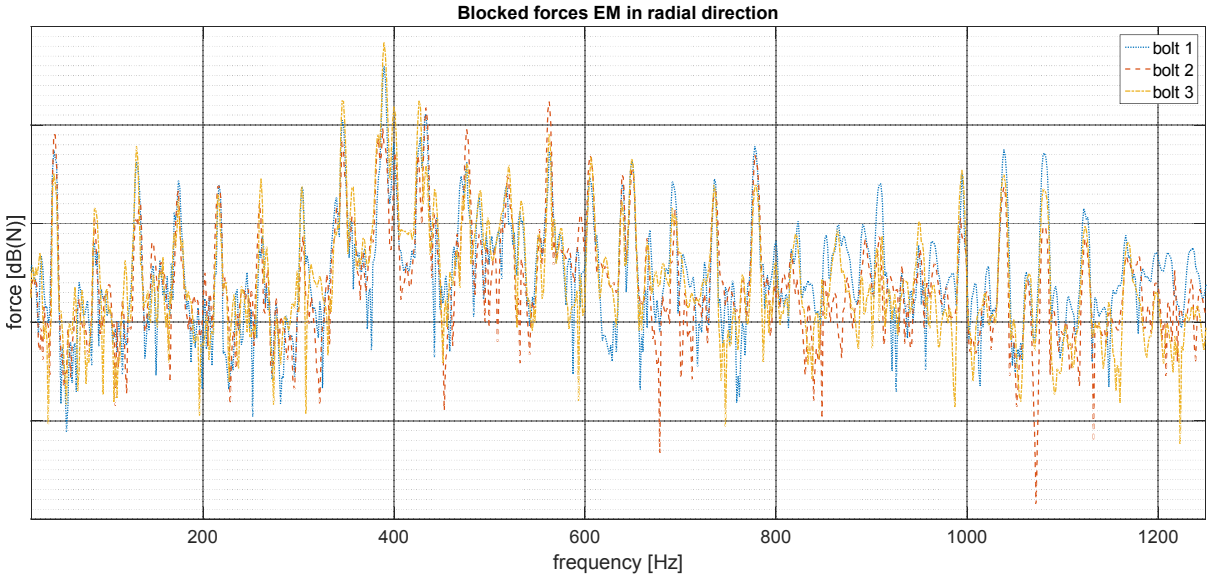

Figure 4.22: Spectra of in-situ blocked forces of an electric motor (EM); radial direction; grid ordinate: 20 dB

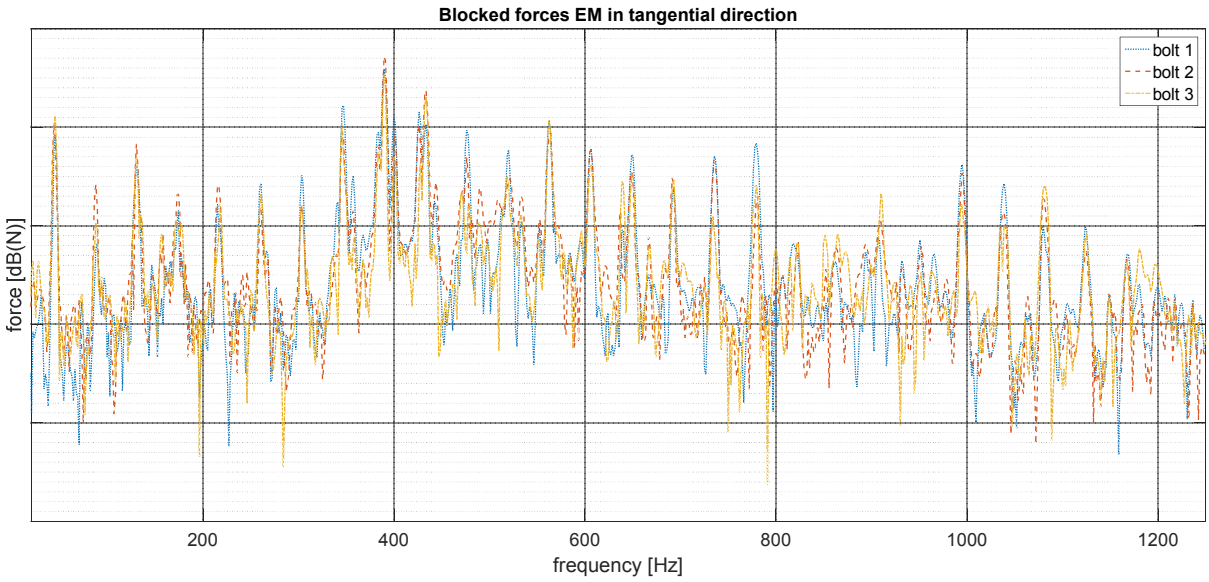

Figure 4.23: Spectra of in-situ blocked forces of an electric motor (EM); tangential direction; grid ordinate: 20 dB[11]

It can be observed from Figure 4.21, Figure 4.22 and Figure 4.23 that the magnitude of the in-situ blocked forces are within 10 dB at the peaksfor one of the three cylindrical directions at every of the three chosen positions near the bolts on the interface. Although there are some exceptions at some peaks, this means that the distribution of the structure-borne sound over the interface can be seen as nearly constant. This behaviour is expected since the used tightening torque for all three bolts was the same and additionally the EM can be assumed as rotationally symmetric.

Every peak of the blocked force in the spectra shown in Figure 4.23 represents one order O of the EM according to the following equation,

[11] In the following all graphs that are related to an EPSapa system and its components only show relative values. However, the grid of the ordinate is always specified in the caption.

$$\omega = On \tag{4.9}$$

where ω denotes the frequency and n the rotating speed of the EM. Since the rotating speed n is constant every peak of the blocked force at a certain frequency can be related easily with an order of the EM. Usually the spectrum induced by an EM are expected to show only a few dominant orders which are related to its functional principle. However, in the presented case the EM was modified[12] which probably caused an imbalance of the shaft. This leads to a first order at a frequency of 43 Hz which can be observed in the spectra shown in Figure 4.23. The first order and its harmonics superpose over the orders which would be expected to be dominant for an EM which is not modified. For the bfTPA approach within an EPSapa system that will be presented in subsection 5.4.3 and subsection 5.4.4 an EM will be used which is not modified at all (except for the MEMS accelerometers) and is therefore expected to show a behaviour where only a few characteristic orders are dominant.

Since the structure-borne sound can be assumed to be constant over the interface one can look in detail at the in-situ blocked forces at just one of the three bolts. The spectra of the in-situ blocked forces at bolt 1 which is shown in Figure 4.24 shows that the forces in axial direction are less dominant compared to the forces in tangential and radial direction. Furthermore it can be observed that the magnitude of the blocked forces in radial and tangential direction are within 5 dB at the peaks.. This means that the structure-borne sound characteristics of the EM is mainly dominated by the forces in tangential and radial direction.

[12] electric motor (EM) can also be used as a shaker

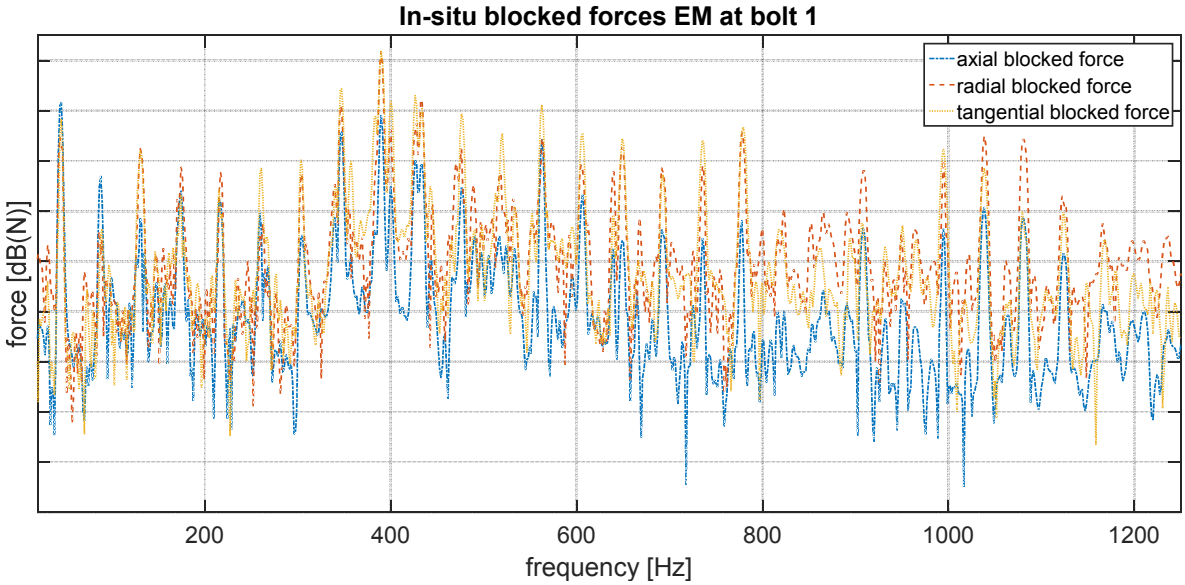

Figure 4.24: Spectrogram of in-situ blocked forces of an electric motor (EM) determined at one bolt which is used for the fixation; grid ordinate: 10dB

In subsection 2.3.5 an on-board methodology approach was outlined to validate the determined in-situ blocked forces. Figure 4.25 shows the on-board validation of the determined in-situ blocked forces of an EM. The figure shows a comparison of the measured and calculated acceleration on a randomly chosen validation point on the plate based on the in-situ blocked forces and the corresponding FRFs.

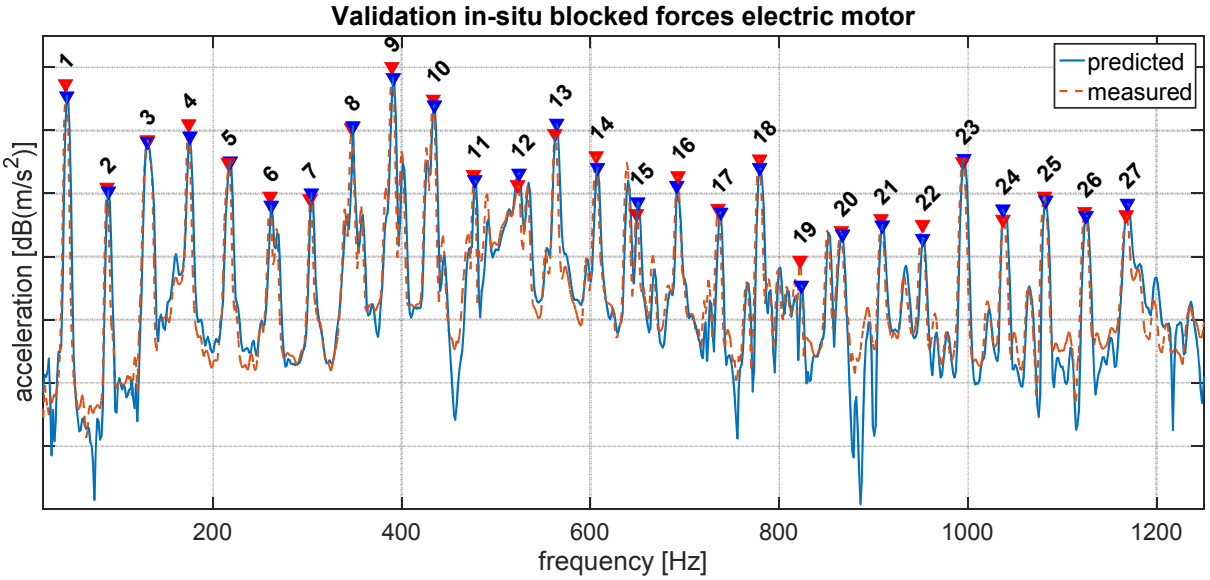

Figure 4.25: On-board validation of the in-situ blocked forces of an electric motor (EM); grid ordinate: 10 dB

It can be seen that the acceleration can be precisely predicted based on the in-situ blocked forces which means that the 9 in-situ blocked forces were determined with a deviation of below 4 dB at the peaks. The peaks represent the orders of an EM which are marked with numbers from 1 to 27. Except for the 12th and the 19th order the deviation is always below 3 dB. The deviation of the predicted and measured 27 orders is depicted as a bar graph in Figure 4.26.

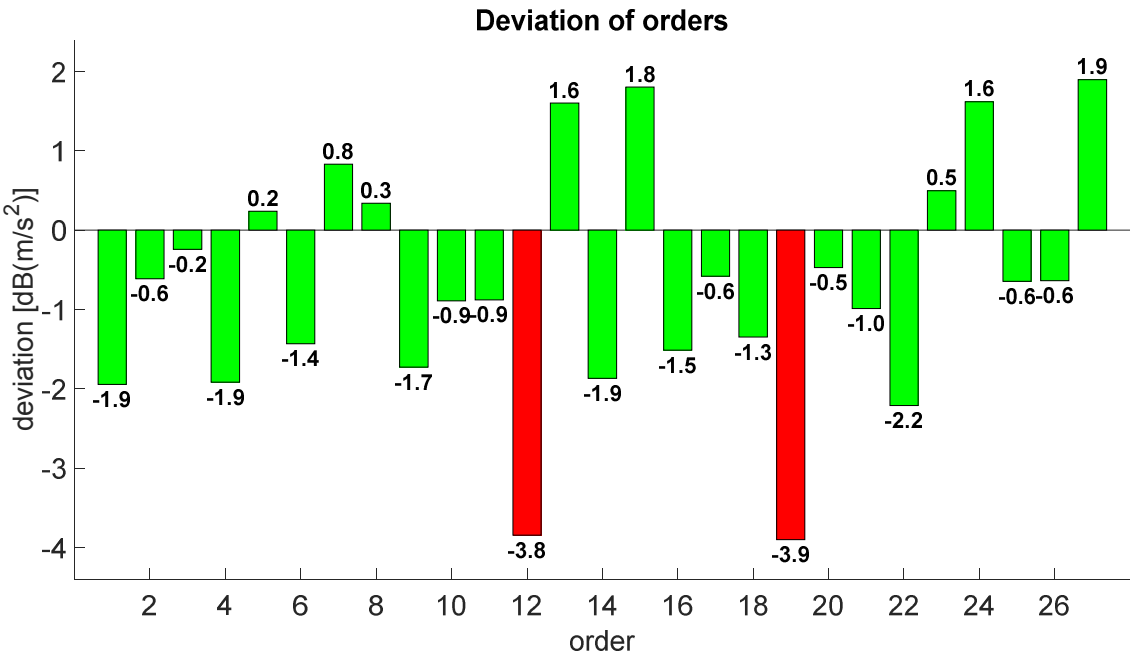

Figure 4.26: Deviation of predicted and measured orders of an electric motor (EM)

Consequently the in-situ blocked forces of an EM can be precisely identified using the in-situ blocked force method and embedded small MEMS accelerometers at the interface between the EM and the plate or any other receiver structure.

4.5.3 Case study II: Ball nut assembly

The second prominent internal source of an EPSapa system, of which the source strength needs to be characterised in terms of in-situ blocked forces, is the ball nut assembly. This part which is important for the functionality of an EPSapa system is usually considered as the least critical of the three internal sources, introduced in subsection 3.3. Furthermore the BNA can be seen as part of an important transmission path within the internal receiver of an EPSapa system according to the explanations of section 3.4.

The test setup, used to determine the in-situ blocked forces of the BNA, is shown in Figure 4.27. An already existing test bench was used which usually functions to detect damaged BNAs according to anomalies of their NVH behaviour.

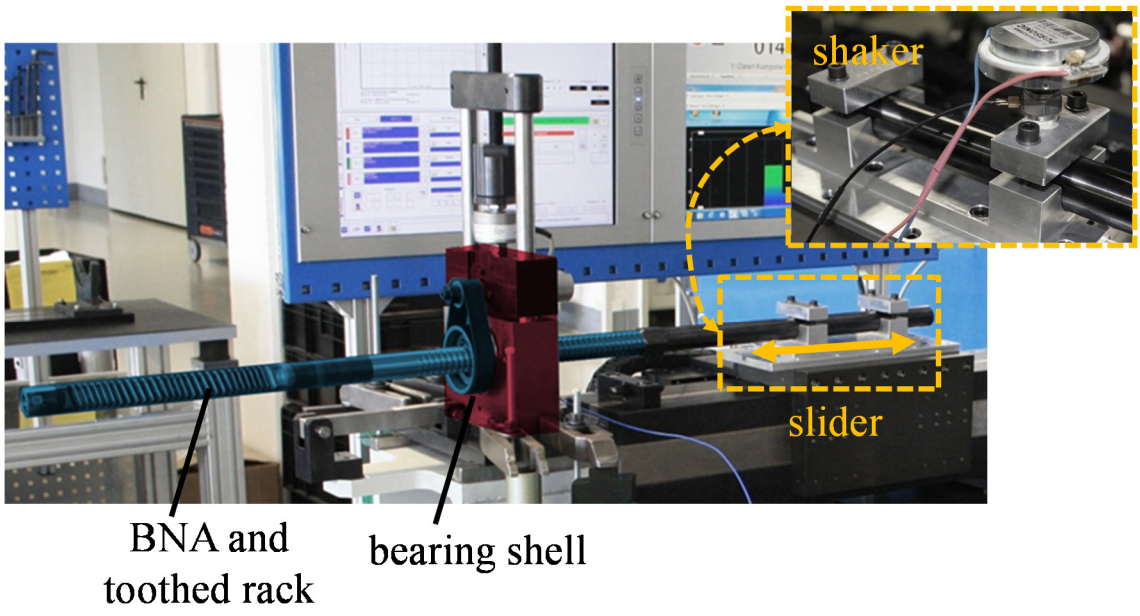

Figure 4.27: Test setup for the determination of in-situ blocked forces of a ball nut assembly (BNA)

The test bench consists of an air-springed slider that functions as a seating for a toothed rack. The toothed rack is connected with the BNA that is embedded inside a bearing shell, coloured in red. The BNA is embedded with a ball bearing. Both the slider and the bearing shell are mounted on a stiff machine bed. Since the slider, which moves the toothed rack in a lateral way and therefore drives the BNA, is air-springed it can be assumed as being the only source present during a test.

As mentioned in subsection 4.2.3 the definition of the interface is important for the determination of in-situ blocked forces. Therefore special care was taken to define the interface correctly. In Figure 4.28 the interface between the BNA and the bearing shell is symbolised as a yellow

dotted circle. The interface is chosen as the outer ring of the ball bearing of the BNA which is a cylindrical surface that was modified with a groove. This can be seen in Figure 4.28 as the blue coloured surface.

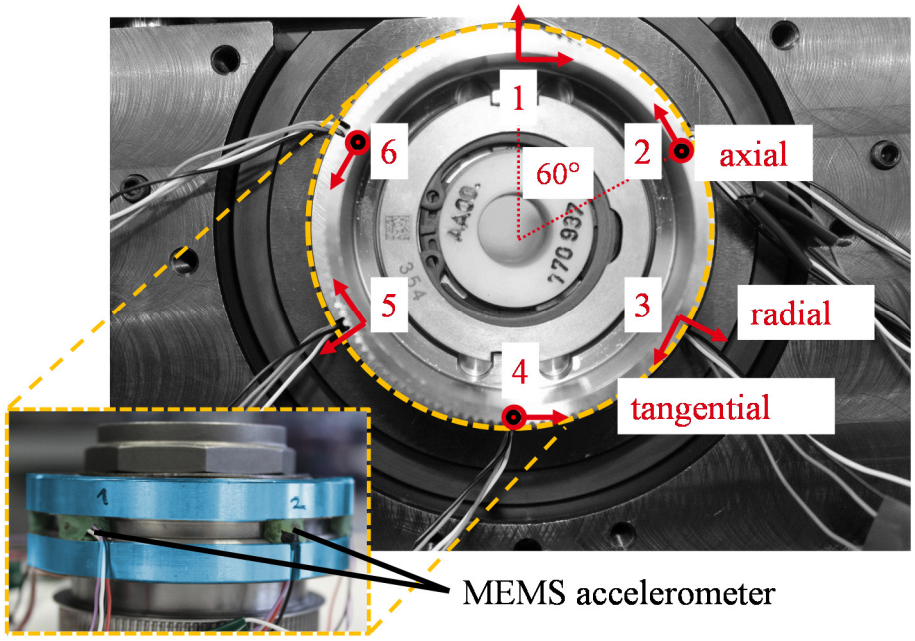

Figure 4.28: Interface between a ball nut assembly (BNA) and a bearing shell of the test rig; accelerometers embedded in outer ring of the ball bearing of a BNA in an array at 60° intervals at the coupling points (CP) 1-6

As mentioned in subsection 4.2.2, it is necessary to modify the interface to embed the MEMS accelerometers necessary to determine the in-situ blocked forces of the BNA. Therefore a groove was ground in the outer ring of the ball bearing, shown in Figure 4.28. The MEMS accelerometers, which allow measurement in two perpendicular directions, are placed in the groove to measure three radial, three axial and six tangential DoFs in total. Therefore an accelerometer is placed in the groove at every 60° angular intervals. The six positions of the MEMS accelerometers on the interface, which are called “coupling points”, can be seen in Figure 4.28.

The coordinate system for the definition of the DoFs is chosen to be cylindrical, because for a symmetrical source it has advantages over a Cartesian coordinate system.

During a measurement, a problem occurred in that the electro-pneumatic device, necessary for the function of the air spring, generated an unwanted background noise which corrupted the measurement of the operational velocities. For that reason an artificial excitation was applied to simulate an operational state. A shaker was mounted on top of the slider on the toothed rack, to excite the BNA without the electro-pneumatic supply for the air spring. The operational state was chosen to be a sine signal with a frequency of 200 Hz.

The measurement points, namely remote points (RP) on the bearing shell are shown in Figure 4.29. The point which is chosen out of the 25 remote points for the on-board validation is labelled RP20.

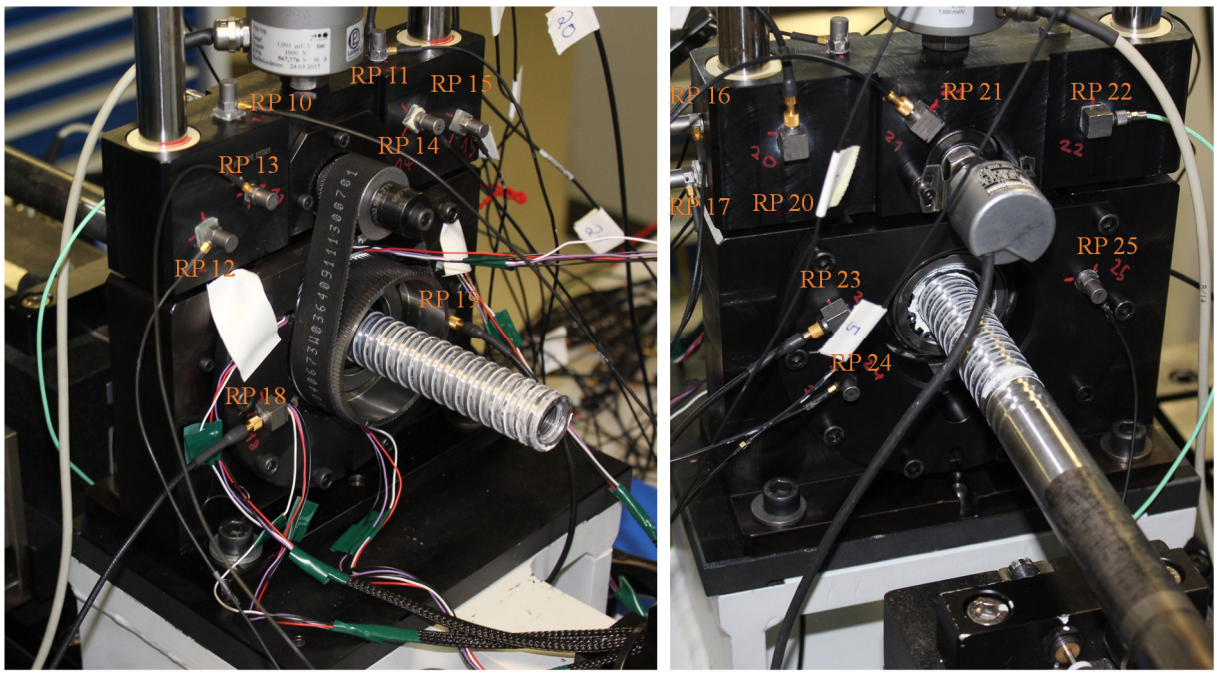

Figure 4.29: Measurement points: 25 remote points (RP) on bearing shell

The colour diagram on top of Figure 4.30 shows the SNR at all 25 remote points. On the bottom the spectra of the acceleration signal and the noise at RP20 is shown. The signal is chosen as a sine with a frequency of 200 Hz.

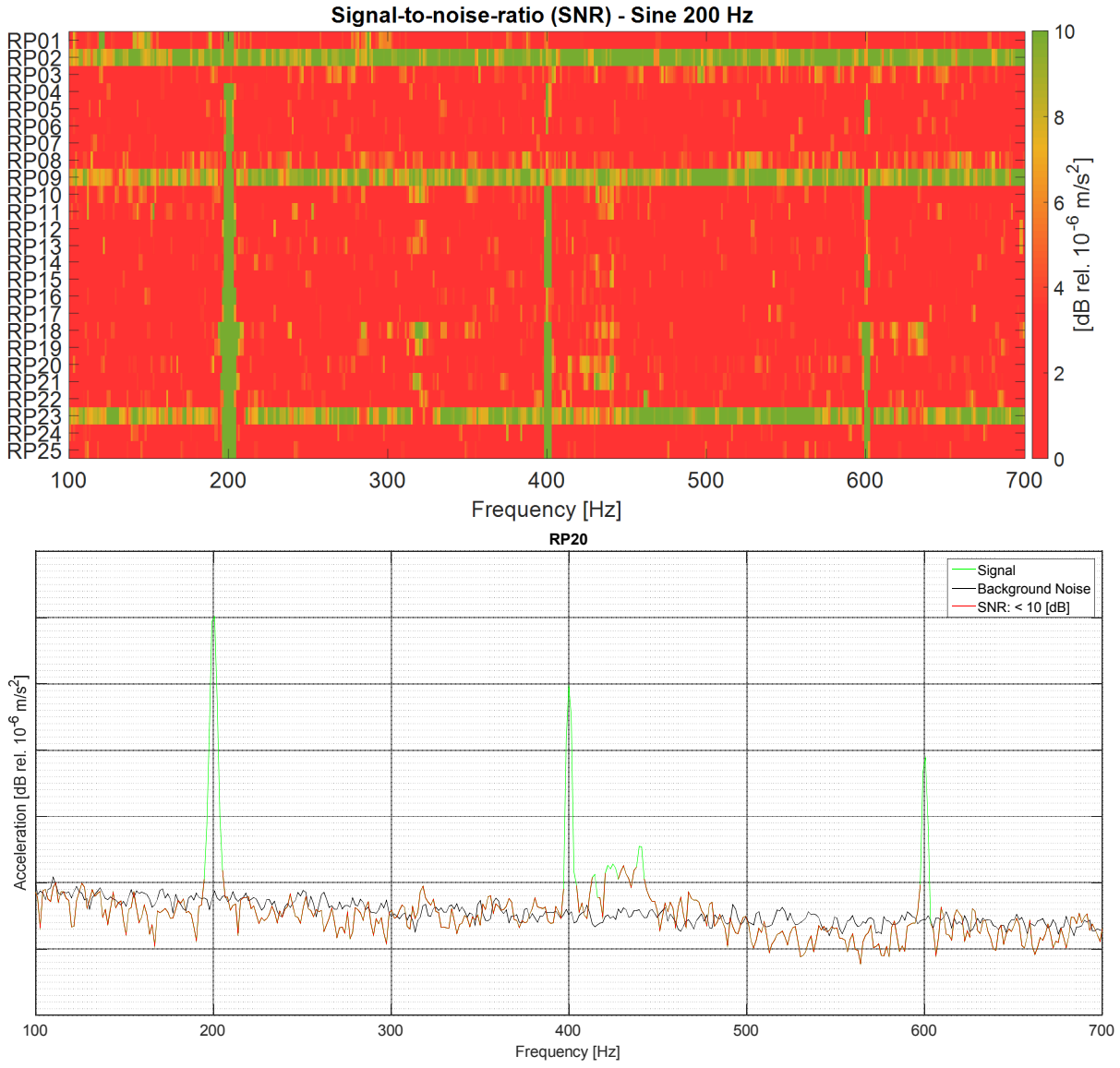

Figure 4.30: Signal-to-noise-ratio (SNR); top: SNR at all 25 remote points (RP); bottom: SNR at RP 20, Grid 10 dB

It can be observed from the top diagram that the SNR in the frequency range between 100 and 700 Hz is generally below 10 dB, except for RP02, RP09 and RP23. However, especially at the relevant peaks of 200 Hz, 400 Hz and 600 Hz, the SNR is always above 10 dB.

The upper bound for the determination of mobility functions is at 2200 Hz for this case. The same approach for the determination of the upper bound is used as shown in Figure 4.17. In Figure 4.31 the mobility functions between the validation point (RP20) and the 9 DoFs at the internal interface (CP 1-6) between the BNA and the bearing shell are shown.

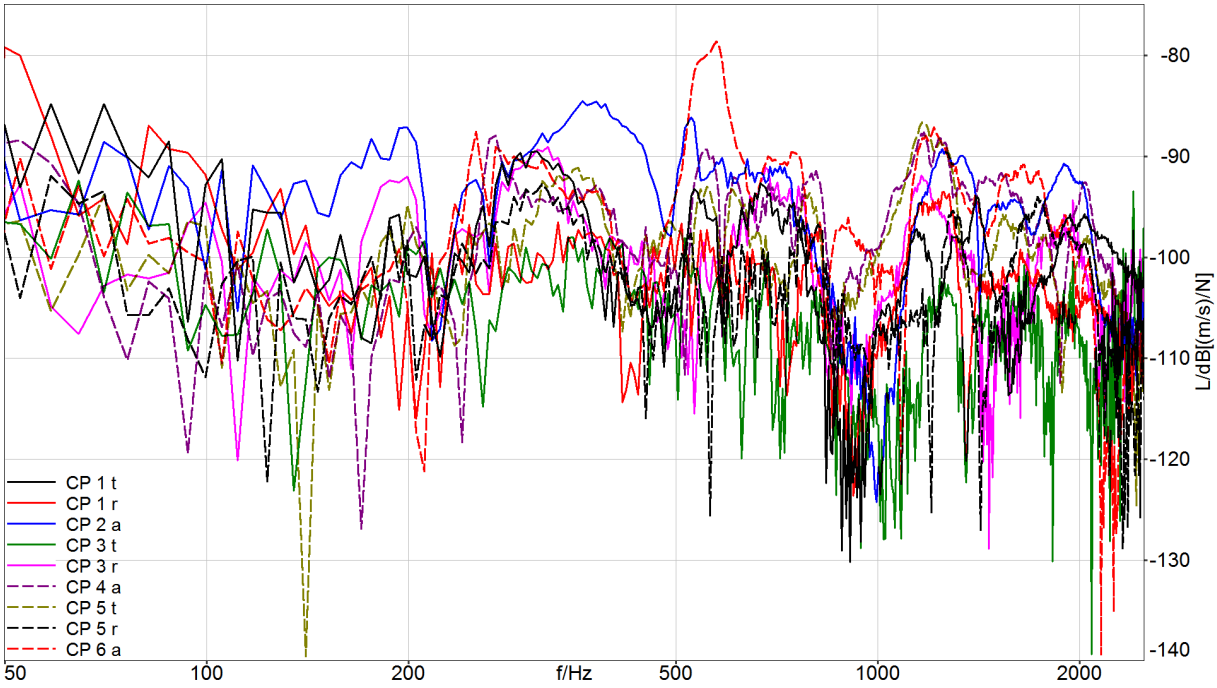

Figure 4.31: Mobility between validation point and degrees of freedom at internal interface

It can be observed that the assembly is stiff and the mobilities in axial (a) direction are dominant in the shown frequency range. In radial (r) and tangential (t) direction the mobilities are comparable. The coherence functions between the validation location and the DoFs at the interface are shown in Figure 4.32.

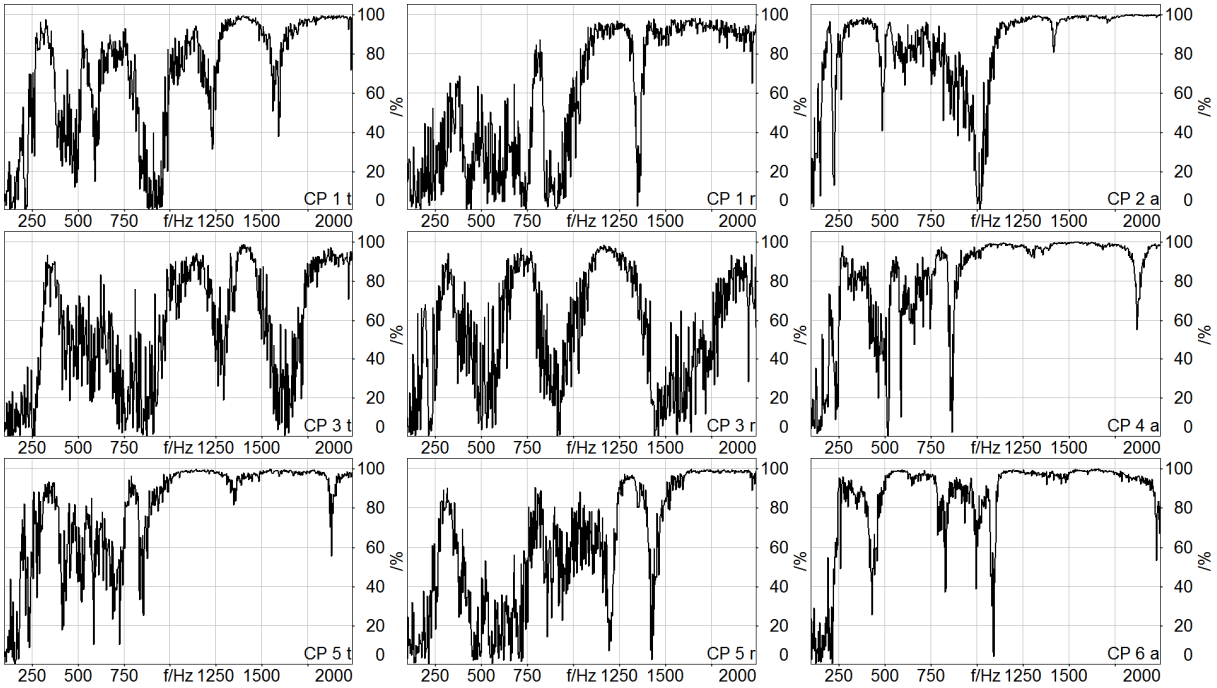

Figure 4.32: Coherence functions between validation point and degrees of freedom at internal interface

It can be observed that the coherence in axial (a) direction is generally above 95% in the frequency range above 1 kHz, except at the anti-resonances. In radial (r) and tangential (t) direction the coherence below 1 kHz is lower than the coherence in axial direction. Often the coherence does not reach values above 90% in radial and tangential direction.

Figure 4.33 shows the spectrum of the condition number of the matrix, which is used for the calculation of the in-situ blocked forces of a ball nut assembly (BNA).

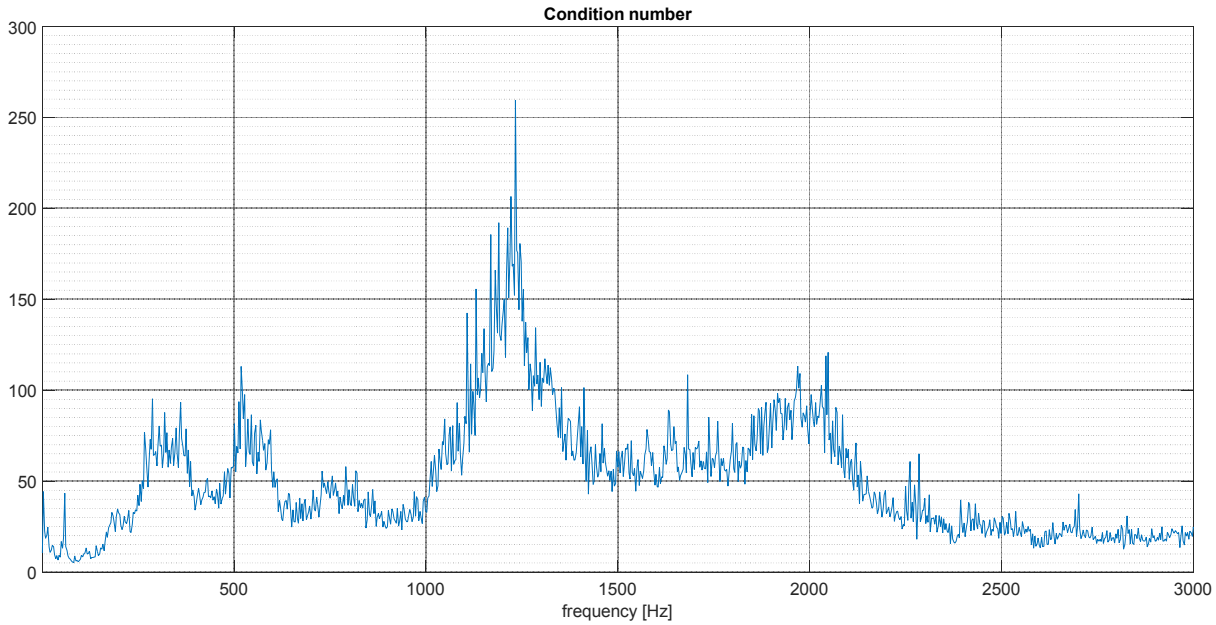

Figure 4.33: Condition number of mobility matrix

Except for frequencies between 1 and 1.3 kHz the condition number is always below 150 in the shown frequency range.

In theory it was possible to determine in total 12 blocked forces, but it was assumed that only 9 forces were needed to characterise the source strength of the BNA. Therefore three forces in tangential direction were omitted. The spectra of the 9 in-situ blocked forces of the BNA for the artificial operational state are shown in Figure 4.34, Figure 4.35 and Figure 4.36. Every figure shows the in-situ blocked forces for one direction. Figure 4.34 shows the in-situ blocked forces in axial direction, Figure 4.35 in radial direction and Figure 4.36 in tangential direction.

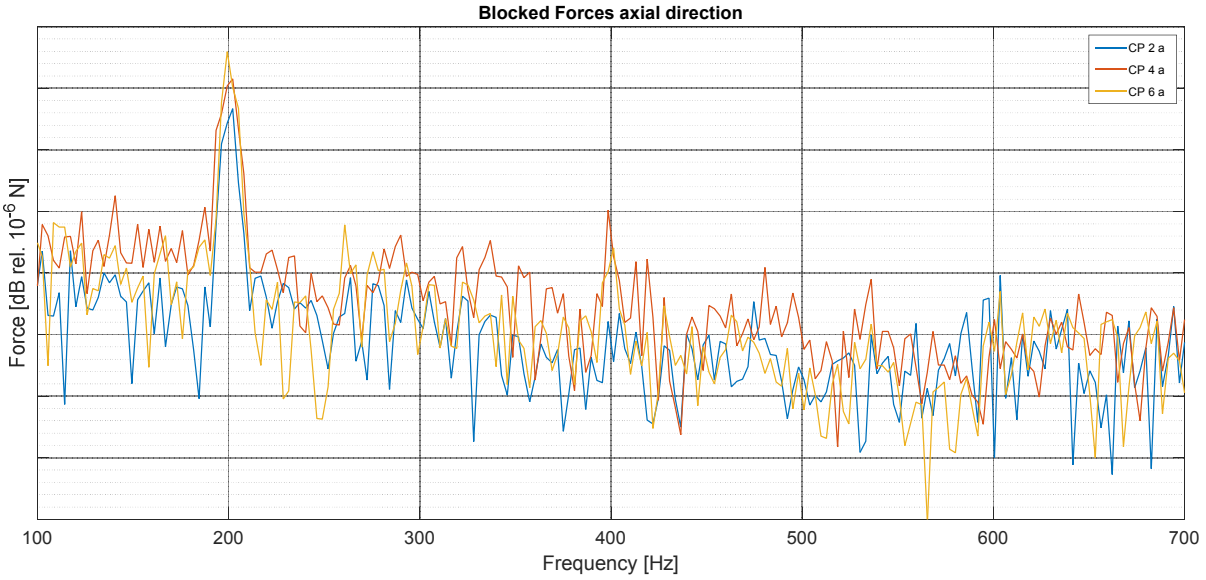

Figure 4.34: Spectra of in-situ blocked forces of a ball nut assembly (BNA) at coupling points (CP); axial direction; grid ordinate: 10 dB

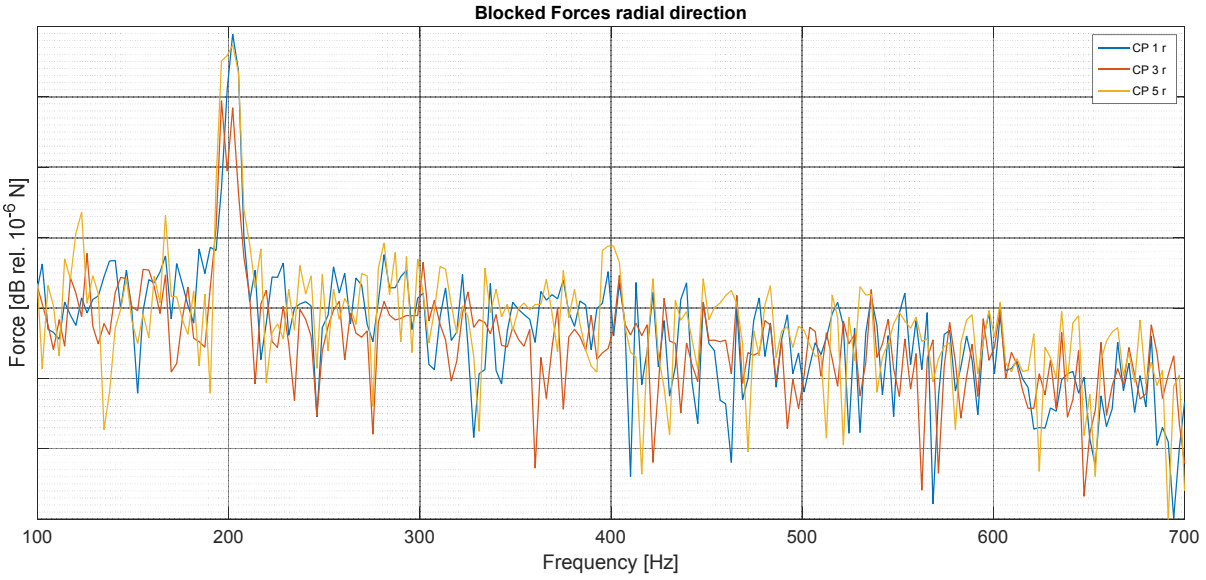

Figure 4.35: Spectra of in-situ blocked forces of a ball nut assembly (BNA) at coupling points (CP); radial direction; grid ordinate: 10 dB

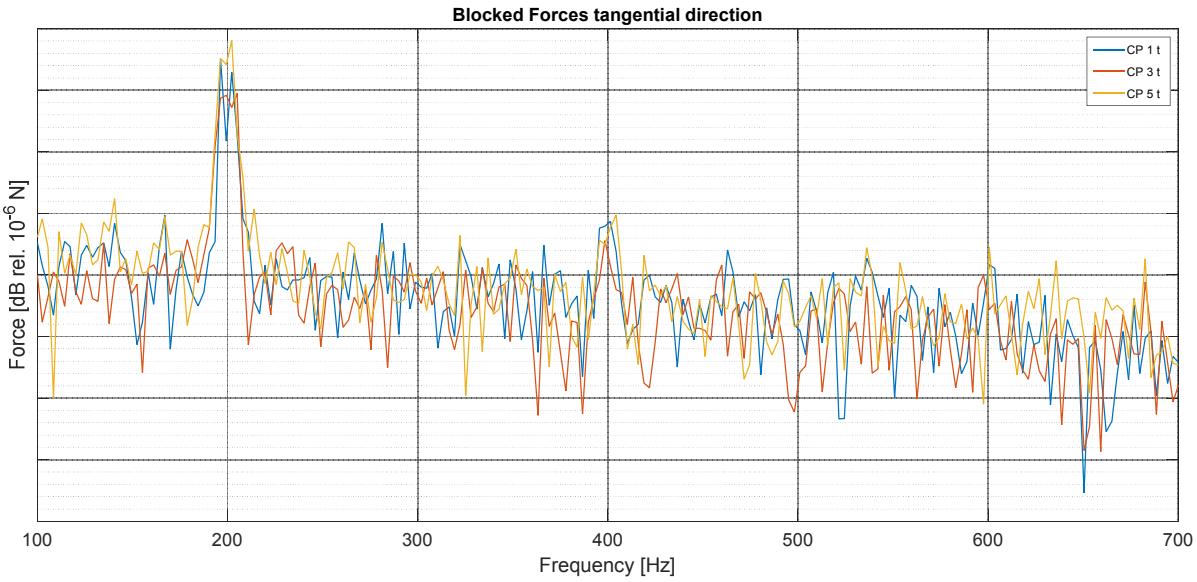

Figure 4.36: Spectra of in-situ blocked forces of a ball nut assembly (BNA) at coupling points (CP); tangential direction; grid ordinate: 10 dB

The determined in-situ blocked forces show dominant peaks at 200 Hz in the depicted frequency range. This is expected since the operational state was chosen as a sine signal with a frequency of 200 Hz. Furthermore the spectra show that the magnitudes of the in-situ blocked forces at the dominant peak at 200 Hz are within 10 dB for one direction. This means that the structure-borne sound transfer from the BNA to the receiver can be seen as nearly constantly distributed over the interface. This is expected behaviour for a fully rotationally symmetric component with a continuous interface.

The result of the on-board validation of the blocked forces is shown in Figure 4.37. It shows the comparison between the acceleration in frequency domain that is measured at a validation point on the receiver structure (bearing shell) and the acceleration at the same point that is predicted using the 9 determined in-situ blocked forces and the corresponding FRFs. This on-board validation approach was described in subsection 2.3.5.

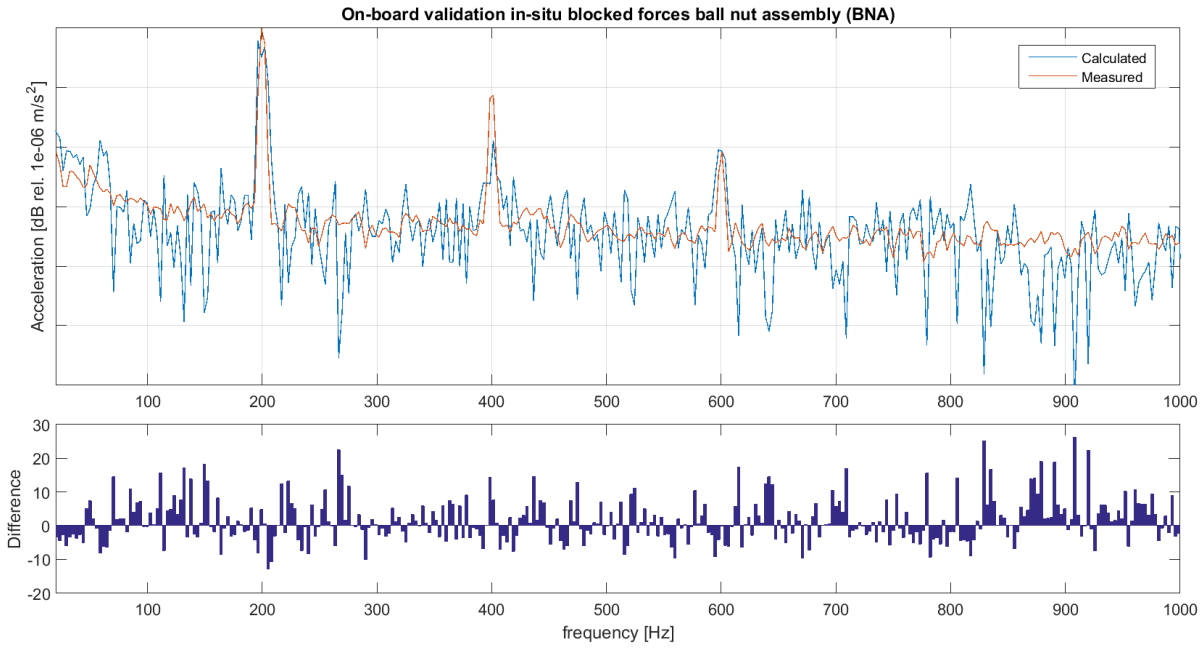

Figure 4.37: On-board validation of the in-situ blocked forces of a ball nut assembly (BNA); grid ordinate: 10 dB

It can be observed that the source characteristics of a BNA can be adequately described using 9 in-situ blocked forces around the circumference of the ball bearing. The 9 in-situ blocked forces compose of each three forces in axial, radial and tangential direction. The magnitude at the main frequency of the swept sine is detected with an accuracy of below 3 dB. The first and the second harmonic are also detected correctly but in contrast to the main frequency the deviation between the calculated and the measured magnitude of the velocity is around 7 dB higher at the first harmonic at 400 Hz. The velocity induced by the second harmonic at 600 Hz is predicted within 2 dB.

4.5.4 Case study III: Toothed belt

In subsection 4.5.2 and subsection 4.5.3 it was demonstrated that it is possible to experimentally determine vectors of in-situ blocked forces which characterise the source strength of an EM and a BNA of an EPSapa system. In order to achieve the results in an accurate manner MEMS accelerometers were embedded at the internal contact interface between BNA and EM, respectively. In this way two of the three prominent internal sources of an EPSapa system are characterised in terms of experimentally determined vectors of in-situ blocked forces at the internal interface DoFs. Thus an important objective of the present thesis is achieved. Both of the aforementioned internal sources (EM and BNA) of an EPSapa system can be characterised with in-situ blocked forces at a rigid and quasi-static interface. However, the in-situ blocked forces of the third main internal source of an EPSapa system which is a toothed belt cannot be experimentally determined in the same way.

Hence, in the following the results of a toothed belt of an EPSapa system are presented. The results are achieved by applying the methodology to determine the in-situ blocked forces of sources with revolving interfaces, proposed in subsection 4.4.3. The assumption is made that the structure-borne sound is generated solely at the teeth which mesh with the toothed disc of the BNA and the pinion of the EM, respectively. This assumption, which is based on the functional principle of a TB, reduces the amount of in-situ blocked forces to be determined. An on-board validation was carried out to prove the aforementioned assumption. Furthermore, two interface cases are compared with each other. The two cases define the rotating interface between the TB and the attached receiver in a different way.

The test rig which is used to determine the in-situ blocked force of the TB is depicted by Figure 4.38. It is constructed of two fixtures which are connected via two bolts. The left fixture plate

of the test rig drives the TB by an electric motor while the right fixture is for the toothed disc which is connected to a magnetic brake. With the help of the brake the TB can be loaded. This way the same operational conditions as an EPSapa system can be set. Furthermore the test rig depicted by Figure 4.38 allows the tension σ of the TB to be set according to the functional and NVH requirements of an EPSapa system. Although the depicted test rig was not specifically designed to determine (in-situ) blocked forces it yields the necessary boundary conditions. Furthermore Figure 4.38 shows the position of the accelerometer for the validation of the determined in-situ blocked forces.

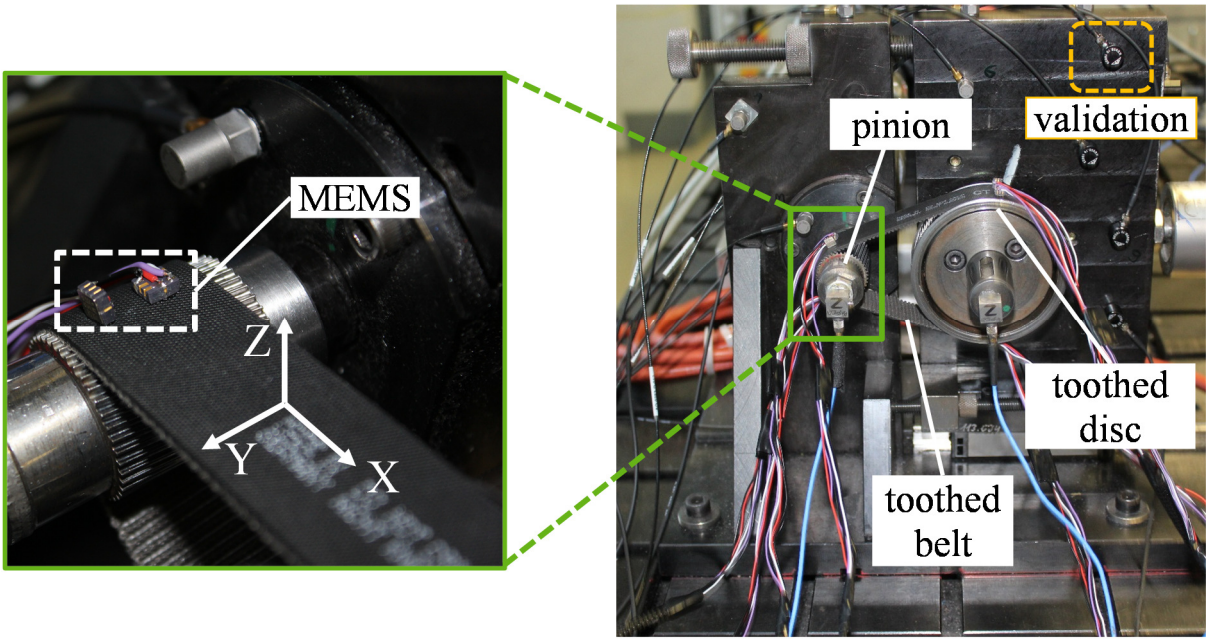

Figure 4.38: Test rig for the determination of in-situ blocked forces of a toothed belt

At the beginning of this subsection it was mentioned that two cases of defining the interface between TB and the receiver was to be compared. Hence the different cases of the revolving interface that are distinguished within this case study are listed in the following:

1. The interface is chosen as the incoming meshing teeth between the TB and the pinion of the EM and the toothed disc of the BNA and the TB, respectively. This results in a total of six internal in-situ blocked forces since three perpendicular forces in a Cartesian coordinate system (compare Figure 4.39) per tooth are defined.
2. The interface is chosen as the centre of the discs which are used to drive the toothed belt on the test rig (compare Figure 4.38). These discs represent the pinion (P) of the EM and the toothed disc (TD) of the BNA when the TB is assembled within an EPSapa system. This results in six internal in-situ blocked forces since three perpendicular forces in a Cartesian coordinate system (compare Figure 4.39) per disc are defined.

The two cases are depicted in Figure 4.39 for a rotation of the TB in clockwise direction. The red lines show the location of the in-situ blocked forces for the second interface case at the centre while the black lines indicate the location for the first interface case at the incoming teeth, respectively.

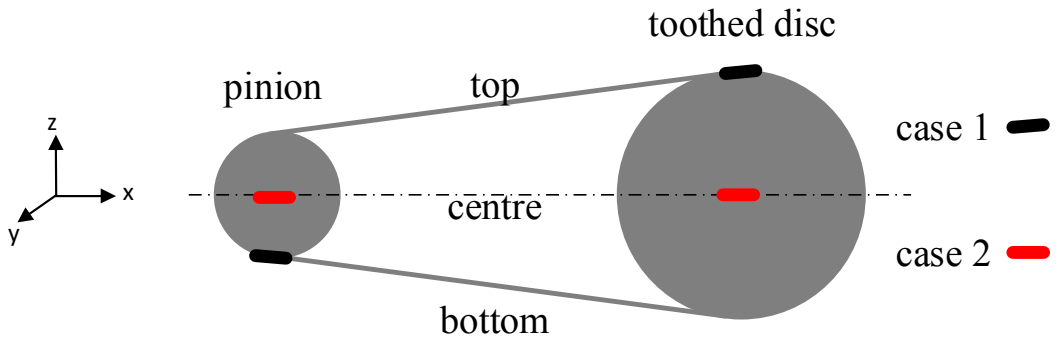

Figure 4.39: Schematic depiction of revolving interface of a toothed belt which meshes with a toothed disc (right interface) and the pinion of an electric motor (left interface)

It will be shown, based on the experimentally determined results of the different interface cases, that the definition of the revolving interface between a TB and the pinion of an EM or a toothed disc of a BNA, respectively, is not obvious or trivial. However, for a bfTPA, the first interface case is to be preferred because of its transferability to the realistic mounting conditions of a TB within an EPSapa system.

The measurement points, namely remote points (RP) on the two plates of the test rig are shown in Figure 4.40. The point which is chosen out of the 13 remote points for the on-board validation is labelled RP07.

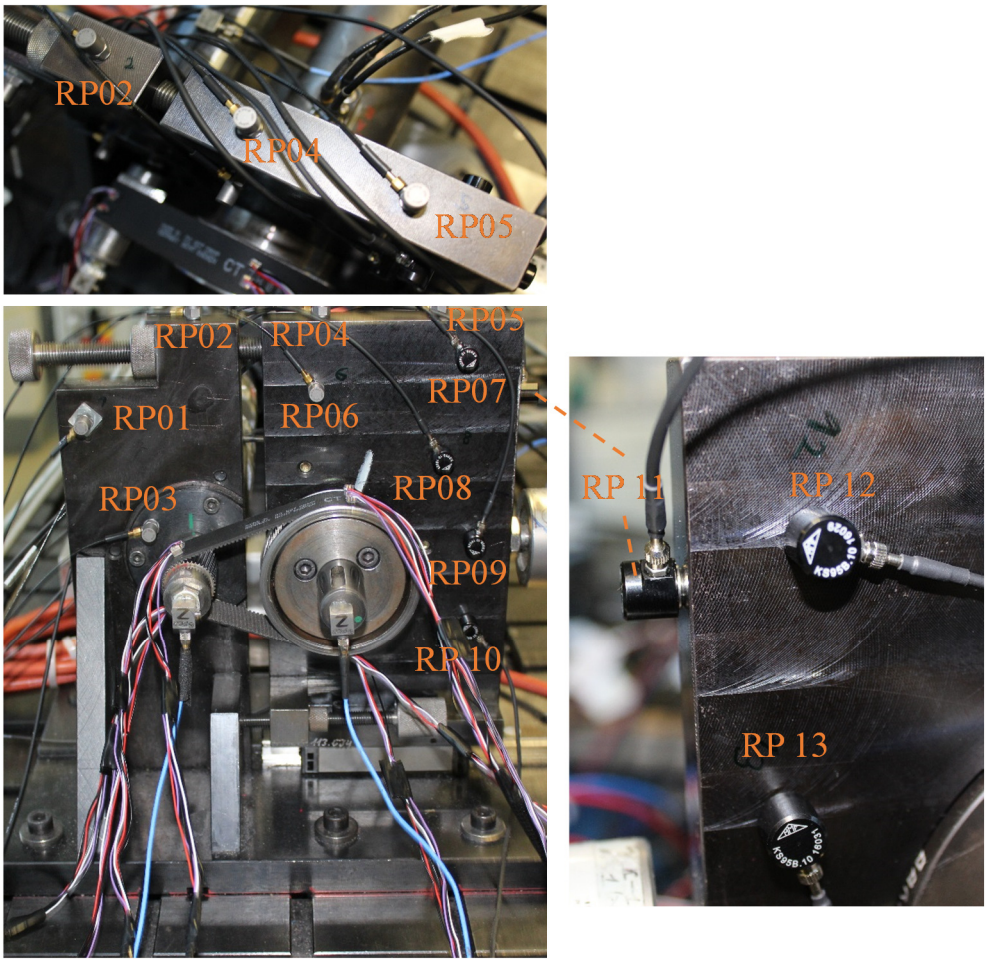

Figure 4.40: Measurement points: 13 remote points (RP) and validation point (RP07) on right plate

The colour diagram on top of Figure 4.41 shows the SNR at all remote points. On the bottom the spectra of the acceleration signal and the noise at the validation location (RP7) is shown.

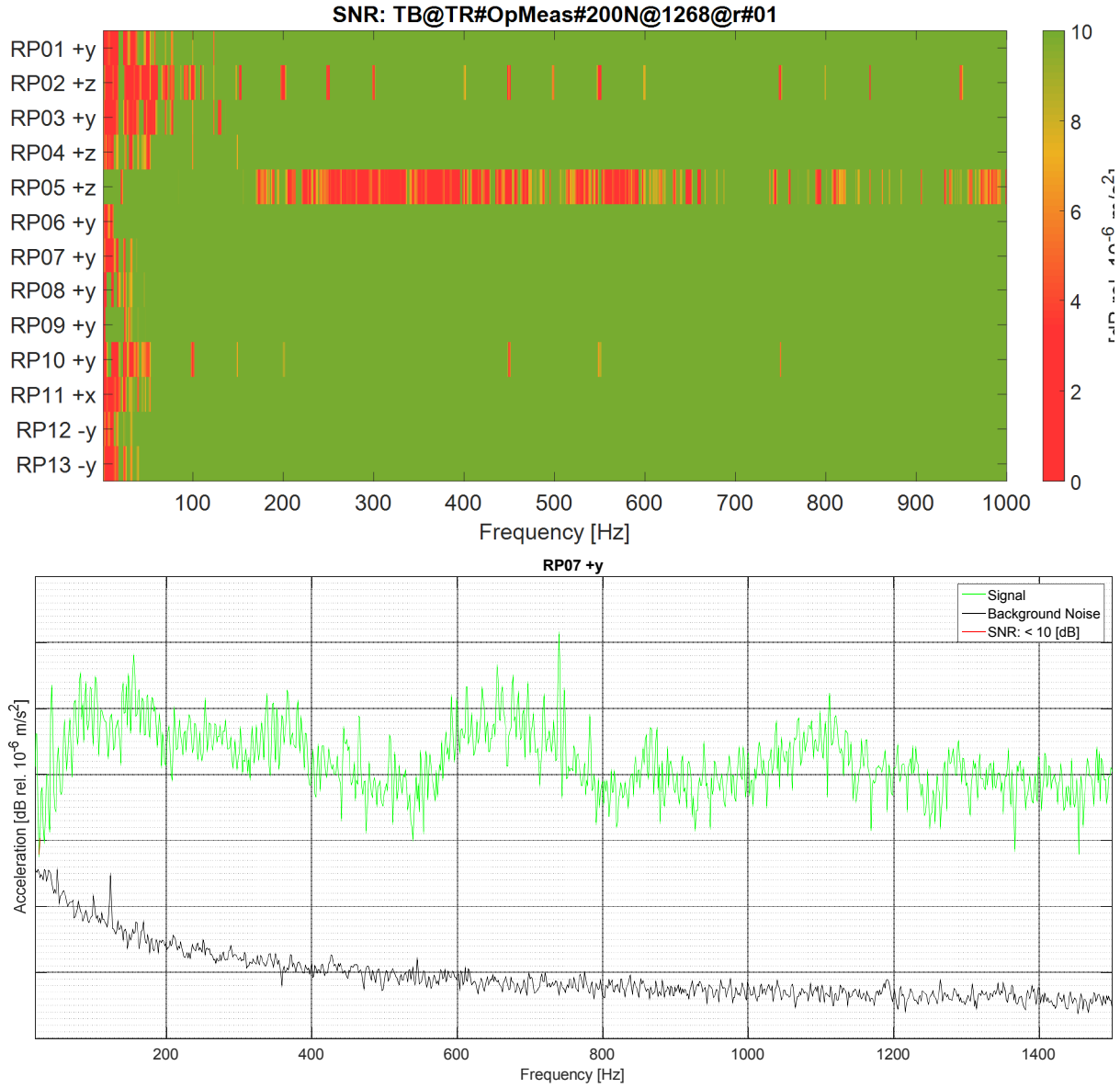

Figure 4.41: Signal-to-noise-ratio (SNR); top: SNR at all 13 remote points (RP); bottom: SNR at RP07 on the right fixation in y-direction; Grid: 10 dB

It can be observed from the top diagram that the SNR is generally above 10 dB, except for RP05.

The upper bound for the determination of mobility functions is at 2100 Hz for this case. The same approach for the determination of the upper bound is used as shown in Figure 4.17. In Figure 4.42 the mobility functions between the validation point and the 6 DoFs at the internal interface between the toothed and the pinion and toothed disc, respectively, are shown.

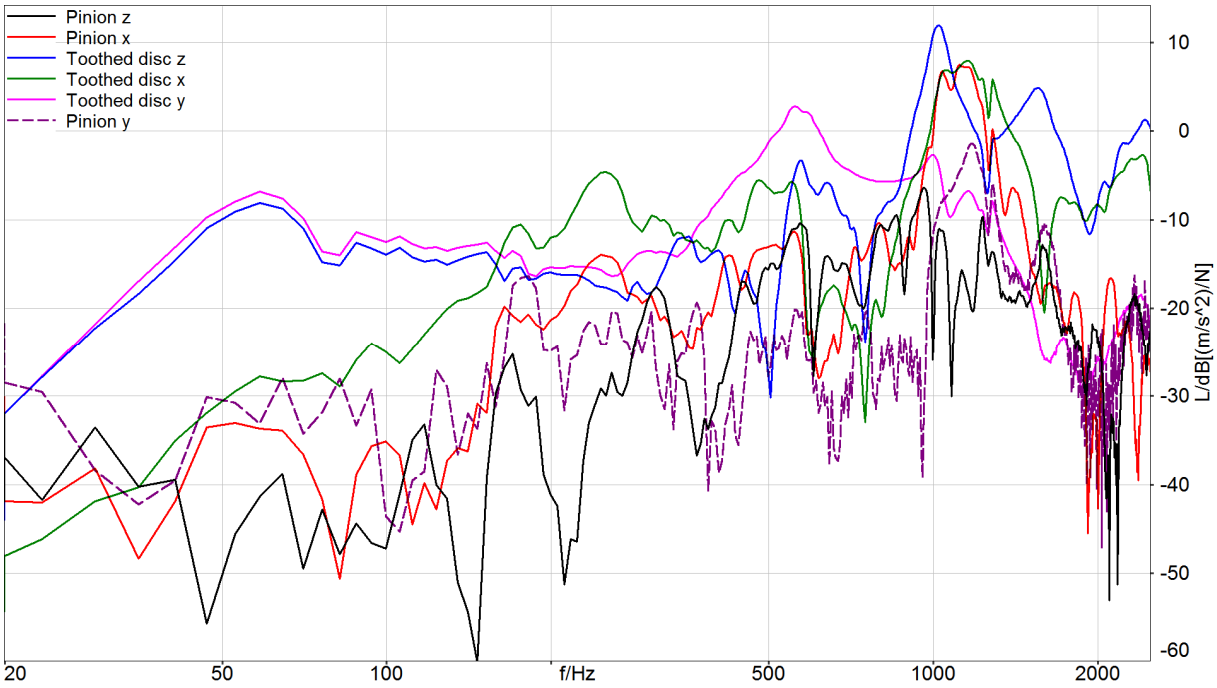

Figure 4.42: Mobility functions between validation point and degrees of freedom at internal interface on toothed belt

It can be observed that especially the mobilities between the validation location (RP07) and the toothed disc are dominant. This is an expected behaviour since the toothed disc and the validation location are on the same plate of the test rig. One dominant resonance is at 1 kHz.

The coherence between the validation location and the DoFs at the internal interface are shown in Figure 4.43.

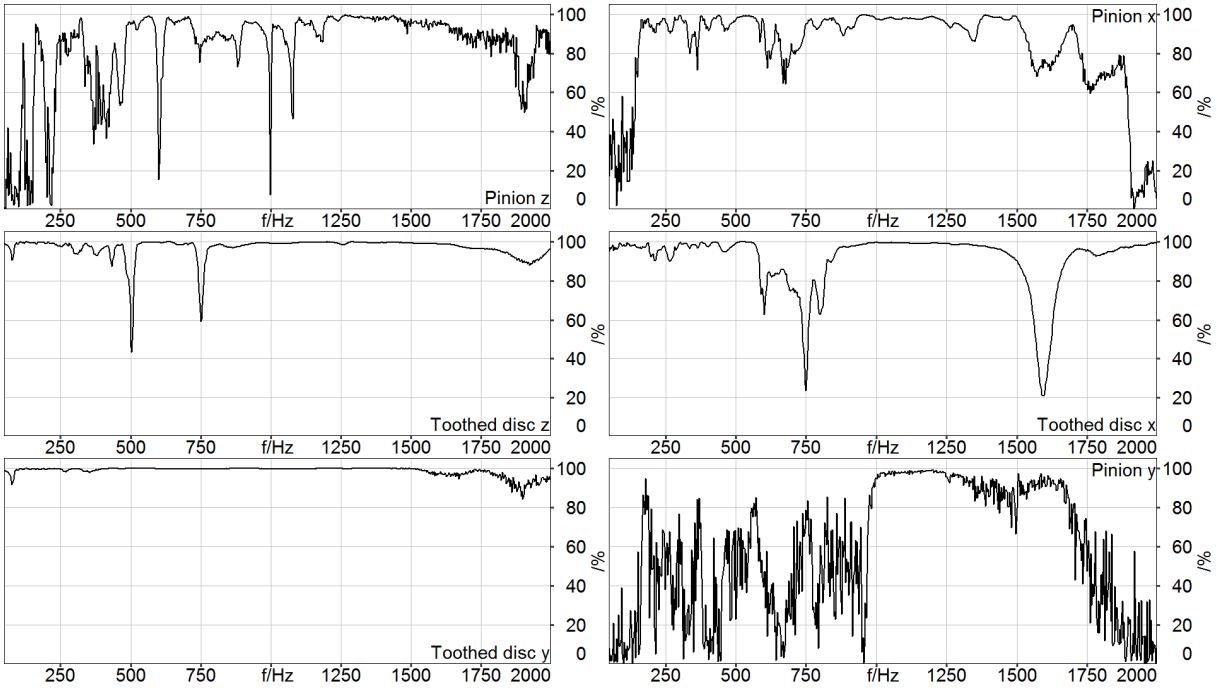

Figure 4.43: Coherence functions between validation point and degrees of freedom at internal interface

It can be observed that the coherence is generally above 95%, except at the anti-resonances. For excitation at RP07 and measurement at the pinion in y direction the coherence is significantly worse than in the other directions. Furthermore the coherence functions for excitation at RP07 and measurement at the pinion is generally worse than at the toothed disc. This is expected since the pinion is fixed on the other plate. Therefore the remote points are placed on both plates in all 3 directions (x, y and z). The test setup, which consists of the test rig and the toothed belt, can be seen as a linear time invariant system.

In the literature condition numbers below 100 are assumed to indicate a very successful inversion of the matrix. The condition number is shown in Figure 4.44.

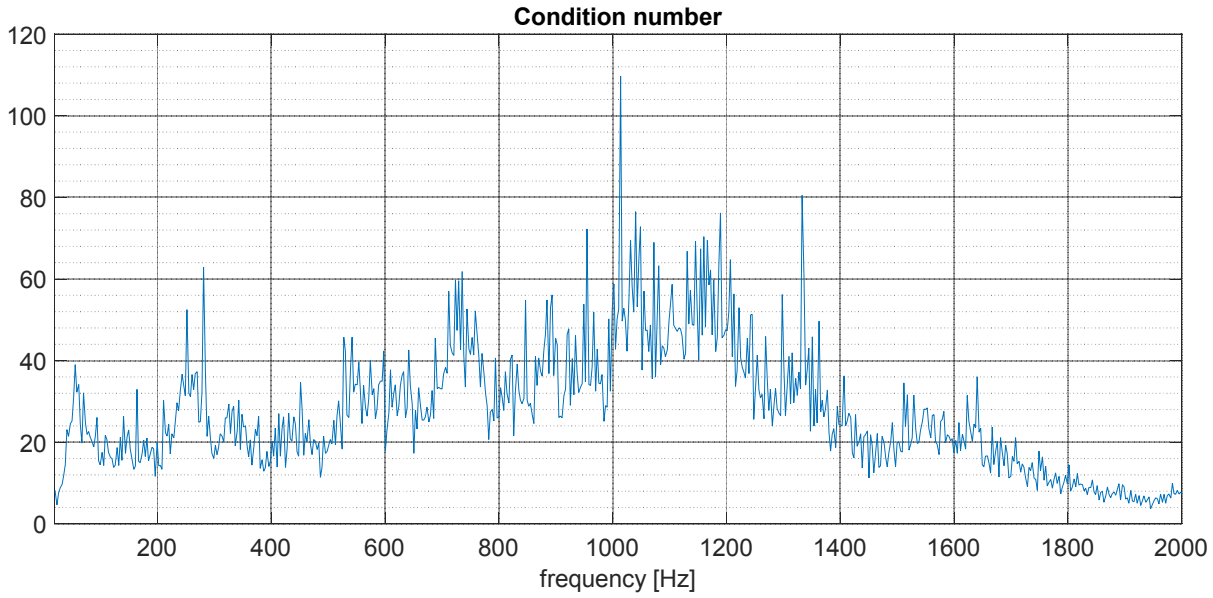

Figure 4.44: Condition number of mobility matrix

Except for one frequency at 1 kHz the condition number is always below 100 in the frequency range, which is important for the toothed belt.

One possibility to validate the calculated in-situ blocked forces of the TB is to use the information about the distinct order generated by the constant gear transmission ratio between the TB and the pinion of the EM. The order is related to frequency according to Eq. (5.3). Since the pinion of the EM has 41 teeth a 41^{st} order, generated by the TB, can be observed. If the TB is driven with a constant rotational speed only one dominant frequency according to Eq. (4.9) should be observable. The spectra of the determined in-situ blocked force of the TB and the acceleration used for OBV, respectively, should therefore only show a dominant peak at this frequency. However because of the electric motor, which drives the toothed belt, a 35^{th} order can also be observed in the spectra of the acceleration used for the OBV and the in-situ blocked forces, respectively.

In the following, the OBV approaches for the both interface cases will be shown separately. This procedure constitutes a deviation to the presentation of the case studies of the EM and the BNA in subsection 4.5.2 and subsection 4.5.3, respectively. However, both aforementioned case studies contained clearly defined interfaces and it was not necessary to compare two choices of interfaces. However, since within the present case study of a TB the choice of the interface should be evaluated at first the OBV approaches of the two different case studies are discussed. The operational state is chosen as a constant run of the TB in clockwise direction with 1268 rpm. By choosing this rotating speed the operational state of the TB correlates with the operational state of an EPSapa system with a constant steering speed of 300°/sec. In the following only the frequency range, which is important for a constant run of the toothed belt with 1268 rpm at the test rig, between 650 and 900 Hz is shown.

At first the OBV approach for the choice of the interface at the incoming meshing teeth is shown by Figure 4.45. The figure shows the spectra of the measured and calculated accelerations (compare subsection 2.3.5).

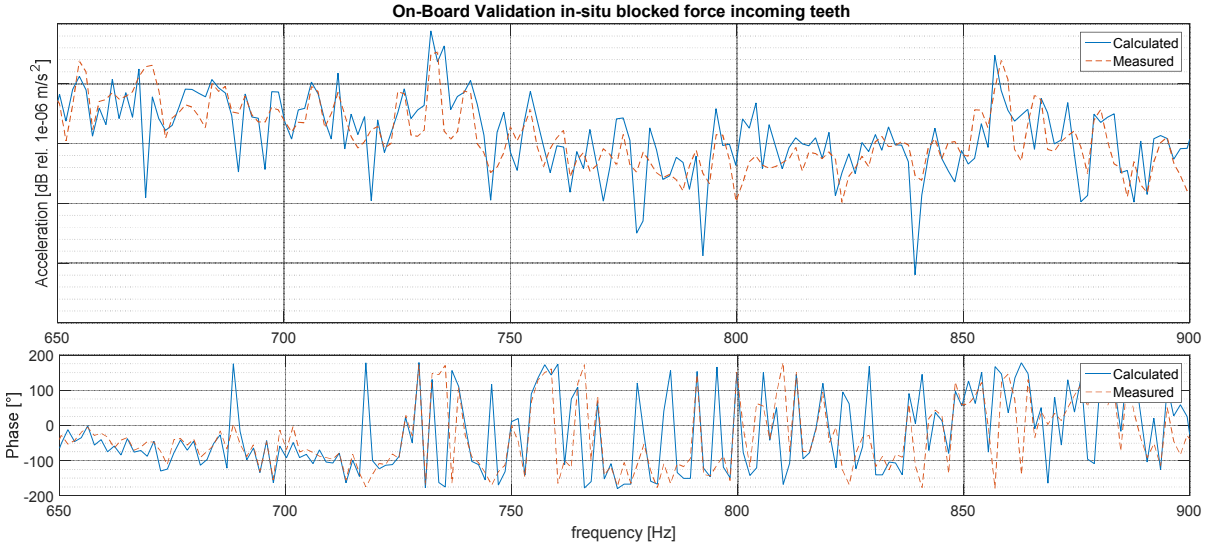

Figure 4.45: On-board validation of the in-situ blocked forces of a toothed belt (TB) determined at the incoming meshing teeth (case 1); grid ordinate: 5 dB

It can be observed from Figure 4.45 that the OBV of the in-situ blocked forces which characterise the source strength of the TB is generally successful. Especially the relevant peak at the main order of the TB at 866 Hz is determined with a deviation below 1 dB. A second peak at 740 Hz can be observed in the spectra of the acceleration which is used for the OBV. This peak is related to the electric motor which drives the pinion and in turn drives the TB which meshes with the pinion.

The OBV approach for the case where the interfaces are chosen as the centres of the discs which drive the toothed belt is shown in Figure 4.46. The same position for the measurement of the acceleration used for the validation is chosen as for the first interface case.

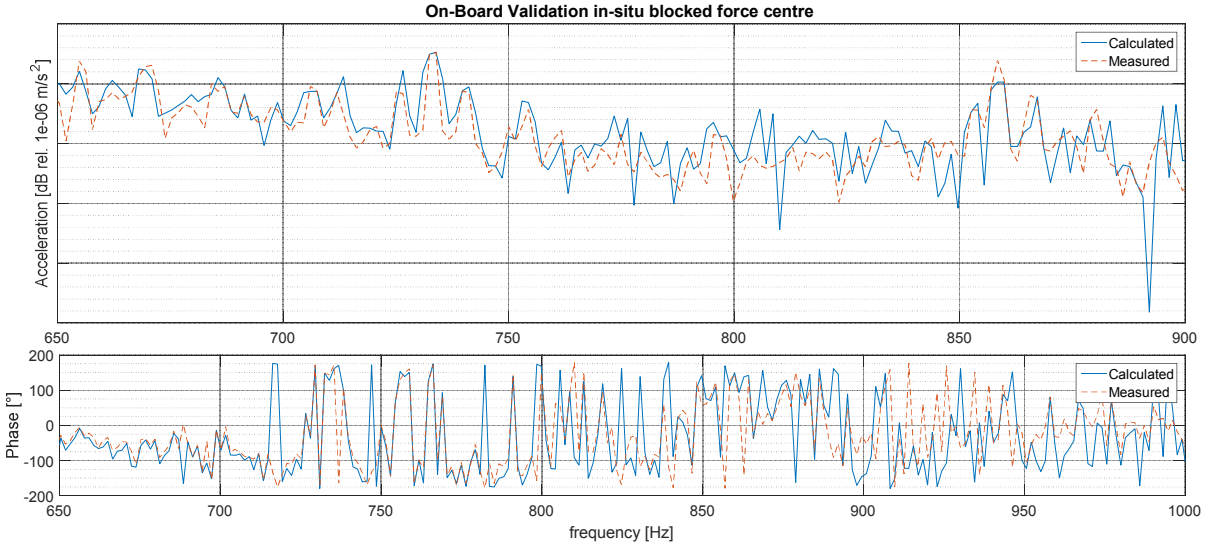

Figure 4.46: On-board validation of the in-situ blocked forces of a TB determined at the centre of the driving discs (case 2), grid ordinate: 5 dB

Figure 4.46 clearly shows that the interface can also be chosen as the centre of the discs. Especially the orders of the electric motor and the toothed belt at 760 and 867 Hz are detected with high accuracy, with a deviation below 2 dB. A reason for the However, this is only a feasible approach if the in-situ blocked forces are determined on the shown test rig (compare Figure 4.38). The order of the belt is observed in the spectrum of the predicted acceleration. Both interface cases show good results.

If only the dominant frequency range is to be observed, a band pass filter can be applied. In this way the influence of the electric motor, which corrupts the measurement, can be neglected. However, the main order of the toothed belt was predicted with an accuracy of below 2 dB for both chosen interface cases. This proves that the in-situ blocked forces of a source with a rotating interface can be determined according to the methodology which is proposed in section 4.3. In the following the determined in-situ blocked forces for the first interface case at the incoming teeth are discussed.

Figure 4.47, Figure 4.48 and Figure 4.49, shows the in-situ blocked forces of the TB divided into the three directions of a Cartesian coordinate system. The directions of the coordinate system in relation to the TB can be seen in Figure 4.39.

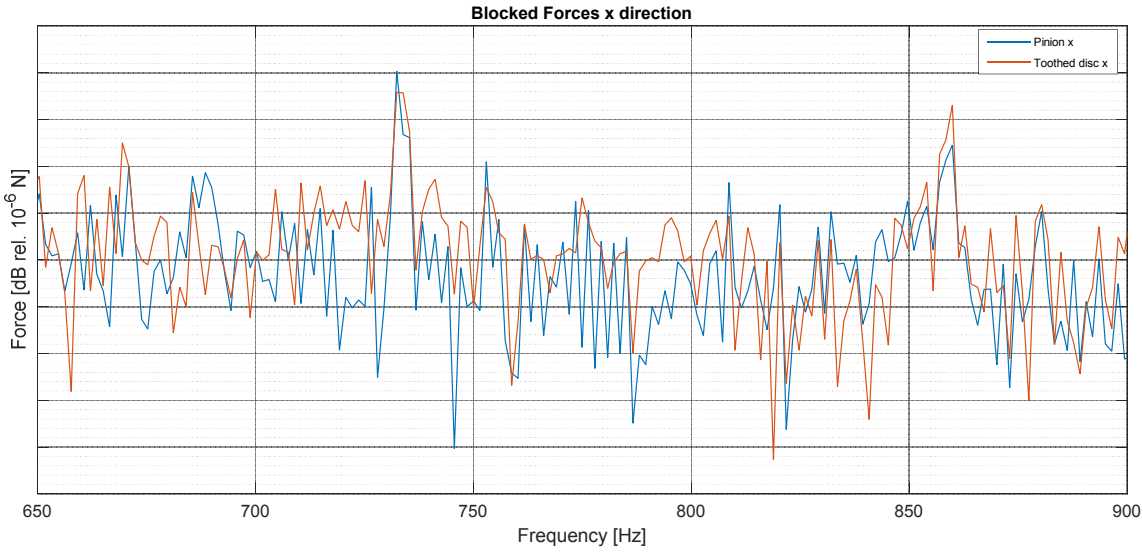

Figure 4.47: Spectrogram of in-situ blocked forces of a toothed belt (TB) at the incoming meshing teeth according to coordinate direction; x-direction; grid ordinate: 5 dB

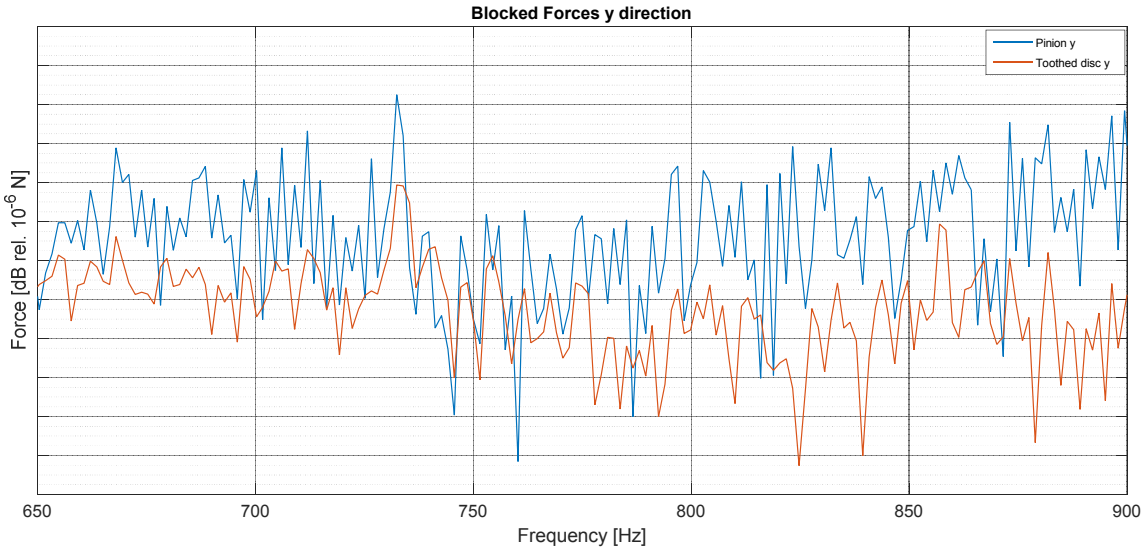

Figure 4.48: Spectrogram of in-situ blocked forces of a toothed belt (TB) at the incoming meshing teeth according to coordinate direction; y-direction; grid ordinate: 5 dB

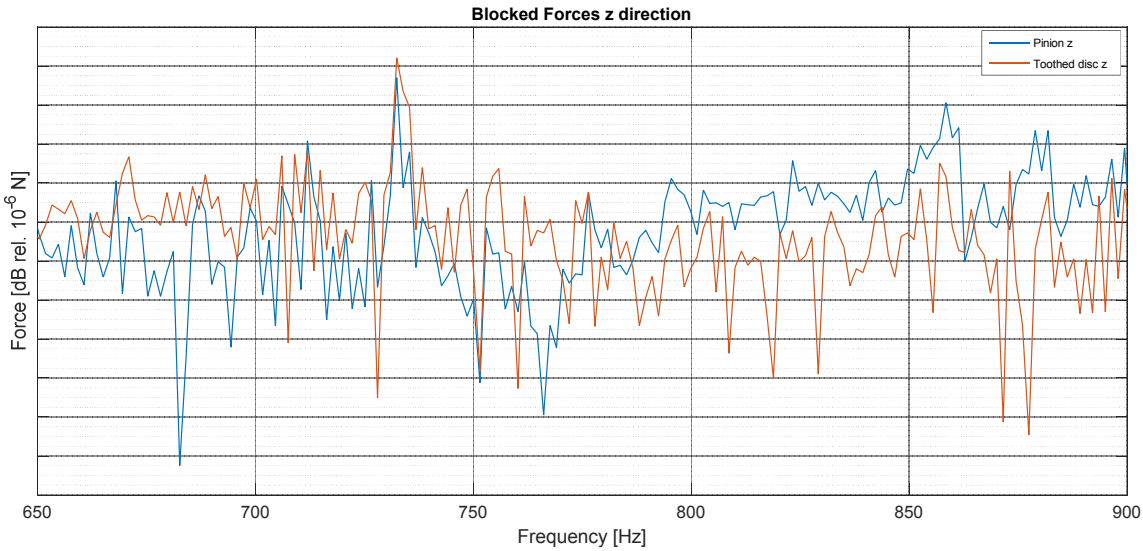

Figure 4.49: Spectrogram of in-situ blocked forces of a toothed belt (TB) at the incoming meshing teeth according to coordinate direction; z-direction; grid ordinate: 5 dB

The force in the x-direction, which is the lateral force of the TB, is of the same magnitude at both interfaces. This means that both tooth mesh at the pinion and the toothed disc side, respectively, generate the same force at the relevant frequency. Furthermore, the shear force in the y-direction at the pinion side of the TB is significantly higher than at the toothed disc side. This is a consequence of the crimping at the toothed disc which guides the TB. However, at the pinion side the TB is not guided which results in a swerve movement. For that reason the in-situ blocked forces are significantly higher at the pinion side, seen in the middle diagram. If the toothed belt is restricted from a shear movement the forces are expected to be lower. The movement in the z-direction which is an up and down movement of the TB is relatively small at the toothed disc side and therefore the resulting in-situ blocked forces need to be small as well. This can also be observed in Figure 4.50 and Figure 4.51 which show the in-situ blocked forces at the pinion side and on the toothed disc side, respectively.

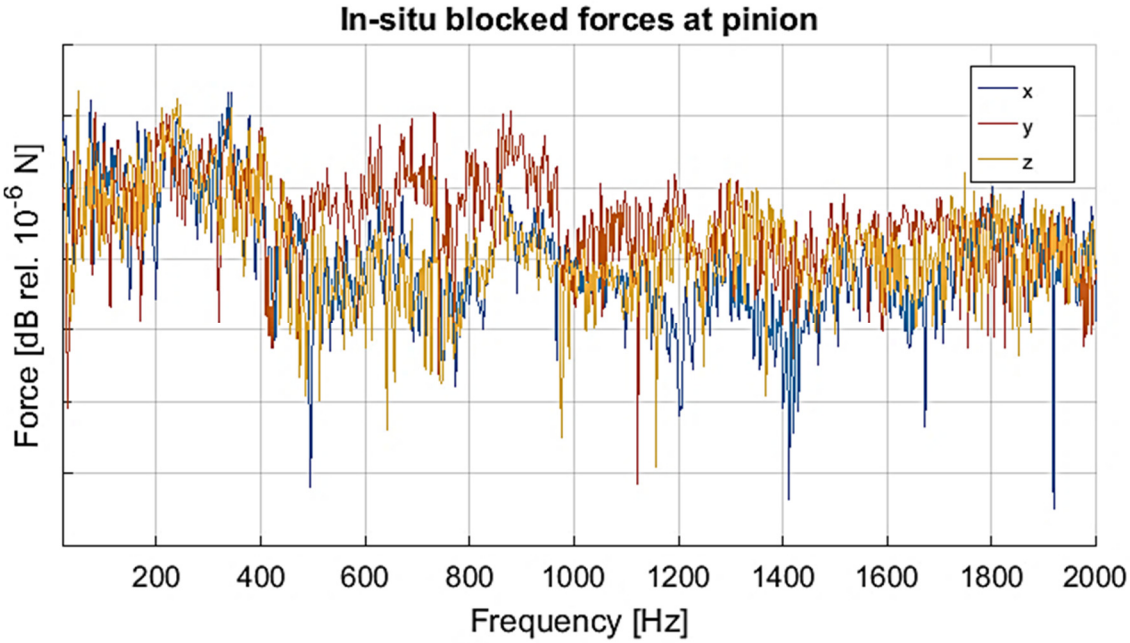

Figure 4.50: Spectra of the in-situ blocked forces of a toothed belt at the incoming teeth according to interface position; forces at pinion side; grid ordinate: 10 dB

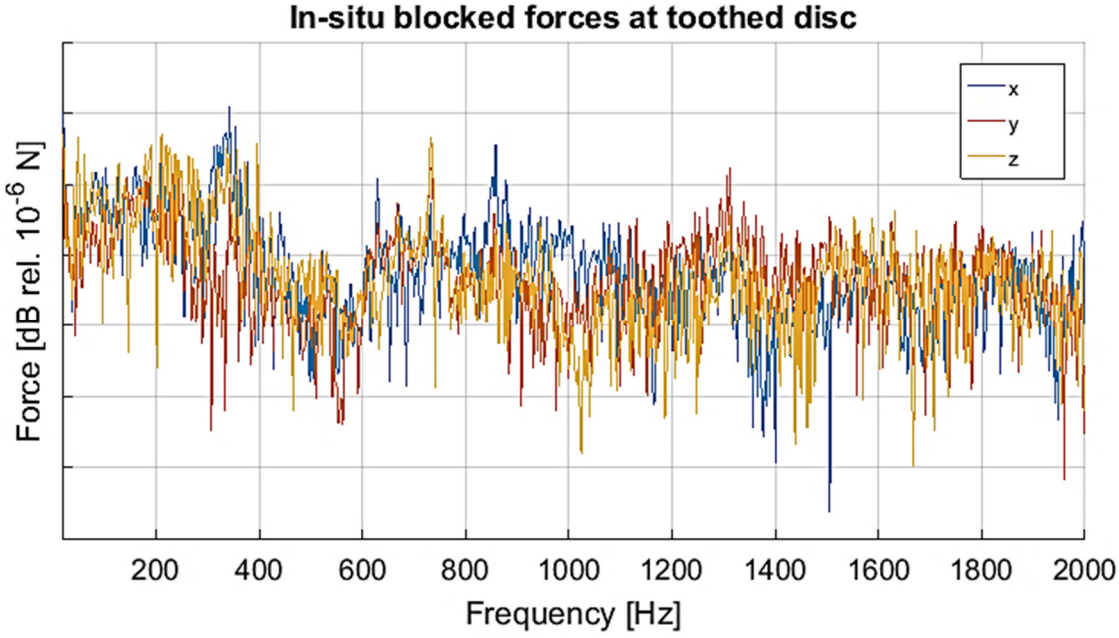

Figure 4.51: Spectra of the in-situ blocked forces of a toothed belt at the incoming teeth according to interface position; lower diagram: forces at toothed disc side; grid ordinate: 10 dB

At the dominant frequency of 867 Hz the determined blocked forces in the z-direction are significantly lower than the forces in the x-direction at the toothed disc side. This is expected since the function of a toothed belt is to generate forces in an x-direction in order to transfer the torque of the electric motor to the ball nut assembly. Furthermore the shear force at the toothed disc in the y-direction is relatively small compared to the lateral forces in the x-direction. This means that the structure-borne sound which is induced by the toothed belt is mainly affected by the forces in the x-direction. At the pinion side the shear forces in the y-direction are dominant. However, if the swerve movement of the TB at the pinion could be restricted, the lateral forces in the x-direction would be dominant at 867 Hz.

4.6 **Summary and concluding remarks**

In section 4.2 a novel application of MEMS accelerometers was presented. It was generally shown that MEMS accelerometers can be embedded within a structure-borne sound source such as an electric motor or a ball nut assembly to determine blocked forces using the in-situ method.

MEMS accelerometers can be embedded using any two component adhesive in small grooves or holes. It was proven that only minor modifications to the very sensitive contact interface between a source and a receiver are necessary to embed the MEMS accelerometers. Furthermore it was shown that the adopted calibration method allows measurement with high accuracy in a broad frequency range, sufficient for most structure-borne sound issues within EPS systems. Additionally the limitations of MEMS accelerometers for inverse force identification in general were elucidated. Generally it can be stated that MEMS accelerometers usually have an unfavourable SNR. Nevertheless the measurement performance of the used MEMS accelerometers is sufficiently accurate for the use to experimentally determine FRFs.

Secondly in section 4.3 it was specified how a structure-borne sound source with a continuous interface between the source and a receiver can be characterised in terms of in-situ blocked forces. Two potential ways to describe the physical behaviour of the interface were discussed. The interface can be discretised through multiple point connections. A second possibility, using Fourier series, was briefly described. However, within this thesis Fourier series are not used to describe the interface. Solely the discretisation of the interface which is discussed in subsection 4.3.2 is used.

Section 4.4 discusses a methodology to determine the in-situ blocked forces of revolving sources such as a TB or a toothed gear. In case of a revolving source the interface is not static but dynamic. However if one is able to determine an interface which is accessible with MEMS or IEPE accelerometers it is possible to determine meaningful in-situ blocked forces. This holds even for sources with interfaces that can be considered as elastic rather than stiff.

The theoretical consideration of section 4.2 - 4.4 were applied to case studies presented in section 4.5. The in-situ blocked forces of the three main internal sources of an EPSapa system were determined. It was shown for all three cases that it is possible to determine in-situ blocked forces. A validation approach which is outlined in subsection 2.3.5 was used to ensure that the blocked forces were determined with a maximum deviation at the relevant frequencies below 5 dB.

Chapter 5

Contribution of multiple internal structure-borne sound sources

5.1 **Introduction**

The main aim of the presented thesis is to develop and subsequently validate a novel TPA methodology. By conducting the proposed novel TPA the partial contribution of every internal source to the entire source strength of an EPSapa system is determined and analysed. In the previous chapter, it was shown that the vectors of in-situ blocked forces characterising the three main internal structure-borne sound sources of an EPSapa system can be determined using MEMS accelerometers embedded at the internal interfaces. This is an essential requirement of the proposed novel TPA that will be introduced and explained in section 5.3. It can be remarked that the presented methodology can in theory be applied to any vibrational structure-borne sound source that can be substructured into its multiple prominent internal sources.

In section 5.2 the advanced internal-source-path-receiver-model is introduced. This model is an extension of the internal-source-path-receiver-model (ISPRM) and is derived, based on the functional principle of an EPSapa system. The model includes all necessary internal sources, internal transmission paths and internal receivers and presents the relationship between all three parts. Based on the advanced ISPRM, the in-situ blocked forces of both the internal sources of an EPSapa system, presented in section 4.5, and the whole EPSapa system will be characterised in terms of in-situ blocked forces. In order to rank order the internal sources the determined vectors of in-situ blocked forces of the internal sources are correlated to the vectors of in-situ blocked forces of the whole EPSapa system. For that reason the so called blocked force transmissibility functions (BFT), which characterise the sound transmission within the housing of the EPSapa system, need to be determined as described in section 5.3. It will be shown that the BFT functions can be determined using MEMS accelerometers. The presented methodology is validated by carrying out three case studies which are outlined in section 5.4.

In section 5.5 a novel approach is presented, which is based on a matrix containing BFT functions and vectors of in-situ blocked forces. This approach aims to virtually assembling a product regarding the NVH requirements of a vehicle manufacturer. The methodology and the benefits of the presented approach, which is called virtual component assembly (VCA), is outlined in section 5.5.

Often it is not possible to characterise the passive behaviour of a source coupled to a receiver with only one set of measured FRFs since the kinematic behaviour of the source changes during operation. Therefore in section 5.6 this issue will be addressed. It will be shown by applying a frequency response assurance criterion (FRAC) analysis, that the internal FRFs of an EPSapa system change significantly during a steering manoeuvre. For that reason an approach will be presented to overcome this problem.

5.2 Advanced internal-source-path-receiver-model

5.2.1 Introduction

In section 1.4 the fundamentals of the internal source-path-receiver-model (ISPRM) are introduced. In this context it is also already generally elucidated that the classical source-path-receiver model (SPRM) is not sufficient to describe the structure-borne sound transfer within an overall vibrational source such as an EPSapa system. This is especially if the contribution of the internal source strength to the overall source strength is to be defined in terms of in-situ blocked forces in order to be receiver independent.

In subsection 5.2.2 the ISPRM is developed and expanded, yielding the advanced ISPRM. By expanding the ISPRM it is easier to include structures such as bearings. In subsection 5.2.3 the

term blocked force transmissibility (BFT) is introduced, which is an important part of advanced ISPRM.

5.2.2 Model as basis for blocked force transmissibility

As briefly mentioned in section 3.2, a technical product that is engineered to fulfil a complex function such as an EPSapa system usually consists of multiple components which generate structure-borne sound. This means that the structure-borne sound of the whole product, which is transferred to an attached overall receiver, is affected by multiple internal source mechanisms. In order to deal with this issue all of the defined internal source mechanisms need to be characterised independently from each other. In subsection 2.3.4 the main benefits of in-situ blocked forces as a possibility to characterise structure-borne sound sources independently from a receiver is outlined. Therefore within the concept of bfTPA, vectors of in-situ blocked forces are used to characterise the internal sources and then related to the overall source strength by a transmissibility function that characterises the passive part of the product such as the housing of an EPSapa.

The advanced internal-source-path-receiver model is depicted in Figure 5.1. The model is derived from the functional design of an EPSapa system but is also valid for other products which consist of multiple internal structure-borne sound sources and internal rigid receiver structures.

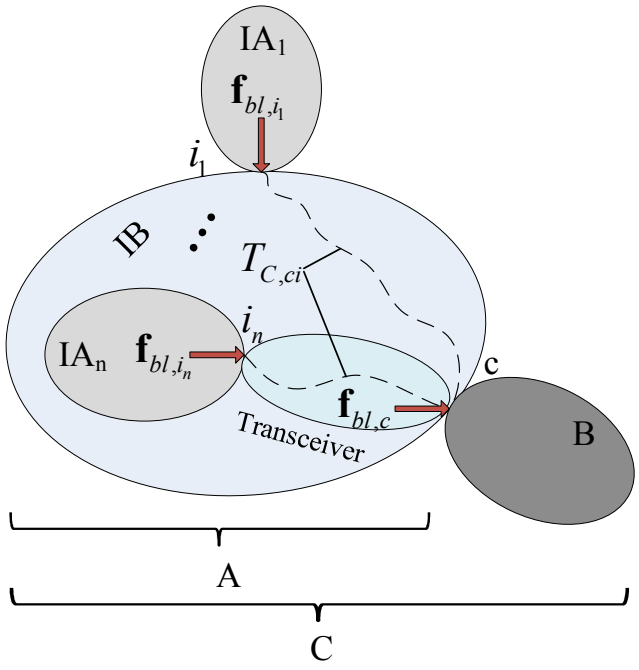

Figure 5.1: Advanced internal-source-path-receiver model

Most complicated engineered products consist of rigid and passive components such as a housing which embeds and carries all the active internal sources (IA_1 … IA_n). This structure is therefore considered as the internal receiver (IB). Mostly the internal sources are embedded inside of the IB and are therefore not accessible with standardised accelerometers. A potential way to overcome that issue was described in section 4.2. Usually there is also some sort of a bearing between the internal sources and the IB to ensure the functional principle of the whole product, source (A). These components were introduced as “transceivers” in subsection 3.4.4.

The overall structure-borne sound of the product (A) can be independently characterised in terms of in-situ blocked forces $\mathbf{f}_{bl,c}$ at interface (c) between the source (A) and the receiver structure (B). The determined in-situ blocked forces $\mathbf{f}_{bl,c}$ are the sum of all the vectors of in-situ

blocked forces $\mathbf{f}_{bl,i_n}$ of the internal sources (IAs) and the transmission paths in terms of a transmissibility matrix $\mathbf{T}_{C,ci}$ within the internal receiver (IB).

Both the in-situ blocked forces $\mathbf{f}_{bl,c}$ of the source (A) at interface (c) and the internal blocked forces $\mathbf{f}_{bl,i_n}$ at the n internal interfaces $(i_1 \ldots i_n)$ are independent from an attached overall receiver structure (B) or internal receiver (IB) respectively. This means that the product, which is the overall source (A) can be disassembled and the in-situ blocked forces $\mathbf{f}_{bl,i_n}$ can be determined independently from each other using a specifically engineered test bench as receiver. Therefore a TPA can be carried out within the source (A) which is based on the in-situ blocked forces of the n internal sources $\mathbf{f}_{bl,i_n}$ as input quantity, the transmissibility matrix $\mathbf{T}_{C,ci}$ within the IB to describe the transmission paths and the in-situ blocked forces $\mathbf{f}_{bl,c}$ of the source (A) as target quantity. In subsection 5.2.3 it is shown how the necessary transmissibility $\mathbf{T}_{C,ci}$ can be determined by measurements and in subsection 5.3.2 the bfTPA method is explained. The proposed model applies for all internal sources with continuous and also revolving internal interfaces, as explained in section 4.3 and section 4.4.

5.2.3 Blocked force transmissibility

The term blocked force transmissibility (BFT) is used to describe the transmissibility functions between a vector of in-situ blocked forces at the external and internal interfaces of an overall source according to advanced ISPRM. The BFT is different from the general approach of transmissibility functions. The experimental determination of the functions is presented in subsection 5.3.2. However, the underlying equations of BFT are first explained.

In contrast to classical and in-situ TPA the target quantity for the analysis of the structure-borne sound within a source (A) is chosen to be a vector of in-situ blocked forces $\mathbf{f}_{bl,c}$ acting at DoFs at interface (c) between source (A) and receiver (B). This is depicted by Figure 5.1. Furthermore the internal sources (IA_1 … IA_n) which induce the structure-borne sound of a source (A) are characterised by a vector of in-situ blocked forces $\mathbf{f}_{bl,i}$ at the corresponding DoFs at the internal interfaces ($i_1 \ldots i_n$) as well. Hence a vector of velocities $\mathbf{v}_c$ at interface (c) between source (A) and receiver (B) can be determined based on the knowledge of the in-situ blocked forces $\mathbf{f}_{bl,i}$ and $\mathbf{f}_{bl,c}$ and corresponding mobilities $\mathbf{Y}_{ci}$ and $\mathbf{Y}_{cc}$ as follows

$$\mathbf{v}_c = \mathbf{Y}_{cc}\mathbf{f}_{bl,c} \tag{5.1}$$

$$\mathbf{v}_c = \mathbf{Y}_{ci}\mathbf{f}_{bl,i} \tag{5.2}$$

Based on Eq. (5.1) and Eq. (5.2) the following relation between the in-situ blocked forces $\mathbf{f}_{bl,i}$ at the internal interfaces $\left(i_1 \cdots i_n\right)$ and the in-situ blocked forces $\mathbf{f}_{bl,c}$ at the external interface (c) can be established

$$\mathbf{f}_{bl,c} = \mathbf{Y}_{cc}^{-1}\mathbf{Y}_{ci}\mathbf{f}_{bl,i} = \mathbf{T}_{C,ci}\mathbf{f}_{bl,i} \tag{5.3}$$

The matrix $\mathbf{T}_{C,ci}$ which relates the two vectors of internal in-situ blocked forces $\mathbf{f}_{bl,i}$ and external in-situ blocked forces $\mathbf{f}_{bl,c}$ is equal to the transpose of the generalised transmissibility matrix, see Ribeiro et al. [15]. Maia et al. [16] proposed an approach to determine the transmissibility based on kinematic quantities only and Moorhouse et al. showed that the generalised transmissibility is invariant to whether the excitation is applied at the interface DoFs or downstream of the interface [29].

The BFT matrix $\mathbf{T}_{C,ci}$ can be theoretically determined in two ways. The first yields the functions which are the generalised transmissibility functions $\mathbf{T}_Y$ and are based on mobilities[13] as follows (compare Figure 5.2)

$$\mathbf{T}_Y = \left(\left(\mathbf{Y}_{C,cc}\right)^T\right)^+ \left(\mathbf{Y}_{C,ic}\right)^T = \left[\left(\mathbf{Y}_{C,ic}\right)\left(\mathbf{Y}_{C,cc}\right)^+\right]^T \tag{5.4}$$

where $\mathbf{Y}_{C,cc}$ is the point mobility matrix of the coupled system (C) for an excitation and a response at the interface (c) between the source (A) and the receiver (B). $\mathbf{Y}_{C,ic}$ denotes a transfer mobility matrix for an excitation at the interface (c) and a response at the internal interface (i) between the internal source (IA) and the internal receiver (IB). This is given by the generalised transmissibility approach by Ribeiro et al. [15]. However, in most cases it is not possible to determine the mobilities $\mathbf{Y}_{C,cc}$ and $\mathbf{Y}_{C,ic}$ because neither interface (c) or interface (i) is accessible with an impact hammer, which is often used in structural dynamics for the excitation of a structure [113]. For that reason a second methodology to determine the transmissibility $\mathbf{T}_{C,ci}$ is presented which is based only on velocities that can be measured without the necessity to excite at interface (c) or (i). The second approach is detailed in subsection 5.3.2. This method will be used for the case studies, presented in section 4.5.

[13] the subscript Y should indicate that this transmissibility function is derived from mobility functions.

5.3 Blocked force transmissibility transfer path analysis

5.3.1 Introduction

In subsection 3.2.2 the functional principle of an EPSapa system was introduced. According to this functional principle an EPSapa system can be substructured into three main internal sources and one internal receiver: the housing of the steering system. Based on this substructuring approach the advanced internal-source-path-receiver model, introduced in section 5.2, is derived. Furthermore it was briefly outlined that the in-situ blocked forces of the whole EPSapa system and the in-situ blocked forces of the internal sources can be related via multiple transmissibility functions which are called BFT functions. The methodology to determine this BFT functions in order to relate vectors of in-situ blocked forces at the internal and external interfaces to each other will be outlined in the following of this section. In this context, the aISPRM serves as the foundation of the derived BFT functions. Furthermore a validation approach is presented to prove the feasibility and validity of the methodology to determine BFT functions. The section ends with a discussion of the benefits and drawbacks of BFT functions.

5.3.2 Methodology to determine blocked force transmissibility

In section 5.2 it was outlined with the help of the advanced internal-source-path-receiver model that the in-situ blocked forces $\mathbf{f}_{bl,c}$ of an EPSapa system or any other product are the sum of the internal source mechanisms in terms of in-situ blocked forces $\mathbf{f}_{bl,i}$ according to Eq. (2.8). In the following of this subsection the methodology to determine the BFT matrix $\mathbf{T}_{C,ci}$ will now be described.

Generally, the transmissibility can be understood as the ratio between velocities measured at interface (c) and (i) for an excitation at interface (c). Moorhouse et al. [29] showed that the generalized transmissibility is independent from the location of the excitation. This means that the excitation can occur directly at the interface (c) or through a coupled structure at interface (b). Based on the findings of Maia et al. [16] and Tcherniak [114], which showed that the transmissibility can be calculated by using response measurements in terms of velocities, only the BFT matrix $\mathbf{T}_{C,ci}$ can be determined using the follow measurement routine (Figure 5.2).

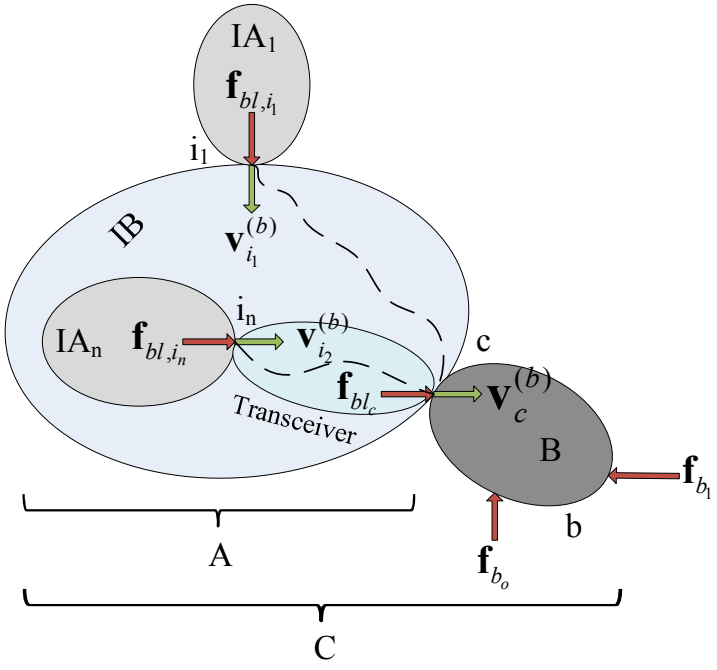

Figure 5.2: Methodology to determine blocked force transmissibility functions

Using different excitations $\left(\mathbf{f}_{b_1} \quad \mathbf{f}_{b_2} \quad \cdots \quad \mathbf{f}_{b_o}\right)$ at interface (b) corresponding responses $\mathbf{v}_{C,c}$ and $\mathbf{v}_{C,i}$ at interface (c) and interface (i) can be measured. Here o is the number of different excitation locations at interface (b). This yields the expression for the transmissibility $\mathbf{T}_{C,ci}$ as follows

$$\begin{aligned}\mathbf{T}_{C,ci} &= \begin{pmatrix} \mathbf{v}_{C,c}^{(b_1)} \\ \mathbf{v}_{C,c}^{(b_2)} \\ \vdots \\ \mathbf{v}_{C,c}^{(b_o)} \end{pmatrix}^{+} \begin{pmatrix} \mathbf{v}_{C,i}^{(b_1)} \\ \mathbf{v}_{C,i}^{(b_2)} \\ \vdots \\ \mathbf{v}_{C,i}^{(b_o)} \end{pmatrix} \\ &= \left(\begin{pmatrix} \mathbf{v}_{C,c}^{(b_1)} & \mathbf{v}_{C,c}^{(b_2)} & \cdots & \mathbf{v}_{C,c}^{(b_1)} \end{pmatrix}^{T} \right)^{+} \begin{pmatrix} \mathbf{v}_{C,i}^{(b_1)} & \mathbf{v}_{C,i}^{(b_2)} & \cdots & \mathbf{v}_{C,i}^{(b_1)} \end{pmatrix}^{T} \\ &= \left(\mathbf{V}_{C,c}^{(b)} \right)^{+} \mathbf{V}_{C,i}^{(b)} \end{aligned} \tag{5.5}$$

The transmissibility matrix $\mathbf{T}_{C,ci}$ based on velocities will be called the BFT matrix in the following. Based on the BFT, the relation between the vector of internal blocked forces $\mathbf{f}_{bl,i}$ and the vector of external blocked forces $\mathbf{f}_{bl,c}$ can be expressed as follows

$$\mathbf{f}_{bl,i} = \left[\left(\mathbf{V}_{C,i}^{(b)} \right)^{+} \left(\mathbf{V}_{C,c}^{(b)} \right) \right] \mathbf{f}_{bl,c} \tag{5.6}$$

Therefore for the determination of the transmissibility matrix $\mathbf{T}_{C,ci}$ the source (A) which is coupled to receiver (B) is excited at multiple locations (b) to yield responses at the internal interfaces ($i_1 \ldots i_n$) and the external interface (c), respectively. A fundamental requirement of this approach is that the number of excitation DoFs *o* is equal to or greater than the DoFs of dynamic loads at the internal interface ($i_1 \ldots i_n$). The vectors of responses at the internal interfaces $\left(\mathbf{v}_{C,i}^{(b_1)} \cdots \mathbf{v}_{C,i}^{(b_o)} \right)$ and the external interface ($\mathbf{v}_{C,c}^{(b_1)} \ldots \mathbf{v}_{C,c}^{(b_o)}$) as a consequence of the *o* excitations are then organised in matrices $\mathbf{V}_{C,i}^{(b)}$ and $\mathbf{V}_{C,c}^{(b)}$.

For stabilisation of the solution to Eq. (5.6) the amount of excitation *o* can be greater than the number of DoFs at the internal interfaces. Hence the matrices $\mathbf{V}_{C,i}^{(b)}$ and $\mathbf{V}_{C,c}^{(b)}$ are not square and

pseudo inversion of $\mathbf{V}_{C,c}^{(b)}$ is needed. The fundamental equation for bfTPA which forms the basis to analyse the transfer path problem of aISPRM is formulated as follows

$$\mathbf{f}_{bl,c} = \mathbf{T}_{C,ci}\mathbf{f}_{bl,i} \tag{5.7}$$

Eq. (5.7) and Eq. (5.6) apply for generalized blocked forces, including blocked moments.

5.3.3 Validation method for blocked force transmissibility transfer path analysis

In the previous subsection a methodology is presented to experimentally determine BFT functions and arrange them in a matrix. The matrix forms the link between a vector of external and internal in-situ blocked forces of a vibrational source. The matrix is determined using artificial excitation at random positions on the receiver.

Since both the vector of internal blocked forces as well as the vector of external in-situ blocked forces are determined using an inverse approach both vectors are known to be error prone [55], [56]. For that reason in the following a validation approach of the developed bfTPA methodology and the corresponding aISPRM is presented, which avoids that problem.

The presented approach is based on the OBV approach which is used to confirm the correct determination of in-situ blocked forces [28]. The approach is to first validate the external in-situ blocked forces $\mathbf{f}_{bl,c}$ at the external interface between the overall source (A) and the overall receiver (B). Afterwards the internal in-situ blocked forces $\mathbf{f}_{bl,i}$ of every internal source are validated. Therefore at first the in-situ blocked forces of the internal sources are used with the

transmissibility functions $\mathbf{T}_{C,ci}$ to predict external in-situ blocked forces $\overline{\mathbf{f}}_{bl,c}$ according to Eq. (5.7). The general approach of the validation is depicted by Figure 5.3.

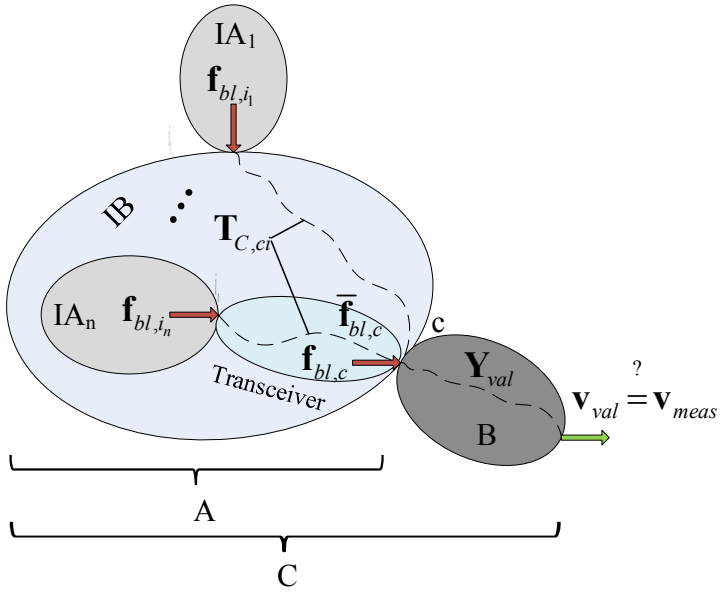

Figure 5.3: Approach to validate the determined internal in-situ blocked forces $\mathbf{f}_{bl,i}$ of an overall source (A)

The predicted external in-situ blocked forces $\overline{\mathbf{f}}_{bl,c}$ and the corresponding FRFs $\mathbf{Y}_{val}$ (compare also Figure 2.7 and subsection 2.3.5) are used to determine a kinematic quantity such as velocity $\mathbf{v}_{val}$ at a validation location on the overall receiver such as a test rig, for instance, as follows

$$\begin{aligned} \mathbf{v}_{val} &= \mathbf{Y}_{val}\mathbf{f}_{bl,c} \\ \overline{\mathbf{v}}_{val} &= \mathbf{Y}_{val}\overline{\mathbf{f}}_{bl,c} = \mathbf{Y}_{val}\underbrace{\left(\mathbf{V}_{C,c}^{(b)}\right)^{+}\left(\mathbf{V}_{C,i}^{(b)}\right)}_{\mathbf{T}_{C,ci}}\mathbf{f}_{bl,i} \end{aligned} \tag{5.8}$$

In this way two measurement techniques are compared. The first technique is the determination of blocked forces at the external interfaces $\mathbf{f}_{bl,c}$ using the in-situ method. In subsection 5.4.4

this will be labelled “in-situ”. The second method uses the BFT functions $\mathbf{T}_{C,ci}$ to derive predicted external in-situ blocked forces $\overline{\mathbf{f}}_{bl,c}$ based on internal in-situ blocked forces. $\mathbf{f}_{bl,i}$. This will be labelled “predicted” in subsection 5.4.4. Both velocities $\mathbf{v}_{val}$ are compared with the measured velocity $\mathbf{v}_{meas}$ at the validation location. In this way the external blocked forces and the internal blocked forces and the corresponding BFT functions are validated. The approach will be applied to validate the results of the case studies of an EPSapa system which are presented in subsection 5.4.3 and subsection 5.4.4.

5.3.4 Drawback of blocked force transmissibility

In the previous subsections the main benefits of the methodology of bfTPA are elucidated. The independence of the approach from the overall receiver and the fact that the approach can be carried out in-situ is highlighted. However, like other transmissibility based TPA approaches the bfTPA approach contains aspects which should be carefully taken into account. Therefore in the course of this subsection the drawbacks of the presented bfTPA approach are discussed.

One of the benefits of bfTPA and also other transmissibility based approaches is the fact that no excessive FRF measurements are necessary [71], [115]. This means that in order to determine the matrix, which relates the internal and the external vectors of in-situ blocked forces operational measurements, can be used. This poses an advantage over FRF based TPA methods since the expenditure of time and the measurement expense is significantly reduced. However, the success of transmissibility based TPA approaches requires knowledge of all relevant transmission paths. Otherwise the contribution of one DoF to the overall source strength can be significantly over predicted. This applies for the bfTPA method as well.

A further risk concerns the potential complexity of the overall source. In theory every DoF that should be investigated by carrying out a bfTPA approach requires a row in the BFT matrix. However, this means that for the generation of a new row an operational state is required, which is linearly independent from the other operational states. Although this is, in theory, possible to achieve through artificial excitation at different receiver locations, in reality the signals which are used for the artificial excitation are not always linearly independent. This is especially if the full frequency range that should be investigated is taken into account. Hence the BFT matrix does not always have full rank. If a sufficient over determination of the system is to be achieved, more artificial excitation signals than DoFs to be investigated are necessary. In subsection 5.4.4 the effect of over determination is discussed. Furthermore a criterion is presented based on coherence to separate excitation signals which contribute to the quality of the BFT matrix by adding a new row to the BFT matrix.

5.4 Case studies: Blocked force transmissibility transfer path analysis

5.4.1 Introduction

In section 5.3 a novel TPA approach called bfTPA is proposed and the underlying equations are derived and presented. The proposed methodology of bfTPA is based on BFT functions which are derived from basic equations of structure-borne sound and the in-situ blocked force method. The derivation of the general equations was shown in section 5.3. For the validation of the novel bfTPA methodology three different case studies are carried out which increase in complexity and are presented in the following subsections.

At first in subsection 5.4.2 the general underlying equations of the bfTPA approach are proven to be valid by using a freely suspended steel beam and artificial excitation to simulate the internal source mechanisms. A steel beam and artificial excitation is chosen because a beam is a technical structure that only allows movement in particular directions. Furthermore this case study contains the determination of in-situ blocked moments to prove the validity of the bfTPA methodology for rotational DoFs. In subsection 5.4.3 and subsection 5.4.4 an EPSapa system as introduced in section 3.2 is used for conducting the bfTPA. The results of this case study are presented and discussed in subsection 5.4.3. In the third case study which is presented in subsection 5.4.4 multiple constant steering manoeuvres are considered and hence a realistic application is simulated.

5.4.2 Case study I: Freely suspended steel beam

This subsection introduces a case study which confirms the feasibility of the novel bfTPA approach (compare section 5.3) for translational and rotational DoFs. For this purpose a steel beam is used as an overall source according to aISPRM (compare section 5.2). Figure 5.4 shows the test setup which is used to carry out the case study.

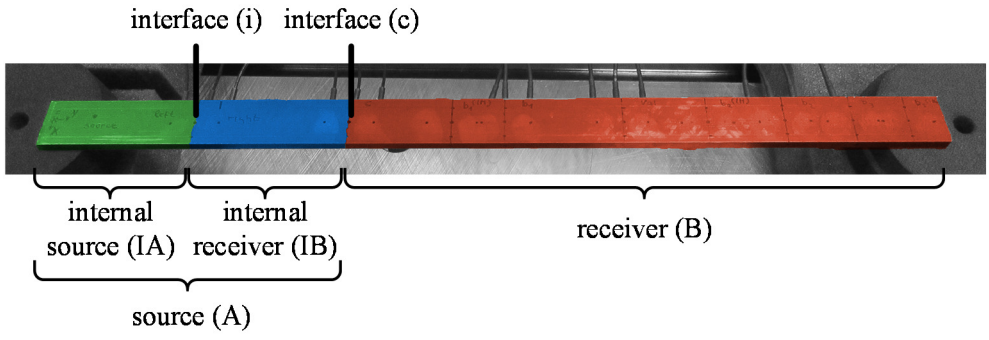

Figure 5.4: Test setup for the determination of the in-situ blocked forces at the external and internal interface and the corresponding BFT functions between interface (i) and (c)

The test setup consists of a steel beam freely suspended on both ends on foam. The free suspension allows for the assumption that solely the internal in-situ blocked forces are taken into consideration and no external unintentional disturbance is present. In order to fulfil the principle of aISPRM the used steel beam is virtually subdivided into three parts. The green coloured part represents an internal source (IA) that is connected to a blue coloured internal receiver (IB) at the internal interface (i). Both parts (green and blue) together form the overall source (A) which is coupled to an orange coloured receiver (B). The overall source and the receiver are attached at the external interface (c). Both the internal and the external interface can be treated as continuous line. Hence discretisation of the interface is necessary as discussed in subsection 4.3.2. However, since the width of the beam is comparably small the interfaces (i) and (c) are each discretised by just one point connection. The considered DoFs at the internal and the external interface (i) and (c), respectively, will be discussed further in this subsection.

The beam is artificially excited in out of plane direction at an arbitrary location on the internal source (IA). This kind of excitation represents an unknown internal source mechanism within (A) which can be characterised with in-situ blocked forces and moments at the internal interface (i). Furthermore the artificial excitation generates dynamic loads at the external interface (c) which are characterised by in-situ blocked forces and moments. The blocked forces and moments at interface (c) and interface (i) are determined according to the in-situ method. For the determination of the in-situ blocked moments the central difference approach by Elliott is used to yield the necessary moment mobilities [48].

The BFT matrix, according to Eq. (5.5), is compared with the ratio of the internal and external in-situ blocked forces and moments at interface (i) and (c), respectively. It can be observed from

the spectra of the in-situ blocked forces and moments, shown by Figure 5.5, that the characteristic of the internal and external blocked forces and moments is different hence making them linearly independent. This fact is a necessary requirement for the validation of the presented methodology of the bfTPA. For a complex product such as a vehicle component it is expected that the internal and external in-situ blocked forces and moments at interface (i) and (c) are linearly independent as well.

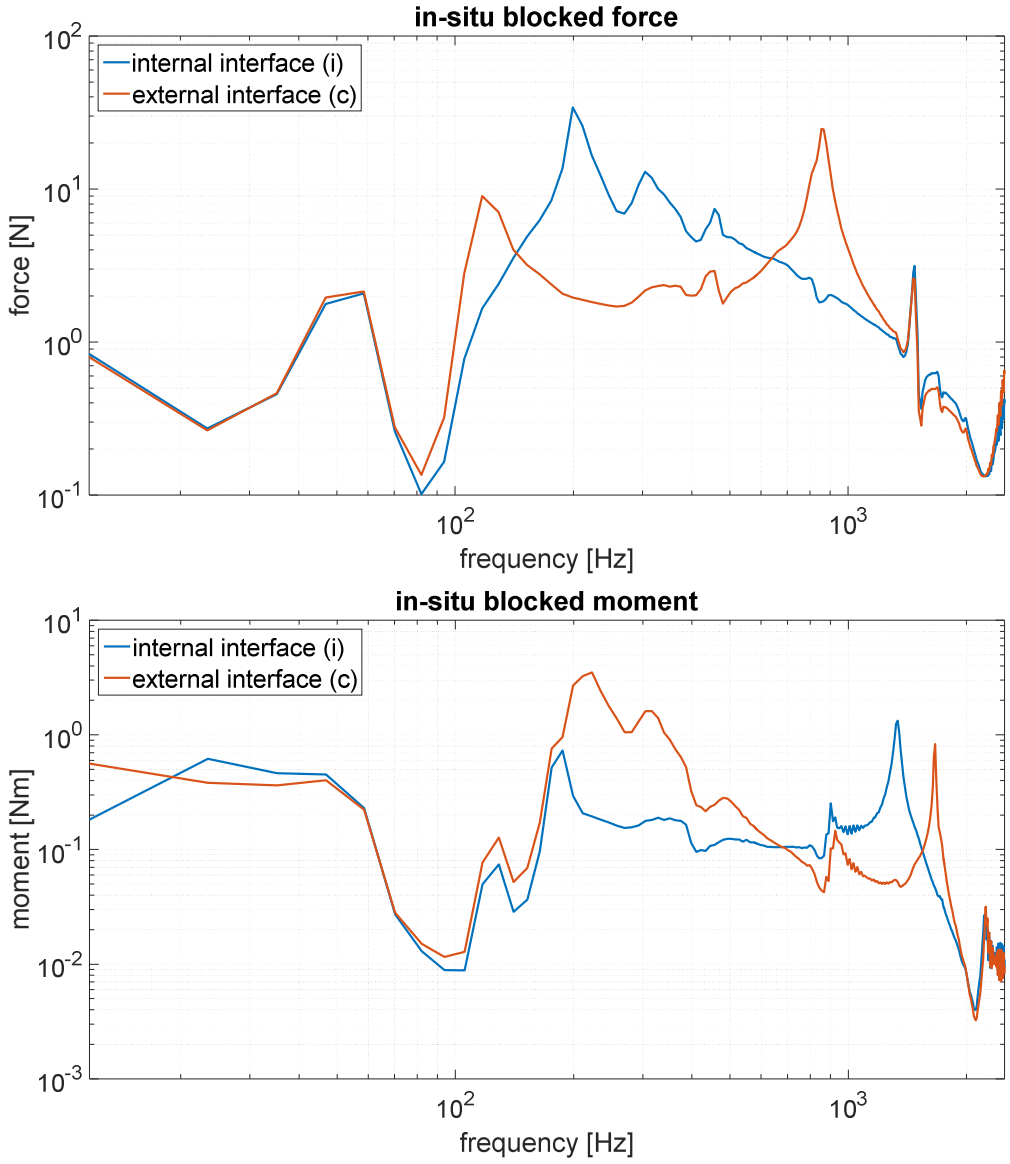

Figure 5.5: In-situ blocked forces (left) and moments (right) at interface (i) and (c)

The comparison of the transmissibility matrix determined by the ratio of the internal and external in-situ blocked forces and moments and the transmissibility matrix determined by velocities according to Eq. (5.5) is shown by Figure 5.6. It can be observed that both the force and moment based transmissibilities are nearly equal to the corresponding velocity and angular velocity based transmissibilities determined according to Eq. (5.5).

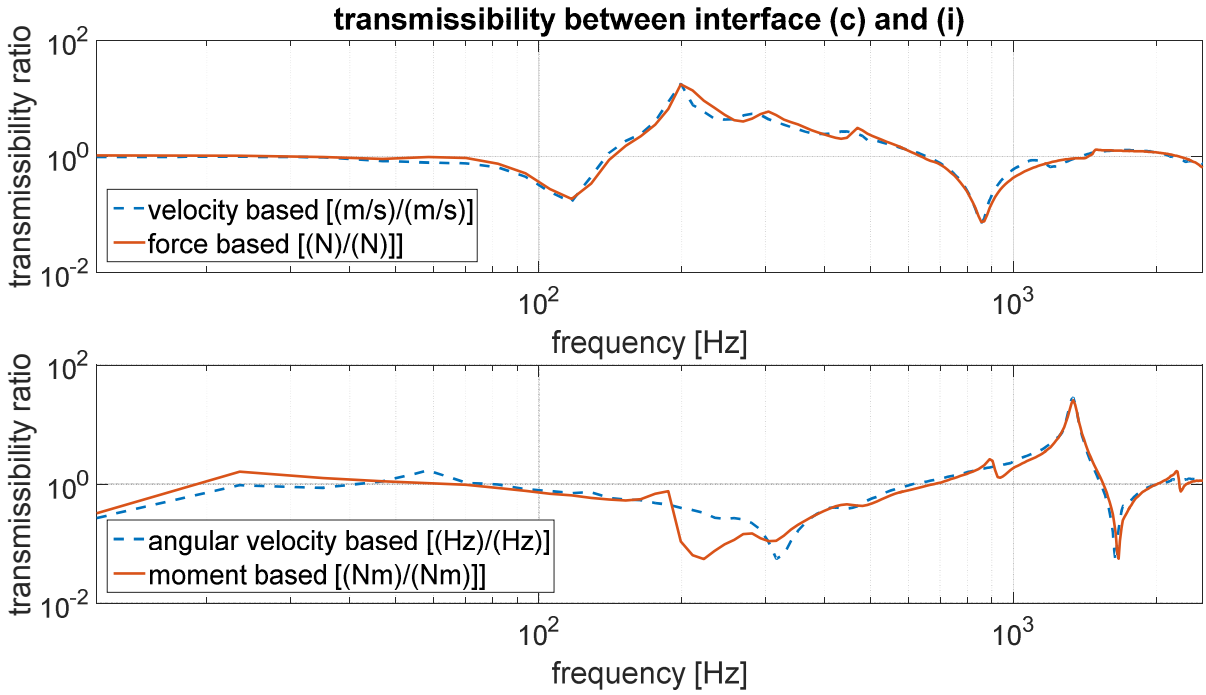

Figure 5.6: Comparison of transmissibility between external interface (c) and internal interface (i); upper diagram: blocked force transmissibility functions; lower diagram: blocked moment transmissibility functions

Based on Eq. (5.7) the determined in-situ blocked forces and moments at the internal interface (i) can be used in combination with the velocity based transmissibility matrix to predict the in-situ blocked forces and moments at the external interface (c). This shows a potential application of the presented methodology. The prediction is shown by Figure 5.7.

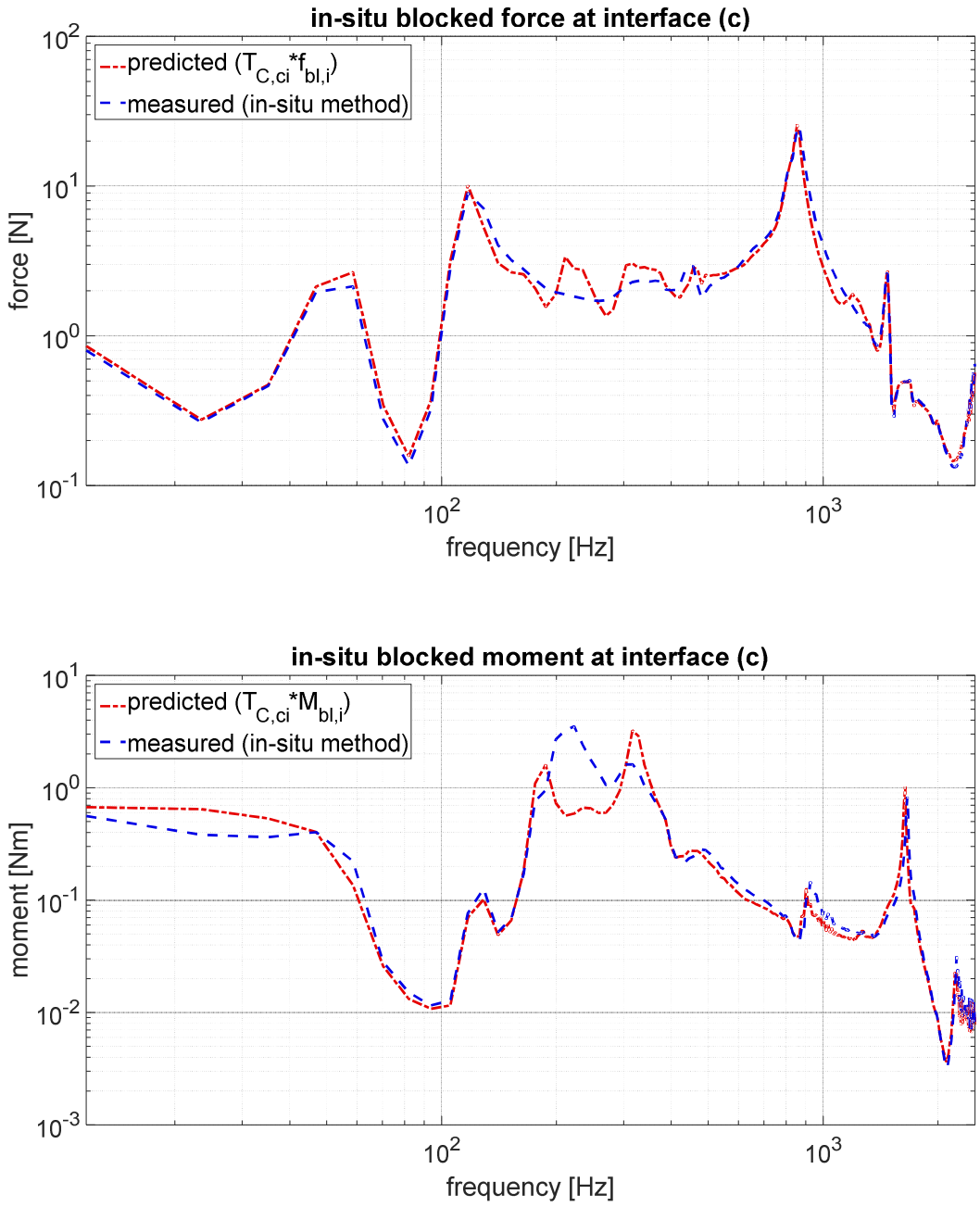

Figure 5.7: Predicted strength of source (A) at external interface (c) based on transmissibility and source strength of internal source (IA) at internal interface (i); upper diagram: in-situ blocked force; lower diagram: in-situ blocked moment

It can be seen that the experimentally determined BFT matrix according to Eq. (5.5) is a solid basis to predict in-situ blocked forces and moments at the external interface (c) based on the knowledge of the in-situ blocked forces and moments at the internal interface (i) and vice versa.

Therefore the internal source mechanisms can be easily observed from the external in-situ blocked forces and moments if the BFT matrix can be experimentally determined using accelerometers.

5.4.3 Case study II: Artificial excitation of electric power steering systems

In the previous subsection it was shown that the developed aISPRM and the underlying equations of the bfTPA method are generally valid. In order to show the validity for both translational as well as rotational DoFs at internal and external interfaces, respectively, a freely suspended steel beam was used. However, at this point the question arises on if the underlying equations of the bfTPA method can be applied with the same or comparable accuracy to a more complicated structure-borne sound source containing multiple internal structure-borne sound sources. For that reason an EPSapa system, which is a particular type of EPS systems, was used as the presented case study. In the following the results and the procedure of the case study are presented.

As described in chapter 3, an EPSapa system consists of three main internal sources and one secondary source, the so called steering pinion. The steering pinion is mentioned for the sake of completeness but is not part of the conducted bfTPA approach since it is considered as a secondary source. The aforementioned dominant internal sources and the corresponding transmission paths within the housing should be rank ordered in relation to their partial contribution to the overall source strength of the EPSapa system in terms of in-situ blocked forces. Theoretically, a classical TPA or an iTPA, instead of a bfTPA, can be carried out to achieve a meaningful rank ordering of the internal source strengths. However, the idea of the proposed novel bfTPA

is to be fully based on quantities that are solely used for the independent characterisation of both the overall source as well as the embedded internal sources.

The general principle of the bfTPA approach for the case of an EPSapa system is schematically shown in Figure 5.8[14].

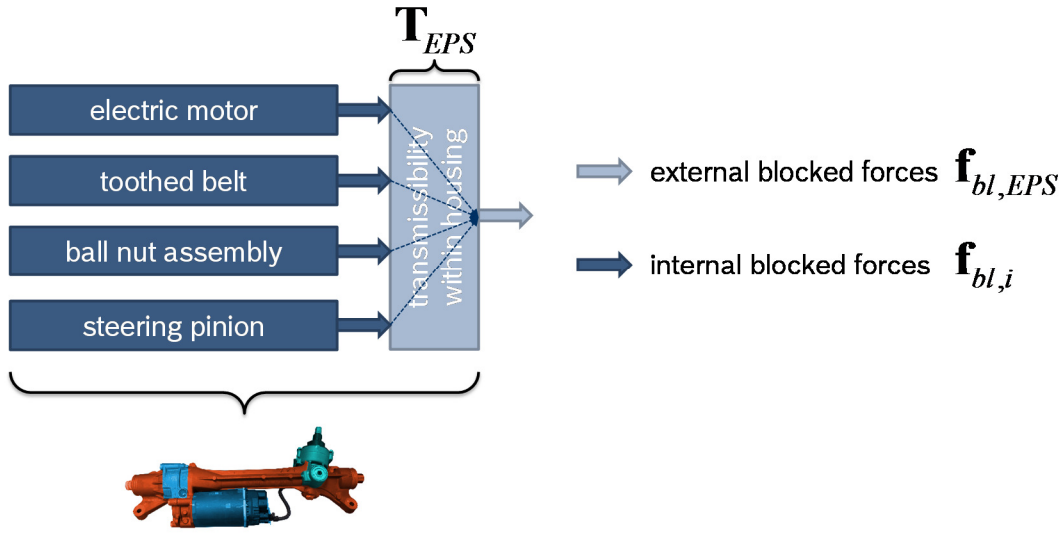

Figure 5.8: Principle of a bfTPA within an EPSapa system based on the external and internal in-situ blocked forces and the corresponding blocked force transmissibility functions

In order to be able to determine the BFT matrix $\mathbf{T}_{EPS}$ experimentally the methodology proposed in section 5.3 is used. The matrix contains the BFT functions which describe the transmission paths within the housing between the DoFs at the external and internal interfaces of an EPSapa system. As already mentioned, the methodology of bfTPA differs from classical TPA and iTPA in the way that the target quantity of the approach is a vector of in-situ blocked forces

[14] The steering pinion is mentioned for completeness since it can be seen as an internal source, but in most cases the structure-borne sound of an EPSapa system is not influenced by the steering pinion.

$\mathbf{f}_{bl,EPS}$ characterising the whole source which is in this case the EPSapa system. The transmission paths within the internal receiver which in this case is the housing of the EPSapa system is characterised by the use of a BFT matrix $\mathbf{T}_{EPS}$ [15] rather than a FRF matrix. Hence, the input quantity of the bfTPA approach are vectors of in-situ blocked forces $\mathbf{f}_{bl,i}$ characterising the vibrational behaviour of the internal sources (electric motor, toothed belt and ball nut assembly) which can be determined independently from each other on specified test rigs.

Since every DoF of the vector of in-situ blocked forces characterising the internal sources $\mathbf{f}_{bl,i}$ is correlated with one transmission path characterised by a BFT function it is possible to determine the partial contribution of each internal source DoFs according to Eq. (5.7). This general principle of a bfTPA approach is the basis for the case study presented in the following and also for the case study presented in subsection 5.4.4. A further benefit of the bfTPA approach for EPSapa systems will be outlined in subsection 5.5.3.

To conduct the bfTPA within an EPSapa system, the steering system is mounted on a test rig which is specifically designed to determine the external in-situ blocked forces of different steering systems. Hence the test rig is called “adaptive test rig” (ATR). The test rig was designed and validated by Lang and further improved by Huttenlauch [116]. Figure 5.9 shows the test rig including the mounted EPSapa system. The ATR consists of four base plates which allow the distances to be altered between the four towers, which are used to fix the steering system. Hence the towers form the external interface with the EPSapa system. In theory other test rigs or a

[15] coupled mobility matrix

front axle carrier can be used, which allow a stiff mounting of the EPSapa system to carry out an EPSapa system.

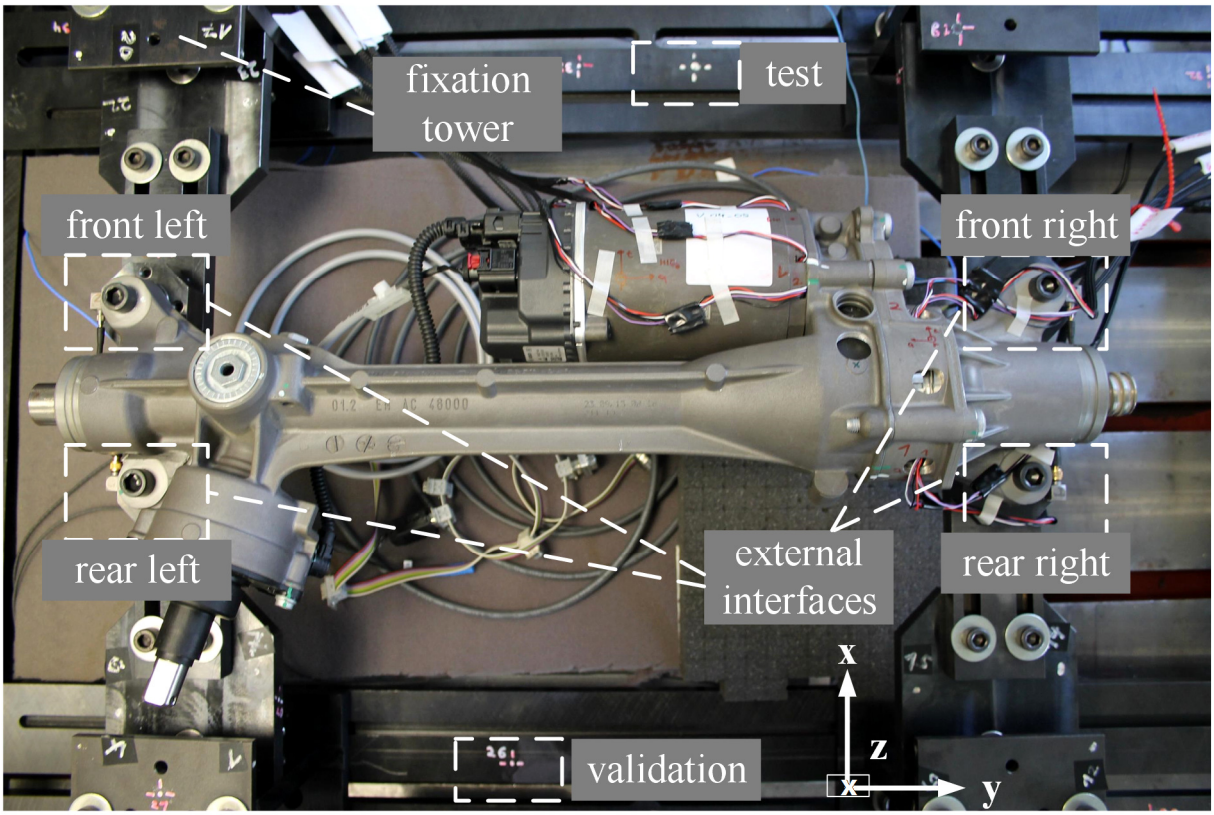

Figure 5.9: Adaptive test rig used for the determination of in-situ blocked forces of an EPSapa system

The EPSapa system is characterised by 12 external in-situ blocked forces (compare subsection 3.4.2) at the external interfaces between the steering system and the test rig. At each of the external interface, namely “front left”, “front right”, “rear left” and “rear right” three perpendicular blocked forces are determined. The naming for each external interface is chosen according to the position of the external interface when the EPSapa system is mounted towards the front axle carrier of a vehicle. The success of characterising an EPSapa system with three translational DoFs at each external interface was shown by Sturm [11], [12], [32], [66], Alber [77], [104] and Bauer [31].

For the experimental determination of the external and internal in-situ blocked forces of the EPSapa system, 36 remote points are used which are positioned on the ATR. In this manner a three times over-determination of the system is used for the inverse calculation of the external in-situ blocked forces. The 36 remote points are defined in a near, mid and far field range according to the position where the EPSapa system is mounted towards the test rig. Each range on the test rig contains 12 remote points. The near field range is close to the external interfaces between EPSapa system and the test rig. The midfield range is defined on the fixation towers. The far field range is defined as the remote points which are placed on the four base plates of the ATR. Furthermore each range contains four remote points per perpendicular direction of the vehicle coordinate system, respectively.

The operational state was created using an artificial excitation. That way the complexity of the case study is reduced and the general applicability of a bfTPA approach within a complex product such as an EPSapa system can be validated. To create the artificial excitation the steering system is not driven but excited at a position on the EM using an impact hammer. Since the TB and the BNA are downstream of the EM in direction to the external interfaces this approach is valid and the EM can be seen as the only active internal source of the EPSapa system. However the internal interface between the EM and the EPSapa system is further subdivided. The first interface is chosen between the housing of the EM and the housing of the EPSapa system. This is the same approach as used in section 4.5.2. Hence 9 DoFs are defined at this interface. The second interface is chosen between the pinion of the EM and the toothed belt. This interface is characterised with three DoFs according to the finding which are presented in section 4.5.4. Hence, in total 12 internal in-situ blocked forces are determined. This way a three times over-determination for the inverse calculation of the defined internal in-situ blocked forces is achieved.

One specific validation point on the test rig is used for the OBV of the external and the internal in-situ blocked forces (Figure 5.9). The validation approach for the bfTPA is described in subsection 5.3.3. The same approach, based on Eq.(5.8), was used for the validation of the artificially excited EM. The results of the aforementioned validation approach for the bfTPA approach are shown in Figure 5.10.

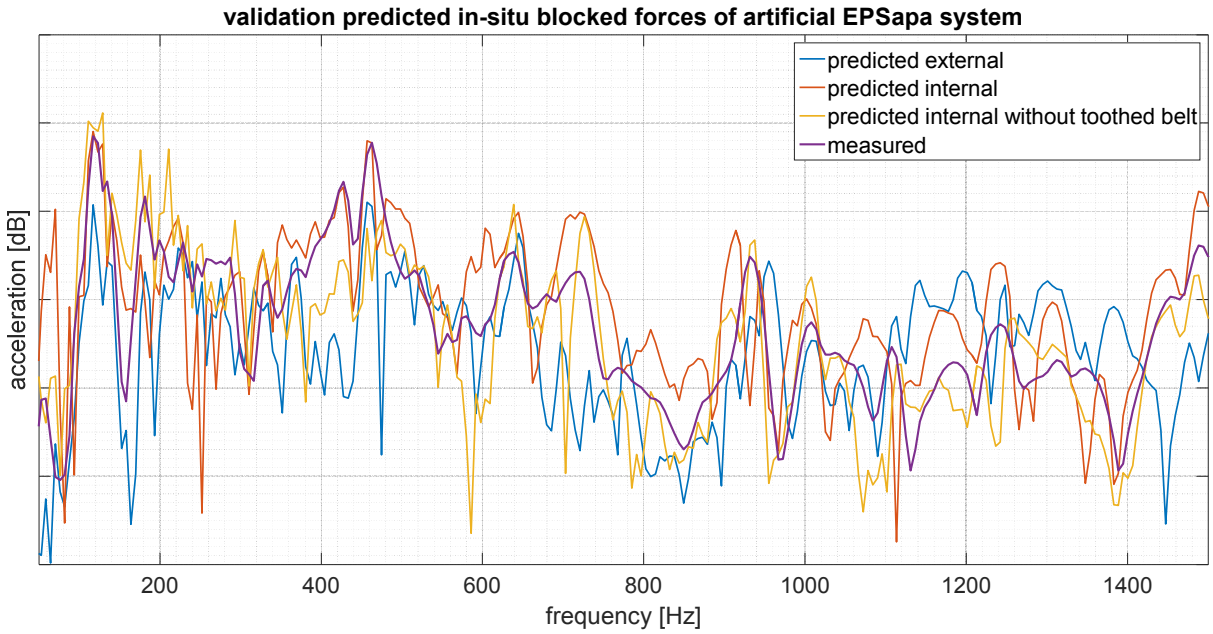

Figure 5.10: Validation of the external and internal in-situ blocked forces of an artificially excited EPSapa system mounted on a test rig; grid ordinate: 10 dB

It can clearly be stated that the internal in-situ blocked forces are successfully determined since the acceleration at the validation point (purple curve) is predicted at the peaks with a deviation below 5 dB high accuracy based on the internal in-situ blocked forces and the corresponding BFT functions (red curve). The OBV approach of the external in-situ blocked forces according to Eq. (2.9) yields the blue curve. It can clearly be seen that the prediction of the acceleration is 5 dB worse compared to the prediction based on the internal in-situ blocked force. Hence the conclusion is drawn that it is favourable to determine the in-situ blocked forces as close as

possible to the location of the internal source generation mechanisms. Figure 5.10 includes the prediction of the acceleration at the validation point if the internal in-situ blocked forces at the interface between pinion and toothed belt and the corresponding BFT functions within the belt are excluded (yellow curve). It can be seen that if this is done the prediction of the acceleration based on Eq. (5.8) gets 5 dB worse. This allows the conclusion that the in-situ blocked forces at the interface between toothed belt and pinion and the corresponding transmission paths are important for the transmission of structure-borne sound within an EPSapa system. Therefore the structure-borne sound induced by the TB cannot be neglected. To take this transfer path into account MEMS accelerometers were placed on the pinion of the EM as depicted by Figure 5.11. This way the BFT functions which describe the sound transfer between the pinion and the external interfaces of an EPSapa system can be taken into account. If the pinion is driven the MEMS accelerometers need to be removed according to what is proposed in section 4.4.

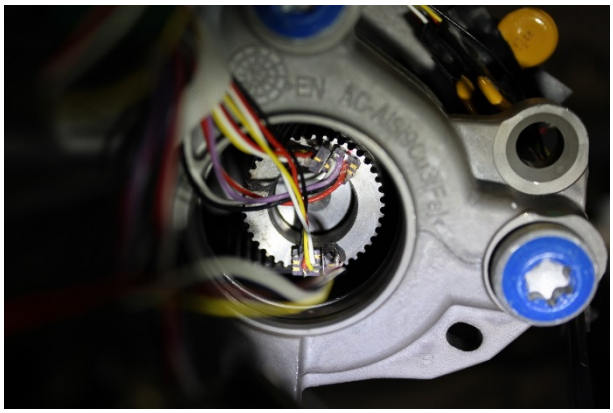

Figure 5.11: MEMS accelerometers placed at pinion of electric motor

One aim of the thesis is to show that rank ordering of internal sources of an EPSapa system can be achieved based by applying the proposed bfTPA approach. For the theory of bfTPA the target quantity should be chosen as an in-situ blocked force at one defined external interface DoF. This would mean that the contribution of the 12 internal in-situ blocked forces to in total 12 in-

situ blocked forces at the external interface needed to be determined within this case study. However, in order to avoid presenting 12 graphs in the following, a different approach to illustrate the contribution of the internal in-situ blocked forces is elucidated. The contribution of the electric motor and the pinion to the external source strength of the EPSapa system are summarised in Figure 5.12. However it is of course theoretically possible by applying Eq. (5.7) to determine the contribution of every internal in-situ blocked force and the corresponding BFT functions to each of the 12 external in-situ blocked forces which characterise an EPSapa system.

However, for the sake of simplicity the target quantity is chosen as a predicted kinematic quantity $\tilde{\mathbf{y}}$ such as acceleration, on the overall receiver (B) which is the ATR. The quantity $\tilde{\mathbf{y}}$ is predicted based on the external in-situ blocked forces $\mathbf{f}_{bl,EPS}$ and the corresponding FRFs $\mathbf{H}_{EPS}$ as follows

$$\tilde{\mathbf{y}}_b = \mathbf{H}_{b,EPS}\mathbf{f}_{bl,EPS} \tag{5.9}$$

Based on the established relationship between $\tilde{\mathbf{y}}$ and $\mathbf{f}_{bl,EPS}$ the contribution of the internal blocked forces of the EM $\mathbf{f}_{bl,EM}$ and the pinion $\mathbf{f}_{bl,P}$ to the external blocked forces $\mathbf{f}_{bl,EPS}$ can be analysed based on the following equation

$$\tilde{\mathbf{y}}_b = \mathbf{H}_{b,EPS}\mathbf{f}_{bl,EPS} = \mathbf{H}_{b,EM}\mathbf{T}_{EM}\mathbf{f}_{bl,EM} + \mathbf{H}_{b,P}\mathbf{T}_P\mathbf{f}_{bl,P} \tag{5.10}$$

where $\mathbf{T}_{EM}$ and $\mathbf{T}_P$ are the BFT matrices containing the BFT functions between the electric motor and the EPSapa system and between the pinion and the EPSapa system, respectively. The FRF matrices $\mathbf{H}_{b,EM}$ and $\mathbf{H}_{b,P}$ relate the internal in-situ blocked forces with the predicted target location on the overall receiver (B).

This approach is consistent with the aim of the bfTPA approach within an EPSapa system to provide information about the contribution of the internal source strengths and be able to use this information in a subsequent VAP approach. If further improvement regarding NVH requirements at each external interface DOFs should be considered the presented bfTPA methodology can be used (compare Figure 5.8). As mentioned before this would yield 12 different analysis which each would show the contribution of each of the 12 internal in-situ blocked forces to one external in-situ blocked force DoF.

Figure 5.12 shows the contribution of the vector of in-situ blocked forces of the electric motor and the pinion to the vector of external in-situ blocked forces of an EPSapa system.

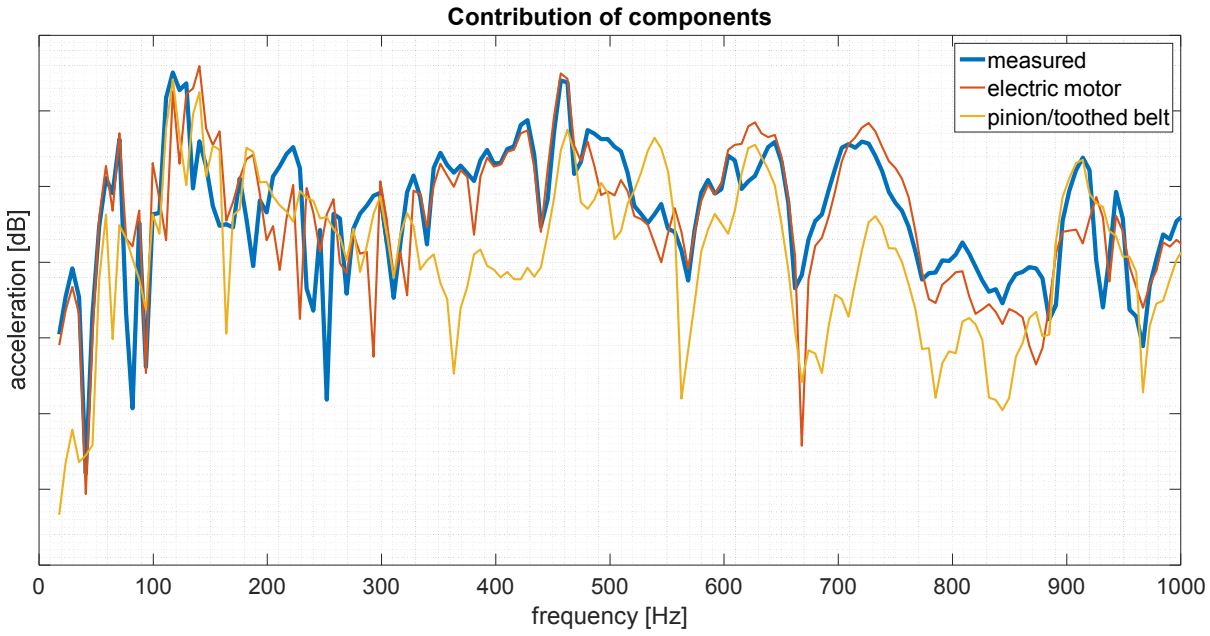

Figure 5.12: Contribution of in-situ blocked forces of electric motor and pinion to structure-borne sound of an artificially excited EPSapa system, grid ordinate: 10 dB

For this particular case of an artificially excited EPSapa system, the in-situ blocked forces of the EM contribute in most frequency ranges more than the in-situ blocked forces at the pinion. This makes sense since the artificial excitation is applied through an impact on the surface of

the EM. Hence it is considered that most of the induced energy of the impact is damped. Furthermore, this case studies proves that the external and the internal in-situ blocked forces of an EPSapa system can be determined with a deviation below 5 dB. Hence, the rank ordering of the internal sources can be achieved. This offers a useful tool for engineers to optimise the internal sources of an EPSapa system. A further discussion of this advantage of bfTPA can be found in section 5.5.

5.4.4 Case study III: Realistic excitation of electric power steering systems

In the course of this thesis it was already shown that it is generally possible to determine external and internal in-situ blocked forces with a deviation below 5 dB for conducting a meaningful bfTPA of MDoF system (see section 5.4.2). Furthermore it was shown in the previous subsection that conducting a bfTPA within an EPSapa system is possible for an artificial case where the EPSapa system is excited with an impact hammer. In the following, a further case study is presented which shows that the description of structure-borne sound within an EPSapa system with realistic boundary conditions is also achievable. Hence, the case study can be seen as the most complex of the case studies.

In order to conduct a meaningful bfTPA of an EPSapa system, both the in-situ blocked forces of every internal source, namely electric motor $\mathbf{f}_{bl,EM}$, ball nut assembly $\mathbf{f}_{bl,BNA}$, toothed belt $\mathbf{f}_{bl,TB}$ and the in-situ blocked forces of the whole EPSapa system $\mathbf{f}_{bl,EPS}$ at the external interfaces, need to be determined. This relationship between the internal and the external in-situ blocked forces of an EPSapa system, via the BFT matrix $\mathbf{T}_{EPS}$, with realistic boundary conditions is shown by Figure 5.13.

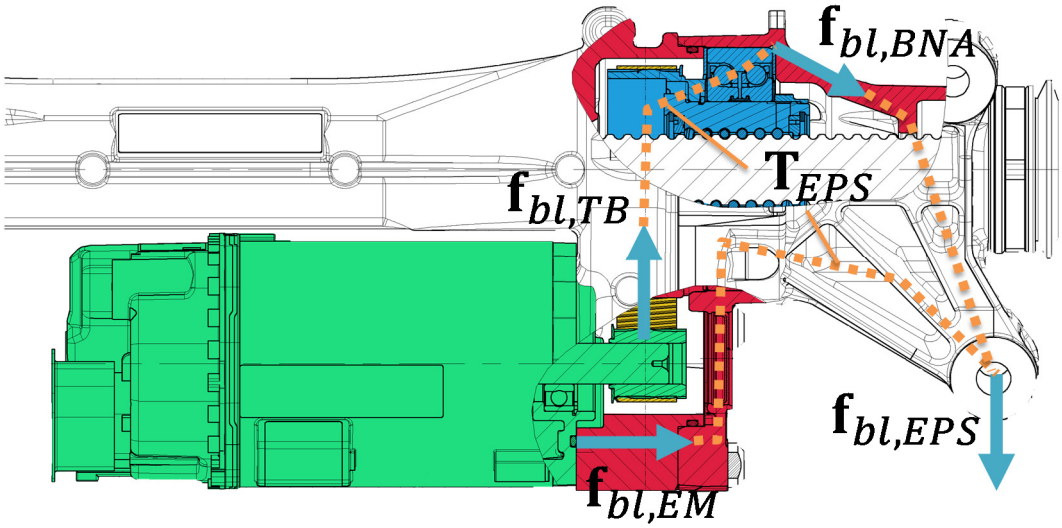

Figure 5.13: bfTPA of an EPSapa system with realistic boundary conditions

The equations for a bfTPA include rotational DoFs at the internal and external interfaces for completeness. However, blocked moments $\boldsymbol{\tau}_{bl}$ and the corresponding angular velocities $\boldsymbol{\alpha}$ and angular velocity matrices $\boldsymbol{\Lambda}$, respectively, are excluded within the case study that is presented in this subsection.

The external in-situ blocked forces and moments $\mathbf{f}_{bl,EPS}$ and $\boldsymbol{\tau}_{bl,EPS}$ of an EPSapa system are related with the internal in-situ blocked forces and moments $\mathbf{f}_{bl,i}$ and $\boldsymbol{\tau}_{bl,i}$ as follows

$$\underbrace{\begin{pmatrix} \underbrace{\mathbf{f}_{bl,EPS}(\xi_{EPS})}_{(12x1)} \\ \underbrace{\boldsymbol{\tau}_{bl,EPS}(\xi_{EPS})}_{(12x1)} \end{pmatrix}}_{(24x1)} = \underbrace{\mathbf{T}_{EPS}(\xi_T)}_{(24x48)} \underbrace{\begin{pmatrix} \mathbf{f}_{bl,i} \\ \boldsymbol{\tau}_{bl,i} \end{pmatrix}}_{(48x1)} \tag{5.11}$$

with ξ_{EPS} and ξ_T being the influences on the in-situ blocked forces and moments and the corresponding BFT functions, respectively. The influences ξ_{EPS} and ξ_T contain the torque of the electric motor M_{EM}, the rotating speed of the electric motor n_{EM}, the tension of the toothed

belt σ_{TB}, the rotating speed of the toothed belt n_{TB}, the rotating speed of the ball nut assembly n_{BNA}, the position of the toothed rack x_{TR}, the so called tie rod forces f_{Trod} which act as external forces on the EPSapa system during a steering manoeuvre and the moments which are defined to mount the EPSapa and its components according to specified assembly conditions M_{AC} as follows

$$\begin{aligned} \xi_{EPS} &= \left(M_{EM}, n_{EM}, \sigma_{TB}, n_{TB}, n_{BNA}, x_{TR}, f_{Trod}\right) \\ \xi_{T} &= \left(M_{AC}, x_{TR}, f_{TR}, \sigma_{TB}\right) \end{aligned} \tag{5.12}$$

The BFT matrix $\mathbf{T}_{EPS}$ contains four sub BFT matrices $\mathbf{T}_{vv}$, $\mathbf{T}_{v\alpha}$, $\mathbf{T}_{\alpha v}$ and $\mathbf{T}_{aa}$. Hence the right hand side of eq. (5.11) can be written as follows

$$\underbrace{\begin{pmatrix} \underbrace{\mathbf{f}_{bl,EPS}(\xi_{EPS})}_{(12x1)} \\ \underbrace{\boldsymbol{\tau}_{bl,EPS}(\xi_{EPS})}_{(12x1)} \end{pmatrix}}_{(24x1)} = \begin{pmatrix} \underbrace{\mathbf{T}_{vv}}_{(12x24)} & \underbrace{\mathbf{T}_{v\alpha}}_{(12x24)} \\ \underbrace{\mathbf{T}_{\alpha v}}_{(12x24)} & \underbrace{\mathbf{T}_{\alpha\alpha}}_{(12x24)} \end{pmatrix} \begin{pmatrix} \underbrace{\mathbf{f}_{bl,EM}}_{(9x1)} \\ \underbrace{\mathbf{f}_{bl,BNA}}_{(9x1)} \\ \underbrace{\mathbf{f}_{bl,TB}}_{(6x1)} \\ \underbrace{\boldsymbol{\tau}_{bl,EM}}_{(9x1)} \\ \underbrace{\boldsymbol{\tau}_{bl,BNA}}_{(9x1)} \\ \underbrace{\boldsymbol{\tau}_{bl,TB}}_{(6x1)} \end{pmatrix} \tag{5.13}$$

The sub BFT matrices $\mathbf{T}_{vv}, \mathbf{T}_{v\alpha}, \mathbf{T}_{\alpha v}$ and $\mathbf{T}_{aa}$ in eq. (5.13) each contain the velocity matrices $\mathbf{V}_C^{(b)}$ and angular velocity matrices $\boldsymbol{\Lambda}_C^{(b)}$, respectively, which are necessary to construct each of the sub BFT $\mathbf{T}_{vv}, \mathbf{T}_{v\alpha}, \mathbf{T}_{\alpha v}$ and $\mathbf{T}_{aa}$ matrices as follows

$$\begin{pmatrix} \underbrace{\mathbf{T}_{vv}}_{(12x24)} & \underbrace{\mathbf{T}_{v\alpha}}_{(12x24)} \\ \underbrace{\mathbf{T}_{\alpha v}}_{(12x24)} & \underbrace{\mathbf{T}_{\alpha\alpha}}_{(12x24)} \end{pmatrix} = \begin{pmatrix} \underbrace{\left(\mathbf{V}_{C,EPS}^{(b)}\right)^{+}}_{(12x12)} \underbrace{\mathbf{V}_{C,i}^{(b)}}_{(12x24)} & \left(\mathbf{V}_{C,EPS}^{(b)}\right)^{+} \mathbf{\Lambda}_{C,i}^{(b)} \\ \left(\mathbf{\Lambda}_{C,EPS}^{(b)}\right)^{+} \mathbf{V}_{C,i}^{(b)} & \left(\mathbf{\Lambda}_{C,EPS}^{(b)}\right)^{+} \mathbf{\Lambda}_{C,i}^{(b)} \end{pmatrix} \tag{5.14}$$

Hence the sub BFT matrices $\mathbf{T}_{vv}$, $\mathbf{T}_{v\alpha}$, $\mathbf{T}_{\alpha v}$ and $\mathbf{T}_{aa}$ can be written as follows

$$\underbrace{\mathbf{T}_{vv}(\omega)}_{(12x24)} = \begin{pmatrix} v_{c,EPS_1}^{(b_1)}(\omega) & \cdots & v_{c,EPS_{12}}^{(b_1)} \\ \vdots & \ddots & \vdots \\ v_{c,EPS_1}^{(b_{12})} & \cdots & v_{c,EPS_{12}}^{(b_{12})} \end{pmatrix}^{+} \begin{pmatrix} v_{c,i_1}^{(b_1)} & \cdots & v_{c,i_{24}}^{(b_1)} \\ \vdots & \ddots & \vdots \\ v_{c,i_1}^{(b_{12})} & \cdots & v_{c,i_{24}}^{(b_{12})} \end{pmatrix} \tag{5.15}$$

Every entrance in the two matrices on the right hand side of Eq. (5.15) such as $v_{c,EPS_1}^{(b_1)}(\omega)$, is dependent on frequency ω. However for the sake of simplicity the variable ω is omitted in the following equations.

$$\underbrace{\mathbf{T}_{v\alpha}}_{(12x24)} = \begin{pmatrix} v_{c,EPS_1}^{(b_1)} & \cdots & v_{c,EPS_{12}}^{(b_1)} \\ \vdots & \ddots & \vdots \\ v_{c,EPS_1}^{(b_{12})} & \cdots & v_{c,EPS_{12}}^{(b_{12})} \end{pmatrix}^{+} \begin{pmatrix} \alpha_{c,i_1}^{(b_1)} & \cdots & \alpha_{c,i_{24}}^{(b_1)} \\ \vdots & \ddots & \vdots \\ \alpha_{c,i_1}^{(b_{12})} & \cdots & \alpha_{c,i_{24}}^{(b_{12})} \end{pmatrix} \tag{5.16}$$

$$\underbrace{\mathbf{T}_{\alpha v}}_{(12x24)} = \begin{pmatrix} \alpha_{c,EPS_1}^{(b_1)} & \cdots & \alpha_{c,EPS_{12}}^{(b_1)} \\ \vdots & \ddots & \vdots \\ \alpha_{c,EPS_1}^{(b_{12})} & \cdots & \alpha_{c,EPS_{12}}^{(b_{12})} \end{pmatrix}^{+} \begin{pmatrix} v_{c,i_1}^{(b_1)} & \cdots & v_{c,i_{24}}^{(b_1)} \\ \vdots & \ddots & \vdots \\ v_{c,i_1}^{(b_{12})} & \cdots & v_{c,i_{24}}^{(b_{12})} \end{pmatrix} \tag{5.17}$$

$$\underbrace{\mathbf{T}_{\alpha\alpha}}_{(12x24)} = \begin{pmatrix} \alpha_{c,EPS_1}^{(b_1)} & \cdots & \alpha_{c,EPS_{12}}^{(b_1)} \\ \vdots & \ddots & \vdots \\ \alpha_{c,EPS_1}^{(b_{12})} & \cdots & \alpha_{c,EPS_{12}}^{(b_{12})} \end{pmatrix}^{+} \begin{pmatrix} \alpha_{c,i_1}^{(b_1)} & \cdots & \alpha_{c,i_{24}}^{(b_1)} \\ \vdots & \ddots & \vdots \\ \alpha_{c,i_1}^{(b_{12})} & \cdots & \alpha_{c,i_{24}}^{(b_{12})} \end{pmatrix} \tag{5.18}$$

Within the presented approach only the sub matrix $\mathbf{T}_{vv}$ which contains solely translational velocities at the internal and external interfaces is considered. Hence solely external and internal in-situ blocked forces are determined. The in-situ blocked moments at the external and internal

interfaces are neglected since previous research at RBAS has shown that moments at the external interfaces can be neglected without reducing the meaning of the source characterisation. As presented in the previous subsection, MEMS accelerometers are embedded at the internal interfaces to determine the internal in-situ blocked forces and the necessary BFT functions between the internal and the external interface DOFs of an EPSapa system. For the determination of the BFT functions the same approach as already elucidated in the previous subsection is used. However, in the following it will be shown how the MEMS accelerometers are placed at the internal interfaces of an EPSapa system.

The MEMS accelerometers are placed on the TB through holes which are added into the housing of the EPSapa system. The placement of the MEMS accelerometers is exemplified for one interface of the TB by Figure 5.14. Two MEMS accelerometers are used in order to be able to determine the in-situ blocked forces in three perpendicular directions (compare subsection 4.5.4 for all DoFs)

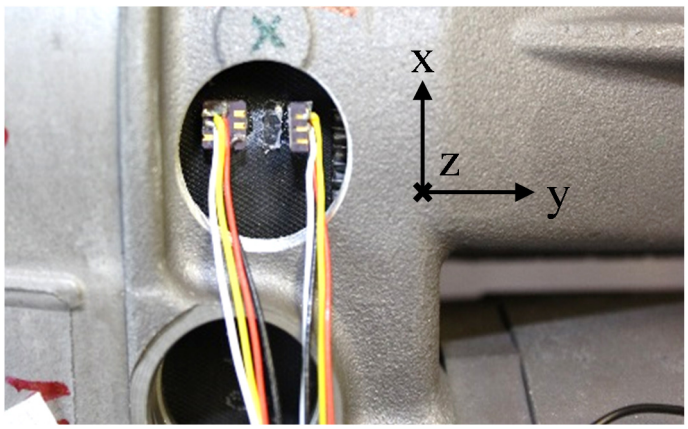

Figure 5.14: MEMS accelerometers placed at toothed belt (TB)

As with the successful embedding of MEMS accelerometers in the outer ring of the ball bearing of a BNA, the same approach was used. However, the housing of the EPSapa system needs to

be modified by adding holes as depicted by Figure 5.15 (left hand side) to place the accelerometers at the outer ring. In contrast to the approach which is proposed in subsection 4.5.3 the two MEMS accelerometers can be placed close to each other as depicted by Figure 5.15 (right hand side)

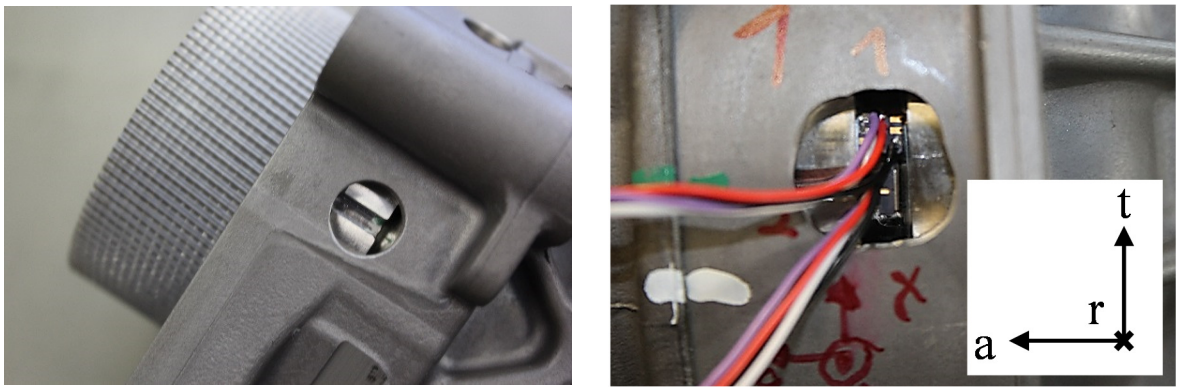

Figure 5.15: Grooves for MEMS accelerometers embedded at ball nut assembly (BNA)

The electric motor is prepared as proposed in section 4.2.2 and section 4.5.2 with six MEMS accelerometers at its interface with the housing of the EPSapa system. Figure 5.16 shows two of the 6 MEMS accelerometers at the interface in order to determine axial, radial and tangential DoFs.

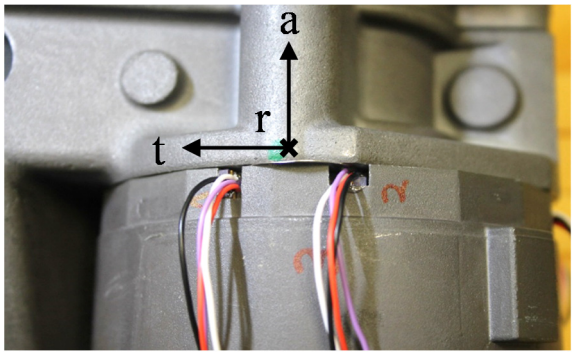

Figure 5.16: MEMS accelerometers embedded at electric motor (EM)

For the operational state of the EPSapa system a constant steering speed and hence a constant speed of the EM is chosen. For this purpose the parking assistant is used, which allows constant speed of the EM and as a consequence a constant steering speed according to the functional principle of an EPSapa system, introduced in subsection 3.2.2. The benefit of a constant speed is the possibility to detect the orders which reflect an internal source in a rather convenient way according to Eq. (4.9). The same approach is used for the case study of the in-situ blocked forces of an EM and a TB, presented in subsection 4.5.2 and subsection 4.5.4, respectively. The main orders for the constant rotational steering speed of the EPSapa system are summarised by the following table.

Table 5.1: Main orders of the internal sources of an EPSapa system

Internal source	*EM*	*BNA*	*TB*
Order	*A;* *B;* *C;* *D;* *E;* *F;* *G;*	*H*	*I*

According to the validation approach for bfTPA, presented in subsection 5.3.3, also the quality of the presented case study is evaluated. In the following the external in-situ blocked forces of the whole EPSapa system are determined according to Eq. (5.6) based on the BFT functions and the corresponding vectors of internal in-situ blocked forces (compare also Figure 5.10).

The predicted external in-situ blocked forces are subsequently validated by using them to predict the acceleration at a validation point on the receiver within an OBV (compare subsection 2.3.5). The validation for the external and internal in-situ blocked forces is shown by Figure 5.17. The red curve shows the measured validation acceleration, the blue curve shows the predicted acceleration based on the internal in-situ blocked forces and the corresponding BFT functions and the red curve shows the prediction if the external in-situ blocked forces are directly multiplied with the corresponding validation mobility matrix (compare also Eq. (5.8)).

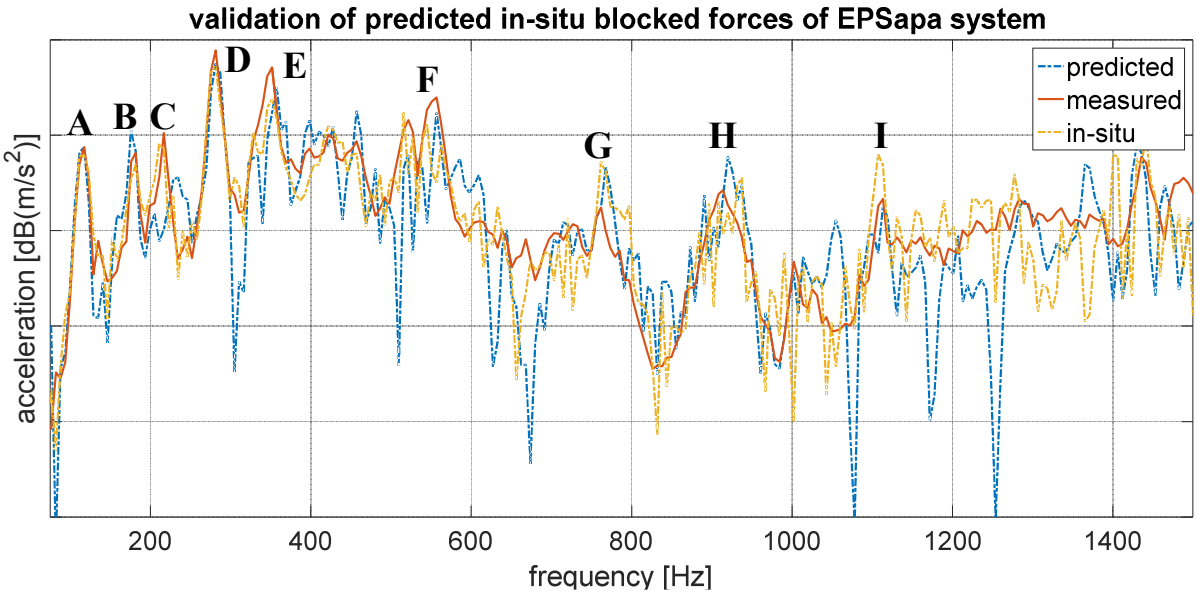

Figure 5.17: Validation predicted blocked forces of an EPSapa system; grid ordinate: 10 dB

It can be observed from the comparison between the measured and the predicted acceleration shown by Figure 5.17 that the internal and external in-situ blocked forces are determined with a deviation below 5 dB at the peaks. . Especially the main orders of the EM (A-G) and the TB (I) can be predicted with a deviation below 3 dB. Furthermore the whole characteristic of the structure-borne sound generated by an EPSapa under realistic operational conditions can be reproduced in a broad frequency range up to 1.5 kHz. In average the deviation between the

prediction and the measurement is generally below 5dB with only a few exceptions at rather unimportant frequencies. These frequencies do not define the sound characteristic of the EPSapa system during a steering manoeuvre and are hence neglected because the generated structure-borne sound energy is too low to excite the receiver structure. In particular the prediction based on the in-situ blocked force yields promising results. This means that the methodology of bfTPA can improve the understanding of the transmission of structure-borne sound within an EPSapa system. Since both the external in-situ blocked forces which characterise the source strength of the whole EPSapa system and the internal in-situ blocked forces which characterise the internal source strengths are validated according to Figure 5.17 the contribution of each of the internal sources can be determined. This is shown in Figure 5.18. The same approach as in the previous subsection is used (compare Eq. (5.10)).

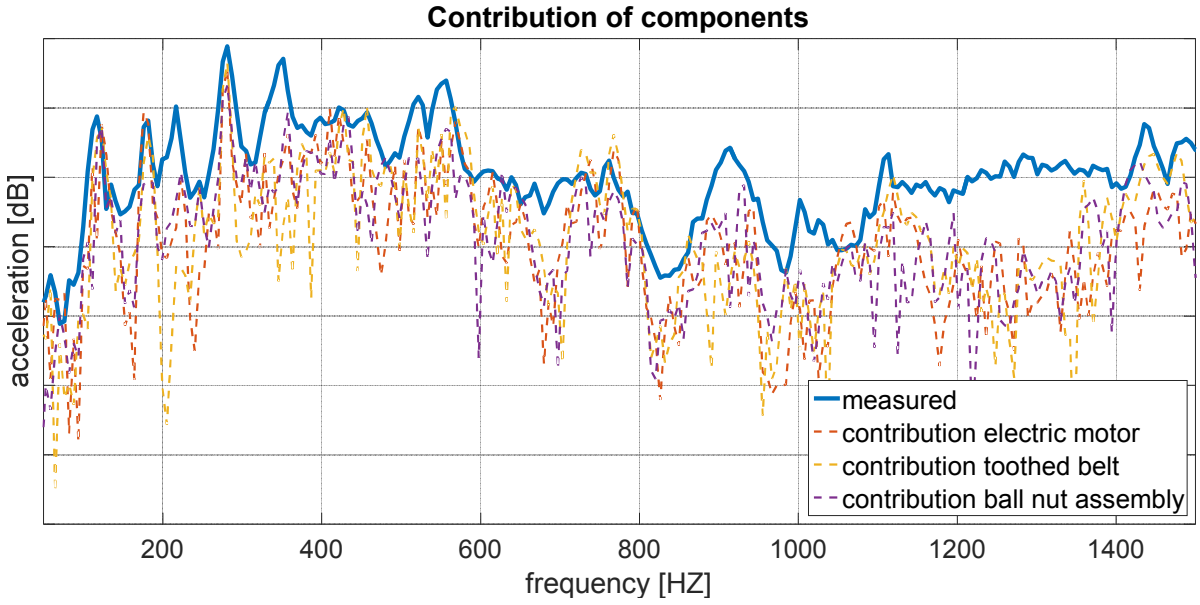

Figure 5.18: Contribution of the internal sources (components) of an EPSapa system to the structure-borne sound generated by the whole EPSapa system; grid ordinate: 10 dB

Generally, the contribution of the EM and the contribution of the TB at the important frequencies (compare Figure 5.17 and Table 5.1) are slightly higher than the contribution of the ball nut assembly. This is not surprising since the structure-borne sound of the ball nut assembly is usually expected to be lower in comparison to the sound generated by the EM and the TB. However since the bearing of the BNA was modified with a groove in its outer ring the contribution at the frequency area around 900 Hz (compare also Figure 5.17) shows a higher contribution of the BNA. Generally, the contribution of the internal sources to the overall source strength of an EPSapa system are nearly equal. This is the consequence of the fact that the internal in-situ blocked forces are determined while the sources are assembled to the EPSapa system. Hence cross coupling between the internal sources exists. If the in-situ blocked forces of the internal sources, namely EM, BNA and TB are determined on test rigs this cross coupling effect would not be present. However, the case study showed that it is possible to determine the contribution of the internal sources of an EPSapa system to its external blocked forces with good accuracy below 5 dB.

5.4.5 Coherence criterion

In order to choose the ideal amount of determined rows of the BFT matrix $\mathbf{Y}_{C,ci}$ a simple criterion is developed. The criterion is based on vectors of coherence functions $\boldsymbol{\gamma}$ which are a quantity to evaluate the linearity of a system. For the determination of the blocked force transmissibility functions the overall receiver is excited at multiple randomly chosen positions and the resulting velocities at the internal and external interfaces are determined (compare subsection 5.3.2). According to the presented methodology of the bfTPA it is not necessary to determine FRFs in order to calculate the needed BFT functions. However, if the excitation is

achieved by using an impact hammer or a shaker it is possible to measure the excitation signal which is a force. Hence it is subsequently possible to determine a coherence functions $\boldsymbol{\gamma}$ between the DoF at the excitation position and the n DoFs at the internal and external interfaces, respectively. For the sake of simplicity the n calculated coherence functions are summarized in a mean value as follows

$$\gamma_{mean} = \frac{\sum_{j=1}^{n} \boldsymbol{\gamma}_j}{n} \tag{5.19}$$

This mean value is an assumption of the quality of the artificial excitation and is used in subsection 5.4.4 to remove the measurements (artificial excitation with an impact hammer) which do not contribute to the quality of the BFT matrix. Therefore a threshold is defined which sets the minimum of the accepted mean value of the coherence functions γ_{mean}. If the mean value γ_{mean} is below the defined threshold it will be removed from the BFT matrix. Hence it will not yield a new row of the BFT matrix. The results of the mean values of the coherence γ_{mean} for each of the 96 artificial excitations which are used to determine the BFT matrix within an EPSapa system are represented in Figure 5.19.

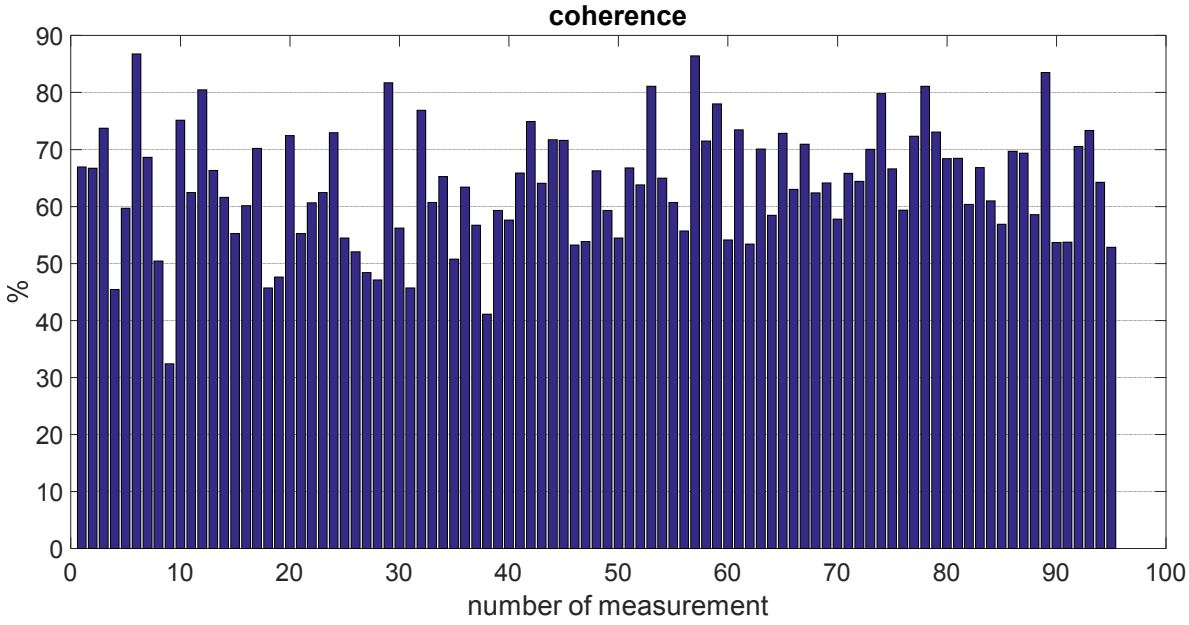

Figure 5.19: Mean values of coherence functions for coherence criterion

It can be observed that if the threshold for the mean value of the coherence is set to 50% out of the 96 measurements (artificial excitations) 8 measurements are deleted. Hence it is proposed to excite the overall receiver at as many positions as possible to yield a sufficient over-determination of the velocity matrices which are necessary to construct the BFT matrix (compare Eq. (5.5)).

5.4.6 Concluding remarks

In section 5.3 a novel transmissibility based TPA approach called bfTPA is presented which aims to analyse the transfer path problem for the introduced advanced internal-source-path-receiver model. Therefore the in-situ blocked forces and moments of an overall source are propagated back to the in-situ blocked forces and moments which characterise the internal source mechanisms at the internal interface with an internal receiver such as a housing, for example.

By carrying out a case study of a freely suspended steel beam the methodology of the introduced bfTPA is validated for a multiple degree of freedom system including rotational DoFs.

It was shown that the blocked force transmissibility (BFT) functions can be determined by measuring only operational kinematic quantities such as velocity or angular velocity at the internal and external interfaces. Thereby the BFT functions can be conveniently determined while the source is passive. Artificial excitation at the overall receiver is applied, to determine the necessary BFT functions using an impact hammer. Furthermore an application of the bfTPA was outlined by predicting the in-situ blocked forces and moments of a source based on the knowledge of the in-situ blocked forces and moments of the internal source as for instance a bearing and corresponding BFT functions between the internal and external interface. Furthermore the presented methodology of the bfTPA allows the in-situ blocked forces and moments at internal interfaces to be determined based on the knowledge of the in-situ blocked forces and moments at the external interface and corresponding velocity based transmissibility functions.

In order to prove the feasibility of the bfTPA methodology for a complex product, two further case studies were carried out. Both case studies concern an EPSapa system. It was shown that the bfTPA methodology can be applied to steering systems. Hence, it is possible to determine the contributions of the in-situ blocked forces of the internal sources namely electric motor, ball nut assembly and toothed belt to the overall source strength by means of external in-situ blocked forces. A coherence criterion is presented which is used to ensure to quality of the BFT matrix in order to increase the reliability of the bfTPA approach.

5.5 Virtual component assembly

5.5.1 Motivation

A perennially potential issue, in the engineering process of an EPSapa system, is the coordination between the domain of Robert Bosch Automotive Steering GmbH (RBAS) and the requirements of a customer regarding NVH quality. This holds not only true for RBAS, but also for the engineering processes of other suppliers of automotive components. However, in the following the motivation will only be elucidated for the products of RBAS and the corresponding engineering process. During the product development the supplier of automotive components has the responsibility of the source description while the customer, which is a car manufacturer, is concerned with the acoustic behaviour of the receiver. This means that the customer usually defines a limit for the sound pressure level (SPL) in the vehicle interior for a defined steering manoeuvre of the vehicle. Such a manoeuvre can be a parking process, for instance.

However, this required limit depends on characteristics of the source, the EPSapa system, for instance, and the receiver including the transmission paths which in this case is the vehicle. This consideration is based on the classical source-path-receiver-model. The defined limit should not be exceeded to guarantee a high comfort of the vehicles according to the NVH requirements of the vehicle manufacturer. The main problem although is the dependence of the SPL on both the characteristics of an EPSapa system which is the active vibrational source and the vehicle which is the passive receiver including the transmission paths for structure-borne sound. For that reason it would be of great benefit for both RBAS and the car manufacturer if it would be possible to clearly separate the responsibilities of both domains. Hence, it would be possible to engineer or to optimise both the active properties of the EPSapa system and the

passive characteristics of the vehicle independent from each other with the overall aim to reduce the SPL in the vehicle interior.

Therefore the in-situ blocked forces of the EPSapa system can be used to characterise the source and hence describe the domain of RBAS. This is state of the art and has been used within on-going projects between RBAS and different vehicle manufacturers. At this stage the question arises if the vector of in-situ blocked forces of an EPSapa system can be assembled from of the vectors of in-situ blocked forces of the internal sources. This question was generally answered as shown in section 5.3.

5.5.2 Methodology

In section 5.4 it was shown that it is in general possible to relate a vector of in-situ blocked forces and moments of an internal embedded source with a vector of in-situ blocked forces of a product which they are part of by using the BFT matrix. It was shown that it is possible to relate the internal sources with the source strength of the whole product in terms of in-situ blocked forces and BFT functions for a product or machinery with multiple inputs and multiple outputs such as an EPSapa system.

This would yield the possibility to virtually assemble a product with due regard to NVH requirements set by a customer. This approach will be called “virtual component assembly” (VCA) and is an extension of the virtual acoustic prototyping approach (VAP) [31], [76] which aims to predict the SPL based on a vector of in-situ blocked forces. Thus the VCA approach is a useful engineering tool, especially at early engineering stages. The general principle of the approach is schematically depicted in Figure 5.20.

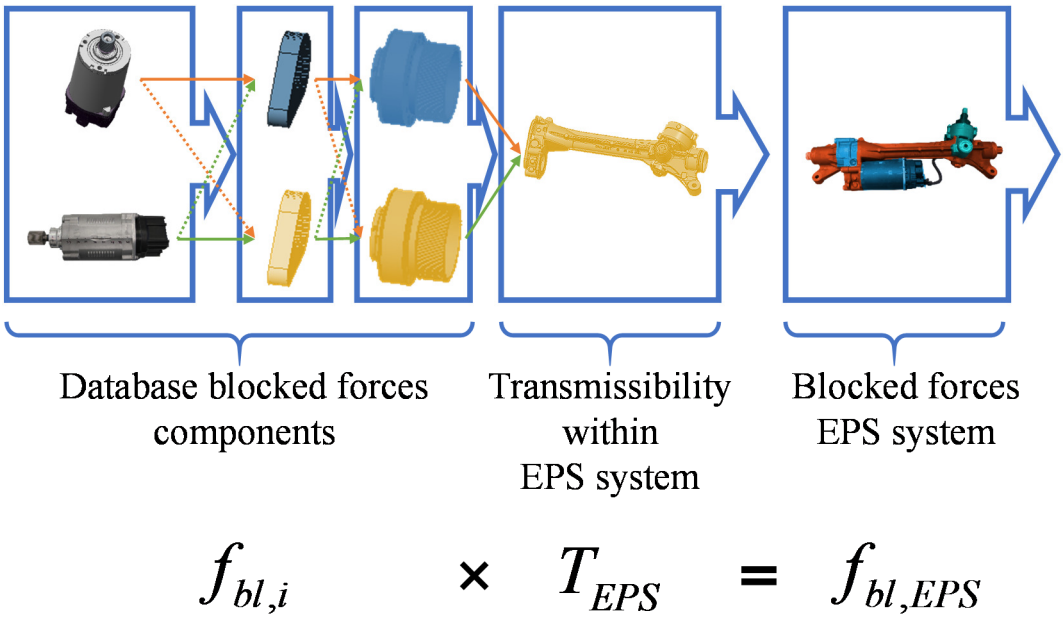

Figure 5.20: Approach of virtual component assembly

The aim of the approach is to determine the active properties of an EPSapa system based on the knowledge of the active properties of each of the internal sources and BFT functions. This can be done by using vectors of internal in-situ blocked forces to describe the active properties. The benefit of in-situ blocked forces is the independence from an attached receiver such as a vehicle. This statement was already outlined in subsection 2.3.4. This offers the possibility to generate a data base system based on in-situ blocked forces $\mathbf{f}_{bl,i}$ of the internal sources of the EPS system and the transmissibility of the housing $\mathbf{T}_{EPS}$. With the help of the database system the blocked forces of the EPSapa system $\mathbf{f}_{bl,EPS}$ can be designed by combining different components of the EPSapa system. Furthermore, this offers the possibility to generate a frequency map [117] of the EPSapa system which highlights the potentially critical frequency ranges.

5.5.3 Benefits and risks for early development stages

Currently the VCA approach is based on vectors of in-situ blocked forces that are determined experimentally. This means that a physically existing prototype of the internal sources or components needs to be available in order to determine the in-situ blocked forces. However, in early development stages often no prototypes are available.

Rapid prototyping which is a commonly used approach during early development stages is no solution for this issue since the material coefficients of the component are crucial for the sound generation and transmission. Unfortunately, rapid prototyping does not provide a prototype which is made of the actual material. However, this is a very important and crucial issue for the determination of transmissibility functions which are an essential part of a VCA approach. It is important to determine the transmissibility functions which are arranged in a transmissibility matrix as precise as possible. Therefore it would be of great benefit if the transmissibility functions could be determined through simulation. Dependent on the complexity of the component to be modelled numerical simulations or finite element methods can be applied. The use of simulation would allow for an early prediction of the structure-borne sound generated by an overall source based on the knowledge of the source strengths of its internal sources (compare Eq. (5.7)).

At this point it needs to be mentioned that the use of transmissibility functions requires a full understanding of the functional principle. Hence all possible transfer paths within a structure-borne sound need to be included. If DoFs are omitted it is possible to predict the in-situ blocked forces of the overall source incorrectly.

5.6 **Kinematic influences**

5.6.1 Introduction

Most technical products such as EPSapa systems consist of multiple lateral moving or rotating components which ensure the functionality of the product. This means, however, that the kinematics within the product can change while the product is operated. Especially if in consequence of the functional principle lever arms or angles between two components change significantly. This implies that the FRFs or transmissibilities which characterise the transmission paths of structure-borne sound within a product can significantly change while the FRFs, describing the transmission of structure-borne sound from the external interface to a target location on a receiver, mostly stay the same.

In case of an EPSapa system the toothed rack which is connected via the tie rods to the wheels of a vehicle moves within the housing from the left to the right end lock and therefore enables the driver to change direction according to the functional principle which was explained in subsection 3.2.2. The change of the position is schematically shown by Figure 5.21. The grey coloured part depicts the BNA which does not change its position relative to the fixed housing of an EPSapa system. The green and blue striped areas show the toothed rack which is moved out of middle position which is depicted by the grey striped part towards the left and right end lock, respectively.

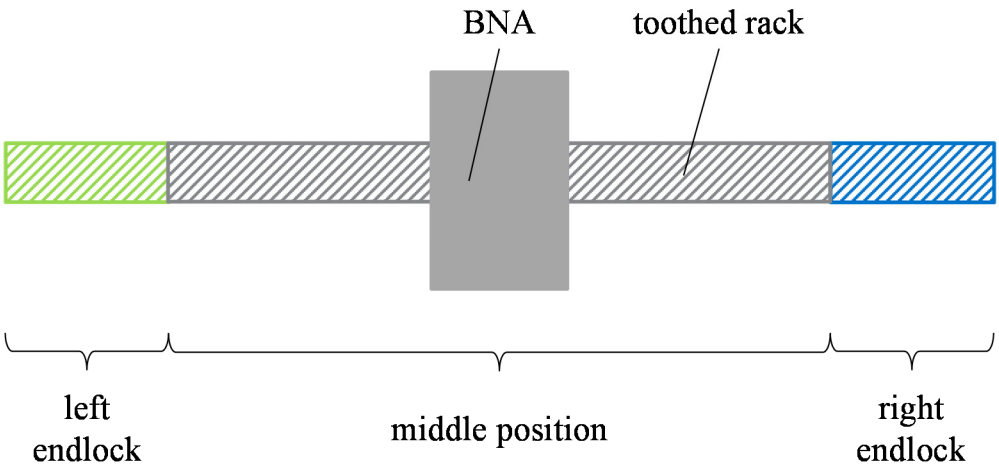

Figure 5.21: Change of the position of a toothed rack within the housing of an electric power steering system

The change of position of the toothed rack relative to the fixed position of the ball nut assembly changes the internal lever arms and therefore also the FRFs which describe the internal behaviour of the EPSapa system change as well. In the following of this section this assumption is further investigated.

5.6.2 Case study: Electric power steering system

When conducting a bfTPA, within an overall source such as an EPSapa system, the external as well as the internal in-situ blocked forces need to be precisely determined. Hence it is important to measure accurate FRFs between defined DoFs at the interfaces and locations on a receiver. This means that on the one hand the external FRFs and on the other hand the internal FRFs need to be experimentally determined in a correct manner. For the case of an EPSapa system the assumption is made that because of the translational movement of the toothed rack the in-

ternal FRFs change while the external FRFs only change in a minor way. For the sake of validating the assumption two cases with different positions of the toothed rack are compared by applying the frequency assurance criterion (FRAC). The aforementioned criterion yields a value between 0 and 1 which is an estimator of frequency changes between two states. The value of 1 means that there are no changes observable in the analysed frequency range. In theory additionally the phase assurance criterion can also be applied, which is omitted within this thesis. Further information about FRAC can be found in [118].

During the first case the toothed rack is in middle position and the whole assembly consisting of the EPSapa system and the test rig which is the fixture for the EPSapa system is excited at a defined position on the test rig (compare Figure 5.9). In this state the steering angle is 0° and the internal and the external FRFs are measured. The external FRFs are determined between DoFs at the interface between the EPSapa system and the test rig and the defined location on the test rig. In total 12 external FRFs are determined since the EPSapa system is mounted at four points with the test rig and every point is described by three translational DoFs. The internal FRFs are determined according to the presented case study of the ball nut assembly in subsection 4.5.3. In total 9 FRFs are determined between the interfaces DoFs between the ball nut assembly and the housing of the EPSapa system and the defined position on the test rig.

In the second case the toothed rack is moved towards the left end lock of the EPSapa system which corresponds to a rotation of the steering wheel of 600°. It can be clearly observed from Figure 5.22 which depicts the FRAC matrix of the two different cases that the assumption which was made is true. The upper four rows of the FRAC matrix represent the external FRFS at the DoFs at the connection points between the EPSapa system and the test rig. It is clearly observable that the FRFs between the connection points of the EPSapa with the test rig and an arbitrary

excitation position on the test rig are not significantly changed. However the internal FRFs between the BNA which are the lower three rows undergo significant changes.

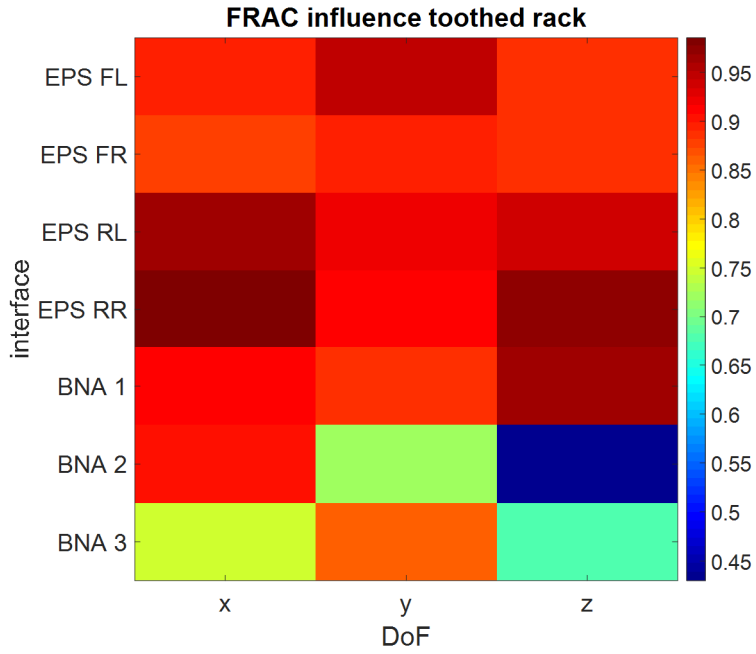

Figure 5.22: Frequency response assurance criterion (FRAC) comparing 600° (end lock) and 0° (middle position) steering angle; row 1-4 frequency response function (FRFs) between the external interface DoFs of an EPSapa system and the defined test position on the test rig; row 5-7 FRFs between the internal interface DoFs of the ball nut assembly (BNA) and the defined test position on the test rig

5.6.3 Improvement of in-situ blocked forces

At this point the question arises how many steps of measuring FRFs are relevant to fully include all kinematic conditions during a steering manoeuvre. In this thesis work, the FRFs were measured at 5° intervals. However, this is not practicable since it would increase the amount of measurements by 120. If the results of a bfTPA should be increased it is worth putting the effort into the FRF measurements.

One could for example think of a case where one measures the mobility for the middle position of the toothed rack $\mathbf{Y}_{middle}$ and for the left and the right end lock $\mathbf{Y}_{left}$ and $\mathbf{Y}_{right}$, respectively. Based on the position of the toothed rack while a steering manoeuvre one could also determine the operational velocities $\mathbf{v}_{op,left}$, $\mathbf{v}_{op,middle}$ and $\mathbf{v}_{op,right}$. According to Eq. (3.5) one can then calculate three sets of blocked forces $\mathbf{f}_{bl,left}$, $\mathbf{f}_{bl,middle}$ and $\mathbf{f}_{bl,right}$ which characterise the total steering manoeuvre in terms of blocked forces $\mathbf{f}_{bl,tot}$ as follows

$$\mathbf{f}_{bl,tot} = \begin{pmatrix} \mathbf{f}_{bl,left} \\ \mathbf{f}_{bl,middle} \\ \mathbf{f}_{bl,right} \end{pmatrix} = \begin{pmatrix} \mathbf{Y}_{left}^{-1}\mathbf{v}_{op,left} \\ \mathbf{Y}_{middle}^{-1}\mathbf{v}_{op,middle} \\ \mathbf{Y}_{right}^{-1}\mathbf{v}_{op,right} \end{pmatrix} \tag{5.20}$$

With this consideration the different parts of a steering manoeuvre are characterised in a more precise manner rather than just using one blocked force vector for the whole steering manoeuvre. Especially if the structural properties in terms of the mobility during a steering manoeuvre change significantly, because of a variable gear ratio for example, this methodology will improve the characterisation of the source. This methodology is not limited to three positions or to steering systems. It can be used for other products and in theory for as many positions as reasonable.

5.7 **Summary and concluding remarks**

In section 5.2 the internal source-path-receiver-model (ISPRM), introduced in section 1.4, was extended yielding the aISPRM. This model forms the basis for the development of the underlying equations of the blocked force transmissibility transfer path analysis (bfTPA), proposed in section 5.3. The extension of ISPRM to the aISPRM is a necessary step in order to be able

to include such parts within an overall source which on the one hand solely transmit structure-borne sound and on the other hand also generate structure-borne sound. If the aforementioned parts of an overall source are defect, as a consequence of misuse, for instance or manufactured incorrectly, the structure-borne sound becomes especially relevant. An example of such a part is a ball bearing which can be found within most technical products. Within an EPSapa system an important ball bearing is used within the ball nut assembly. Hence ball bearings were taken into consideration.

In section 5.3 the methodology of bfTPA is introduced and explained in detail. It was shown that the necessary BFT matrix can be conveniently determined using artificial excitation at random locations on the overall receiver such as a test rig or vehicle. In order to apply the artificial excitation an impact hammer or a shaker can be used. Furthermore it is elucidated that embedded MEMS accelerometers are successfully used in the determination of the BFT matrix. Since the process of embedding the MEMS accelerometers at the internal interfaces is necessary for the determination of internal in-situ blocked forces anyway, no additional steps are required. In subsection 5.3.3 a validation based on the OBV approach, is developed and presented [28]. The aim of the approach is to show that an experimentally determined vector of internal in-situ blocked forces can be derived from a vector of external in-situ blocked forces by using the linear relationship with the BFT matrix.

Besides the advantages of the bfTPA, the potential drawbacks of the proposed TPA within an overall structure-borne sound source are discussed. It was outlined in subsection 5.3.4 that a significant amount of impacts is necessary to yield a BFT matrix with linearly independent rows or columns, respectively. This means that a significant amount of linearly independent excitation signals are required, which is a severe challenge. Furthermore, the functional principle of

the overall structure-borne sound source to be analysed needs to be fully understood in order to include all necessary internal sources and corresponding transmission paths.

Three experimental case studies were carried out to prove the validity and the applicability of the bfTPA within different kinds of structure-borne sound source. The procedure and the results were presented in section 5.4. The first case study was of a steel beam and demonstrated the possibility to include rotational DoFs. Generally, all three case studies independently prove the methodology of the bfTPA and the underlying equations as valid. Furthermore it was possible to show, in the third case study, that is possible to predict in-situ blocked forces of an EPSapa system based on the knowledge of the in-situ blocked forces characterising the internal sources. Since it was possible to prove the feasibility of the aforementioned approach the virtual component assembly (VCA) approach which is presented in section 5.5 was possible to implement.

Since the internal kinematics of an EPSapa system change during a steering manoeuvre, as a result of the movement of the toothed rack, the internal transmission paths within an EPSapa system were investigated. It was shown by means of a FRAC analysis that in contrast to the internal transmission paths between BNA and a reference position the external transmission paths between the external interfaces and the same reference position are mostly unchanged. In order to prove this the FRFs were determined in the middle position of the toothed rack and while the toothed rack was moved towards the end lock of the EPSapa system. Based on the results an improvement for the in-situ blocked forces of an EPSapa system was proposed by sub dividing a steering manoeuvre into multiple parts and determine the corresponding mobility matrices $\mathbf{Y}_{C,bc}$ for the determination of in-situ blocked forces.

Chapter 6

Concluding remarks and future work

6.1 **Concluding remarks**

The outcomes of the present thesis work, which were briefly summarized at the ends of chapters 3 to 5, will be outlined in more detail. This chapter also aims to define a more global range and relate all concluding remarks to each other.

At the beginning of this thesis in section 1.1 and section 1.2 it was stated that in automotive industry TPA methods are widely used to analyse the NVH characteristics of structure-borne sound sources. As a specific example of structure-borne sound sources EPS systems which are further outlined in chapter 3 were introduced. In this context, it was emphasised that the contribution of the source strength of an EPS system to the sound pressure level at well-defined target positions in the vehicle interior is of interest for NVH engineers at Robert Bosch Automotive Steering GmbH (RBAS). Commonly used forces to characterise structure-borne sound sources such as EPS systems, for instance, were identified as contact forces or blocked forces[16]. Both experimentally determined forces were discussed in section 2.3. However, in this thesis, only in-situ blocked forces were used for the purpose of source characterisation (compare subsection 2.3.4). Six experimental case studies were carried out in which structure-borne sound sources such as an EPSapa system and its components were characterised by means of in-situ blocked forces. That way the characterisation of the source strengths were independent of the receiver's dynamic behaviour. Hence a crucial objective of the thesis project, stated in subsection 1.5, was fulfilled.

[16] directly measured blocked forces or in-situ blocked forces

A novel transmissibility based TPA method that was developed to analyse the structure-borne sound transmission within a complex engineered product such as an EPSapa system. The terms "overall source" and "internal source" (IA), respectively, were proposed to describe EPSapa systems and other products that consist of multiple internal source mechanisms. It was shown that the proposed novel transmissibility based TPA method provides the possibility to determine the necessary transmissibility functions within the internal receiver (IB) through artificial excitation on the overall receiver side with an impact hammer.

The novel transmissibility based TPA approach was the "blocked force transmissibility transfer path analysis" (bfTPA). This included a validation approach. With the help of aISPRM the terms "internal source, internal receiver, overall source and overall receiver" were introduced and set into relation with an EPSapa system.

The proposed bfTPA method was validated in three experimental case studies which increased in complexity. The results of the three case studies which prove the general feasibility of bfTPA for MIMO and LTI systems were presented in section 5.4. Especially the first case study (compare subsection 5.4.2) highlights the applicability of the developed bfTPA method for systems with rotational and translational DoFs at the internal and external interfaces, respectively.

Moreover, in section 5.5 a further aspect of bfTPA was elucidated. It was shown that the methodology of bfTPA allows to construct a so called "virtual acoustic prototype" (VAP) based on the derived vectors of external in-situ blocked forces. Hence the methodology of bfTPA was introduced as an extension to a VAP approach since it delivers the input quantity for a VAP based on the determined strengths of the IAs such as an electric motor (EM), a ball nut assembly (BNA) or a toothed belt (TB).

In subsection 5.3.3 a force validation approach for bfTPA which is based on the so called on-board validation (OBV) is presented (compare subsection 2.3.5). The validation approach is based on the prediction of vectors of external in-situ blocked forces from vectors of internal in-situ blocked forces and the corresponding transmissibility functions. Subsequently the predicted vectors of in-situ blocked forces at the external interface DoFs are further used within an OBV approach as reviewed in subsection 2.3.5. The proposed validation approach was successfully applied within all the three presented bfTPA case studies. Thus it was generally shown that the developed methodology of bfTPA is valid for even complex products such as EPSapa systems and its components EM, BNA and TB.

Within the first bfTPA case study (compare subsection 5.4.2) a freely suspended steel beam was virtually subdivided into three parts according to the proposed aISPRM. The first two parts of the beam represent an IA and an internal receiver, respectively, which together build an overall structure-borne sound source. The overall source is then again attached to the third part of the beam which represents the overall receiver such as a vehicle, for example. Furthermore, it was shown that also rotational DoFs can be included within bfTPA since in-situ blocked moments were successfully included.

The second bfTPA case study comprises an EPSapa system mounted on a special developed adaptive test rig (ATR) which functions as an overall receiver. The purpose of this case study was to employ the methodology of bfTPA to a complex technical product such as an EPSapa system. In order to at first reduce the complexity of the case study the tie rod forces were set to zero and the system was excited artificially with an impact hammer at the housing of the electric motor. This way only one IA in the form of the EM is active. The results of the case study proved that bfTPA can be applied to even complex products with multiple internal transmission

paths with high accuracy. Furthermore it was shown that the internal transmission path through the TB within an EPSapa system cannot be neglected.

The third case study increased the complexity of the second case study since the parking assistant of the steering system is used to generate the operational state. In this manner it is theoretically possible to reproduce the same operational conditions of the IAs on test rigs. This is important to be able to compare the internal in-situ blocked forces which are determined in the assembled EPSapa system with forces which are determined on special component test rigs. Generally the results of the case study showed that by applying bfTPA the internal transmission of structure-borne sound within an EPSapa system can be analysed and the contribution of the IAs can be rank ordered. Within all three bfTPA case studies MEMS accelerometers were successfully used to determine the in-situ blocked forces which characterise the IAs EM, BNA and TB. Hence the presented methodologies to determine in-situ blocked forces at continuous and revolving internal interfaces which are proposed in section 4.3 and section 4.4, respectively, were validated.

In theory the methodologies of both classical TPA and in-situ TPA (compare section 2.4.1 and 2.4.2, respectively) can be used to analyse the structure-borne sound transmission within a product such as an EPSapa system, for instance. However, both methodologies only determine the contribution of the internal source strengths to a kinematic target quantity at the external interface DOFs with an overall receiver. Unfortunately, the analysed kinematic target quantity cannot be further processed in a subsequent VAP approach. This main drawback of classical TPA as well as in-situ TPA regarding a further use of their results for a VAP approach was discussed in the course of this thesis in section 5.5. Furthermore, at this point it was elucidated that the input quantity of a VAP approach needs to be the source strength in terms of (in-situ) blocked

forces rather than a kinematic input such as velocity or acceleration, for instance. Hence, it was stated that both classical TPA and in-situ TPA cannot be used within an EPSapa system as basis for a subsequent VAP approach in a vehicle.

By proposing the novel bfTPA method a solution of the aforementioned issue of VAP is developed and validated through the conduction of three case studies whose results were presented and discussed in section 5.4. However, before presenting the results of the case studies, in section 5.3 the main advantage of bfTPA was highlighted. Besides the fact that the proposed methodology of bfTPA can be applied to analyse structure-borne sound transmission within a technical product such as an EPSapa system, for instance, it also yields a receiver independent description of the internal and external source strengths. Vectors of in-situ blocked forces serve as the characterisation and the target quantity of the TPA at the internal and external interface DoFs, respectively. That way the overall source strength as well as the strength of the IAs which are embedded within the overall source are characterised solely without the influence (damping and stiffness) of the internal and overall receiver, respectively. Since both the input quantities and the target quantity of the proposed bfTPA method are of the same kinetic quantity (compare section 5.2) only transmissibility functions rather than frequency response functions (FRFs) can be used to describe the internal transmission paths. Therefore special transmissibility functions which describe the transmission of the generated structure-borne sound within the internal receiver were developed and introduced in subsection 5.2.3. These transmissibility functions are called “blocked force transmissibility” or in abbreviated form BFT. In general it can be stated that in chapter 5 it was shown that the concept of BFT functions is reasonable and can be applied to even complex products, such as EPSapa systems.

In order to determine transmissibility functions usually the overall source is operated and vibrations at the relevant DoFs at the defined interfaces and target positions are observed. However, within this thesis a different approach to determine transmissibility functions is presented. The approach is based solely on artificial excitation on the overall receiver. This way the aforementioned approach which is presented in chapter 5 and used to determine the BFT functions differs from the commonly used approaches since the transmissibility functions are determined while the internal source mechanisms within the overall source are passive. However, like for all transmissibility approaches it is crucial to identify all relevant transmission paths and the corresponding DoFs at the interfaces. Otherwise the energy flux within the observed vibrational system is likely to be misinterpreted.

Besides the fact that a bfTPA approach can be used on the one hand to analyse the structure-borne sound transmission within a source based on in-situ blocked forces and transmissibility functions the benefit of the bfTPA is on the other hand to predict the in-situ blocked forces of the overall source. This approach is introduced as “virtual component assembly” (VCA). A VCA approach which is introduced in section 5.5 is proposed as an extension to a VAP. By applying the methodology of VCA the in-situ blocked forces of an overall source can be designed based on the knowledge of the internal in-situ blocked forces. This way it is possible to establish a database system of internal sources which can be used to design an optimised overall source regarding NVH requirements.

In order to conclude the conceptual development of the bfTPA method the drawbacks of the proposed approach were elucidated and discussed in subsection 5.3.4. It was discussed that the necessity of linearly independent rows of the BFT matrix is crucial for the success of the presented bfTPA approach. In subsection 5.4.4 the necessary factor of over determination of the

BFT matrix in order to achieve meaningful results is presented. However, it was furthermore discussed that a factor of over determination between 2 and 4 improves the reliability of bfTPA significantly. Other factors above 4 can deduce the reliability of the BFT matrix which is a key factor for the conduction of a bfTPA approach. A coherence criterion was presented to choose the right transmissibility functions for the BFT matrix. This criterion was successfully applied within the case study of an EPSapa system which was presented in subsection 5.4.4.

The kinematic properties of an EPSapa system change during a steering manoeuvre because of its functional principle and the resulting movement of the toothed rack (compare subsection 3.2.2). Consequently the different positions of the toothed rack in relation to the housing of the EPSapa system affect the FRFs which are necessary to determine the internal in-situ blocked forces. The influences of the position of the toothed rack were considered in section 5.6. It was shown by a frequency assurance criterion (FRAC) analysis that in contrast to the external FRFs the internal FRFs of an EPSapa system change significantly. Thus an approach was proposed in order to further improve the determination of internal in-situ blocked forces by taking the change of the position of the toothed rack into account.

However, before it is possible to conduct a bfTPA approach within an overall source such as an EPSapa system at first the overall source needs to be substructured. For that reason a substructuring approach of an EPSapa system is introduced in chapter 3. The approach is based on the so called internal-source-path-receiver-model (ISPRM) which is a proposed extension of the classical source-path-receiver-model by Bolt and Ingaard. ISPRM is briefly introduced in section 1.4 of this thesis and further extended to the advanced ISPRM (aISPRM) for complex structures such as an EPSapa system in section 5.2. The aISPRM is especially developed to include structures such as bearings which on the one hand generate structure-borne sound and

on the other hand only transmit sound generated by other IAs. Furthermore based on the introduced substructuring approach of an EPSapa system a general methodology for the substructuring of other technical products or machinery is presented and elucidated in section 3.5. Four steps were presented which can be followed to substructure a product for the conduction of bfTPA.

Often it is not possible to access the embedded internal interfaces within an overall source with standard IEPE accelerometers. Furthermore the aforementioned measurement devices cannot be mounted on the surface of an IA. Hence in chapter 4 of this thesis an application of the in-situ blocked force method is introduced to avoid this issue. The methodology is based on the use of micro-electro-mechanical-systems (MEMS) accelerometers which can be embedded at the sensitive contact interfaces. In subsection 2.2 it was reviewed that the benefit of these types of accelerometers is their low cost and small size. Hence MEMS accelerometers were successfully used within the scope of this thesis to fulfil the measurement tasks in order to determine internal in-situ blocked forces and the corresponding BFT functions. However the drawback of MEMS accelerometers is the fact that often they need to be calibrated in a rather complex way to ensure the measurement quality. A potential way to do the calibration was therefore presented in section 4.2.

Furthermore in chapter 4 all relevant primary IAs of an EPSapa system were characterised with in-situ blocked forces at the defined internal interfaces. By using an OBV approach it was shown that the general idea to discretise the continuous interfaces of an EM and a BNA, respectively, with a housing by three point connection provides sufficient accuracy. The deviation between the velocity based on the determined in-situ blocked forces of an EM and a BNA, respectively, compared to a measured velocity does not excide 5 dB in the relevant frequency

range. Furthermore the results of the determined in-situ blocked forces of a TB were presented and validated using the OBV approach, which is reviewed in subsection 2.3.5. Because of the high accuracy of the OBV it can be stated that it is also possible to use the in-situ blocked force method for IAs of an EPSapa system. Furthermore it was proven that the in-situ blocked force method is feasible for IAs with continuous and revolving interfaces, respectively.

6.2 **Future work**

According to the findings and conclusions of the present thesis the following future work can be defined.

Currently all the IAs of an EPSapa system are characterised with vectors of in-situ blocked forces only. However, in theory also blocked moments are present at the DoFs at the internal interfaces between an EM and the housing of the EPSapa system. Although the OBV for the determined in-situ blocked forces of an EM already showed good accuracy it is assumed that by including blocked moments the validation can be improved. The central difference method by Elliott can be used to further investigate this.

Additionally the development of a criterion to evaluate the necessity to include rotational DoFs at the internal and external interfaces is proposed as future research. The round trip identity can be used to develop this criterion. Furthermore the assumption is made that the prediction of the external in-situ blocked forces of an EPSapa system can be further improved by including rotational DoFs. This means that the BFT matrix should include, besides translational velocities also angular velocities.

A methodology to deal with continuous interfaces based on Fourier series was briefly discussed but within the scope of the thesis all continuous interfaces of an EPSapa system are discretised through multiple point connections. The question arises how many point connections are necessary to characterise the source strength of the IAs of an EPSapa system. Future research can be conducted to answer this question for a BNA and an EM of an EPSapa system.

Since MEMS accelerometers were used to determine in-situ blocked forces and BFT functions, further research should be focused on MEMS accelerometers. Thereby two questions arise. Can MEMS accelerometers be embedded within a rigid structure and be calibrated after the embedding? Can MEMS accelerometers be embedded on the receiver side of the interface to determine meaningful in-situ blocked forces? This could lead to the design of special test rigs for the determination of the source strength of IAs by means of in-situ blocked forces.

Furthermore the question arises on if the sound generation mechanisms within an EM can be characterised by in-situ blocked forces. A promising approach by Wienen is available [44]. If the root cause of the structure-borne sound of an EM is seen as the current or voltage then it should be possible to introduce a novel frequency response function (FRF). The FRF should describe the "vibro-electrical" behaviour of any sort of product that has an electrical root cause. The resulting vibro-electrical FRF relates the dynamic forces of an electric component such as an EM at the interface with a receiver to the current or voltage of the electrical component. If it can be proven that these FRFs are linearly scalable by changing the current or voltage in that sense the in-situ blocked forces of an electrical component can be predicted if the vibro-electrical FRFs are known.

Additionally it is also desirable to further develop the methodology of bfTPA regarding the stability of the BFT matrix. This includes especially the experimental determination of the BFT

matrix through artificial excitation. Within the scope of this thesis it was shown that the concept of transmissibility is generally prone to errors if an inversion of a big BFT matrix is required. Especially if MEMS sensors are used to determine the transmissibility functions between an external and an internal interface, great care should be taken on measurement accuracy. Therefore further work should be focussed on the reliability of the BFT matrix. Although sufficient over determination through a significant amount of excitation locations on the receiver side was shown to be beneficial, it is necessary to determine the minimum amount of over determination needed.

Further research could also be focused on the proposed VCA approach. It would be also interesting to investigate if the BFT functions can also be determined by simulation. Furthermore research should be focused on the transferability between different internal receivers such as housing of EPSapa systems.

References

[1] M. Pflüger, F. Brandl, B. Ulrich, and K. Feitzelmayer, *Automotive Acoustics (Fahrzeugakustik (in German))*. Wien New York: Springer, 2010.

[2] K. Genuit, "Designing acoustics in the development of vehicles (Akustikgestaltung in der Fahrzeugentwicklung (in German))," in *Sound-Engineering in automotive section - Methods for measurement and analysis of sound and vibration (Sound-Engineering im Automobilbereich - Methoden zur Messung und Auswertung von Geräuschen und Schwingungen (in German))*, Berlin: Springer, 2010.

[3] J. Du and D. Ouyang, "Progress of Chinese electric vehicles industrialization in 2015: A review," *Applied Energy*, vol. 188, 2017, pp. 529–546.

[4] P. Pfeffer, "Requirements of electric power steering systems (Anforderungen an die Lenkung (in German))," in *Steering handbook - Steering system, Steering feeling, driving dynamics of vehicles (Lenkungshandbuch - Lenksysteme, Lenkgefühl, Fahrdynamik von Kraftfahrzeugen (in German))*, Wiesbaden: Springer Vieweg, 2013, pp. 43–50.

[5] M. A. Panza, "A review of experimental techniques for NVH analysis on a commercial vehicle," *Energy Procedia*, vol. 82, 2015, pp. 1017–1023.

[6] J. Plunt, "Strategy for transfer path analysis (TPA) applied to vibro-acoustic systems at medium and high frequencies," in *Proceedings of the 23rd International Conference on Noise and Vibration Engineering (ISMA 23)*, no. 1, pp. 16–18, 1998.

[7] J. Plunt, "Finding and fixing vehicle NVH problems with transfer path analysis," *Sound And Vibration*, no. November, 2005, pp. 12–16.

[8] J. W. Verheij, "Multi-path sound transfer from resiliently mounted shipboard machinery: Experimental methods for analyzing and improving noise control," Thesis, Delft University of Technology, 1982.

[9] A. S. Elliott, A. T. Moorhouse, T. Huntley, and S. Tate, "In-situ source path contribution analysis of structure borne road noise," *Journal of Sound and Vibration*, vol. 332, no. 24, Nov. 2013, pp. 6276–6295.

[10] A. S. Elliott and A. T. Moorhouse, "In-situ characterisation of structure borne noise from a building mounted wind turbine," in *Proceedings of the International Conference on Noise and Vibration Engineering (ISMA 2010)*, pp. 2055–2068, 2010.

[11] M. Sturm, T. Alber, A. T. Moorhouse, D. Zabel, and Z. Wang, "The in-situ blocked force method for characterization of complex automotive structure-borne sound sources and its use for virtual acoustic prototyping," in *Proceedings of the international conference on Noise and Vibration Engineering (ISMA 2016)*, 2016.

[12] M. Sturm, M. Yankonis, C. Marchand, S. Sherman, M. Priebe, and A. T. Moorhouse, "Robust NVH Development of Steering Systems Using In-Situ Blocked Forces from Measurements with Low-Noise Driver Simulators," in *Proceeding of Noise-Con 2017*, 2017.

[13] F. X. Magrans, "Method of measuring transmission paths," *Journal of Sound and Vibration*, vol. 74, no. 3, Feb. 1981, pp. 321–330.

[14] W. Liu and D. J. Ewins, "Transmissibility properties of MDOF systems," in *Proceedings*

of the International Modal Analysis Conference - IMAC, pp. 847–854, 1998.

[15] A. M. R. Ribeiro, J. M. M. Silva, and N. M. M. Maia, "On the Generalisation of the Transmissibility Concept," *Mechanical Systems and Signal Processing*, vol. 14, no. 1, 2000, pp. 29–35.

[16] N. M. M. Maia, J. M. M. Silva, and A. M. R. Ribeiro, "The Transmissibility Concept in Multi-Degress-of-Freedom Systems," *Mechanical Systems and Signal Processing*, vol. Vol. 15, N, 2001, pp. 129–137.

[17] P. Gajdatsy, K. Janssens, W. Desmet, and H. van der Auweraer, "Application of the transmissibility concept in transfer path analysis," *Mechanical Systems and Signal Processing*, vol. 24, no. 7, Oct. 2010, pp. 1963–1976.

[18] Y. E. Lage, N. M. M. Maia, M. M. Neves, and A. M. R. Ribeiro, "Force identification using the concept of displacement transmissibility," *Journal of Sound and Vibration*, vol. 332, no. 7, 2013, pp. 1674–1686.

[19] Y. E. Lage, M. M. Neves, N. M. M. Maia, and D. Tcherniak, "Force transmissibility versus displacement transmissibility," *Journal of Sound and Vibration*, vol. 333, no. 22, 2014, pp. 5708–5722.

[20] J. Jové and O. Guasch, "Direct response and force transmissibilities in the characterization of coupled structures," *Journal of Sound and Vibration*, vol. 407, 2017, pp. 1–15.

[21] B. L. Kim, J. Y. Jung, and I. K. Oh, "Modified transfer path analysis considering transmissibility functions for accurate estimation of vibration source," *Journal of Sound and Vibration*, vol. 398, 2017, pp. 70–83.

[22] A. M. R. Ribeiro, N. M. M. Maia, and J. M. M. Silva, "Experimental evaluation of the transmissibility matrix," in *Proceedings of IMAC*, pp. 1126–1129, 1999.

[23] D. Zabel, T. Alber, M. Sturm, and A. T. Moorhouse, "Internal transfer path analysis based on in-situ blocked forces and transmissibility functions," in *Proceedings of 24 International Congress on Sound and Vibration (ICSV 24)*, 2017.

[24] Knowles Electronics, "Datasheet Vibration Transducer (BU-21771-000)." Knowles Electronics, Itasca.

[25] Analog Devices Inc., "Datasheet ADXL103/ADXL203." Analog Devices, Inc., Norwood, 2014.

[26] A. S. Elliott, "Characterisation of structure borne sound sources in-situ," Thesis, University of Salford, 2009.

[27] A. T. Moorhouse, A. S. Elliott, and T. A. Evans, "In situ measurement of the blocked force of structure-borne sound sources," *Journal of sound and vibration*, vol. 325, no. 4, 2009, pp. 679–685.

[28] A. S. Elliott, J. W. R. Meggitt, and A. T. Moorhouse, "Blocked forces for the characterisation of structure borne noise," in *Conference Proceedings of Internoise and Noise-Con Congress*, vol. 250, no. 1, pp. 5798–5805, 2015.

[29] A. T. Moorhouse, T. A. Evans, and A. S. Elliott, "Some relationships for coupled structures and their application to measurement of structural dynamic properties in situ," *Mechanical Systems and Signal Processing*, vol. 25, no. 5, 2011, pp. 1574–1584.

[30] C. M. Harris, *Handbook of Noise Control*. McGraw-Hill, 1957.

[31] M. Bauer, "Virtual acoustic prototyping : characterisation of a steering system and

prediction of structure-borne sound," Thesis, University of Salford, 2011.

[32] M. Sturm, "Identification and quantification of transient structure-borne sound sources within electrical steering systems," Thesis, University of Salford, 2013.

[33] D. Lennström, M. Olsson, F. Wullens, and A. Nykänen, "Validation of the blocked force method for various boundary conditions for automotive source characterization," *Applied Acoustics*, vol. 102, 2016, pp. 108–119.

[34] A. Moorhouse, A. S. Elliot, and Y. Heo, "Intrinsic characterisation of structure-borne sound sources and isolators from in-situ measurements.," in *Proceedings of Meetings on Acoustics*, vol. 19, pp. 1–9, 2013.

[35] R. a Fulford and B. M. Gibbs, "Structure-Borne Sound Power and Source Characterization in Multi-Point-Connected Systems. Part 2: About mobility functions and free velocities," *Journal of Sound and Vibration*, vol. 220, no. 2, 1999, pp. 203–224.

[36] M. V. van der Seijs, E. Pasma, D. de Klerk, and D. Rixen, "A robust Transfer Path Analysis method for steering gear vibrations on a test bench," in *Proceedings of the international conference on noise and vibration engineering (ISMA 2014)*, pp. 4027–4040, 2014.

[37] M. Bao, *Analysis and design principles of MEMS devices*. Elsevier, 2005.

[38] A. Albarbar, A. Badri, J. K. Sinha, and A. Starr, "Performance evaluation of MEMS accelerometers," *Measurement: Journal of the International Measurement Confederation*, vol. 42, no. 5, 2009, pp. 790–795.

[39] A. Albarbar, S. Mekid, A. G. Starr, and R. Pietruszkiewicz, "Suitability of MEMS accelerometers for condition monitoring: An experimental study," *Sensors*, vol. 8, no. 2,

2008, pp. 784–799.

[40] J. Vollmer and T. Neumann, "Integration of low-cost accelerometers in machinery for constant condition monitoring (Integration von Low-Cost Schwingungsmesssystemen in Maschinen und Anlagen zur permanenten Schwingungsüberwachung (in German))," *VDI-Berichte*, no. 2093, 2010.

[41] A. Badri, J. K. Sinha, and A. Albarbar, "A method to calibrate the measured responses by MEMS accelerometers," *Strain: An International Journal for Experimental Mechanics*, vol. 47, no. s2, 2011, pp. 242–257.

[42] A. E. Badri, J. K. Sinha, and A. Albarbar, "A typical filter design to improve the measured signals from MEMS accelerometer," *Measurement: Journal of the International Measurement Confederation*, vol. 43, no. 10, 2010, pp. 1425–1430.

[43] C. J. Fisher, "Using an accelerometer for inclination sensing," *Analog Devices: AN-1057 - Application note*. pp. 1–8, 2010.

[44] K. Wienen, "Experimental determination of electro-magnetic forces in the air gap of a permanent magnet synchronous motor (Experimentelle Bestimmung elektro-magnetischer Kräfte im Luftspalt einer permanenterregten Synchronmaschine (in German))," Thesis, University of Stuttgart, 2017.

[45] F. Fauser, "Application of low cost accelerometers for the inverse calculation of blocked forces (Anwendung von low cost Beschleunigungsaufnehmern für die inverse Bestimmung von Kurzschlußkräften (in German))," Thesis, Hochschule Esslingen, 2015.

[46] S. Marschall, "Optimization of low-cost accelerometers for the characterization of

electric power steering systems with in-situ blocked forces (in German)," Thesis, Hochschule Aalen, 2015.

[47] M. Schulz, "Application of miniature accelerometers for acoustic measurement of electric steering systems (Anwendung von Miniatur- Beschleunigungssensoren zur akustischen Bewertung elektrischer Lenksysteme (in German))," Thesis, Hochschule Aalen, 2016.

[48] A. S. Elliott, A. T. Moorhouse, and G. Pavić, "Moment excitation and the measurement of moment mobilities," *Journal of Sound and Vibration*, vol. 331, no. 11, May 2012, pp. 2499–2519.

[49] S. Jianxin and C. M. Mak, "Direct measurement of moment mobility and a moment excitation system," *Applied Acoustics*, vol. 63, no. 2, 2002, pp. 139–151.

[50] M. a. Sanderson and C. R. Fredö, "Direct measurement of moment mobility: Part I: A theoretical study," *Journal of Sound and Vibration*, vol. 179, no. 4, 1995, pp. 669–684.

[51] H. G. Choi, A. N. Thite, and D. J. Thompson, "Comparison of methods for parameter selection in Tikhonov regularization with application to inverse force determination," *Journal of Sound and Vibration*, vol. 304, no. 3–5, Jul. 2007, pp. 894–917.

[52] H. G. Choi, A. N. Thite, and D. J. Thompson, "A threshold for the use of Tikhonov regularization in inverse force determination," *Applied Acoustics*, vol. 67, no. 7, Jul. 2006, pp. 700–719.

[53] Y. Kim and P. A. Nelson, "Optimal regularisation for acoustic source reconstruction by inverse methods," *Journal of Sound and Vibration*, vol. 275, no. 3–5, 2004, pp. 463–487.

[54] Y. Liu and W. S. Shepard, "Dynamic force identification based on enhanced least squares

and total least-squares schemes in the frequency domain," *Journal of Sound and Vibration*, vol. 282, no. 1–2, Apr. 2005, pp. 37–60.

[55] A. N. Thite and D. J. Thompson, "The quantification of structure-borne transmission paths by inverse methods. Part 1: Improved singular value rejection methods," *Journal of Sound and Vibration*, vol. 264, no. 2, Jul. 2003, pp. 411–431.

[56] A. N. Thite and D. J. Thompson, "The quantification of structure-borne transmission paths by inverse methods. Part 2: Use of regularization techniques," *Journal of Sound and Vibration*, vol. 264, no. 2, Jul. 2003, pp. 433–451.

[57] S. H. Yoon and P. A. Nelson, "Estimation of Acoustic Source Strength By Inverse Methods: Part I, Experimental Investigation of Methods for Choosing Regularization Parameters," *Journal of Sound and Vibration*, vol. 233, no. 4, 2000, pp. 665–701.

[58] P. C. Hansen, "The L-Curve and its Use in the Numerical Treatment of Inverse Problems," *in Computational Inverse Problems in Electrocardiology, ed. P. Johnston, Advances in Computational Bioengineering*, vol. 4, 2000, pp. 119–142.

[59] P. A. Gauthier, A. Gérard, C. Camier, and A. Berry, "Acoustical inverse problems regularization: Direct definition of filter factors using signal-to-noise ratio," *Journal of Sound and Vibration*, vol. 333, no. 3, 2014, pp. 761–773.

[60] "ISO 9611: 1996-08 Acoustics -- Characterization of sources of structure-borne sound with respect to sound radiation from connected structures -- Measurement of velocity at the contact points of machinery when resiliently mounted." 1996.

[61] F. Fahy and J. Walker, *Advanced Applications in Acoustics, Noise and Vibration*. London: Spon Press, 2004.

[62] T. ten Wolde, J. W. Verheij, and H. F. Steenhoek, "Reciprocity method for the measurement of mechano-acoustical transfer functions," *Journal of Sound and Vibration*, vol. 42, no. 1, 1975, pp. 49–55.

[63] A. Gaudin and L. Gagliardini, "Recent improvements in road noise control," *SAE TECHNICAL PAPER SERIES*, no. 2358, 2007.

[64] J. Park, P. Gu, M.-R. Lee, and A. Ni, "A New Experimental Methodology to Estimate Tire / Wheel Blocked Force for Road NVH Application," *SAE TECHNICAL PAPER SERIES*, no. 724, 2005.

[65] Z. Wang, "Methods for the in-situ determination of dynamic forces of electric power steering systems (Verfahren zur In-Situ-Bestimmung dynamischer Kräfte an elektrischen Lenksystemen (in German))," Thesis, University of Stuttgart, 2016.

[66] M. Sturm, A. T. Moorhouse, W. Kropp, and T. Alber, "Robust calculation of simultaneous multi-channel blocked force signatures from measurements made in-situ using an adaptive algorithm in time domain," in *Proceeedings of 20th International Congress on Sound and Vibration (ICSV 20)*, vol. 2, no. July, pp. 1610–1617, 2013.

[67] M. Hudelmaier, "Characterisation of an electrical power steering system as structure borne sound source in frequency and time domain using inverse methods," Thesis, University of Salford, 2012.

[68] C. Picard, Y. Guibert, and A. Sanon, "Prediction of forces induced by a windscreen wiper system on a car body," in *SIA conference paper*, pp. 1–10, 2010.

[69] A. T. Moorhouse *et al.*, "Defra NANR244: Noise and vibration from building-mounted micro wind turbines Part 2: Results of measurements and analysis," 2011.

[70] D. de Klerk, "Dynamic response characterization of complex systems through operational identification and dynamic substructuring," Thesis, Delft University of Technology, 2009.

[71] M. V. van der Seijs, D. de Klerk, and D. J. Rixen, "General framework for transfer path analysis: History, theory and classification of techniques," *Mechanical Systems and Signal Processing*, 2015, pp. 1–28.

[72] M. V. van der Seijs, "Experimental Dynamic Substructuring: Analysis and Design Strategies for Vehicle Development," Thesis, Delft University of Technology, 2016.

[73] J. W. Verheij, "Measuring sound transfer through resilient mountings for separate excitation with orthogonal translations and rotations," in *Internoise and Noise-Con Congress and Conference Proceedings*, vol. 1980, no. 2, pp. 723–726, 1980.

[74] H. Van Der Auweraer, P. Mas, S. Dom, A. Vecchio, K. Janssens, and P. Van De Ponseele, "Transfer Path Analysis in the Critical Path of Vehicle Refinement: The Role of Fast, Hybrid and Operational Path Analysis," *SAE TECHNICAL PAPER SERIES*, no. 724, 2007, pp. 776–790.

[75] A. T. Moorhouse, N. Zafeiropoulos, A. Mackay, and U. Senapati, "A Comparison of Two In-Situ Transfer Path Analysis Methods," in *11th International Conference - Recent Advances in Structural Dynamics*, no. July, 2013.

[76] A. T. Moorhouse and G. Seiffert, "Characterisation of an airborne sound source for use in a virtual acoustic prototype," *Journal of Sound and Vibration*, vol. 296, no. 1–2, 2006, pp. 334–352.

[77] T. Alber, M. Sturm, and A. T. Moorhouse, "Independent characterization of structure-

borne sound sources using the in-situ blocked force method," in *INTER-NOISE and NOISE-CON Congress and Conference Proceedings*, no. August, pp. 601–612, 2016.

[78] M. Hesselmeier, "Virtual Acoustic Prototyping - A virtual model for the prediction of vehicle interior sound based on the experimental analysis of electric steering systems," Thesis, Hochschule für angewandte Wissenschaften Coburg, 2012.

[79] D. de Klerk, D. J. Rixen, and S. N. Voormeeren, "General framework for dynamic substructuring: History, review and classification of techniques," *AIAA Journal*, vol. 46, no. 5, May 2008, pp. 1169–1181.

[80] J. H. Gordis, R. L. Bielawa, and W. G. Flannelly, "A general theory for frequency domain structural synthesis," *Journal of Sound and Vibration*, vol. 150, no. 1, 1991, pp. 139–158.

[81] M. V. van der Seijs, E. Pasma, D. van den Bosch, and M. Wernsen, "A benchmark structure for validation of Experimental Substructuring , Transfer Path Analysis and Source Characterisation," in *Dynamics of Coupled Structures, Volume 4*, no. February, Cham: Springer, 2017, pp. 295–305.

[82] P. Pfeffer, "Electromechanical systems (Elektromechanische Systeme (EPS) (in German))," in *Steering handbook - Steering system, Steering feeling, driving dynamics of vehicles (Lenkungshandbuch - Lenksysteme, Lenkgefühl, Fahrdynamik von Kraftfahrzeugen (in German))*, Springer Vieweg, 2013, pp. 347–408.

[83] B. Hans-Hermann and U. Seiffert, *Vieweg handbook automotive engineering (Vieweg Handbuch Kraftfahrzeugtechnik (in German))*. Springer Vieweg, 2013.

[84] Robert Bosch Automotive Steering GmbH, "Electric power steering system

Servolectric® - servo unit at a second pinion (Elektrolenkung Servolectric® - Servoeinheit an einem zweiten Ritzel (in German))." 2015.

[85] Robert Bosch Automotive Steering GmbH, "Electric power steering system Servolectric® - servo unit at the steering colum (Elektrolenkung Servolectric® - Servoeinheit an der Lenksäule (in German))." 2015.

[86] P. Pfeffer, "Acoustics and vibration (Akustik und Schwingungen (in German))," in *Steering handbook - Steering system, Steering feeling, driving dynamics of vehicles (Lenkungshandbuch - Lenksysteme, Lenkgefühl, Fahrdynamik von Kraftfahrzeugen (in German))*, Springer Vieweg, 2013, pp. 101–124.

[87] W. Ashby, *An introduction to cybernetics*. London: Chapman & Hail Ltd., 1956.

[88] M. V. van der Seijs, D. D. van den Bosch, D. J. Rixen, and D. de Klerk, "An improved methodology for the virtual point transformation of measured frequency response functions in dynamic substructuring," in *4th ECCOMAS Thematic Conference on Computational Methods in Structural Dynamics and Earthquake Engineering*, no. June, pp. 12–14, 2013.

[89] M. Blau, "Inverse force synthesis : State of the art and future research," in *Proceedings of Inter-Noise*, pp. 1–6, 2000.

[90] B. J. Dobson and E. Rider, "A review of the indirect calculation of excitation forces from measured structural response data," *Proceedings of the Institution of Mechanical Engineers, Part C: Journal of Mechanical Engineering Science 1989-1996 (vols 203-210)*, vol. 204, no. 23, 1990, pp. 69–75.

[91] M. Tanaka, "An industrial and applied review of new MEMS devices features,"

Microelectronic Engineering, vol. 84, no. 5–8, 2007, pp. 1341–1344.

[92] N. Okubo, S. Tanabe, and T. Tatsuno, "Identification of forces generated by a machine under operating condition," in *Proceedings of IMAC*, vol. 3, p. 92, 1985.

[93] P. Nelson, "Some inverse problems in acoustics," in *International Congress on Sound and Vibration, 6 th, Technical Univ. of Denmark, Lyngby, Denmark*, pp. 7–32, 1999.

[94] Dytran Instruments, "Accelerometer Mounting Considerations." Dytran Instruments, Inc., Chatsworth.

[95] A. Acri, G. Offner, E. Nijman, and J. Rejlek, "Substructuring of multibody systems for numerical transfer path analysis in internal combustion engines," *Mechanical Systems and Signal Processing*, vol. 79, 2016, pp. 254–270.

[96] H. Bonhoff, "Interface Mobilities for Low-Noise Design of Structure-Borne Sound Sources," in *Forum Acusticum*, 2011.

[97] S. Mathiowetz and H. a. Bonhoff, "Interface mobilities for characterization of structure-borne sound sources resiliently mounted via multiple contact points," *Journal of Sound and Vibration*, vol. 332, no. 22, 2013, pp. 5789–5803.

[98] H. A. Bonhoff and B. A. T. Petersson, "The influence of cross-order terms in interface mobilities for structure-borne sound source characterization: Force-order distribution," *Journal of Sound and Vibration*, vol. 322, no. 1–2, 2009, pp. 241–254.

[99] H. A. Bonhoff and B. A. T. Petersson, "The influence of cross-order terms in interface mobilities for structure-borne sound source characterization," *Journal of Sound and Vibration*, vol. 329, no. 16, 2010, pp. 3280–3303.

[100] H. A. Bonhoff and A. T. Petersson, "Interface mobilities for structure-borne sound source

characterization and the description of the transmission process," in *DAGA 2010*, pp. 63–64, 2010.

[101] H. A. Bonhoff and A. Eslami, "Interface Mobilities for Characterization of Structure-Borne Sound Sources with Multi-Point Coupling," *Acta Acustica united with Acustica*, vol. 98, no. 3, 2012, pp. 384–391.

[102] H. A. Bonhoff and B. A. T. Petersson, "The influence of cross-order terms in interface mobilities for structure-borne sound source characterization: Plate-like structures," *Journal of Sound and Vibration*, vol. 311, no. 1–2, 2008, pp. 473–484.

[103] H. A. Bonhoff and B. A. T. Petersson, "The influence of cross-order terms in interface mobilities for structure-borne sound source characterization: Frame-like structures," *Journal of Sound and Vibration*, vol. 319, no. 1–2, 2009, pp. 305–319.

[104] D. Zabel, M. Sturm, T. Alber, and A. Moorhouse, "Embedded MEMS accelerometers for the in-situ measurement of blocked forces in coupled structures," in *DAGA 2017*, no. 1, pp. 7–10, 2017.

[105] M. V. van der Seijs, D. de Klerk, D. J. Rixen, and S. Rahimi, "Validation of current state frequency based substructuring technology for the characterisation of steering gear-vehicle interaction," in *Topics in Experimental Dynamic Substructuring - Proceedings of the 31st IMAC, A Conference on Structural Dynamics, 2013*, vol. 2, pp. 253–266, 2014.

[106] M. V. van der Seijs, E. A. Pasma, D. de Klerk, and D. J. Rixen, "A comparison of two component TPA approaches for steering gear noise prediction," in *Dynamics of Coupled Structures, Volume 4*, pp. 71–79, 2015.

[107] M. van der Seijs, "Experimental Dynamic Substructuring - Analysis and Design Strategies for Vehicle Development," Thesis, Delft University of Technology, 2016.

[108] A. T. Moorhouse, A. S. Elliott, and T. A. Evans, "In situ measurement of the blocked force of structure-borne sound sources," *Journal of Sound and Vibration*, vol. 325, no. 4, 2009, pp. 679–685.

[109] A. T. Moorhouse *et al.*, "Defra NANR244: Noise and vibration from building-mounted micro wind turbines Part 3: Prediction methodology," 2011.

[110] A. T. Moorhouse *et al.*, "Defra NANR244: Noise and vibration from building-mounted micro wind turbines Part 1: Review and proposed methodology," 2011.

[111] D. Lennström, M. Olsson, F. Wullens, and A. Nykänen, "Validation of the blocked force method for various boundary conditions for automotive source characterization," *Applied Acoustics*, vol. 102, 2016, pp. 108–119.

[112] A. T. Moorhouse, "Simplified calculation of structure-borne sound from an active machine component on a supporting substructure," *Journal of Sound and Vibration*, vol. 302, no. 1–2, 2007, pp. 67–87.

[113] B. W. G. Halvorsen, A. Corporation, D. L. Brown, and V. November, "Impulse technique for structural frequency response," *Sound and Vibration*, vol. 11, 1977, pp. 8–21.

[114] D. Tcherniak and A. P. Schuhmacher, "Application of decomposition based technique in NVH source contribution analysis," in *Proceedings of the International Conference on Noise and Vibration Engineering (ISMA 2008)*, 2008.

[115] D. de Klerk and A. Ossipov, "Operational transfer path analysis: Theory, guidelines and tire noise application," *Mechanical Systems and Signal Processing*, vol. 24, no. 7, 2010,

pp. 1950–1962.

[116] L. Huttenlauch, “Optimization of a universal test rig for the determination of dynamic forces of electric power steering systems (Optimierung eines Universalprüfstandes zur in-situ Bestimmung dynamischer Kräfte an elektrischen Lenksystemen (in German)),” Thesis, Hochschule Aalen, 2018.

[117] D. Zabel, “Investigation of motor orders and structural resonances of electric adjustable steering columns as a basis for optimization (Untersuchung der Antriebsordnungen und Strukturresonanzen elektrisch verstellbarer Lenksäulen als Basis für Optimierungsmaßnahmen ,” Thesis, University of Stuttgart, 2014.

[118] R. J. Allemang, “The Modal Assurance Criterion - Twenty Years of Use and Abuse,” *Sound and Vibration*, vol. 1, no. August, 2003, pp. 14–21.